



Distributed Coordination in Multiantenna Cellular Networks

RASMUS BRANDT

Doctoral Thesis in Electrical Engineering
Stockholm, Sweden, 2016

TRITA-EE 2016:047
ISSN 1653-5146
ISBN 978-91-7595-916-0

Kungliga Tekniska högskolan
Skolan för elektro- och systemteknik
Avdelningen för signalbehandling
Osqudas väg 10
100 44 Stockholm

Akademisk avhandling som med tillstånd av Kungliga Tekniska högskolan framläggas till offentlig granskning för avläggande av teknologie doktorsexamen i elektro- och systemteknik fredagen den 29 april 2016 klockan 13.15 i Kollegiesalen, Brinellvägen 8, Stockholm.

© Rasmus Brandt, april 2016.

Tryck: Universitetservice US AB.

Abstract

Wireless communications are important in our highly connected world. The amount of data being transferred in cellular networks is steadily growing, and consequently more capacity is needed. This thesis considers the problem of downlink capacity improvement from the perspective of multicell coordination. By employing multiple antennas at the transmitters and receivers of a multicell network, the inherent spatial selectivity of the users can be exploited in order to increase the capacity through linear precoding and receive filtering. For the coordination between cells, distributed algorithms are often sought due to their low implementation complexity and robustness. In this context, the thesis considers two problem domains: base station clustering and coordinated precoding.

Base station clustering corresponds to grouping the cell base stations into disjoint clusters in order to reduce the coordination overhead. This is needed in intermediate-sized to large networks, where the overhead otherwise would be overwhelmingly high. Two solution methods for the clustering problem are proposed: an optimal centralized method, as well as a heuristic distributed method. The optimal method applies to a family of throughput models and exploits the structure of the model to find bounds that can be used to focus the search for the optimal clustering into promising territories. The distributed method instead uses notions from coalitional game theory, where the base stations are modelled as rational and intelligent players in a game. By letting the players make individual deviations that benefit them in the game, i.e. switching clusters, a distributed coalition formation algorithm is obtained.

Coordinated precoding is the act of finding the linear precoders and receive filters that maximize the network performance, given a base station clustering. Four specific challenges are studied in this problem domain. First, coordinated precoding under intercluster interference is considered. The channels of the intercluster links are not explicitly estimated due to overhead reasons, and these links thus lead to intercluster interference. By exploiting the known statistics of the intercluster channels, a robust and distributed coordinated precoding algorithm is developed. Second, coordinated precoding under imperfect channel state information is considered. Relying on the channel reciprocity under time-division duplex operation, a distributed estimation framework is proposed. Given the estimated channels, a robust and distributed coordinated precoding algorithm is then derived. Third, coordinated precoding under imperfect radio hardware is considered. By modelling the radio frequency distortion noises, a distributed coordinated precoding method that accounts for the imperfections is proposed. Fourth, joint coordinated precoding and discrete rate selection is considered. By bounding and linearizing an originally intractable optimization problem, a heuristic algorithm is derived which selects the transmit rate from a finite set and simultaneously forms the linear precoders and receive filters.

Sammanfattning

Trådlös kommunikation är ett viktigt verktyg i dagens ständigt uppkopplade värld. Datamängden som överförs i mobilnätverk ökar stadigt och därmed behovet av mer kapacitet. För att öka kapaciteten i nedlänken så utvecklar denna avhandling nya metoder för koordinering av multicellnätverk. Med flerantenniga sändare och mottagare så kan den spatiala selektiviteten hos mottagarna utnyttjas för att separera dem, vilket ger en ökad kapacitet. För denna koordinering är distribuerade algoritmer ofta att föredra eftersom de är robusta och har låg implementeringskomplexitet. I detta sammanhang undersöker denna avhandling två problemområden: basstationsgruppering och samordnad förkodning.

Basstationsgruppering innebär att basstationerna delas in i disjunkta grupper, vilket minskar overheadkostnaden för samordningen. Detta är framför allt nödvändigt i medelstora till stora nätverk, eftersom overheadkostnaden för koordineringen av dessa annars skulle bli för stor. Två lösningar för basstationsgruppering presenteras: dels en optimal och centraliserad metod samt dels en heuristisk och distribuerad metod. Den optimala och centraliserade metoden kan hantera en familj av modeller för den totala datatakten och utnyttjar strukturen i modellen för att fokusera sökandet efter den optimala grupperingen mot lovande områden. Den heuristiska och distribuerade metoden bygger på spelteori för koalitioner och modellerar basstationerna som rationella och intelligenta spelare i ett spel. En distribuerad algoritm för koalitionsformering härleds genom att låta spelarna göra individuella förflyttningar, dvs. byta grupp, när det gynnar dem under spelets regler.

Vid samordnad förkodning använder de flerantenniga sändarna och mottagarna linjära förkodare och mottagningsfilter för att maximera nätverkets prestanda. Inom detta problemområde undersöks fyra olika specifika problem. Först undersöks problemet när det finns störningar mellan basstationsgrupperna. För att hålla nere mängden overhead så skattas inte kanalerna mellan grupperna, vilket ger upphov till störningar hos mottagarna. Genom att utnyttja den kända statistiska informationen för dessa okända kanaler kan en robust och distribuerad samordningsmetod för förkodningen utvecklas. Därefter undersöks problemet då kanalkännedomen är bristfällig i allmänhet. Reciprociteten som uppstår vid tidsdelningsduplexning utnyttjas och flera distribuerade skattningsmetoder härleds. Givet den skattade kanalkännedomen föreslås en robust metod för samordnad förkodning. Därefter undersöks problemet med samordnad förkodning då radiohårdvaran är bristfällig. En modell för det distortionsbrus som skapas av den bristfälliga hårdvaran används för att föreslå en robust distribuerad metod för samordnad förkodning för detta scenario. Slutligen undersöks valet av diskret datatakt med simultan samordnad förkodning. En heuristisk algoritm utvecklas som löser ett begränsat optimeringsproblem. Algoritmen väljer sänddatatakten från en ändlig mängd och bestämmer simultant de linjära förkodarna och mottagningsfiltrena.

Acknowledgements

This thesis is the result of five years' worth of work, and many people deserve thanks for supporting me in the endeavour towards the Ph. D. degree.

First and foremost, I am deeply grateful for the helpful and encouraging guidance that I have received from my supervisor Prof. Mats Bengtsson. Since I got to know Mats in 2010, while working on my M. Sc. thesis under his supervision, we have had countless technical discussions that have pushed me forward in my research. He has taught me many things, ranging from how to approach complicated technical problems, to how to deal with the trickiest computer issues. I am appreciative that his door was always open for unscheduled meetings. I would also like to thank my co-advisor Prof. Joakim Jaldén, who always finds the critical issues in my technical presentations and who gives good general advice. Thanks go to Prof. Peter Händel and Prof. Magnus Jansson for giving excellent Ph. D. level courses, which helped me in my research. I am also thankful to Prof. Magnus Jansson for notifying me of the open Ph. D. student position at the department.

In my scientific papers, I have been fortunate to have the opportunity to collaborate with several colleagues: thanks go to Dr. Rami Mochaourab, Prof. Emil Björnson, Dr. Per Zetterberg, Hadi Ghanch, Henrik Asplund, Vijaya Yajnanarayana, Klas Magnusson, Dr. Satyam Dwivedi, and Prof. Peter Händel. In particular, I would like to thank Rami for teaching me about coalitional game theory and for being very enthusiastic over the base station clustering work. His willingness to give advice has meant a lot to me. The discussions with, and feedback from, Emil has also been very helpful.

The working environment at plan 4 and 3 of the Q building is very creative and positive, and I am happy to have had a lot of great colleagues. Special thanks go to Ehsan Olfat, Hadi Ghanch, Marie Maros, Nima Najari Moghadam, and Rami Mochaourab for helping me in proofreading this thesis. Hadi also deserves a lot of thanks for our regular discussions, for a great conference trip to CAMSAP, and for the good times outside of work. During my years sharing an office with Klas Magnusson, we have had countless of interesting conversations on wildly varying topics.

I have thoroughly enjoyed the fika and lunchtime discussions with Martin Sundin, Arash Owrang, Johan Wahlström and Satyam Dwivedi. My conference trips would have been less fun without my travel mates Alla Tarighati, Arun Venkitaraman, and Ehsan Olfat. Outside of work, it has been really nice to hang out with Farshad Naghibi and Serveh Shalmashi. For the help with all the administrative details, I am thankful to Tove Schwartz.

I wish to thank Prof. Ignacio Santamaría from Universidad de Cantabria, Spain, for taking the time to serve as the faculty opponent.

I am happy for all my friends in Stockholm, Uppsala, and other parts of the world. There are many of you, and I am truly lucky for having all of you as friends.

The support from my family has been important to me during my Ph. D. studies. I am happy for the great family holidays in Canada with parents-in-law Elaine and Glenn and brother-in-law Charles and his wife Erika. Thank you to my brother Oskar and his partner Johanna for the video and board game sessions. Most of all, I am deeply thankful for the encouragement and the unrelenting support from my parents Eva-Britt and Ingvar.

As always, the most important person is Melissa. Thank you for complementing me so perfectly.

Rasmus Brandt
Stockholm, March 2016

Contents

Nomenclature	xi
1 Introduction	1
1.1 Multiantenna Cellular Networks	1
1.2 Distributed Coordination	4
1.3 Performance Evaluation	6
2 Background and Contributions	11
2.1 System Model	11
2.2 Fundamental Limits and Throughput Maximization	19
2.3 Contributions and Thesis Outline	28
2.A Convex Optimization	39
2.B Weighted MMSE Minimization	39
I Base Station Clustering	45
3 Optimal Base Station Clustering	47
3.1 General Throughput Model	47
3.2 Branch and Bound	51
3.3 Performance Evaluation	56
3.4 Conclusions	58
4 Distributed Base Station Clustering	59
4.1 Frame Structure	59
4.2 Long-Term Throughput Model	62
4.3 Coalition Formation	69
4.4 Performance Evaluation	73
4.5 Conclusions	79
4.A Proof of Theorem 4.1	80

II Coordinated Precoding	83
5 Coordinated Precoding with Intercluster Interference	85
5.1 Throughput Bound	85
5.2 Distributed WMMSE Algorithm	88
5.3 Performance Evaluation	90
5.4 Conclusions	91
6 Coordinated Precoding with Imperfect Channel State Information	93
6.1 Uplink/Downlink Model	94
6.2 Distributed CSI Acquisition	96
6.3 Inherent and Enforced Robustness	107
6.4 Robust and Distributed WMMSE Algorithm	114
6.5 Performance Evaluation	115
6.6 Conclusions	124
6.A Proof of Theorem 6.1	125
6.B Proof of Theorem 6.2	127
7 Coordinated Precoding with Hardware Impairments	131
7.1 Distortion Noise Model	131
7.2 Semi-Distributed WMMSE Algorithm	135
7.3 Distributed Implementation for Constant-EVM Transceivers	139
7.4 Performance Evaluation	145
7.5 Conclusions	148
8 Joint Coordinated Precoding and Discrete Rate Selection	151
8.1 Discrete Rate Model	151
8.2 Semi-Distributed Algorithm	157
8.3 Performance Evaluation	159
8.4 Conclusion	162
8.A Proof of Theorem 8.1	163
9 Conclusions	165
Bibliography	169

Nomenclature

Abbreviations and Acronyms

3GPP	3rd Generation Partnership Project
a.s.	Almost surely
BS	Base Station
CSI	Channel State Information
dB	decibel
EVM	Error Vector Magnitude
FDD	Frequency-Division Duplex
FDMA	Frequency-Division Multiple Access
IA	Interference Alignment
IIA	Intracluster (intracoalition) Interference Alignment
IBC	Interfering Broadcast Channel
IC	Interference Channel
i.i.d.	independent and identically distributed
KKT	Karush-Kuhn-Tucker
LTE	3GPP Long-Term Evolution standard
LTI	Linear and Time-Invariant
MCS	Modulation and Coding Scheme
MIMO	Multiple-Input Multiple-Output

MISO	Multiple-Input Single-Output
MMSE	Minimum Mean Squared Error
MS	Mobile Station
MSE	Mean Squared Error
MVU	Minimum Variance Unbiased (estimator)
OFDM	Orthogonal-frequency division multiplexing
RF	Radio Frequency
SINR	Signal-to-Interference-and-Noise Ratio
SINDR	Signal-to-Interference-plus-Noise-and-Distortions Ratio
SIMO	Single-Input Multiple-Output
SISO	Single-Input Single-Output
SNR	Signal-to-Noise Ratio
SOCP	Second-Order Cone Program
TDD	Time-Division Duplex
TDMA	Time-Division Multiple Access
WMMSE	Weighted Minimum Mean Squared Error
w.r.t.	with respect to

Mathematical Notation

a	Scalars are written in normal font
$ a $	The absolute value of the scalar a
\mathbf{a}	Vectors are written in lower-case bold font
\mathbf{a}_{i_k}	A vector corresponding to MS i_k (thesis specific; see Section 2.1)
$\ \mathbf{a}\ _2$	Euclidean norm of the vector \mathbf{a}
\mathbf{A}	Matrices are written in upper-case bold font
\mathbf{A}_{i_k}	A matrix corresponding to MS i_k (thesis specific; see Section 2.1)
$\mathbf{a}_{i_k,n}$	The n th column of the matrix \mathbf{A}_{i_k}

$[\mathbf{A}]_{nm}$	The (n, m) th element of the matrix \mathbf{A}
$[\mathbf{A}]_{:,1:m}$	The matrix formed from columns 1 through m of the matrix \mathbf{A}
$[\mathbf{A}]_{1:n,:}$	The matrix formed from rows 1 through n of the matrix \mathbf{A}
\mathbf{A}^{-1}	The inverse of the square matrix \mathbf{A}
\mathbf{A}^H	The Hermitian transpose of the matrix \mathbf{A}
\mathbf{A}^T	The transpose of the matrix \mathbf{A}
\mathbf{A}^*	The complex conjugate of the matrix \mathbf{A}
\mathbf{I}_n	The identity matrix of size $n \times n$
$\text{Tr}(\mathbf{A})$	The trace of the matrix \mathbf{A} , i.e. the sum of the diagonal elements of the matrix \mathbf{A}
$\det(\mathbf{A})$	The determinant of the square matrix \mathbf{A}
$\text{diag}(\mathbf{a})$	The diagonal matrix with the elements from the vector \mathbf{a} along the main diagonal and zeros elsewhere
$\text{Diag}(\mathbf{A})$	The diagonal matrix with the elements from the main diagonal of the matrix \mathbf{A} along the main diagonal and zeros elsewhere
$\lambda_{\max}(\mathbf{A})$	The eigenvalue of the matrix \mathbf{A} with the largest magnitude
$\lambda_{\min}(\mathbf{A})$	The eigenvalue of the matrix \mathbf{A} with the smallest magnitude
$\lambda_n(\mathbf{A})$	The eigenvalue of the matrix \mathbf{A} with the n th largest magnitude
$\ \mathbf{A}\ _F^2$	The Frobenius norm squared of the matrix \mathbf{A} , i.e. the sum of singular values of the matrix \mathbf{A}
\mathcal{A}	Sets are written in calligraphic font
$\{a_1, a_2, a_3\}$	The set of elements a_1 , a_2 , and a_3
$\{a_{j_l}\}$	The set of elements a_{j_l} for all $j \in \mathcal{I}, l \in \mathcal{K}_j$ (thesis specific; see Section 2.1)
$\mathcal{B} \subseteq \mathcal{A}$	The set \mathcal{B} is a subset of the set \mathcal{A}
$\mathcal{B} \subset \mathcal{A}$	The set \mathcal{B} is a proper subset of the set \mathcal{A}
$a \in \mathcal{A}$	The element a is in the set \mathcal{A}
$\forall a \in \mathcal{A}$	For all elements a in the set \mathcal{A}
$ \mathcal{A} $	The cardinality of the set \mathcal{A}
$2^{\mathcal{A}}$	The power set of \mathcal{A}

\mathbb{B}_I	The I th Bell number, i.e. the number of ways to partition a set of cardinality I into disjoint non-empty subsets
\mathbb{N}	The set of natural numbers
\mathbb{R}	The set of real numbers
\mathbb{R}_+	The set of non-negative real numbers
\mathbb{R}_{++}	The set of positive real numbers
\mathbb{C}	The set of complex numbers
$\operatorname{Re}(c)$	Real part of the complex number $c \in \mathbb{C}$
$\operatorname{Im}(c)$	Imaginary part of the complex number $c \in \mathbb{C}$
\ln	The natural logarithm
\log_a	The base- a logarithm
$E_1(\xi)$	The exponential integral
$\binom{n}{k}$	The (n, k) th binomial coefficient
$f(x) \in O(g(x))$	The asymptotic growth of $f(x)$ is no faster than that of $g(x)$ (“Big-O”)
$f(x) \in o(g(x))$	The asymptotic growth of $f(x)$ is strictly slower than that of $g(x)$ (“Little-O”)
$\arg \max_x f(x)$	The argument which maximizes the function $f(x)$
$\arg \min_x f(x)$	The argument which minimizes the function $f(x)$
\sup	Supremum, the least upper bound of a set
\limsup	Limit superior, the limiting least upper bound of a sequence
$a \sim b$	The random variable a is distributed according to the probability distribution b
$\mathbb{E}(b)$	The expected value of the random variable b
$\mathcal{CN}(\mathbf{m}, \mathbf{C})$	The circularly-symmetric complex Gaussian probability distribution with mean \mathbf{m} and covariance \mathbf{C}

Introduction

Wireless communications is abundant in today's world. Industry sources expect that there will be 28 billion connected devices by the year 2021 [Eri15], and the total amount of data transferred in wireless networks worldwide is projected to grow exponentially for the foreseeable future [Cis15]. These numbers show the importance of wireless connectivity and are also partially the *raison d'être* of research in wireless communications.

Many types of radio-based wireless systems exist, ranging from e.g. ZigBee and Bluetooth [Haa00] for personal area networks, to IEEE 802.11 WiFi [BKP13] for wireless local area networks and the 3GPP releases [DPS11] for wide area cellular networks. Different systems have different use cases and requirements. In this thesis, we use mathematics to consider a theoretical model of a wireless system. Based on constraints and challenges faced by practical systems, we develop and evaluate mathematical methods for optimizing the performance of our theoretical system. Although our theoretical results are applicable to many types of systems, we generally assume a cellular system infrastructure.

In this first chapter of the thesis, we introduce the notion of cellular networks and how multiple antennas can be used to exploit the available spatial selectivity of the wireless channel.

1.1 Multiantenna Cellular Networks

In the cellular network paradigm, the geographical service area is split up into disjoint *cells*. Each cell contains a *base station* (BS), which *serves* multiple *mobile stations* (MSs) within the cells.¹ The MSs can be e.g. smartphones, tablets, or laptop computers. The cellular network connects the MSs to the outside world (e.g. the Internet). There is both data traffic going from the outside world to the MSs (called the *downlink*), as well as data traffic going from the MSs to the

¹Sometimes we refer to the MSs as *users*.

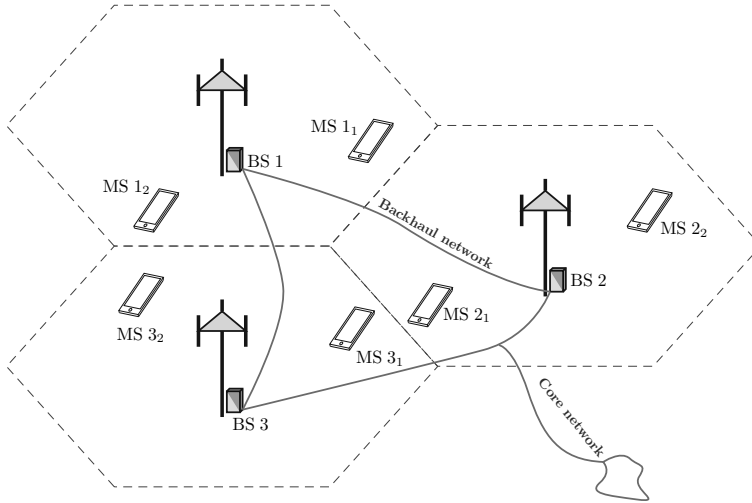


Figure 1.1. Example of multicell network with $I = 3$ BSs and $K = 2$ MSs per cell. The BSs are connected to each other using the backhaul network. Communication with other networks occur over the core network.

outside world (called the *uplink*). It is the responsibility of the serving BS in a cell to transmit data to, and receive data from, the respective MSs in the cell. The BS then relays this data to, and from, the outside world. This happens over the *backhaul network*, which connects the BSs with each other, and the *core network*, which connects the BSs to other networks.

The benefit of the cellular paradigm is that if two MSs want to communicate with each other (through e.g. a phone call, text message, data transfer, etc.), they do not have to set up a direct wireless connection in between themselves. Instead, the initiating MS (wirelessly) connects to its serving BS, which in its turn relays the data over the (wired) backhaul or core networks to the serving BS of the receiving MS, which finally (wirelessly) transmits the message to the receiving BS. Since the distance traversed by the radio waves typically is shorter when communicating between the MS and the serving BS (and vice versa), than if the MSs were to communicate directly with each other, the achieved *signal quality* over the radio links is higher, leading to a higher quality of service.²

In Figure 1.1, we show a schematic illustration of a cellular network with $I = 3$ BSs, each serving $K = 2$ MSs in their respective cells.

²Note that if the MSs are close to each other, they might actually achieve a higher quality of service by connecting directly to each other. This is called *device-to-device communications*. We do not consider this case in this thesis, but instead point the interested reader to the recent Ph.D. thesis [Sha15] in this research area.

1.1.1 Multiple Access in Cellular Networks

The wireless radio channel is a broadcast medium, meaning that many receivers may be able to receive the radio waves transmitted by a single transmitter. If intended and unintended radio transmissions are received simultaneously at a receiver, the intended message is corrupted by *interference* from the unintended message. This can especially be a problem for *cell edge* MSs, as these may have similar distances to their serving BS and the closest interfering BS, meaning that the desired signal power will be on the same order as the interference signal power. Some form of separation of the transmissions to the MSs is therefore clearly needed; this is the notion of *multiple access*.

There are several dimensions that can be used for multiple access: time, frequency, code, or space [TV08, Chapter 1.2]. In this thesis, we mainly consider space-division multiple access (SDMA) [OR96], which means that the spatial selectivity of the MSs is used to separate their corresponding intended transmissions [DADSC04]. This is done by employing multiple antennas at the transmitters and receivers, effectively sampling in space [TV08, Chapter 7.3.7]. The multiple antennas can then be used to *beamform* or *precode*³ the signals spatially at the transmitter, or *receive filter* the signals at the receiver.⁴ When several cells (i.e. the BSs and their corresponding MSs) jointly coordinate their selection of precoders and receive filters, they are performing *coordinated precoding*.

The benefit of using SDMA instead of time-division multiple access (TDMA) or frequency-division multiple access (FDMA) is that the time/frequency resources are more efficiently used, as explained by this simple example:

Example 1.1. *A single BS serves two MSs in the downlink. The BS has two antennas, and the MSs have one antenna each. With TDMA or FDMA, the time/frequency resources are split evenly between the two receivers, leading to a resource utilization of 50% per MS. If SDMA is used instead, zero-forcing beamforming [SSH04] can be used at the BS. This spatially cancels the interference at both MSs, and a time/frequency resource utilization of 100% per MS is achieved.*

The example above is very simplified, but conveys the main benefit of SDMA: the spectral efficiency is improved at the cost of having multiple antennas.

Multiple Antennas at the MSs

In this thesis, we focus on downlink transmissions for the case when both BSs as well as MSs have multiple antennas. This is called a *multiple-input multiple-*

³As is common in the literature, in this thesis the term “beamforming” is used when a single spatial data stream is transmitted whereas the term “precoding” is used when multiple spatial data streams are transmitted.

⁴This can intuitively be thought of as transmitting or receiving in some spatial direction. This is how the human hearing works: since we have two ears, we are able to “hear” the direction of incoming sounds. Without twisting our heads, we cannot spatially direct our speech, however, since we only have one mouth.

output (MIMO) system, in contrast to e.g. the case with single-antenna MSs which is called a *multiple-input single-output* (MISO) system. The MIMO case is often harder to mathematically optimize than the MISO case [BJ13, Chapter 4.6], but we still consider the former due to its increased possibility of performance gains. For the interested reader, the recent treatise [BJ13] gives a good overview of the state-of-the-art for the MISO case.

In addition to multiple access, the multiple antennas can be employed for other tasks: multiple spatial data streams can be transmitted to a single user, the received signal quality can be increased, or the coverage area can be extended while maintaining the received signal quality. The former is called *multiplexing gain*⁵, whereas the two latter correspond to an increase in *diversity*. There is a fundamental trade-off between these two concepts [ZT03], i.e., one cannot simultaneously achieve the maximum multiplexing gain and the maximum diversity.

1.1.2 Channel State Information Acquisition

In order for the coordinated precoding to be effective, the transmitters/receivers must adapt their precoders/receive filters based on the realization of the wireless channel. This means that some *channel state information* (CSI) is required. The CSI in the downlink direction can be estimated at the MS side, using e.g. transmitted training sequences and channel estimation [BG06]. The estimated CSI can then be used for the local receive filter design. In order for the BSs to get the estimate CSI, *feedback* [LHNL⁺08, EAH12] from the MSs to the serving BSs is often used. The BSs then use the fed back CSI in their precoder design.

We group the CSI estimation and feedback together and call this the *CSI acquisition* stage. Although necessary for effective coordinated precoding, the CSI acquisition leads to some *overhead*, which is time/frequency resources not directly used for data transmission.

1.2 Distributed Coordination

The goal of this thesis is to propose algorithms for *coordination* in multicell systems. Specifically, we are interested in designing systems which rely on CSI acquisition and coordinated precoding for maximizing the performance of the network. In this pursuit, we will consider two main problem domains: base station clustering and coordinated precoding.

In both cases, we formulate the problem as a mathematical optimization problem where the goal is to maximize some system-level performance metric that describes the efficiency of the entire network. Solving the optimization problem can be done using *centralized* schemes where the network-wide CSI is gathered in one central location. The optimization problem is then solved in the central location,

⁵Note that using SDMA for multiple access actually is a form of spatial multiplexing, where the multiple spatial data streams are served to different users.

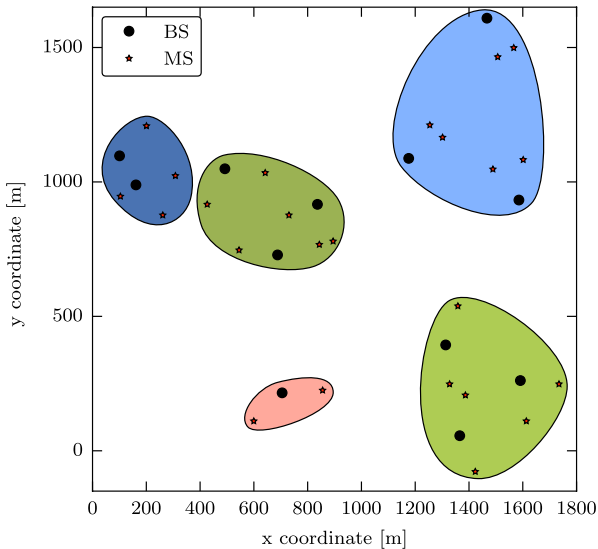


Figure 1.2. Example of a clustered network. The different clusters are marked by the background colour.

and the results are disseminated to all BSs and MSs in the network. Although effective, this type of solution is not efficient, since it may require a lot of communication overhead. Therefore, we consider *distributed* coordination schemes instead. In distributed coordination, the BSs/MSs are able to make *local* decisions based on locally available CSI, which leads to lower communication overhead and implementation complexity than the corresponding centralized approach.

1.2.1 Base Station Clustering

In intermediate-sized to large networks, regardless if the operation is centralized or distributed, not all BSs can coordinate their decisions. This is due to both fundamental aspects (e.g. there is not enough time available to acquire the CSI before it is outdated [LHA13]), and practical aspects (e.g. the complexity of coordinating a large number of BSs may be too high [GHH⁺10]). The idea of *base station clustering* approaches this problem by deciding which BSs that should coordinate their decisions. Disjoint sets of BSs form smaller *clusters*, and the coordination (i.e. CSI acquisition and coordinated precoding) only takes place within the cluster. After the cluster formation there is no coordination between the clusters, leading to a reduction in overhead and complexity at the cost of some unmitigated interference.

An example of a clustered network can be seen in Figure 1.2.

1.2.2 Coordinated Precoding

Given a base station clustering and acquired CSI, the next challenge is how to design the precoders and receive filters. As already mentioned, this is the problem of coordinated precoding. In its basic form, there have been several solutions proposed (see e.g. [SSB⁺13] and references therein). In this thesis, we however consider the problem given specific challenges such as intercluster interference, imperfect CSI, imperfect hardware, and discrete data rates. We generally formulate the coordinated precoding problem as an optimization problem, which we then solve.

1.3 Performance Evaluation

Before diving into the mathematical details of how the base station clustering and coordinated precoding is performed, we will first provide two examples of the performance gains that can be achieved through coordinated precoding.

Outdoors Macrocell Network

The first example⁶ considers an outdoors macrocell deployment, where $I = 3$ macrocell BSs each serve a single MS. We use channel measurements provided by Ericsson Research, and use the data to emulate a multicell system. The BS locations can be seen in Figure 1.3 on the next page. The MS positions are randomly drawn from the marked line segments. We assume an unclustered network, and compare two coordinated precoding methods (*WMMSE* and *MaxSINR*; more details will be given later in the thesis) to the traditional FDMA solution and to the case of no coordination with full frequency reuse.

As can be seen in Figure 1.4 on the facing page, the coordinated precoding methods provide gains of about 15-20% over the traditional FDMA solution. The coordinated precoding methods are also significantly better than the uncoordinated approach, which saturates at high signal-to-noise ratios (SNRs).

⁶For more details about this particular example, we direct the reader to [BAB12].

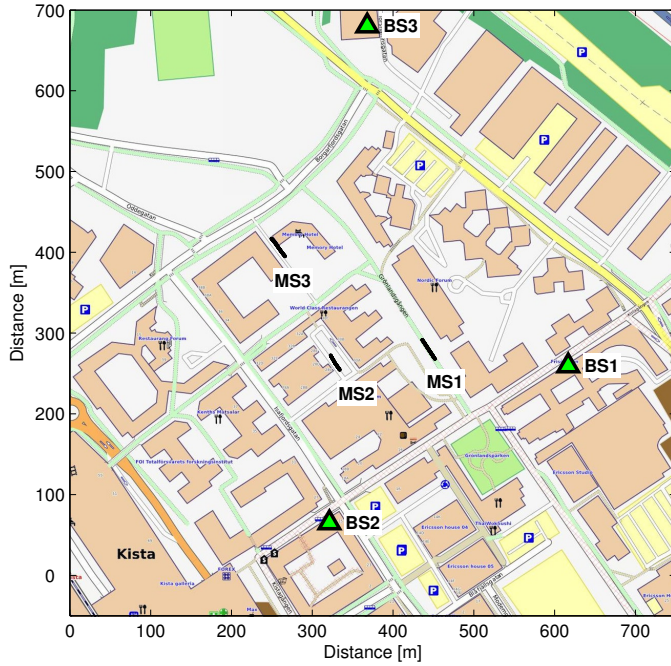


Figure 1.3. Map over outdoors measurement area. © OpenStreetMap contributors, CC-BY-SA, <http://creativecommons.org/licenses/by-sa/2.0>

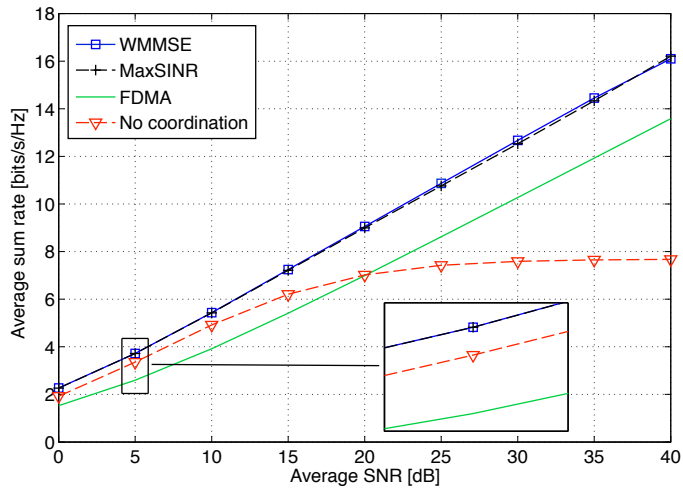


Figure 1.4. Sum rate for algorithms evaluated on outdoors measurements.

Indoors Heterogeneous Network

The second example⁷ considers an indoors heterogeneous network (HetNet) deployment, where $I = 10$ BSs each serve a single MS. We use channel measurements from another measurement campaign performed by Ericsson Research. A map over the measurement area is found in Figure 1.5 on the next page. The BS locations are taken from the “Indoor panel”, “Indoor omni”, and “Outdoor pico” points, and the MS locations are randomly selected within the measurement area. We compare the same coordinated precoding methods as in the previous example, but now the benchmarks are the traditional TDMA solution and uncoordinated approach with full time-reuse.

The results are shown in Figure 1.6 on the facing page. The coordinated precoding methods again show large gains over the traditional methods. At high SNR, the coordinated precoding methods achieves up to 50 % gain over the traditional TDMA solution.

⁷For more details about this particular example, we direct the reader to [BZB13].

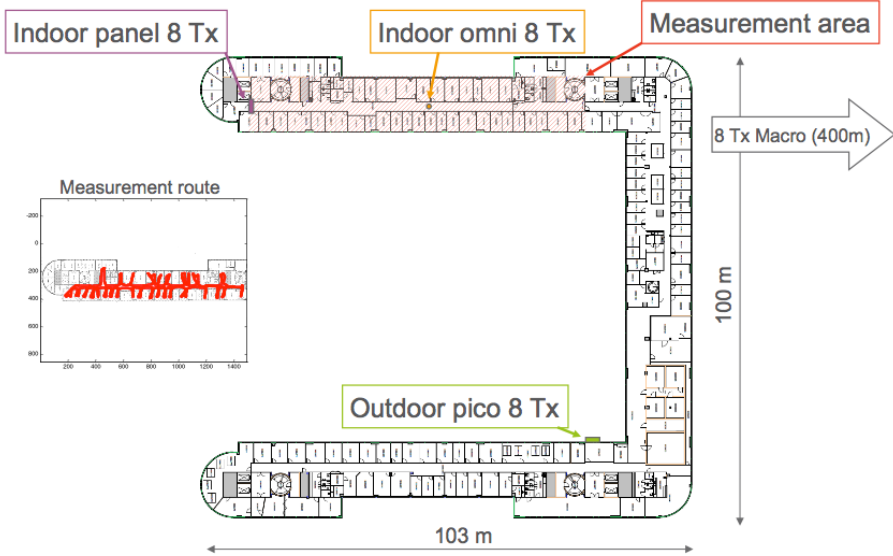


Figure 1.5. Map over indoors measurement area. © Ericsson Research, reproduced with permission.

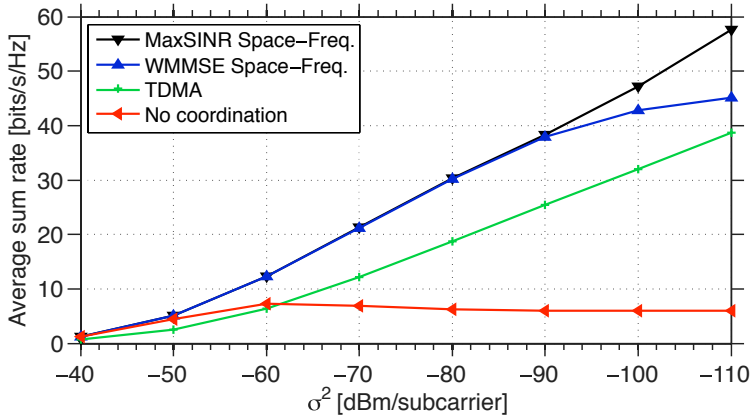


Figure 1.6. Sum rate for algorithms evaluated on indoors measurements.

Background and Contributions

In this chapter, we provide some mathematical preliminaries together with the basic assumptions of this thesis. We describe the problems that we are considering in more detail, discuss some relevant background, and list the specific contributions of the thesis.

2.1 System Model

2.1.1 Interfering Broadcast Channel

Since the wireless radio channel is fundamentally a broadcast medium, we need a model that describes the multiuser interaction between the transmitters and receivers. For this, we will use the *interfering broadcast channel* (IBC) [PL12], which can be seen as a combination of the information theoretic concepts of the *interference channel* (IC) and the *broadcast channel* (BC) [CT06, Chapter 15]. In the IBC, there are I BSs¹, which we will index using the set $\mathcal{I} = \{1, \dots, I\}$. Each BS *serves* one² or many MSs, and for BS i we index these served MSs using the set $\mathcal{K}_i = \{1, \dots, K_i\}$. Each MS is served by a single BS, meaning that this BS is responsible for transmitting data in the downlink to that MS, and receiving data in the uplink from that MS.³ For brevity, we will often abbreviate the BS-MS pair (i, k) by i_k , meaning the k th MS served by the i th BS. We call the BS and its associated MSs a *cell*.

We assume that BS i has $M_i \in \mathbb{N}$ antennas, and correspondingly that MS i_k has $N_{i_k} \in \mathbb{N}$ antennas.⁴ The narrowband complex-valued equivalent baseband channel

¹An IBC with a single BS is a broadcast channel.

²An IBC where all BSs serve a single MS each is an interference channel.

³Contrary to the neighbouring concept of *joint transmission coordinated multipoint transmission* (JT-CoMP), the MSs in the IBC only receive desired signals from one transmitter, i.e. their serving BS.

⁴There is nothing in our exposition that precludes single-antenna BSs or MSs, but in general, we assume that both BSs and MSs have multiple antennas.

[TV08, Chapter 2.2] between BS j and MS i_k is denoted $\mathbf{H}_{i_k j} \in \mathbb{C}^{N_{i_k} \times M_j}$ (see Section 2.1.2 for the channel model). In the downlink,⁵ BS i serves MS i_k with $d_{i_k} \in \mathbb{N}$ data streams. The data is modulated onto a signal $\mathbf{x}_{i_k} \in \mathbb{C}^{d_{i_k}}$. For tractability, we generally⁶ assume that $\mathbf{x}_{i_k} \sim \mathcal{CN}(0, \mathbf{I}_{d_{i_k}})$, and we always assume that the signals to different MSs are statistically independent. We further assume that all data buffers are full, i.e. that there is always data to transmit to all MSs.⁷

We restrict ourselves to *linear* precoding of the data signals \mathbf{x}_{i_k} . This means that BS i applies a linear precoder $\mathbf{V}_{i_k} \in \mathbb{C}^{M_i \times d_{i_k}}$ to the data signal intended for MS i_k , such that the total transmitted signal from BS i is $\mathbf{s}_i = \sum_{k \in \mathcal{K}_i} \mathbf{V}_{i_k} \mathbf{x}_{i_k}$. In an unclustered network,⁸ the received signal at MS i_k is then modelled as

$$\mathbf{y}_{i_k} = \underbrace{\mathbf{H}_{i_k i} \mathbf{V}_{i_k} \mathbf{x}_{i_k}}_{\text{desired signal}} + \underbrace{\sum_{l \in \mathcal{K}_i \setminus \{k\}} \mathbf{H}_{i_k i} \mathbf{V}_{i_l} \mathbf{x}_{i_l}}_{\text{intracell interference}} + \underbrace{\sum_{\substack{j \in \mathcal{I} \setminus \{i\} \\ l \in \mathcal{K}_j}} \mathbf{H}_{i_k j} \mathbf{V}_{j_l} \mathbf{x}_{j_l}}_{\text{intercell interference}} + \underbrace{\mathbf{z}_{i_k}}_{\text{noise}}. \quad (2.1)$$

Notice that there are two types of interference in (2.1): intercell and intracell interference. The intracell interference is received over the same channel as the desired signal, whereas the intercell interference is received over different channels. By lumping these two types of interference together, we get the standard representation of the IBC as:

$$\mathbf{y}_{i_k} = \underbrace{\mathbf{H}_{i_k i} \mathbf{V}_{i_k} \mathbf{x}_{i_k}}_{\text{desired signal}} + \underbrace{\sum_{\substack{j \in \mathcal{I}, l \in \mathcal{K}_j \\ (j,l) \neq (i,k)}} \mathbf{H}_{i_k j} \mathbf{V}_{j_l} \mathbf{x}_{j_l}}_{\text{interference}} + \underbrace{\mathbf{z}_{i_k}}_{\text{noise}}. \quad (2.2)$$

In this model, the thermal noise term is $\mathbf{z}_{i_k} \sim \mathcal{CN}(0, \sigma_{i_k}^2 \mathbf{I}_{N_{i_k}})$ and there are no other forms of *distortions* [Sch08].⁹

See Figure 2.1 on the next page for a schematic illustration of the IBC.

Symmetric Networks

In some chapters of this thesis, we consider *symmetric networks*. In these, the I BSs each serve K MSs. The BSs have M antennas each, and the MSs have N antennas each. All BSs use a transmit power of P , and serve each MS with d data streams. All MSs have a noise power of σ^2 .

⁵We mainly consider downlink transmissions in this thesis. With the advent of smartphones, in deployed cellular networks there can on average be more than 10 times more data flowing in the downlink than in the uplink [Nok14].

⁶This is not the case in Chapter 8, where the transmitted messages are drawn from a set of finite constellations.

⁷This is a strong assumption, which however significantly simplifies our system modelling.

⁸In an *unclustered* network, *all* BSs coordinate their precoding. We discuss the extension to clustered networks in Section 2.1.4.

⁹In Chapter 7 we generalize to the case with additive distortions due to hardware impairments.

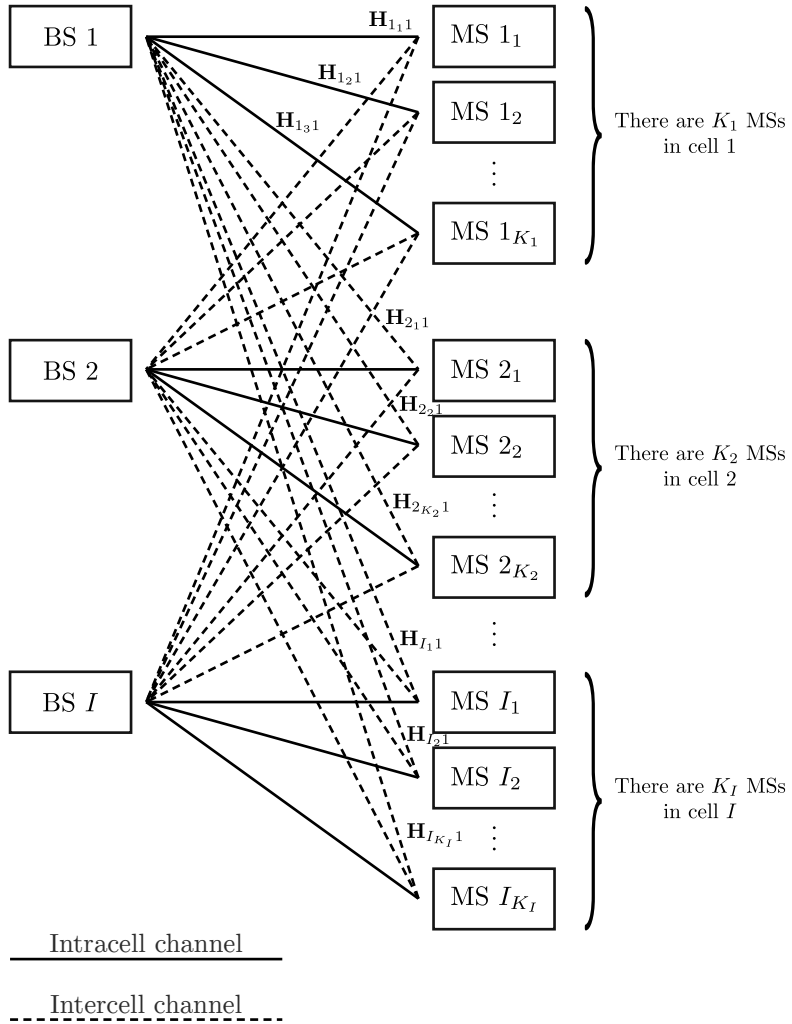


Figure 2.1. Schematic illustration of the IBC. For space reasons, only the channels originating from BS 1 are labelled.

Covariance Matrices

The covariance matrix for the received signal at MS i_k in (2.2) on page 12 is

$$\Phi_{i_k}(\{\mathbf{V}_{jl}\}) = \mathbb{E}(\mathbf{y}_{i_k} \mathbf{y}_{i_k}^H) = \sum_{j \in \mathcal{I}, l \in \mathcal{K}_j} \mathbf{H}_{i_k j} \mathbf{V}_{jl} \mathbf{V}_{jl}^H \mathbf{H}_{i_k j} + \sigma_{i_k}^2 \mathbf{I}, \quad (2.3)$$

where we have used the independence assumption of the transmitted signals. The corresponding interference-and-noise covariance matrix is

$$\Phi_{i_k}^{i+n}(\{\mathbf{V}_{jl}\}) = \Phi_{i_k} - \mathbf{H}_{i_k i} \mathbf{V}_{i_k} \mathbf{V}_{i_k}^H \mathbf{H}_{i_k i} = \sum_{\substack{j \in \mathcal{I}, l \in \mathcal{K}_j \\ (j,l) \neq (i,k)}} \mathbf{H}_{i_k j} \mathbf{V}_{jl} \mathbf{V}_{jl}^H \mathbf{H}_{i_k j} + \sigma_{i_k}^2 \mathbf{I}. \quad (2.4)$$

For brevity of presentation, in the following we will often drop the explicit dependence on the precoders in these expressions.

2.1.2 Channel Model

In the literature, there is a lot of work done on the modelling of wireless channels; see e.g. [ECS⁺98, ABB⁺07] and references therein. Since the main concern of this thesis is resource allocation in the multiuser setting however, we intentionally use simple channel models. This both reduces complexity as well as simplifies the performance evaluation in the simulations.

We assume that the channel is defined by three independent components: path loss, shadow fading, and small-scale fading [TV08, Chapter 2]. The two former are collectively known as the large-scale fading and together describe the macro parameters of the channel. The latter, the small-scale fading, describes the microscopic fading, which changes much quicker than the large-scale parameters.

We assume *block fading* [TV08, Chapter 5.4] for both the large-scale as well as the small-scale parameters. This means that the channel is constant for some time (the *coherence time* [TV08, Chapter 2]) and then abruptly changes to another realization. We will generally consider the coherence time of the large-scale fading to be long, such that we do not need to model it. The coherence time of the small-scale fading (defined as L_c) will however have an important impact of the CSI acquisition overhead, as used in e.g. the long-term throughput model of Chapter 4.

For the path loss, we use a model on the form $\text{PL}_{\text{dB}} = a + b \log_{10}(\text{distance [m]})$ where a [dB] is an offset and b is the path loss exponent. For the shadow fading, we use a log-normal distribution. Finally, the small-scale fading is taken as i.i.d. Rayleigh fading, meaning that $[\mathbf{H}_{i_k j}]_{nm} \sim \mathcal{CN}(0, \gamma_{i_k j})$, where $\gamma_{i_k j}$ is the large-scale fading determined by the path loss and shadow fading realizations. The Rayleigh fading assumption models non-line-of-sight transmission with a rich scattering environment at both the transmitter and the receiver. In urban scenarios, this is generally a reasonable assumption to make [TV08, Chapter 7.3.8] [CLW⁺03].

An example of the time-frequency evolution of an indoors channel from the measurement set in Figure 1.5 can be seen in Figure 2.2 on the next page.

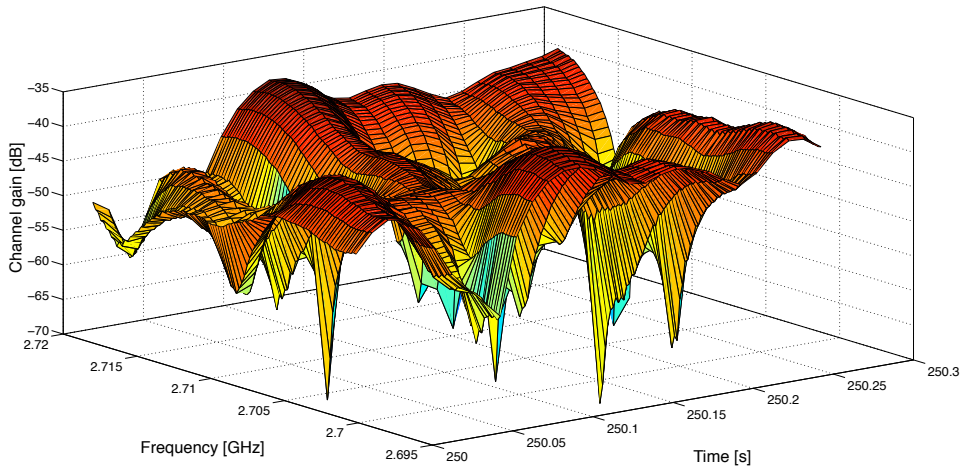


Figure 2.2. Example of the time-frequency surface for a wideband channel measured indoors. (See map of measurement location in Figure 1.5 on page 9.)

Orthogonal Frequency-Division Multiplexing

We only directly consider narrowband channels in this thesis. Most wireless systems are however wideband, meaning that some form of equalization [Mad08, Chapter 5] is necessary to handle the dispersive nature of the wideband channel. We implicitly avoid considering the equalization by assuming that *orthogonal frequency-division multiplexing* (OFDM) [Mad08, Chapter 8.3] is applied. Through OFDM, the linear and time-invariant (LTI) wideband channel can be transformed into a set of parallel narrowband channels called *subcarriers*. The transformation is done by preprocessing the transmitted data symbols with the inverse discrete Fourier transform (implemented as an inverse fast Fourier transform), and postprocessing the received data symbols with the discrete Fourier transform (implemented as a fast Fourier transform) [Lat05, Chapter 8]. By adding a cyclic prefix, the linear convolution of the channel with the transmitted signal becomes a cyclic convolution whose matrix representation is a circulant matrix. For this extended system, the circulant matrix is diagonalized by the discrete Fourier (inverse) transforms, meaning that each subcarrier can be equalized separately. The equalization per subcarrier is trivial: it is a simple division by the corresponding channel coefficient of the Fourier transformed extended channel.

The presentation in this thesis will assume that all operations are performed on a single narrowband subcarrier. The presented ideas can then be extended to the wideband case through the usage of OFDM.

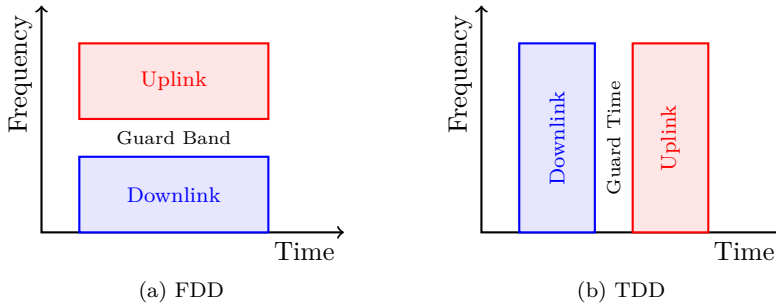


Figure 2.3. Comparison of frequency-division duplex (FDD) and time-division duplex (TDD).

Uplink/Downlink Duplexing

Although we are mainly concerned with optimizing the downlink transmissions, the system also allows for uplink transmissions. The uplink and downlink are duplexed onto the same physical channels by separating them in time or in frequency. In the former case, time-division duplexing (TDD) [TV08, Chapter 4.1] splits up the available time into chunks, which are dedicated for either the uplink or the downlink. In the latter case, frequency-division duplexing (FDD) [TV08, Chapter 4.1] splits the available frequency into chunks, which similarly are dedicated for either the uplink or the downlink. A schematic picture of the differences between these approaches can be seen in Figure 2.3.

In some chapters of this thesis we will assume FDD operation, and in some other chapters we will assume TDD operation. FDD is the most common paradigm in deployed cellular networks [Eri15], but TDD does have some benefits. For example, in TDD the *reciprocity* [Smi04] of the wireless channel can be exploited to gain channel state information at the transmitters through uplink pilot transmissions rather than feedback. We discuss this in more detail in Chapter 6.

2.1.3 System Operation

We assume that our multicell network operates in stages, which cycle indefinitely:

1. **User association:** The MSs are associated to their serving BSs, forming the cells.¹⁰
2. **CSI statistics acquisition:** The large-scale fading parameters are estimated by the MSs and then acquired by the serving BSs through feedback or reciprocity.
3. **Base station clustering:** Given the CSI statistics, the BSs form disjoint clusters.
4. **CSI acquisition:** Within the clusters, the small-scale fading parameters are estimated by the MSs and then acquired by the serving BSs through feedback or reciprocity.
5. **Coordinated precoding:** Given the CSI, the BSs design their precoders within their respective clusters using a coordinated precoding algorithm.
6. **Estimation of effective CSI:** The final effective channels¹¹ are estimated by the MSs.
7. **Data transmission:** The downlink data is transmitted by the BSs using the designed precoders, and receive filtered by the MSs using the estimated effective channels.

Whenever the CSI or the CSI statistics change, i.e. at the end of the corresponding coherence block, these need to be re-estimated. This restarts the cycle from the corresponding stage. In most channel models, the CSI changes significantly faster than the CSI statistics, meaning that stage 4–6 will need to be re-performed more frequently than stage 1–3.

Backhaul and Feedback

The BSs are connected to each other through a backhaul network, which can be used to aid the coordination. The MSs, in virtue of being roaming devices, are not connected to the backhaul network however. All feedback from the MSs go to their serving BS, which may then share the fed back information over the backhaul with other BSs.

¹⁰We do not address this issue in the thesis, but simply assume that a user association is provided to us. The field of joint user association and precoding has recently seen some movement within the research community, see e.g. [GMBS15].

¹¹An effective channel is the channel multiplied by a precoder, e.g. $\mathbf{H}_{i_k i} \mathbf{V}_{i_k}$.

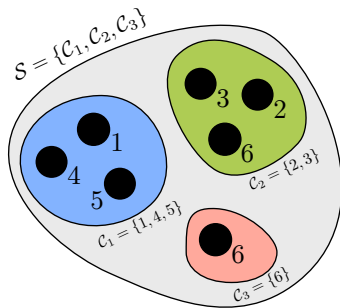


Figure 2.4. Example of a set partition \mathcal{S} when $\mathcal{I} = \{1, 2, 3, 4, 5, 6\}$. The BSs are represented by the black dots, and the clusters are represented by the coloured areas.

2.1.4 Base Station Clustering

As mentioned in Section 1.2.1, there is a need to cluster the BSs in large multicell networks. There are several reasons for this, including CSI acquisition overhead, backhaul delays, and implementation complexity constraints [GHH⁺10, LHA13]. In this thesis, we consider the CSI acquisition overhead as the major reason for the need of the clustering. The CSI acquisition overhead in a cluster depends on the number of member BSs: for each BS that joins the cluster, the interfering channels to all MSs in the other cells in the cluster should be acquired. Under FDD, the overhead is mainly due to the required feedback of the estimated channels [EAH12, BT09], whereas under TDD, the overhead is due to the pilot orthogonality required to avoid pilot contamination [JAMV11, MBB15] effects. In several different models [EAH12, KV13, BMB16a], the overhead scales *quadratically* with the number of BSs in a cluster.

Mathematically, we define a base station clustering using the notion of a set partition:

Definition 2.1 (Set partition). *A set partition $\mathcal{S} = \{C_1, \dots, C_S\}$ is a partition of the BS set \mathcal{I} into disjoint and non-empty sets C_s called clusters, such that $\emptyset \neq C_s \subseteq \mathcal{I}$ for all $C_s \in \mathcal{S}$ and $\bigcup_{s=1}^S C_s = \mathcal{I}$. For a BS $i \in C_s$, we let $\mathcal{S}(i) = C_s$ map to its cluster and $\mathcal{S}^\perp(i) = \mathcal{I} \setminus C_s$ to the complement.*

With this definition, we can describe the IBC in the following way:

$$\mathbf{y}_{i_k} = \underbrace{\mathbf{H}_{i_k i} \mathbf{V}_{i_k} \mathbf{x}_{i_k}}_{\text{desired signal}} + \underbrace{\sum_{\substack{j \in \mathcal{S}(i), l \in \mathcal{K}_j \\ (j, l) \neq (i, k)}} \mathbf{H}_{i_k j} \mathbf{V}_{j_l} \mathbf{x}_{j_l}}_{\text{intracluster interference}} + \underbrace{\sum_{j \in \mathcal{S}^\perp(i), l \in \mathcal{K}_j} \mathbf{H}_{i_k j} \mathbf{V}_{j_l} \mathbf{x}_{j_l}}_{\text{intercluster interference}} + \underbrace{\mathbf{z}_{i_k}}_{\text{noise}}, \quad (2.5)$$

where we distinguish between the *intracluster* interference and the *intercluster* interference at MS i_k . The intracluster interference corresponds to channels that are

acquired during the CSI acquisition stage, and it can thus be handled by the succeeding coordinated precoding. The intercluster interference corresponds to channels that are not estimated, and it will thus give rise to unmitigated intercluster interference.

In networks with small clusters, the intercluster interference limits the performance in the high-SNR regime, whereas in networks with large clusters, the CSI acquisition overhead limits the general performance [LHA13]. It is thus the purpose of the base station clustering to strike a good balance between these two limiting factors. By appropriately including the strong interferers in the same clusters, most of the benefit of full coordinated precoding can be achieved at reasonable overheads.

For a schematic example of a set partition, see Figure 2.4 on the preceding page.

2.2 Fundamental Limits and Throughput Maximization

The main goal of this thesis is to design algorithms which maximize the performance of the multicell network. In order to formulate the optimization problems that will be solved, we first need to mathematically define how we measure the performance. Before defining the throughput, which will be our main performance metric, we will discuss some fundamental limits on the achievable performance.

2.2.1 Capacity

The fundamental limits of wireless communication are described using information theory [CT06]. This field was pioneered by C. E. Shannon in his formative paper [Sha48].¹² In this paper, Shannon showed that a strictly positive data rate is achievable with arbitrarily low error probability, a fact that was not thought to be true before its publication.

Information theory is partly concerned with finding the channel *capacity* for different channel models. These capacities are described by coding theorems, which generally comprise two parts: the converse and the achievability construction. The converse describes an upper bound on performance that no channel code can surpass. The achievability construction gives a channel code that can achieve a certain performance. If the achievable performance of a particular code coincides with the upper bound, the code achieves the capacity of the system. In order to not get entangled in the details of information theory, we will use the following operational definition of channel capacity: the channel capacity is the highest rate of information that can be transmitted over a channel with arbitrarily low error probability [CT06, p. 184]. In loose terms, it is given by the maximum mutual information between the transmitted signal x and the received signal y , when maximized over all possible input distributions p_X . When the noise is Gaussian, the input distribution p_X that maximizes the mutual information is the Gaussian distribution. The interested reader can find more details in the excellent textbook [CT06].

¹²As trivia, we note that this landmark paper has 80 585 citations according to Google Scholar, at the time of this writing.

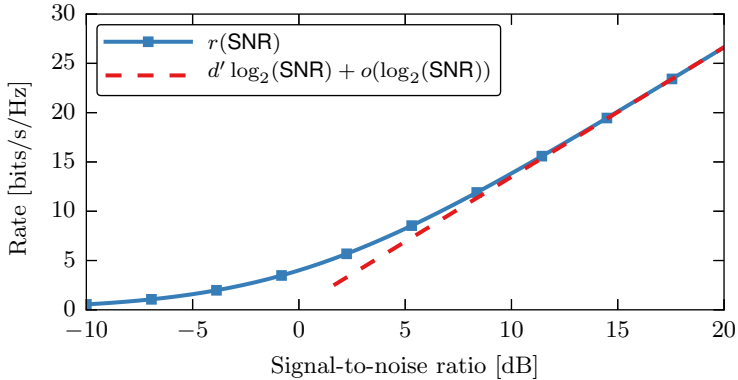


Figure 2.5. Example of how the DoF d' can be interpreted as the high-SNR slope of the rate curve $r(\text{SNR})$.

2.2.2 Degrees of Freedom

There are in total $K_{\text{tot}} = \sum_{i \in \mathcal{I}} K_i$ MSs in the system. The capacity of the entire system is therefore given by a K_{tot} -dimensional *capacity region*, which we denote as $\mathcal{R} \subset \mathbb{R}_+^{K_{\text{tot}}}$. Given a *signal-to-noise ratio* (SNR), we let $r_{i_k}(\text{SNR})$ denote an achievable rate for MS i_k . We let $\mathbf{r}(\text{SNR}) = (r_{1_1}(\text{SNR}), \dots, r_{I_{K_I}}(\text{SNR}))^\top$ denote an achievable rate vector and the capacity region $\mathcal{R}(\text{SNR})$ is then defined as the closure of the set of achievable rate vectors [Car78].¹³ Each point in $\mathcal{R}(\text{SNR})$ represents a different trade-off between the achievable rates of the different MSs.

For the IBC, and its cousin the IC, a full characterization of the capacity region has eluded information theorists for many decades. Lately, a lot of focus has instead been put on the related concept of *degrees of freedom* (DoF). The DoF d'_{i_k} of MS i_k can intuitively be interpreted as the slope of the user rate $r_{i_k}(\text{SNR})$ as the SNR grows large, or equivalently, as the number of interference-free data streams that can successfully be transmitted through the network to MS i_k . The DoF region determines what individual DoFs are jointly achievable, and thus partially characterizes the capacity region at high SNR.

The DoF region of the IBC is defined as (see [CJ08]):

$$\mathcal{D}_{\text{DoF}} = \left\{ (d'_{1_1}, \dots, d'_{I_{K_I}}) \in \mathbb{R}_+^{K_{\text{tot}}} : \forall (\omega_{1_1}, \dots, \omega_{I_{K_I}}) \in \mathbb{R}_+^{K_{\text{tot}}} \right. \quad (2.6)$$

$$\left. \sum_{i \in \mathcal{I}, k \in \mathcal{K}_i} \omega_{i_k} d'_{i_k} \leq \limsup_{\text{SNR} \rightarrow \infty} \left(\sup_{\mathbf{r}(\text{SNR}) \in \mathcal{R}(\text{SNR})} \frac{1}{\log_2(\text{SNR})} \left(\sum_{i \in \mathcal{I}, k \in \mathcal{K}_i} \omega_{i_k} r_{i_k}(\text{SNR}) \right) \right) \right\}.$$

¹³The capacity region can be made convex through *time sharing*, see e.g. [CT06, Chapter 15].

In this definition, the DoF d'_{i_k} can be interpreted as the number of interference-free data streams that can successfully be communicated to MS i_k . We visualize this interpretation in Figure 2.5 on the facing page, where we for a single user plot the rate $r(\text{SNR})$ and an affine curve whose slope, in decibels, is d' . The system-level metric the *sum-DoF* is defined as $d'_{\text{sum}} = \sum_{i \in \mathcal{I}, k \in \mathcal{K}_i} d'_{i_k}$ and describes the total number of interference-free data streams that can be successfully transmitted in the entire network.

Remark 2.1. *Note that the number of spatial data streams allocated to MS i_k , i.e. d_{i_k} , may or may not be equal to the DoF of MS i_k , i.e. d'_{i_k} . The former is simply decided at transmission, whereas the latter describes the fundamental limit of the network. In the high-SNR regime, it is thus generally wise to select $d_{i_k} \leq d'_{i_k}$, $\forall i_k$.*

2.2.3 Interference Alignment

A technique whose development has followed the investigation of the sum-DoF of the IC is the idea of *interference alignment* (IA) [MAMK08, CJ08, Jaf11]. The main idea of IA is to align all received interference into lower-dimensional subspaces at all receivers. Then using simple linear¹⁴ techniques such as receiver zero-forcing, the interference can be completely removed, thus converting the system into a noise-limited system. Our interest in IA lies in the fact that it has been shown to achieve the *optimal* sum-DoF of the IC [CJ08].

Linear IA is performed in some dimension, e.g. time, frequency, or space. In the two former, a diagonal channel matrix is formed by means of time extensions or frequency extensions. The extended channel is then used for the IA. In this thesis, we are however only concerned with spatial IA over the MIMO channel matrices $\{\mathbf{H}_{i_k j}\}_{j \in \mathcal{I}, l \in \mathcal{K}_j}$. For more details about time/frequency-extended IA, we direct the interested reader to [BAB12, BZB13].

Before describing the spatial IA mathematically, we introduce the idea of a *linear receive filter*. These filters are similar to the precoders at the transmitters, except that they are applied to the received signal at the receivers. Each MS i_k has a linear receive filter $\mathbf{U}_{i_k} \in \mathbb{C}^{N_k \times d_{i_k}}$, and the correspondingly received filtered signal is

$$\hat{\mathbf{x}}_{i_k} = \mathbf{U}_{i_k}^H \mathbf{y}_{i_k} = \underbrace{\mathbf{U}_{i_k}^H \mathbf{H}_{i_k i} \mathbf{V}_{i_k} \mathbf{x}_{i_k}}_{\text{filtered desired signal}} + \underbrace{\sum_{\substack{j \in \mathcal{I}, l \in \mathcal{K}_j \\ (j,l) \neq (i,k)}} \mathbf{U}_{i_k}^H \mathbf{H}_{i_k j} \mathbf{V}_{j_l} \mathbf{x}_{j_l}}_{\text{filtered interference}} + \underbrace{\mathbf{U}_{i_k}^H \mathbf{z}_{i_k}}_{\text{filtered noise}}. \quad (2.7)$$

A set of receive filters and precoders $\{\mathbf{U}_{i_k}, \mathbf{V}_{i_k}\}_{i \in \mathcal{I}, k \in \mathcal{K}_i}$ is then an *IA solution* if it completely cancels all the interference present in the second term of (2.7). The

¹⁴Here we only consider linear IA. There is also non-linear IA (see e.g. [Jaf11, Chapter 4.7]), which however would require receivers with infinite floating-point precision, thus mainly contributing theoretical value.

conditions for this to happen at MS i_k are:

$$\mathbf{U}_{i_k}^H \mathbf{H}_{i_k j} \mathbf{V}_{j_l} = \mathbf{0}, \quad \forall j \in (\mathcal{I} \setminus \{i\}), l \in \mathcal{K}_i, \quad (2.8)$$

$$\mathbf{U}_{i_k}^H \mathbf{H}_{i_k i} \mathbf{V}_{i_l} = \mathbf{0}, \quad \forall l \in (\mathcal{K}_i \setminus \{k\}), \quad (2.9)$$

$$\text{rank}(\mathbf{U}_{i_k}^H \mathbf{H}_{i_k i} \mathbf{V}_{i_k}) = d_{i_k}. \quad (2.10)$$

Due to equations (2.8) and (2.9), no residual interference will be present after receive filtering. In order to avoid the trivial solution, equation (2.10) enforces full rank effective channels for the desired signals.

A schematic example of aligned interference is shown in Figure 2.6 on the next page.

Feasibility

At first, IA seems like a great idea: converting an interference-limited system into a noise-limited system would lead to good performance in high-SNR scenarios, where the interference is the main culprit. However, a solution may not always exist to the spatial IA equations in (2.8)–(2.10). The notion of the *feasibility* of IA describes the existence of a solution to the IA equations. Depending on the scenario, there may be 0, 1, or many solutions [GBS15]. There are several results in the literature which give conditions on a.s. existence of solutions to the IA equations under generic channel models,¹⁵ such as ours in Section 2.1.2. In [YGJK10], the notion of *properness*—meaning that there are more variables than equations in the IA equations—was introduced as a proxy for the feasibility. The connection to feasibility was made rigorous in [RLL12], where necessary and sufficient conditions were proposed for different scenarios. The results were extended to the IBC in [ZBH11, LY13]. Another approach was taken in [GBS14], where a numerical test was proposed for testing the feasibility of arbitrary configurations. For the special case of square symmetric systems, i.e. where $N = M$, necessary and sufficient conditions were derived in [BCT14].

All derived IA feasibility conditions depend on the scenario studied, but the gist is that “enough” antennas must be available in order to be able to align the interference and simultaneously maintain the rank of the desired channels. For the particular case of a symmetric IBC, the necessary and sufficient condition for IA feasibility is given in [LY13] as:

$$IKd \leq M + N - d. \quad (2.11)$$

¹⁵For a fixed realization of channels however, checking the existence of an IA solution is NP-hard if the nodes have more than 2 antennas each [RSL12].

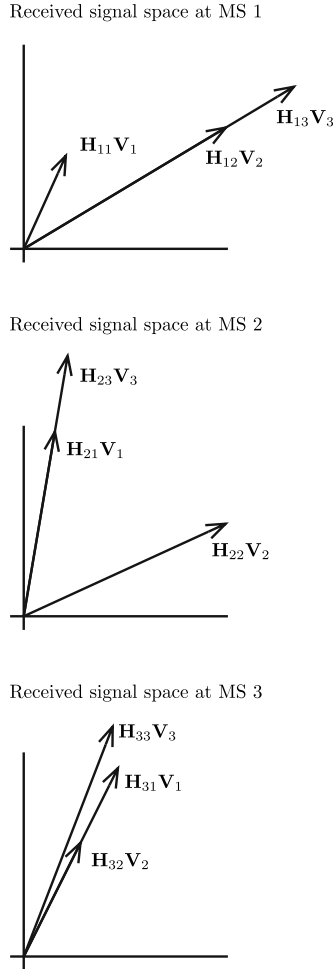


Figure 2.6. Schematic example of an interference alignment solution in a symmetric network with $I = 3$ BSs serving $K = 1$ MSs each. For notational brevity, we drop the BS index in the channel and precoder subscripts. The received signal space has two dimensions. Notice how all the interference is simultaneously colinear at all receivers. Since the desired signals have a component which is orthogonal to the interference subspace, receive zero-forcing can be applied to completely remove the interference at all receivers. This comes at the cost of losing the desired signal power which lies in the interference subspace. In this particular example, this will hurt MSs 1 and 3 especially: the desired signal power at MS 1 is low (this can be seen by noting that the desired signal vector is “short” in comparison to the interference vectors), and the desired signal vector at MS 3 is almost colinear with the interference subspace.

Algorithms

For a given IA feasible scenario, the equations in (2.8)–(2.10) on page 22 do not prescribe any particular solution methodology. The equations are bi-linear in the set of receive filters and precoders $\{\mathbf{U}_{i_k}, \mathbf{V}_{i_k}\}_{i \in \mathcal{I}, k \in \mathcal{K}_i}$, and are thus hard to solve in general. Some solution approaches are presented in [GS11, GLS14].

Instead of directly trying to solve the IA equations, there has been a significant push in the research community for algorithms that solve the IA equations by optimizing proxy functions. Among the first was [GCJ11], where the famous MinWLI algorithm was presented. This algorithm iteratively minimizes the *interference leakage*, which is the sum power of received interference in the network. An algorithmically identical version to the MinWLI algorithm was presented in [PH09]. In [SGHP10], leakage minimization was combined with a step along the sum rate gradient on the Grassmann manifold. Leakage minimization for wideband channels was proposed in [GLV⁺12, LGV⁺12]. Another approach was taken in the line of works [PD12, DRSP13, SY15b], where the rank of the interference subspace was minimized through convexification and block coordinate descent. Instead of minimizing the leakage, an MMSE interference alignment technique was proposed in [SCB⁺09]. In [GCJ11], the MaxSINR method was proposed, which iteratively maximizes the SINRs of the different spatial streams of the network. The convergence of this heuristic has not been proven, but empirically it often works very well [GCJ11, BAB12]. Modified versions of the SINR maximization in [GCJ11], with proven convergence, have been proposed in [PH11] and [WV13].

Testbeds

IA appeared as a theoretical concept for achieving the optimal sum-DoF, but it has also gathered some attention from experimental researchers working on wireless testbeds. The first work appeared in [GPK09], where a hybrid form of IA combined with successive interference cancellation was tested on 20 nodes. Performance evaluation by means of recorded measurements from a testbed was presented in [EPH10], where the practical feasibility of IA was confirmed. Real-time transmissions were performed on a testbed at KTH Royal Institute of Technology [ZM12, Zet14a, Zet14b, MFZS14, MFZ15], as well as on a joint testbed at the Universities of A Coruña and Cantabria [GRS⁺11, GNCG⁺11, LGGN⁺15]. Both testbeds reported success in implementing IA in the real world, and showed the importance of considering hardware impairments and CSI imperfections as performance-limiting factors.

2.2.4 Throughput

IA is a useful tool for completely cancelling the interference in the network, but that is only a fruitful approach in the high-SNR regime where the interference is the main performance-limiting factor. Further, IA is only relevant in networks that are IA feasible. It is our goal in this thesis to maximize the performance in more general

scenarios, and we will therefore not directly maximize the DoFs. Instead, we will consider another performance metric. There are many other possible performance metrics proposed in the wireless communications literature and a non-exhaustive list of examples could include: bit error rate, mean squared error, energy efficiency, etc. The choice of performance metric heavily influences the system design. In this thesis, we will choose the performance metric to be that of *throughput*. In our definition, the throughput is the *effective data rate* in [bits/s/Hz]¹⁶ that can be achieved with vanishingly low error probability at the receiver, as the length of the codewords grows large. Mathematically, it is composed of two quantities: the *pre-log factor* α_{i_k} and the *rate* $r_{i_k}(\{\mathbf{V}_{j_l}\})$, such that the throughput for MS i_k is

$$t_{i_k}(\{\mathbf{V}_{j_l}\}) = \alpha_{i_k} r_{i_k}(\{\mathbf{V}_{j_l}\}) \text{ [bits/s/Hz]}. \quad (2.12)$$

Pre-Log Factor

The pre-log factor $0 \leq \alpha_{i_k} \leq 1$ describes how efficiently the spectral resources are used in serving MS i_k with data. It measures what fraction of the resources are used for overhead (i.e. CSI acquisition) compared to the fraction used for data transmission. It does not depend on the precoders, but may depend on the base station clustering.

The specific definition of the pre-log factor depends on the assumptions on the CSI acquisition scheme used and we therefore defer its definition to the relevant Chapters 3 and 4. In Chapters 6–8, we do not explicitly model the CSI acquisition overhead, thus implicitly assuming unity pre-log factors.

Rate

The rate $r_{i_k}(\{\mathbf{V}_{j_l}\})$ describes the spectral efficiency of the system *during* the data transmission stage. It depends on the current signal quality condition for MS i_k , i.e. the desired effective channel $\mathbf{H}_{i_k i}$ and the signal-plus-interference-and-noise covariance matrix $\Phi_{i_k}^{i+n}(\{\mathbf{V}_{j_l}\})$ (defined in (2.4) on page 14). For mathematical tractability, and in order to decrease the complexity of the decoder, we always assume that the received interference is treated as noise in the decoder.¹⁷ For the multi-stream decoding case, we thus define the rate as

$$r_{i_k}(\{\mathbf{V}_{j_l}\}) = \log_2 \det \left(\mathbf{I}_{d_{i_k}} + \mathbf{V}_{i_k}^H \mathbf{H}_{i_k i}^H (\Phi_{i_k}^{i+n}(\{\mathbf{V}_{j_l}\}))^{-1} \mathbf{H}_{i_k i} \mathbf{V}_{i_k} \right) \text{ [bits/s/Hz]}, \quad (2.13)$$

which is the *mutual information* [CT06, Chapter 2] between \mathbf{x}_{i_k} and \mathbf{y}_{i_k} in the IBC model of (2.2) on page 12 [Tel99]. By claiming that (2.13) describes an *achievable*

¹⁶Note that the dimension of the data rate contains [Hz] in the denominator, and thus is normalized w.r.t. the spectrum usage. The for the layperson more common dimension of [bits/s] can easily be obtained by multiplying the throughput with the available bandwidth.

¹⁷This is generally suboptimal in the capacity sense, but leads to simple and practical receiver algorithms.

rate, we are implicitly requiring long codewords, an optimal receiver, and perfect CSI at the receiver. These are all fundamental requirements in the channel coding theorem of Shannon [Sha48], from which we base the definition in (2.13).

In some chapters, we use a slightly different definition of the rate: in Chapters 3 and 4, we consider the long-term average of the single-stream decoding rate; in Chapter 5, we consider the single-stream decoding rate; and in Chapter 8, we consider an altogether different rate definition based on a discrete set of rates together with corresponding SINR requirements. In these cases, we explicitly state the rate model in the corresponding chapter.

Remark 2.2. *Note that the expression in (2.13) is non-convex (see Section 2.A) in the precoders $\{\mathbf{V}_{j_l}\}_{j \in \mathcal{I}, l \in \mathcal{K}_j}$, since they show up both as an outer quadratic term, as well as inner quadratic terms inside $\Phi_{i_k}^{i+n}(\{\mathbf{V}_{j_l}\})$. This has implications for the complexity of mathematically optimizing the rate.*

2.2.5 Weighted Sum Throughput Maximization

The performance of the entire system is now given by a K_{tot} -dimensional *throughput region*, which we denote as $\mathcal{T} \subset \mathbb{R}_+^{K_{\text{tot}}}$. Each point in \mathcal{T} represents a different trade-off between the throughputs of the different MSs. The *Pareto boundary* describes all operating points where the throughput of some MS cannot be increased without decreasing the throughput of at least some other MS [BV04, Chapter 4.7]. One particular point on the Pareto boundary of \mathcal{T} is the *maximum sum throughput*, which is the point that maximizes the sum of the MS throughputs.

In order to focus on the system as a whole, we formulate a *scalarized* [BV04, Chapter 4.7.4] optimization problem using a single system-level objective. There are many ways of weighting together the individual throughputs of the MSs into a single scalar; in this thesis we mainly choose the *weighted sum throughput* function. With MS weights $\omega_{i_k} \in \mathbb{R}_+$, the weighted sum throughput problem is

$$\begin{aligned} & \underset{\{\mathbf{V}_{i_k}\}_{i \in \mathcal{I}, k \in \mathcal{K}_i}}{\text{maximize}} && \sum_{i \in \mathcal{I}, k \in \mathcal{K}_i} \omega_{i_k} t_{i_k}(\{\mathbf{V}_{j_l}\}) \\ & \text{subject to} && \sum_{k \in \mathcal{K}_i} \|\mathbf{V}_{i_k}\|_{\text{F}}^2 \leq P_i, \quad \forall i \in \mathcal{I}, \end{aligned} \tag{2.14}$$

where P_i denotes the transmit power constraint of BS i . This network utility maximization problem [PC06] is non-convex, since the rates in (2.13) are non-convex in $\{\mathbf{V}_{j_l}\}_{j \in \mathcal{I}, l \in \mathcal{K}_j}$.¹⁸ Contrary to the IA equations in (4.2)–(4.4), the problem is always feasible. In essence, the weighted sum rate describes the ultimate performance of the system when fairness is not directly taken into account. That is, the system will completely turn off MSs (through power allocation) if that benefits the system-level

¹⁸The formulation in (2.14), as well as the derived optimization problems in Chapters 5–8, have per-BS sum power constraints. The applied solution algorithm (see below) can however be generalized to other types of convex power constraints; see e.g. [Bra14a, Section 2.3.3].

performance. By suitably selecting the weights $\{\omega_{i_k}\}_{i \in \mathcal{I}, k \in \mathcal{K}_i}$, all Pareto optimal points that coincide with the convex hull of the Pareto boundary can be found [BJ13]. The weights can be thought to describe the relative importance of the MSs and can e.g. be selected to achieve a proportionally fair solution [KMT98].

The system-level optimization problem in (2.14) is a more general approach to coordinated precoding than directly applying IA, in the sense that the problem in (2.14) is relevant in cases such as the intermediate-SNR regime, scenarios when IA is not feasible, or scenarios where the sum-DoF is zero. The latter can happen whenever there is any un-aligned interference left in system, i.e. due to intercluster interference, imperfect hardware, etc. Although our goal in designing our coordinated precoding algorithms will be to solve optimization problems of the form as the one in (2.14), we will remain inspired by the intuition from IA.

Algorithms

The problem in (2.14) is NP-hard [LZ08, LDL11], and as such we can practically only hope to find a *local* maximum of the problem. There have been many algorithms proposed for this task in the literature and the papers [PH11, SSB⁺13] provide a good overview of the different approaches taken in MIMO scenarios. In this thesis, we will mainly use ideas from the *weighted minimum mean squared error* (WMMSE) algorithms proposed in [CACC08, SRLH11]. The gist of the WMMSE approach is to lift the optimization problem into a higher-dimensional space, and then apply a tight linearization.¹⁹ The paper [CACC08] proposed this approach for a single-cell MIMO system, and a similar method was directly applied to multicell MIMO systems in [NSGS10, SM12]. It was however not until [SRLH11] that a rigorous connection to the multicell weighted sum rate problem was presented.

The original WMMSE algorithm of [CACC08, SRLH11] provides a nice building block for deriving more specific resource allocation algorithms for multicell networks, as will be clear by the contributions in Chapters 5–8. In the literature, extensions of the original WMMSE algorithm has been reported in [RHL13b], where it was used for max-min fairness; in [HSBL13], where it was combined with short-term base station clustering; in [BHL⁺14], where it was used as a building block in a cross-layer system design; in [SRL14], where it was combined with user association; in [LHLL14], where it was combined with base station activation; and in [RBCL14], where it was combined with orthogonal user grouping.

The WMMSE algorithms generally only find a locally optimal point, and thus the *initialization* of the algorithm may matter for which locally optimal point that is found. The work in [SY15a] proposes to use an interference alignment solution as the initial point to the algorithm.

¹⁹A detailed outline of this approach is given in Appendix 2.B.

2.3 Contributions and Thesis Outline

With the needed mathematical preliminaries presented, we now summarize the contributions of the thesis and give an outline of the presentation.

2.3.1 Chapter 1: Introduction

In this chapter, we described the setting of the thesis. We also provided a small nugget of motivation, through some performance evaluation results from [BAB12, BZB13], for considering coordination in multicell networks.

2.3.2 Chapter 2: Background and Contributions

In the current chapter, we have mathematically described the system model and provided some background for the problems considered in this thesis. We describe the contributions of the thesis in detail, and we will end the chapter with some reference material on convex optimization and the weighted minimum mean squared error maximization framework for resource allocation in multicell networks.

Reference

Parts of this chapter is based on material in:

[Bra14a] R. Brandt. Coordinated Precoding for Multicell MIMO Networks. Tech. Lic. thesis, KTH Royal Institute of Technology, 2014.

2.3.3 Chapter 3: Optimal Base Station Clustering

As described in Section 2.1.3, when the CSI statistics have been acquired, the first step in the system operation is to form the base station clusters. We therefore start the thesis by providing an algorithm which finds the optimal base station clustering. The algorithm is centralized and has high complexity, and it is thus intended for benchmarking of more practical methods.

Prior Work

Assuming IA precoding, suboptimal base station clustering algorithms have earlier been proposed in [PH12, CC14]. To the best of our knowledge however, no works in the literature have addressed the problem of finding the optimal base station clustering for IA-based systems. Naive exhaustive search over all possible clusterings is not tractable, due to its super-exponential complexity. Yet, the globally optimal base station clustering is important in order to benchmark more practical schemes, such as the ones in e.g [PH12, CC14] and Chapter 4.

Contribution

The contribution in this chapter is a structured method for optimal base station clustering based on branch and bound [LD60]. We consider a generalized long-term throughput model which encompasses the models in [PH12, CC14] and Chapter 4. When evaluated using the long-term throughput model of Chapter 4, empirical evidence shows that the resulting algorithm finds the optimum at an average complexity which is orders of magnitude lower than that of exhaustive search.

Reference

The material presented in this chapter has been published in:

[BMB16b] R. Brandt, R. Mochaourab, and M. Bengtsson. Globally optimal base station clustering in interference alignment-based multicell networks. *IEEE Signal Process. Lett.*, vol. 23, no. 4, pages 512–516, 2016.

For reproducibility reasons [VKV09], we provide the simulation source code for this contribution at [Bra16a].

2.3.4 Chapter 4: Distributed Base Station Clustering

The algorithm for base station clustering proposed in Chapter 3 is good for benchmarking, but its complexity is too high for practical use. In this chapter, we therefore again consider the base station clustering problem, but now focus on distributed solutions with low complexity. We also use first principles to derive a long-term throughput model for IA-based base station clustering.

Prior Work

In [PH12], the clusters were orthogonalized in time and a simple CSI acquisition model was proposed for the pre-logs in the throughputs. In [CC14], the clusters were not orthogonalized and the CSI acquisition overhead was not explicitly accounted for. Both of these papers further proposed base station clustering heuristics; the former based on user grouping, and the latter based on graph partitioning of an interference graph with fixed edge weights. In [PBS⁺13], a coalitional game in partition form was used for IA-based femtocell clustering. The CSI acquisition overhead was modelled in terms of transmission power which limited the amount of power left for data transmission. Static base station clustering using IA was explored in [TG09], where a hexagonal cell setup was studied numerically. In [PLH16], a geographic partition of the plane based on second-order Voronoi regions was used for static pair-wise base station clustering.

Contribution

The contribution in this chapter is a novel long-term throughput model for clustered multicell networks and a distributed clustering heuristic based on coalitional game theory. The long-term throughput model accounts for both the pre-log factors and the long-term rates, under the assumption of intracluster IA precoding. The clustering heuristic is an instance of a coalition formation algorithm, which models the base stations as rational players in a game. The players are allowed to make individual deviations, until the state of individual stability has been reached. In this state, no player has an incentive to move to another cluster, and the algorithm has thus converged. Numerical performance evaluations show the performance of the coalition formation algorithm to be close to the optimal method of Chapter 3.

References

The material presented in this chapter has been published/submitted in:

- [BMB15] R. Brandt, R. Mochaourab, and M. Bengtsson. Interference alignment-aided base station clustering using coalition formation. In *Proc. Asilomar Conf. Signals, Systems, Computers*, pages 1087–1091, 2015.²⁰
- [BMB16a] R. Brandt, R. Mochaourab, and M. Bengtsson. Distributed long-term base station clustering in cellular networks using coalition formation. *IEEE Trans. Signal Inf. Process. Netw.*, accepted in Mar. 2016.

The simulation source code for the contributions in [BMB15] and [BMB16a] is made available at [Bra15b].

2.3.5 Chapter 5: Coordinated Precoding with Intercluster Interference

In the long-term throughput model of Chapter 4, intracluster IA precoding was assumed and there was no coordination between clusters. This allowed for a tractable performance model characterization, but the unmitigated intercluster interference impacted the performance detrimentally. By exploiting knowledge of the CSI statistics for the intercluster interference however, the performance can be improved without having to resort to acquiring the CSI of the intercluster channels.

Prior Work

Existing work on coordinated precoding which is robust against intercluster interference is scarce. One existing work is [CC14], where a fixed diagonal loading term was applied to the MaxSINR algorithm of [GCJ11]. The diagonal loading was numerically shown to lead to robust precoders.

²⁰This paper was awarded a Best Student Paper Award (2nd prize) in the Student Paper Contest of the Asilomar'15 conference.

Contribution

The contribution in this chapter is a robustified WMMSE algorithm, which optimally accounts for the intercluster interference given only knowledge of the CSI statistics and filter norms for the interfering links. The numerical performance evaluation shows the improved performance of our approach, compared to earlier naive and robust approaches applied to the same problem.

Reference

The material presented in this chapter has been submitted in:

- [BMB16a] R. Brandt, R. Mochaourab, and M. Bengtsson. Distributed long-term base station clustering in cellular networks using coalition formation. *IEEE Trans. Signal Inf. Process. Netw.*, accepted in Mar. 2016.

2.3.6 Chapter 6: Coordinated Precoding with Imperfect Channel State Information

In the earlier chapters, the CSI was always assumed to be perfectly estimated. In this chapter, we relax that assumption and propose distributed CSI acquisition techniques that exploit the reciprocal channels attained under TDD operation with calibrated hardware. Given the estimated channels, we then derive an WMMSE algorithm which is robust to the CSI imperfections.

Prior Work

Earlier work on bidirectional channel estimation includes [SBH14], where a reciprocal channel was exploited to directly estimate the filters maximizing the SINR, requiring no other signalling. In [KTJ13], signalling strategies for obtaining the necessary CSI were proposed. TDD reciprocity was assumed, and the MSs used combinations of intercell and intracell effective channel pilot transmissions.

Earlier work on robust precoding under CSI imperfections includes [JPKR11], where a robust WMMSE algorithm was suggested for the case of norm bounded channel uncertainty arising from limited quantized feedback. Other robustified versions of the WMMSE algorithm, where the contribution of the downlink channel estimation errors in the involved covariance matrices was averaged out, were proposed in [SM12, LKY13]. The same approach was taken in [RBCL13], where it was mentioned that this corresponds to optimizing a lower bound on the achieved performance, and in [NGS12] where the lower bound was explicitly derived. The work in [SM12, LKY13, RBCL13, NGS12] was mainly focused on proposing robust WMMSE methods and thus the actual CSI acquisition was not conclusively studied, contrary to this chapter. The major assumption in the system model of [SM12, LKY13, RBCL13, NGS12] is that channel estimation is only performed at

the MSs, leading to a large amount of feedback which would typically be implemented using a centralized CSI acquisition infrastructure.

Contribution

The contributions in this chapter are distributed CSI acquisition protocols and a robustified WMMSE algorithm for imperfect CSI. Three different CSI acquisition protocols are proposed, corresponding to different levels of required feedback and backhaul coordination. All of the protocols exploit the reciprocity of the channel in order to gather the CSI at the transmitters. The robust WMMSE algorithm is obtained by enforcing an invariant of the filters and weights at the MSs, and by heuristically scaling the power constraint at the BSs. The simulations show that the robustifications are effective, and the proposed distributed coordinated precoding system is shown to perform well.

Reference

The material presented in this chapter has been published in:

- [BB16a] R. Brandt and M. Bengtsson. Distributed CSI acquisition and coordinated precoding for TDD multicell MIMO systems. *IEEE Trans. Veh. Technol.*, accepted in Apr. 2015 (in press).

The simulation source code for the contribution in [BB16a] is made available at [Bra16b].

2.3.7 Chapter 7: Coordinated Precoding with Hardware Impairments

Another major assumption so far in the thesis is that of perfect radio hardware. In this chapter, we instead consider imperfect hardware which exhibit distortion noises. We adapt an existing model for the distortion noises to the MIMO case and show how to account for the distortions in the coordinated precoding.

Prior Work

All physical radio transceivers suffer from various hardware impairments, such as phase noise, I/Q imbalance, power amplifier non-linearities, etc [Sch08]. A large amount of previous work has focused on these individual impairments, and on proposing corresponding compensation schemes; see e.g. [Sch08] and references therein. A simple model was proposed in [SWB10], where the aggregate effect of the residual hardware impairments, after compensation, was studied. For their hardware setup, it was shown that the distortion noises from the residual hardware impairments were Gaussian. This type of residual hardware impairments was shown to fundamentally limit performance in the high-SNR regime for a MIMO point-to-point system [BZBO12]. A pure simulation study was performed in [GGLF08],

for a more complicated system with path loss. With a generalized model for the residual impairments compared to the one proposed in [SWB10], the optimal beamforming problem for a MISO multicell network was solved in [BZBO12] and [BJ13, Chapter 4.3].

Contribution

The contribution in this chapter is employing the hardware impairments model from [BJ13, Chapter 4.3] to the coordinated precoding problem in MIMO systems. We show how the extra distortion noise terms can be handled under the WMMSE framework, and provide distributed and semi-distributed coordinated precoding algorithms. The impairments-aware algorithms are numerically shown to significantly outperform the impairments-ignorant algorithms, although the achieved high-SNR slope of the sum rate curve is zero.

References

The material presented in this chapter has been published in:

- [BBB14] R. Brandt, E. Björnson, and M. Bengtsson. Weighted sum rate optimization for multicell MIMO systems with hardware-impaired transceivers. In *Proc. IEEE Conf. Acoust., Speech, and Signal Process.*, pages 479–483, 2014.
- [Bra14a] R. Brandt. Coordinated Precoding for Multicell MIMO Networks. Tech. Lic. thesis, KTH Royal Institute of Technology, 2014.

The simulation source code for the contribution in [BBB14] is made available at [Bra14b].

2.3.8 Chapter 8: Joint Coordinated Precoding and Rate Selection

In the final chapter of the thesis, we consider the case when the user performance is modelled by a set of discrete rates corresponding to a finite number of modulation and coding schemes (MCSs). This is a more practical assumption than what was previously assumed in the thesis, i.e. optimal receivers and transmitted codewords with infinite granularity.

Prior Work

Existing work on joint beamforming and discrete rate selection is limited, and only considers the MISO and SISO models. In [WLM13], a convex approximation of the sum rate was proposed for the MISO case. Through a reweighting procedure, some gains over the state-of-the-art in continuous rate optimization was shown. In [CP15], a mixed integer second order cone program (MISOCP) was formulated for the MISO case. The problem was mathematically reformulated to be applicable to the commercial branch-and-cut solver CPLEX, which numerically gave the optimal

solution. Two heuristics, based on solving a sequence of SOCP problems, were also proposed. In [WJN13], the problem was considered for a subcarrier-based SISO system, and an optimal branch-and-bound algorithm was proposed.

Contribution

The contribution in this chapter is developing a model for the joint precoder design and discrete rate selection problem for MIMO systems and providing a convergent heuristic algorithm. We let the system designer choose which domain is used for the modelling of the discrete rate functions, which then lead to different approximations. Using numerical simulations and MCSs selected from the IEEE 802.11ac WiFi standard [BKP13], we show how our heuristic algorithm outperforms all benchmarks significantly.

Reference

The material presented in this chapter has been submitted in:

- [BB16b] R. Brandt and M. Bengtsson. Joint coordinated precoding and discrete rate selection in multicell MIMO networks. *IEEE Signal Process. Lett.*, submitted in Mar. 2016.

2.3.9 Chapter 9: Conclusions

We end the thesis with some conclusions and an outlook on future research.

2.3.10 Chapter Assumption Comparison

The assumptions of the different chapters are summarized in Table 2.1 on the next page.

2.3.11 Summary of Contributions to the Papers by the Author

The papers cited above are the results of collaboration between me and the co-authors. In the list below, I summarize my contributions to these papers in relation to the contributions of the co-authors:

- [BBB14] The second author proposed the original distortion noise model in [BZB12], but I adapted it to the MIMO setting. I derived the robust algorithm, performed the simulations, and wrote the paper. The second and third authors were helpful with technical discussions and proofreading.
- [BMB15] I formulated the problem, derived the long-term throughput model, performed the simulations, and wrote the paper except for the section about coalition formation. Me and the second author came up with the algorithm together. The second author also wrote the section about coalition formation,

Table 2.1. Summary of Chapter Assumptions

Chapter	3	4	5	6	7	8
Utility/optimization time scale						
Long term	✓	✓	—	—	—	—
Short term	—	—	✓	✓	✓	✓
MS utility						
Throughput	✓	✓	✓	—	—	—
Rate	—	—	—	✓	✓	—
Discrete rate	—	—	—	—	—	✓
System assumptions						
Intercluster interference	✓	✓	✓	—	—	—
Imperfect CSI	—	—	—	✓	—	—
Imperfect hardware	—	—	—	—	✓	—
Suboptimal receivers	—	—	—	—	—	✓

helped with technical discussions, and proofread the paper. The third author helped with technical discussions and proofread the paper.

[BMB16a] I formulated the problem, derived the long-term throughput model, came up with the attach-or-supplant deviation, derived the robust precoding algorithm, performed the simulations, and wrote the paper. The second author provided the technical background for the coalitional formation, helped with technical discussions, and proofread the paper. The third author helped with technical discussions and proofread the paper.

[BMB16b] I formulated the problem, came up with the algorithm, performed the simulations, and wrote the paper. The co-authors helped with technical discussions and proofreading.

[BB16a] The second author came up with the original idea of distributed CSI estimation, but I derived the three CSI acquisition methods. I further formulated the robustification heuristics, performed the simulations, and wrote the paper. The second author was helpful with technical discussions and proofreading.

[BB16b] I formulated the problem, came up with the algorithm, performed the simulations, and wrote the paper. The second author helped with technical discussions and proofreading.

2.3.12 Copyright and Relation to Existing Publications

The material presented in this thesis comes from the compilation of results from the publications cited above. Some passages may be taken verbatim from the respective publication. Accepted and published papers are ©IEEE. The submitted papers may have their copyright transferred to the IEEE in the future. All material is used with permission.

2.3.13 Contributions Outside the Thesis

Some of the published papers by the author were deemed to not fit thematically within this thesis. These contributions are summarized below.

CSI Selection

In Chapters 3 and 4, we consider the problem of base station clustering to handle the fact that not all BSs can coordinate in large networks. Instead of disjointly forming clusters to reduce the CSI acquisition overhead, a similar goal could be achieved by independently selecting which interfering links to feed back during the CSI acquisition. This is the problem of *CSI selection*, which is studied in [MBGB15]. Using the game theoretical notion of stable matching, a distributed algorithm for finding a good CSI selection was provided. The performance of the proposed algorithm was shown to equal that of a centralized design.

[MBGB15] R. Mochaourab, R. Brandt, H. Ghauch, and M. Bengtsson. Overhead-aware distributed CSI selection in the MIMO interference channel. In *Proc. European Signal Process. Conf.*, pages 1043–1047, 2015.

Fast-Convergent Coordinated Precoding

In Chapter 6, we consider iterative optimization of the precoders exploiting the reciprocity of the TDD operation. Since the coherence time of the channel may be low, it is important to achieve a good sum rate solution using few iterations. In [BB15], the problem of how to actively design an algorithm which is fast to reach convergence is considered. This is done by considering a scalarized multi-objective optimization problem, where a linear combination of the sum rate and the sum-DoF is optimized. This is done by approximating the non-smooth DoF function using a technique from the compressive sensing literature, combined with the WMMSE optimization technique. This leads to an algorithm with the desired properties, which is shown to outperform the state-of-the-art.

[BB15] R. Brandt and M. Bengtsson. Fast-convergent distributed coordinated precoding for TDD multicell MIMO systems. In *Proc. IEEE Int. Workshop Computational Advances Multi-Sensor Adaptive Process.*, pages 457–460, 2015.

The simulation source code for this contribution is made available at [Bra15a].

Feasibility of Space-Frequency-IA

Since IA can be performed in space or frequency, an interesting research question is whether combining these dimension for a joint space-frequency IA gives any benefits. In [BZB13], this problem is considered. A properness criterion for the model is derived, and the possible gain over space-only IA is shown. Further, some existing algorithms that have been adapted to this model are evaluated using measurements from an indoors picocell testbed set up by Ericsson Research. The results show that a large performance gain can be achieved using space-frequency IA and the traditional TDMA solution.

The plot in Figure 1.6 is taken from [BZB13], but no other material has been included in this thesis.

- [BZB13] R. Brandt, P. Zetterberg, and M. Bengtsson. Interference alignment over a combination of space and frequency. In *Proc. IEEE Int. Conf. Commun. Workshop: Beyond LTE-A*, pages 149–153, 2013.

Performance Evaluation of Frequency-IA

Although this thesis focused on IA in the spatial domain, both time and frequency extensions can be used as well. In [BAB12], IA in a frequency-extended multicarrier system is considered. The performance of a variety of IA algorithms is evaluated using measurements from a macrocell testbed set up by Ericsson Research in Kista, Sweden. The results show that IA is a highly viable approach for sum rate improvements over the traditional FDMA solution, even with single-antenna transceivers.

The plot in Figure 1.4 is taken from [BAB12], but no other material has been included in this thesis.

- [BAB12] R. Brandt, H. Asplund, and M. Bengtsson. Interference alignment in frequency – a measurement based performance analysis. In *Proc. Int. Conf. Systems, Signals and Image Process.*, pages 227–230, 2012.

Pulse Scheduling in Many-to-Many Communications

In a different research direction than this thesis, [YMB⁺16] considers the scheduling of transmitted pulses in a network where the propagation time is not negligible in relation to the pulse length. If the ranges between nodes is known a priori, this information can be used in the scheduling. The problem can be formulated as a travelling salesman problem, where the visited cities corresponds to different pulse transmit orders. When the pulses are tightly packed in time, high data rates can be achieved.

- [YMB⁺16] V. Yajnanarayana, K. E. G. Magnusson, R. Brandt, S. Dwivedi, and P. Händel. Optimal scheduling for interference mitigation by range information. *IEEE Trans. Mobile Comput.*, submitted in Feb. 2016.

Polynomial Singular Value Decomposition

In another research direction, [BB11] considers the diagonalization of polynomial matrices describing the channel impulse response of a wideband MIMO channel. Using an existing polynomial singular value decomposition (PSVD) algorithm, the wideband MIMO channel is diagonalized and water-filling power allocation is performed. The performance of this approach is compared to the traditional OFDM scheme with per-subcarrier SVD beamforming. Although theoretically interesting, the results of [BB11] show the traditional OFDM method to be superior to the PSVD approach.

[BB11] R. Brandt and M. Bengtsson. Wideband MIMO channel diagonalization in the time domain. In *Proc. IEEE Int. Symp. Indoor, Mobile Radio Commun.*, pages 1958–1962, 2011.

The simulation source code for this contribution is made available at [Bra11].

2.A Convex Optimization

The weighted sum throughput problem in (2.14) on page 26 is non-convex, and possibly NP-hard in general. It is therefore hard to solve, and we will only venture to find locally optimal solutions. This will be done using weighted minimum mean squared error minimization, which will be described in the next appendix. For completeness, we will however first shortly discuss convex optimization problems in this section.

A function $f : \mathbb{C}^L \rightarrow \mathbb{R}$ is said to be convex if it satisfies

$$f(c\mathbf{x} + (1 - c)\mathbf{y}) \leq cf(\mathbf{x}) + (1 - c)f(\mathbf{y}) \quad (2.15)$$

for all $\mathbf{x} \in \mathbb{C}^L$, $\mathbf{y} \in \mathbb{C}^L$ and $c \in [0, 1]$. A set \mathcal{X} is said to be convex if

$$c\mathbf{x} + (1 - c)\mathbf{y} \in \mathcal{X} \quad (2.16)$$

for any $\mathbf{x}, \mathbf{y} \in \mathcal{X}$ and $c \in [0, 1]$. Applying these concept to mathematical optimization, we can formulate a convex optimization problem as

$$\begin{aligned} & \underset{\mathbf{x}}{\text{minimize}} && f(\mathbf{x}) \\ & \text{subject to} && \mathbf{x} \in \mathcal{X}. \end{aligned} \quad (2.17)$$

This is a *convex optimization problem*, since the objective function is a convex function and the feasible set is a convex set. A particularly prominent feature of convex optimization problems is that any local optimum is also a global optimum [BV04]. This makes this class of problem “easy” to solve to global optimality, a property which does not hold in general for non-convex optimization problems.

For a general non-convex optimization problem, under some regularity conditions [Ber06, Chapter 3.3], the Karush-Kuhn-Tucker (KKT) conditions [BV04, Chapter 5.5], [Ber06, Chapter 3.3], give necessary conditions for a point to be locally optimal. For the special case of convex optimization problems, and assuming e.g. that a strictly feasible point exists²¹, the KKT conditions are both necessary and sufficient [BV04, Chapter 5.5]. Finding the optimum to a convex optimization problem therefore amounts to solving the KKT conditions. In some cases, closed-form solutions can be found, but in general, numerical methods must be used to solve them. In the last couple of decades, *interior-point methods* [BV04] have been the state-of-the-art for solving constrained convex optimization problems.

2.B Weighted MMSE Minimization

For reference value, we will now summarize the WMMSE technique developed in [CACC08, SRLH11] for finding a local maximum to the weighted sum throughput problem in (2.14) on page 26. The gist of the algorithm is that by enlarging

²¹This is known as Slater’s constraint qualification [BV04].

the search space and applying a tight lower bound to the user rates, an iterative algorithm that monotonically converges to a stationary point can be found. This algorithm belongs to the larger class of block successive upper-bound minimization (BSUM) algorithms, as further described in [RHL13a, HRLP16].

Rate/MMSE Relationship

First, we assume that a linear receive filter is used at the MSs, similarly as in (2.7) on page 21. With the estimate of the transmitted signal $\hat{\mathbf{x}}_{i_k} = \mathbf{U}_{i_k}^H \mathbf{y}_{i_k}$, the *mean squared error* (MSE) matrix for MS i_k is

$$\begin{aligned} \mathbf{E}_{i_k}(\mathbf{U}_{i_k}, \{\mathbf{V}_{j_l}\}) &= \mathbb{E} \left((\mathbf{x}_{i_k} - \hat{\mathbf{x}}_{i_k}) (\mathbf{x}_{i_k} - \hat{\mathbf{x}}_{i_k})^H \right) = \\ &= \mathbf{I} - \mathbf{U}_{i_k}^H \mathbf{H}_{i_k i} \mathbf{V}_{i_k} - \mathbf{V}_{i_k}^H \mathbf{H}_{i_k i}^H \mathbf{U}_{i_k} + \mathbf{U}_{i_k}^H \mathbf{\Phi}_{i_k}(\{\mathbf{V}_{j_l}\}) \mathbf{U}_{i_k}. \end{aligned} \quad (2.18)$$

The MSE is another user performance metric, and the optimal receive filter in sum-MSE sense is the well known *MMSE filter*. We obtain this by minimizing $\text{Tr}(\mathbf{E}_{i_k}(\mathbf{U}_{i_k}, \{\mathbf{V}_{j_l}\}))$ w.r.t. \mathbf{U}_{i_k} , giving the optimal filter as

$$\mathbf{U}_{i_k}^{\text{MMSE}}(\{\mathbf{V}_{j_l}\}) = (\mathbf{\Phi}_{i_k}(\{\mathbf{V}_{j_l}\}))^{-1} \mathbf{H}_{i_k i} \mathbf{V}_{i_k}. \quad (2.19)$$

Note that since \mathbf{y}_{i_k} and \mathbf{x}_{i_k} have a linear relationship and are jointly Gaussian, the optimal receiver structure is linear [Kay93, Chapter 15]. The receiver in (2.19) is therefore *the* MSE optimal receiver and not just the best receiver (in MSE sense) amongst all linear receivers.

The MMSE filter has an interesting connection to the rate. By substituting (2.19) into (2.18), through the matrix inversion lemma [HJ85, Section 0.7.4], it can be shown that

$$\begin{aligned} \mathbf{E}_{i_k}^{\text{MMSE}}(\{\mathbf{V}_{j_l}\}) &= \mathbf{E}_{i_k}(\mathbf{U}_{i_k}^{\text{MMSE}}, \{\mathbf{V}_{j_l}\}) \\ &= \mathbf{I} - \mathbf{V}_{i_k} \mathbf{H}_{i_k i}^H (\mathbf{\Phi}_{i_k}(\{\mathbf{V}_{j_l}\}))^{-1} \mathbf{H}_{i_k i} \mathbf{V}_{i_k} \\ &= \left(\mathbf{I} + \mathbf{V}_{i_k} \mathbf{H}_{i_k i}^H (\mathbf{\Phi}_{i_k}^{\text{I+n}}(\{\mathbf{V}_{j_l}\}))^{-1} \mathbf{H}_{i_k i} \mathbf{V}_{i_k} \right)^{-1}. \end{aligned} \quad (2.20)$$

From (2.13) on page 25, we thus note that

$$\begin{aligned} r_{i_k}(\{\mathbf{V}_{j_l}\}) &= \log_2 \det \left((\mathbf{E}_{i_k}^{\text{MMSE}}(\{\mathbf{V}_{j_l}\}))^{-1} \right) \\ &= \max_{\mathbf{U}_{i_k}} \log_2 \det \left((\mathbf{E}_{i_k}(\mathbf{U}_{i_k}, \{\mathbf{V}_{j_l}\}))^{-1} \right) \\ &= - \min_{\mathbf{U}_{i_k}} \log_2 \det (\mathbf{E}_{i_k}(\mathbf{U}_{i_k}, \{\mathbf{V}_{j_l}\})). \end{aligned} \quad (2.21)$$

The second equality in (2.21) can be shown by noting that the gradient [HG07] of $\text{Tr}(\mathbf{E}_{i_k})$ w.r.t. \mathbf{U}_{i_k} and the gradient of $-\log_2 \det(\mathbf{E}_{i_k})$ w.r.t. \mathbf{U}_{i_k} are such that, when set to zero, they both give the same solution. Since both functions are convex

w.r.t. \mathbf{U}_{i_k} , the corresponding unconstrained optimization problems have the same solution. This connection has long been known for the single-user MIMO scenario [PCL03], the multiuser MIMO scenario [CACC08], and it was noted for the multicell MIMO scenario in [SRLH11].

Transformed Optimization Problem

Our goal is to find a local optimum to the weighed sum throughput problem (2.14) on page 26. The first step in the WMMSE approach, as pioneered by [CACC08], is to enlarge the search space to $\{\mathbf{U}_{i_k}, \mathbf{V}_{i_k}\}_{i \in \mathcal{I}, k \in \mathcal{K}_i}$ and use (2.21) to replace $\alpha_{i_k} r_{i_k}(\{\mathbf{V}_{j_l}\}) \rightarrow -\alpha_{i_k} \log_2 \det(\mathbf{E}_{i_k}(\mathbf{U}_{i_k}, \{\mathbf{V}_{j_l}\}))$ in the objective function. Then the concave $\log_2 \det(\mathbf{E}_{i_k})$ can be upper bounded by its first-order Taylor approximation, around a point $\bar{\mathbf{E}}_{i_k}$:

$$\log_2 \det(\mathbf{E}_{i_k}) \leq \log_2(e) (-\ln \det(\bar{\mathbf{E}}_{i_k}^{-1}) + \text{Tr}(\bar{\mathbf{E}}_{i_k}^{-1} \mathbf{E}_{i_k}) - d_{i_k}), \quad \forall \bar{\mathbf{E}}_{i_k} \succ \mathbf{0} \quad (2.22)$$

where $e = 2.718\dots$ is Euler's number. Next, additional optimization variables $\{\mathbf{W}_{i_k}\}_{i \in \mathcal{I}, k \in \mathcal{K}_i}$, where $\mathbf{W}_{i_k} \succ \mathbf{0}_{d_{i_k}}$, are introduced such that $\mathbf{W}_{i_k} = \bar{\mathbf{E}}_{i_k}^{-1} \forall i_k$. These optimization variables thus determine the current linearization point of the user rates. Lastly, by *minimizing* the weighted sum of the right-hand side of (2.22), we arrive at the following *weighted MMSE* problem²²,

$$\begin{aligned} & \underset{\substack{\{\mathbf{V}_{i_k}\}, \{\mathbf{U}_{i_k}\} \\ \{\mathbf{W}_{i_k} \succ \mathbf{0}\}}} \text{minimize} && \log_2(e) \sum_{i \in \mathcal{I}, k \in \mathcal{K}_i} \omega_{i_k} \alpha_{i_k} (\text{Tr}(\mathbf{W}_{i_k} \mathbf{E}_{i_k}(\mathbf{U}_{i_k}, \{\mathbf{V}_{j_l}\})) - \ln \det(\mathbf{W}_{i_k}) - d_{i_k}) \\ & \text{subject to} && \sum_{k \in \mathcal{K}_i} \|\mathbf{V}_{i_k}\|_{\text{F}}^2 \leq P_i, \quad \forall i \in \mathcal{I}, \end{aligned} \quad (2.23)$$

where $\mathbf{E}_{i_k}(\mathbf{U}_{i_k}, \{\mathbf{V}_{j_l}\})$ is given in (2.18) on the preceding page. This optimization problem is still non-convex over the joint set $\{\mathbf{U}_{i_k}, \mathbf{W}_{i_k}, \mathbf{V}_{i_k}\}_{i \in \mathcal{I}, k \in \mathcal{K}_i}$. It is however convex in any block ($\{\mathbf{U}_{i_k}\}_{i \in \mathcal{I}, k \in \mathcal{K}_i}$, $\{\mathbf{W}_{i_k}\}_{i \in \mathcal{I}, k \in \mathcal{K}_i}$ or $\{\mathbf{V}_{i_k}\}_{i \in \mathcal{I}, k \in \mathcal{K}_i}$), when the remaining two blocks are kept fixed. Further, a stationary point can be found through block coordinate descent²³ [Ber06, Chapter 2.7] over the blocks $\{\mathbf{U}_{i_k}\}_{i \in \mathcal{I}, k \in \mathcal{K}_i}$, $\{\mathbf{W}_{i_k}\}_{i \in \mathcal{I}, k \in \mathcal{K}_i}$, and $\{\mathbf{V}_{i_k}\}_{i \in \mathcal{I}, k \in \mathcal{K}_i}$ [SRLH11]. There is a one-to-one correspondence between the stationary points of (2.14) and the stationary points of (2.23) [SRLH11]. As will be shown later, in every iteration the bound in (2.22) is locally tight. Therefore, block coordinate descent of (2.23) will also converge to a stationary point of (2.14) [RHL13a]. Unless started from a local maximum, the WMMSE iterations will converge to a local minimum, since the objective in (2.23) is minimized in each iteration. It can also be shown that the global solutions to (2.14) and the global solutions to (2.23) coincide [SRLH11].

²²Note that the $\log_2(e)$ and d_{i_k} constants can be removed from the objective without changing the optimal solution.

²³This technique is also known as *alternating minimization* or the *block nonlinear Gauss-Seidel* method in the literature.

Distributed Algorithm

The *WMMSE algorithm*, as termed by [SRLH11], follows from applying block coordinate descent to (2.23) over the blocks of variables. Assuming that the nodes have perfect knowledge of their local CSI, the WMMSE algorithm is an example of a distributed resource allocation algorithm [SSB⁺13]. We will deliberate on this fact more in Chapter 6, where we will also discuss how to obtain the local CSI in a distributed fashion.

The first step in the WMMSE algorithm is to find the solution to (2.23) w.r.t $\{\mathbf{U}_{i_k}\}_{i \in \mathcal{I}, k \in \mathcal{K}_i}$, for fixed $\{\mathbf{W}_{i_k}, \mathbf{V}_{i_k}\}_{i \in \mathcal{I}, k \in \mathcal{K}_i}$. It is clear that it suffices to solve

$$\underset{\{\mathbf{U}_{i_k}\}}{\text{minimize}} \quad \sum_{i \in \mathcal{I}, k \in \mathcal{K}_i} \omega_{i_k} \alpha_{i_k} \text{Tr}(\mathbf{W}_{i_k} \mathbf{E}_{i_k}(\mathbf{U}_{i_k}, \{\mathbf{V}_{j_l}\})). \quad (2.24)$$

This problem decouples naturally over the MSs, and since $\mathbf{W}_{i_k} \succ 0$, $\forall i_k$, the solution to the quadratic program for MS i_k is, as in (2.19),

$$\mathbf{U}_{i_k}^* (\{\mathbf{V}_{j_l}\}) = \mathbf{U}_{i_k}^{\text{MMSE}} (\{\mathbf{V}_{j_l}\}) = (\Phi_{i_k}(\{\mathbf{V}_{j_l}\}))^{-1} \mathbf{H}_{i_k i} \mathbf{V}_{i_k}. \quad (2.25)$$

That is, the optimal receive filter is the MMSE receiver. Next, fixing $\{\mathbf{U}_{i_k}, \mathbf{V}_{i_k}\}_{i \in \mathcal{I}, k \in \mathcal{K}_i}$, the problem again decouples over the MSs. For MS i_k , we should solve

$$\underset{\mathbf{W}_{i_k}}{\text{minimize}} \quad \text{Tr}(\mathbf{W}_{i_k} \mathbf{E}_{i_k}(\mathbf{U}_{i_k}, \{\mathbf{V}_{j_l}\})) - \ln \det(\mathbf{W}_{i_k}). \quad (2.26)$$

This corresponds to updating the linearization point of $\ln \det(\mathbf{E}_{i_k})$ and the solution for MS i_k is

$$\mathbf{W}_{i_k}^* (\mathbf{U}_{i_k}, \{\mathbf{V}_{j_l}\}) = \mathbf{E}_{i_k}^{-1} (\mathbf{U}_{i_k}, \{\mathbf{V}_{j_l}\}) = \left(\mathbf{I} - \mathbf{V}_{i_k}^H \mathbf{H}_{i_k}^H (\Phi_{i_k}(\{\mathbf{V}_{j_l}\}))^{-1} \mathbf{H}_{i_k i} \mathbf{V}_{i_k} \right)^{-1}, \quad (2.27)$$

where the last equality comes from plugging in $\mathbf{U}_{i_k}^* = \mathbf{U}_{i_k}^{\text{MMSE}}$ (cf. (2.20) on page 40).

With the new iterates for \mathbf{U}_{i_k} and \mathbf{W}_{i_k} , it remains to solve (2.23) w.r.t $\{\mathbf{V}_{i_k}\}_{i \in \mathcal{I}, k \in \mathcal{K}_i}$ for fixed $\{\mathbf{U}_{i_k}, \mathbf{W}_{i_k}\}_{i \in \mathcal{I}, k \in \mathcal{K}_i}$. Removing terms that are constant w.r.t. \mathbf{V}_{i_k} , this is equivalent to solving

$$\begin{aligned} & \underset{\{\mathbf{V}_{i_k}\}}{\text{minimize}} \quad \sum_{i \in \mathcal{I}, k \in \mathcal{K}_i} \omega_{i_k} \alpha_{i_k} \text{Tr}(\mathbf{W}_{i_k} \mathbf{E}_{i_k}(\mathbf{U}_{i_k}, \{\mathbf{V}_{j_l}\})) \\ & \text{subject to} \quad \sum_{k \in \mathcal{K}_i} \|\mathbf{V}_{i_k}\|_{\text{F}}^2 \leq P_i, \quad \forall i \in \mathcal{I}. \end{aligned} \quad (2.28)$$

By using properties of the trace and dropping constant terms, it can be shown that the following optimization problem is equivalent to (2.28):

$$\begin{aligned} & \underset{\{\mathbf{V}_{i_k}\}}{\text{minimize}} \quad \sum_{i \in \mathcal{I}, k \in \mathcal{K}_i} \text{Tr}(\mathbf{V}_{i_k}^H \mathbf{\Gamma}_i(\{\mathbf{U}_{j_l}, \mathbf{W}_{j_l}\}) \mathbf{V}_{i_k}) - 2\omega_{i_k} \alpha_{i_k} \text{Re}(\text{Tr}(\mathbf{W}_{i_k} \mathbf{U}_{i_k}^H \mathbf{H}_{i_k i} \mathbf{V}_{i_k})) \\ & \text{subject to} \quad \sum_{k \in \mathcal{K}_i} \|\mathbf{V}_{i_k}\|_{\text{F}}^2 \leq P_i, \quad \forall i \in \mathcal{I}. \end{aligned} \quad (2.29)$$

Algorithm 2.1 WMMSE Algorithm [SRLH11]

1: **repeat** *At MS* i_k :2: Find MSE weights: $\mathbf{W}_{i_k} = \mathbf{I} + \mathbf{V}_{i_k}^H \mathbf{H}_{i_k}^H (\Phi_{i_k}^{i+n})^{-1} \mathbf{H}_{i_k} \mathbf{V}_{i_k}$ 3: Find MMSE receive filters: $\mathbf{U}_{i_k} = \Phi_{i_k}^{-1} \mathbf{H}_{i_k} \mathbf{V}_{i_k}$ *At BS* i :4: Find μ_i which satisfies $\sum_{k \in \mathcal{I}} \|\mathbf{V}_{i_k}\|_F^2 \leq P_i$ 5: $\mathbf{V}_{i_k} = \sqrt{\omega_{i_k} \alpha_{i_k}} (\mathbf{\Gamma}_i + \mu_i \mathbf{I})^{-1} \mathbf{H}_{i_k}^H \mathbf{U}_{i_k} \mathbf{W}_{i_k}$, $k \in \mathcal{K}_i$.6: **until** convergence criterion met, or fixed number of iterations

where $\mathbf{\Gamma}_i(\{\mathbf{U}_{j_l}, \mathbf{W}_{j_l}\}) = \sum_{j \in \mathcal{I}, l \in \mathcal{K}_j} \omega_{j_l} \alpha_{j_l} \mathbf{H}_{j_l}^H \mathbf{U}_{j_l} \mathbf{W}_{j_l} \mathbf{U}_{j_l}^H \mathbf{H}_{j_l}$ is a signal-plus-interference covariance matrix for BS i in the uplink. The solution is

$$\mathbf{V}_{i_k}^*(\{\mathbf{U}_{j_l}\}, \mathbf{W}_{i_k}) = \omega_{i_k} \alpha_{i_k} (\mathbf{\Gamma}_i(\{\mathbf{U}_{j_l}, \mathbf{W}_{j_l}\}) + \nu_i^* \mathbf{I})^{-1} \mathbf{H}_{i_k}^H \mathbf{U}_{i_k} \mathbf{W}_{i_k}, \quad \forall i_k, \quad (2.30)$$

where the $\nu_i^* \geq 0$ are the optimal Lagrange multipliers for the I per-BS constraints. If $\nu_i^* = 0$ satisfies the constraint for BS i , the problem is solved. Otherwise, $\nu_i^* > 0$ is found such that $\sum_{k \in \mathcal{K}_i} \|\mathbf{V}_{i_k}^*\|_F^2 = P_i$ is satisfied. This can be done using bisection, since $\sum_{k \in \mathcal{K}_i} \|\mathbf{V}_{i_k}^*\|_F^2$ can be shown to be monotonically decreasing in ν_i^* .

When the precoders $\{\mathbf{V}_{i_k}\}_{i \in \mathcal{I}, k \in \mathcal{K}_i}$ have been found, the iterations start over by solving for $\{\mathbf{U}_{i_k}\}_{i \in \mathcal{I}, k \in \mathcal{K}_i}$ again. With each update of $\{\mathbf{U}_{i_k}\}_{i \in \mathcal{I}, k \in \mathcal{K}_i}$, $\{\mathbf{W}_{i_k}\}_{i \in \mathcal{I}, k \in \mathcal{K}_i}$ and $\{\mathbf{V}_{i_k}\}_{i \in \mathcal{I}, k \in \mathcal{K}_i}$, the objective value of (2.23) cannot increase. Since the objective value in (2.23) can be bounded, the objective value therefore converges monotonically. Unless started from a local maximum, the algorithm will find a local minimum, since it minimizes the objective function in every iteration. The convergence was shown for the per-BS sum power constraint in [SRLH11], but the convergence for the general case is a straightforward generalization that can be shown using e.g. [Ber06, Prop. 2.7.1], [RHL13a] or [GS00].

We summarize the WMMSE algorithm in Algorithm 2.1.

Remark 2.3. *In this section, we explicitly wrote out all dependencies of all variables for clarity. In the contributions chapters however, we will instead focus on brevity, meaning that all dependencies may not be explicitly stated. We hope that any dependencies will be clear from the context however.*

Part I

Base Station Clustering

Optimal Base Station Clustering

As described in Section 2.1.3, one of the stages of the system operation involves forming disjoint clusters of the BSs. This is due to the CSI acquisition overhead and general complexity of coordinating a large number of BSs. In a clustered multicell network, direct coordination only occurs within the clusters whereas interference between the clusters is not directly handled.

Given the need for clustering, the question on how to design the clusters arises. In this chapter, we provide a structured approach for finding the *optimal* clustering. The complexity of the solution algorithm will be high, and thus the main purpose of the method is to act as a benchmark for other, more practical, clustering schemes. One such scheme is presented in Chapter 4, where coalitional game theory is used to develop a distributed heuristic for the clustering.

3.1 General Throughput Model

As described in Section 2.1.3, the clustering takes place on a long-term time scale, and it only depends on the CSI statistics of the network. Thus, in order to formulate the clustering optimization problem, we need to define a performance metric as a function of the available CSI statistics. In this chapter, we propose a general model which is able to describe a family of long-term throughput functions. The branch and bound algorithm to be developed can operate on any specific throughput model which adheres to the requirements of the general throughput model. One such specific throughput model is derived in Chapter 4.

3.1.1 Model Assumptions

For tractability, in this chapter we consider a symmetric¹ multicell network where the I BSs each serve K MSs in the downlink. BS i allocates a power of P_{i_k} to

¹Recall that in a symmetric network, the BSs each have M antennas, the MSs each have N antennas and each MS is served d spatial data streams.

MS i_k , in total using a power of $P_i = \sum_{k=1}^K P_{i_k}$. Further, recall that MS i_k has a thermal noise power of $\sigma_{i_k}^2$ and that the average large-scale fading between BS j and MS i_k is $\gamma_{i_k j}$.

We assume that IA is used to completely cancel the intracluster interference.² Within each cluster, both intracell as well as intercell interference is therefore cancelled. This is reflected in the long-term SINRs of the MSs:

Assumption 3.1 (Long-term SINR). *Intracluster IA is used to cancel all interference within the clusters. The long-term SINR of MS i_k , $\rho_{i_k} : 2^{\mathcal{I}} \rightarrow \mathbb{R}_+$, is then*

$$\rho_{i_k}(\mathcal{S}(i)) = \frac{\gamma_{i_k i} P_{i_k}}{\sigma_{i_k}^2 + \sum_{j \in \mathcal{I} \setminus \mathcal{S}(i)} \gamma_{i_k j} P_j}, \quad (3.1)$$

where $\mathcal{S}(i)$ is defined in Definition 2.1 on page 18.

Our general throughput model assumes that the long-term MS throughputs only depend on the long-term SINR and the size of the cluster which the serving BS is a member of. The rationale behind this assumption is that the long-term SINR determines the rate, whereas the cluster size determines the CSI acquisition overhead. Mathematically, we formalize these assumptions as follows:

Assumption 3.2 (Long-term throughput). *For a cluster size $|\mathcal{S}(i)|$ and a long-term SINR $\rho_{i_k}(\mathcal{S}(i))$, the throughput of MS i_k is given by*

$$\bar{t}_{i_k}(\mathcal{S}) = v_{i_k}(|\mathcal{S}(i)|, \rho_{i_k}(\mathcal{S}(i))), \quad (3.2)$$

where the function $v_{i_k} : \mathbb{N} \times \mathbb{R}_+ \rightarrow \mathbb{R}_+$ is unimodal in its first argument and non-decreasing in its second argument.

The unimodality of the first argument models the effect from the cluster size to the pre-log factor, whereas the non-decreasingness in the second argument models the effect from the long-term SINR to the long-term rate. The monotonicity properties of $v_{i_k}(\cdot, \cdot)$ and the structure of $\rho_{i_k}(\cdot)$ will be used in the throughput bound to be derived in Theorem 3.1.

Remark 3.1. *In our model, any fixed power levels can be used, e.g. obtained from some single-cell power allocation method [BJ13, Chapter 1.2]. Generalizing to adaptive multicell power allocation would however lead to loss of tractability in the SINR bound of Theorem 3.1, due to $\rho_{i_k}(\cdot)$ not being supermodular [McC05] when the powers are adaptive.*

3.1.2 Existing Models Satisfying the Assumptions

The proposed throughput model is quite general and is compatible with several existing specific throughput models:

²The corresponding IA feasibility constraint is modelled in the optimization problem in (3.10).

Example 3.1 (Intercluster time sharing with CSI acquisition overhead). In [PH12], the clusters are orthogonalized using time sharing, and no intercluster interference is thus received. Each BS owns $1/I$ of the coherence time L_c , which is contributed to the corresponding cluster. Larger clusters give more time for data transmission but also require more CSI acquisition overhead, which in [PH12] is modelled as a quadratic function, giving the throughput model as:

$$v_{i_k}(|\mathcal{S}(i)|, \cdot) = \left(\frac{|\mathcal{S}(i)|}{I} - \frac{|\mathcal{S}(i)|^2}{L_c} \right) d \log_2(1 + \varrho_{i_k}), \quad (3.3)$$

where

$$\varrho_{i_k} = \frac{\gamma_{i_k i} P_{i_k}}{\sigma_{i_k}^2} \quad (3.4)$$

is the constant long-term SNR. The function in (3.3) is strictly unimodal in its first argument and independent of its second argument, thus satisfying Assumption 3.2.

Example 3.2 (Intercluster spectrum sharing without CSI acquisition overhead). In [CC14], the clusters are operating using spectrum sharing and the CSI acquisition overhead is not accounted for. A slightly modified³ version of their throughput model is then:

$$v_{i_k}(\cdot, \rho_{i_k}(\mathcal{S}(i))) = d \log_2(1 + \rho_{i_k}(\mathcal{S}(i))). \quad (3.5)$$

The function in (3.5) is independent of its first argument, and strictly increasing in its second argument, thus satisfying Assumption 3.2.

Example 3.3 (Intercluster time sharing/spectrum sharing with CSI acquisition overhead). In Chapter 4, intercluster time sharing and intercluster spectrum sharing are used in two different orthogonal phases.⁴ For the CSI acquisition overhead model during the time sharing phase, a model similar to the one in [PH12] is used. For the achievable rates during the spectrum sharing phase, long-term averages are derived involving an exponential integral. The model is thus

$$v_{i_k}(|\mathcal{S}(i)|, \rho_{i_k}(\mathcal{S}(i))) = \alpha_{i_k}^{(1)}(|\mathcal{S}(i)|) \bar{r}_{i_k}^{(1)} + \bar{r}_{i_k}^{(2)}(\rho_{i_k}(\mathcal{S}(i))) \quad (3.6)$$

where

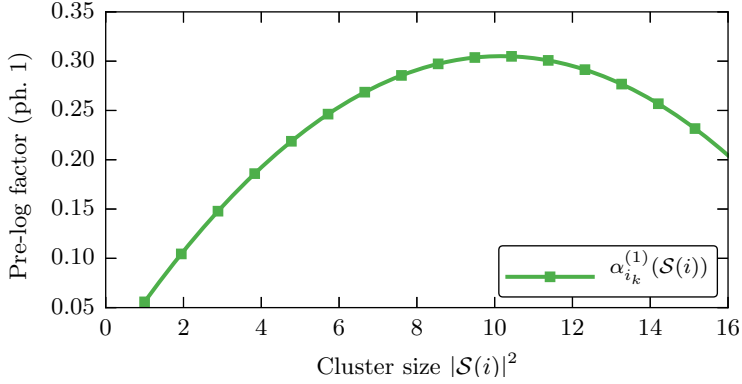
$$\alpha_{i_k}^{(1)}(|\mathcal{S}(i)|) = \frac{|\mathcal{S}(i)|}{I} - \frac{(M + K(N + d)) |\mathcal{S}(i)| + KM |\mathcal{S}(i)|^2}{L_c}, \quad (3.7)$$

$$\bar{r}_{i_k}^{(1)} = d e^{1/\varrho_{i_k}} \int_{1/\varrho_{i_k}}^{\infty} t^{-1} e^{-t} dt, \quad (3.8)$$

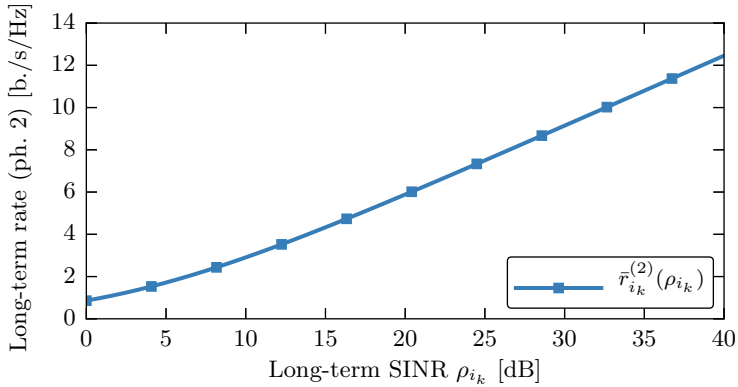
$$\bar{r}_{i_k}^{(2)}(\rho_{i_k}(\mathcal{S}(i))) = d e^{1/\rho_{i_k}(\mathcal{S}(i))} \int_{1/\rho_{i_k}(\mathcal{S}(i))}^{\infty} t^{-1} e^{-t} dt. \quad (3.9)$$

³The original SINR model in [CC14] includes the impact of the instantaneous IA filters, which we neglect here in order to avoid the cross-dependence between the IA solution and the clustering. This corresponds to how the approximated interference graph weights are derived in [CC14].

⁴The full derivations of this model can be found in Section 4.2.



(a) Pre-log factor in phase 1



(b) Long-term rate in phase 2

Figure 3.1. Visualization of the long-term throughput model in Example 3.3. We plot the pre-log factor in phase 1 and the long-term rate in phase 2 for a system with $I = 16$ BSs, each serving $K = 2$ MSs. The BSs had $M = 4$ antennas, the MSs had $N = 2$ antennas and were served $d = 1$ data streams each. We let $L_c = 2700$, corresponding to an MS speed of 30 km/h at a carrier frequency of 2 GHz and coherence bandwidth of 300 kHz [JL10].

The function in (3.6) is strictly unimodal in its first argument and strictly increasing in its second argument, thus satisfying Assumption 3.2. We visualize this model in Figure 3.1 on the facing page.

Given the long-term throughput model, the system-level objective is:

Definition 3.1 (Objective). *The long-term performance of the entire multicell system is given by $f(\mathcal{S}) = g(t_{1_1}(\mathcal{S}), \dots, t_{I_K}(\mathcal{S}))$, where $g: \mathbb{R}_+^{I \cdot K} \rightarrow \mathbb{R}_+$ is an argument-wise non-decreasing function.*

The function $f(\mathcal{S})$ maps a set partition to the corresponding system-level objective. Typical examples of supported objective functions are the weighted sum $f_{\text{WSR}}(\mathcal{S}) = \sum_{(i,k)} \omega_{i_k} \bar{t}_{i_k}(\mathcal{S})$ and the minimum weighted throughput $f_{\text{min}}(\mathcal{S}) = \min_{(i,k)} \omega_{i_k} \bar{t}_{i_k}(\mathcal{S})$.

3.2 Branch and Bound

The optimal base station clustering \mathcal{S}^* is now described by the solution to the following combinatorial optimization problem:

$$\begin{aligned} \mathcal{S}^* &= \arg \max_{\mathcal{S}} f(\mathcal{S}) \\ &\text{subject to } \mathcal{S} \text{ satisfying Definition 2.1} \\ &|\mathcal{S}(i)| \leq D, \forall i \in \mathcal{I}. \end{aligned} \tag{3.10}$$

The cardinality constraint is used to model cluster size constraints due to IA feasibility (see Section 2.2.3), CSI acquisition feasibility (see Definition 4.3 on page 66), implementation feasibility, etc.

3.2.1 Restricted Growth Strings and Exhaustive Search

In order to succinctly describe a set partition in the algorithm to be proposed, we will use the following alternate representation:

Definition 3.2 (Restricted growth string, [Knu11, Section 7.2.1.5]). *A set partition \mathcal{S} can equivalently be expressed using a restricted growth string $a = a_1 a_2 \dots a_I$ with the property that $a_i \leq 1 + \max(a_1, \dots, a_{i-1})$ for $i \in \mathcal{I}$. Then $a_i \in \mathbb{N}$ describes which cluster cell i belongs to. We let \mathcal{S}_a denote the mapping from a to the set partition \mathcal{S} , and $a_{\mathcal{S}}$ as its inverse.*

For example, the set partition $\mathcal{S}_a = \{\{1, 3\}, \{2\}, \{4\}\}$ would be encoded as $a_{\mathcal{S}} = 1213$.

One approach to solve the optimization problem in (3.10) is now by enumerating all restricted growth strings of length I , using e.g. Algorithm H of [Knu11,

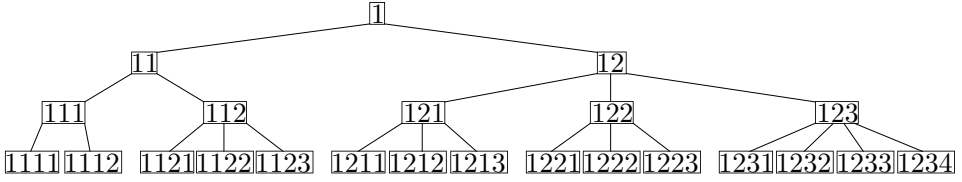


Figure 3.2. Example of branch and bound partial solution tree for $I = 4$.

Section 7.2.1.5]. The complexity of this approach is however \mathbb{B}_I , the I th Bell number,⁵ which grows super-exponentially.

3.2.2 Branch and Bound Algorithm

Most of the possible set partitions are typically not interesting in the sense of the objective of (3.10) however. For example, most set partitions will include clusters whose member cells are placed far apart, thus leading to low long-term SINRs of their correspondingly served MSs. By prioritizing set partitions with a potential to achieve large throughputs, the complexity of finding the optimal set partition can be decreased significantly compared to that of exhaustive search. This is the idea of the branch and bound approach [LD60], which entails bounding the optimal value $f(\mathcal{S}^*)$ from above and below for a sequence of *partial solutions*. When the bounds converge, the optimal solution has been found. The partial solutions are described using *partial restricted growth strings*:

Definition 3.3 (Partial restricted growth string). *The restricted growth string $\bar{a} = \bar{a}_1\bar{a}_2\dots\bar{a}_l$ is partial if $l = \text{LENGTH}(\bar{a}) \leq I$. The corresponding partial set partition, where only the first l cells are constrained into clusters, is denoted $\mathcal{S}_{\bar{a}}$.*

The branch and bound method considers the sequence of partial solutions by dynamically exploring a partial solution tree (see Figure 3.2, at the top of the page), in which each interior node corresponds to a partial restricted growth string. By starting at the root and traversing down the partial solution tree,⁶ more cells are constrained into clusters, ultimately giving the leaves of the tree which describe all possible (non-partial) restricted growth strings.

Bounds

We now provide the bounds that will be used to avoid exploring large parts of the partial solution tree.

⁵The I th Bell number describes the number of set partitions of \mathcal{I} [Bru09, p. 287], and can be bounded as $\mathbb{B}_I < (0.792I/\ln(1+I))^I$ [BT10]. The 16 first Bell numbers are 1, 1, 2, 5, 15, 52, 203, 877, 4140, 21147, 115975, 678570, 4213597, 27644437, 190899322, 1382958545.

⁶At level $i \leq I$ of the tree, there are \mathbb{B}_i nodes.

Lemma 3.1 (Objective bound). *Let $\check{t}_{i_k}(\mathcal{S}_{\bar{a}})$ be an upper bound of the long-term throughput of MS i_k for all leaf nodes in the sub-tree below the node described by \bar{a} . Then the function*

$$\check{f}(\mathcal{S}_{\bar{a}}) = g(\check{t}_{1_1}(\mathcal{S}_{\bar{a}}), \dots, \check{t}_{I_K}(\mathcal{S}_{\bar{a}})) \quad (3.11)$$

is an upper bound of the objective in (3.10) for all leaves in the sub-tree below the node described by \bar{a} .

Proof: This follows directly from the argument-wise monotonicity of $g(t_{1_1}, \dots, t_{I_K})$ in Definition 3.1 on page 51. ■

Given a node described by \bar{a} , we now introduce the following three sets:

$$\mathcal{P}_{\bar{a}} = \{1, \dots, \text{LENGTH}(\bar{a})\} \subseteq \mathcal{I}, \quad (3.12)$$

$$\mathcal{P}_{\bar{a}}^\perp = \mathcal{I} \setminus \mathcal{P}_{\bar{a}}, \quad (3.13)$$

$$\mathcal{F}_{\bar{a}} = \{i \in \mathcal{P}_{\bar{a}} : |\mathcal{S}_{\bar{a}}(i)| < D\} \cup \mathcal{P}_{\bar{a}}^\perp. \quad (3.14)$$

The set $\mathcal{P}_{\bar{a}}$ describes the cells which are constrained into clusters as given by $\mathcal{S}_{\bar{a}}$. The complement set $\mathcal{P}_{\bar{a}}^\perp$ describe the remaining cells which are still unconstrained.⁷ Finally, the set $\mathcal{F}_{\bar{a}}$ describes the set of cells which could accommodate more members in the corresponding clusters.⁸ Our proposed throughput bound then follows as:

Theorem 3.1 (Throughput bound). *Let $\bar{t}_{i_k}(\mathcal{S}_a(i))$ be the long-term throughput of MS i_k for some leaf node in the sub-tree below the node described by \bar{a} . It can be bounded as*

$$\bar{t}_{i_k}(\mathcal{S}_a) = v_{i_k}(|\mathcal{S}_a(i)|, \rho_{i_k}(\mathcal{S}_a(i))) \leq v_{i_k}(\check{B}_{i_k}, \check{\rho}_{i_k}) \quad (3.15)$$

where

$$\begin{aligned} \check{\rho}_{i_k} &= \underset{|\mathcal{E}_{i_k}| \leq D}{\text{maximize}} && \rho_{i_k}(\mathcal{E}_{i_k}) \\ &\text{subject to} && \text{if } i \in \mathcal{P}_{\bar{a}}: \\ &&& \mathcal{S}_{\bar{a}}(i) \subseteq \mathcal{E}_{i_k} \subseteq (\mathcal{S}_{\bar{a}}(i) \cup \mathcal{P}_{\bar{a}}^\perp) \\ &&& \text{else if } i \in \mathcal{P}_{\bar{a}}^\perp: \\ &&& \{i\} \subseteq \mathcal{E}_{i_k} \subseteq \mathcal{F}_{\bar{a}} \end{aligned} \quad (3.16)$$

and

$$B_{i_k}^* = \arg \max_{b \in \mathbb{N}, b \leq D} \bar{t}_{i_k}(b, \check{\rho}_{i_k}), \quad (3.17)$$

$$\check{B}_{i_k} = \begin{cases} |\mathcal{S}_{\bar{a}}(i)| & \text{if } |\mathcal{S}_{\bar{a}}(i)| \geq B_{i_k}^*, \\ \min(|\mathcal{S}_{\bar{a}}(i)| + |\mathcal{P}_{\bar{a}}^\perp|, B_{i_k}^*) & \text{else if } i \in \mathcal{P}_{\bar{a}}, \\ \min(|\mathcal{F}_{\bar{a}}|, B_{i_k}^*) & \text{else if } i \in \mathcal{P}_{\bar{a}}^\perp. \end{cases} \quad (3.18)$$

⁷In the sub-tree below the node described by \bar{a} , there is a leaf node for all possible ways of constraining the cells in $\mathcal{P}_{\bar{a}}^\perp$ into clusters.

⁸For the sake of this definition, we consider the non-constrained cells in $\mathcal{P}_{\bar{a}}^\perp$ to be in singleton clusters.

Proof: First note that $\check{\rho}_{i_k}$ is an upper bound of the achievable long-term SINR for MS i_k in the considered sub-tree, since the requirement of disjoint clusters is not enforced in the optimization problems.⁹ We therefore have that

$$v_{i_k}(|\mathcal{S}_a(i)|, \rho_{i_k}(\mathcal{S}_a(i))) \leq v_{i_k}(|\mathcal{S}_a(i)|, \check{\rho}_{i_k}), \quad (3.19)$$

due to the monotonicity property of $v_{i_k}(\cdot, \cdot)$. Now the fact that

$$v_{i_k}(|\mathcal{S}_a(i)|, \check{\rho}_{i_k}) \leq v_{i_k}(\check{B}_{i_k}, \check{\rho}_{i_k}) \quad (3.20)$$

holds is proven. Note that $B_{i_k}^*$ is the optimal size of the cluster, in terms of the first parameter of $v_{i_k}(\cdot, \check{\rho}_{i_k})$. If $|\mathcal{S}_{\bar{a}}(i)| \geq B_{i_k}^*$, the cluster is already larger than what is optimal, and keeping the size is thus a bound for all leaves in the sub-tree. On the other hand, if $|\mathcal{S}_{\bar{a}}(i)| < B_{i_k}^*$ and $i \in \mathcal{P}_{\bar{a}}$, \check{B}_{i_k} is selected as close to $B_{i_k}^*$ as possible, given the number of unconstrained cells that could conceivably be constrained into $\mathcal{S}_{\bar{a}}(i)$ further down in the sub-tree. If $i \in \mathcal{P}_{\bar{a}}^\perp$ however, we similarly bound \check{B}_{i_k} , except that we only consider cells in non-full clusters for cell i to conceivably be constrained to further down in the sub-tree. Due to the unimodality property of $v_{i_k}(\cdot, \check{\rho}_{i_k})$ and the fact that \check{B}_{i_k} is selected optimistically, we have that

$$v_{i_k}(|\mathcal{S}_a(i)|, \check{\rho}_{i_k}) \leq v_{i_k}(\check{B}_{i_k}, \check{\rho}_{i_k}), \quad (3.21)$$

which gives the bound. ■

As the algorithm explores nodes deeper in the partial solution tree, $\text{LENGTH}(\bar{a})$ gets closer to I , and there is less freedom in the bounds. For $\text{LENGTH}(\bar{a}) = I$, the bounds are tight.

Algorithm

The proposed branch and bound method is described in Algorithm 3.1 on the next page. The algorithm starts by getting an initial incumbent solution from a heuristic (e.g. from Algorithm 3.2 on page 56, Algorithm 4.1 on page 73, or from [PH12, CC14]), and then sequentially studies the sub-tree which currently has the highest upper bound.¹⁰ By comparing the upper bound $\check{f}(\mathcal{S}_{\bar{a}})$ to the currently best lower bound $f(\mathcal{S}_{a_{\text{incumbent}}}) \leq f(\mathcal{S}^*)$, the *incumbent solution*, the sub-tree below \bar{a} can be *pruned* if it provably cannot contain the optimal solution, i.e. if $\check{f}(\mathcal{S}_{\bar{a}}) < f(\mathcal{S}_{a_{\text{incumbent}}})$. If a node \bar{a} cannot be pruned, all children of \bar{a} are built by a branching function and stored in a list for future exploration by the algorithm. If large parts of the partial solution tree can be pruned, few nodes

⁹The optimal solution to the optimization problem in (3.16) can be found by minimizing the denominator of $\rho_{i_k}(\mathcal{E}_{i_k})$ in (3.1), which is easily done using greedy search over the feasible set. The set-function $\rho_{i_k}(\mathcal{E}_{i_k})$ is *supermodular* [McC05], i.e. demonstrating “increasing returns”, which is the structure that admits the simple solution of the optimization problem. Without changes, Theorem 3.1 would indeed hold for any other supermodular set-function $\rho_{i_k}(\mathcal{E}_{i_k})$.

¹⁰This graph traversal strategy is called *best first search*. Other traversal strategies, such as *depth first search*, can also be applied without altering the convergence result in Theorem 3.2.

Algorithm 3.1 Branch and Bound Algorithm for Base Station Clustering

Input: Initial $a_{\text{incumbent}}$ from some heuristic, $\epsilon \geq 0$

```

1: live  $\leftarrow [1]$ 
2: while LENGTH(live) > 0 do
3:    $\bar{a}_{\text{parent}} \leftarrow$  node from live with highest upper bound
4:   if  $\check{f}(\mathcal{S}_{\bar{a}_{\text{parent}}}) - f(\mathcal{S}_{a_{\text{incumbent}}}) < \epsilon$  then go to line 15 end if
5:   for all  $a_{\text{child}}$  from BRANCH( $\bar{a}_{\text{parent}}$ ) do
6:     if  $\check{f}(\mathcal{S}_{\bar{a}_{\text{child}}}) > f(\mathcal{S}_{a_{\text{incumbent}}})$  then
7:       if LENGTH( $\bar{a}_{\text{child}}$ ) =  $I$  then
8:          $a_{\text{incumbent}} \leftarrow \bar{a}_{\text{child}}$ 
9:       else
10:        Append  $\bar{a}_{\text{child}}$  to live
11:      end if
12:    end if
13:  end for
14: end while
15: return optimal  $a_{\text{optimal}} = a_{\text{incumbent}}$ 

```

```

1: function BRANCH( $\bar{a}_{\text{parent}}$ )
2:   Initialize empty list children = []
3:   for  $b = 1 : (1 + \max(\bar{a}_{\text{parent}}))$  do
4:     Append  $[\bar{a}_{\text{parent}}, b]$  to children
5:   end for
6:   return children
7: end function

```

need to be explicitly explored, leading to a complexity reduction. The algorithm ends when the optimality gap for the current incumbent solution is less than a pre-defined $\epsilon \geq 0$.

Theorem 3.2. *Algorithm 3.1 converges to an ϵ -optimal solution of the optimization problem in (3.10) in at most $\sum_{i=1}^I \mathbb{B}_i$ iterations.*

Proof: Only sub-trees in which the optimal solution cannot be are pruned. Since all non-pruned leaves are explored, the global optimum will be found. No more than all $\sum_{i=1}^I \mathbb{B}_I$ nodes of the partial solution tree can be traversed. ■

In Section 3.3 we empirically show that the average complexity is significantly lower than the worst case.

3.2.3 Heuristic Base Station Clustering

In order to obtain the initial incumbent to be used in Algorithm 3.1, we now propose a heuristic base station clustering algorithm. We heuristically let the con-

Algorithm 3.2 Heuristic for Base Station Clustering

Input: $\mathcal{L} = \{(i, j) \in \mathcal{I} \times \mathcal{I} \mid i \neq j\}$, $\mathcal{S} = \{\{1\}, \dots, \{I\}\}$

- 1: **while** $|\mathcal{L}| > 0$ **do**
- 2: $(i^*, j^*) = \arg \max_{(i,j) \in \mathcal{L}} \sum_{k=1}^K \log_2 (1 + \gamma_{i_k j} P_j / \sigma_{i_k}^2)$
- 3: Let $\Xi_{(i^*, j^*)} \leftarrow \mathcal{S}(i^*) \cup \mathcal{S}(j^*)$
- 4: **if** $|\Xi_{(i^*, j^*)}| \leq D$ **then**
- 5: Let $\mathcal{S} \leftarrow (\mathcal{S} \setminus \{\mathcal{S}(i^*), \mathcal{S}(j^*)\}) \cup \{\Xi_{(i^*, j^*)}\}$
- 6: **end if**
- 7: Let $\mathcal{L} \leftarrow \mathcal{L} \setminus \{(i^*, j^*)\}$
- 8: **end while**
- 9: **return** heuristic solution $a_{\text{heuristic}} = a_{\mathcal{S}}$

stant $\log_2 (1 + \gamma_{i_k j} P_j / \sigma_{i_k}^2)$ describe the value of MS i_k being part of the same cluster as BS j . Then by summing over all MSs in cell i , the constant

$$\sum_{k=1}^K \log_2 \left(1 + \frac{\gamma_{i_k j} P_j}{\sigma_{i_k}^2} \right) \quad (3.22)$$

describes the value of BS j joining the cluster of BS i .¹¹ The heuristic algorithm then greedily maximizes the sum of these values, while respecting the cluster size constraint.

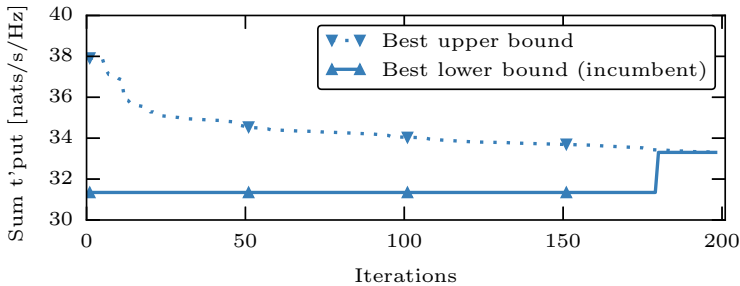
The resulting algorithm is described in Algorithm 3.2. Since the cell-pair values in (3.22) are constant, these can be computed in a preprocessing step and stored in an array. By further sorting the array, the operation on row 2 in Algorithm 3.2 can then be implemented using a simple linear search during the online phase of the algorithm. This heuristic is similar to the hierarchical clustering in Ward's method [War63].

3.3 Performance Evaluation

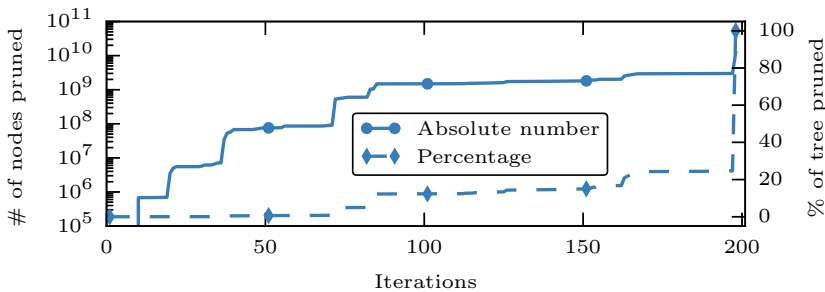
For the numerical performance evaluation, we consider a network of $I = 16$ BSs, $K = 2$ MSs per cell, and $d = 1$ data streams per MS. We employ the long-term throughput model from Chapter 4 (see Example 3.3 on page 49) and use the unweighted sum throughput $f(\mathcal{S}) = \sum_{(i,k)} \bar{t}_{i_k}(\mathcal{S})$ as the system-level objective. We let the number of antennas be $M = 8$ and $N = 2$. This gives a hard size constraint as $D = 4$ cells per cluster, due to IA feasibility [LY13].

We consider a large-scale setting with path loss $15.3 + 37.6 \log_{10}(\text{distance [m]})$, i.i.d. log-normal shadow fading with 8 dB standard deviation, and i.i.d. $\mathcal{CN}(0, 1)$ small-scale fading. The BSs are randomly dropped in a $2000 \times 2000 \text{ m}^2$ square and

¹¹Although this constant has the same form as a sum rate, it should just be thought of as a heuristic way of transforming the normalized interference levels (i.e. $\gamma_{i_k j} P_j / \sigma_{i_k}^2$ in this case) into a form which makes sense to sum over the MSs in a single cell.



(a) Example of convergence of the algorithm for one realization.



(b) Pruning evolution for the realization in Figure 3.3a.

Figure 3.3. Evolution of algorithm quantities for a single realization.

the BS-MS distance is 250 m. We let $L_c = 2700$, corresponding to an MS speed of 30 km/h at a carrier frequency of 2 GHz and a coherence bandwidth of 300 kHz.

Convergence

In Figure 3.3a, we show the convergence of the best upper bound and the incumbent solution, respectively, for one network realization with $\text{SNR} = P_{i_k}/\sigma_{i_k}^2 = 20$ dB. The number of iterations needed was 198 and a total of 908 nodes were bounded. Naive exhaustive search would have needed exploring $\mathbb{B}_{16} = 10480109379$ nodes, and the proposed algorithm was thus around $1 \cdot 10^7$ times more efficient for this realization. Also note that $\sum_{i=1}^{16} \mathbb{B}_i = 12086679035$, i.e. the actual running time of the algorithm was significantly lower than the worst-case running time.

The number and fraction of nodes pruned during the iterations is shown in Figure 3.3b. At convergence, 99.9999% of the partial solution tree had been pruned.

Complexity

In Figure 3.4 on the following page, we show the average number of iterations as a function of the network size. The average complexity of the proposed algorithm is

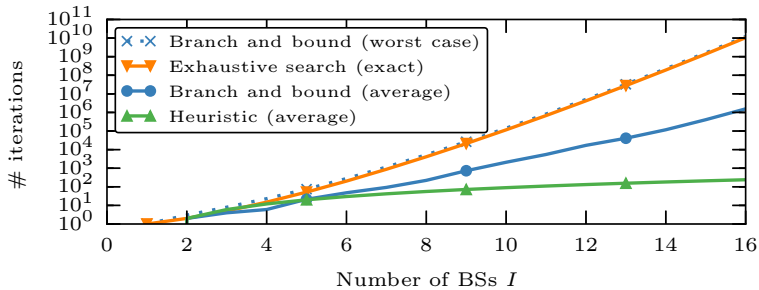


Figure 3.4. Average complexity as a function of I .

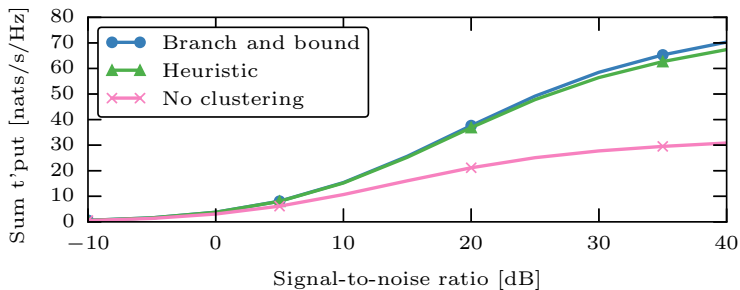


Figure 3.5. Sum throughput performance as a function of SNR.

orders of magnitude lower than the corresponding worst-case complexity. It is also orders of magnitude lower than the complexity of naive exhaustive search.

Sum Throughput

In Figure 3.5, we show the sum throughput performance as a function of SNR, averaged over 250 network realizations. The heuristic algorithm performs well: up to a doubling of throughput is seen compared to the case of no clustering, where $\mathcal{S} = \{\{1\}, \dots, \{I\}\}$. The grand cluster $\mathcal{S} = \{\mathcal{I}\}$ has zero sum throughput since $I > D$, and is therefore not shown.

3.4 Conclusions

Using a structured branch and bound approach, we have solved the base station clustering problem to optimality. The algorithm is mainly intended for benchmarking intermediate sized networks, and it is significantly faster than the naive exhaustive search.

Distributed Base Station Clustering

With the results from Chapter 3, we now have an algorithm for finding the optimal base station clustering. Although efficient compared to exhaustive search, the complexity of this centralized algorithm is however still much too high for practical implementation. In this chapter, we therefore aim to design a low complexity distributed algorithm for base station clustering. For this, we will use the perspective of coalitional games [SHD⁺09].

We will first derive a specific long-term throughput model¹ for the MSs in the clustered network. We then model the cells as rational players in a hedonic coalitional game [DG80], where the utilities of the players are given by the derived long-term throughput model together with two additional concepts: a stabilizing history set [SHZ⁺12] and a deviation search budget [MBB15]. By allowing for individual deviations, where a player leaves its current coalition to join another coalition, we provide a distributed coalition formation algorithm with low complexity and low communication overhead. The algorithm is shown to reach an individually stable [BJ02] coalition structure, and empirical evidence shows that this is done within just a few deviation searches per player.

For consistency with the game theory literature, in this chapter we will refer to a cluster as a *coalition* and the set of clusters (i.e. a set partition, see Definition 2.1 on page 18) as the *coalition structure* [DG80]. A schematic example of a coalition structure is given in Figure 4.1 on the following page.

4.1 Frame Structure

The specific long-term throughput model to be derived assumes that the system operates over two time scales: the long term and the short term.

¹A sneak preview of this model has already been presented in Example 3.3 on page 49.

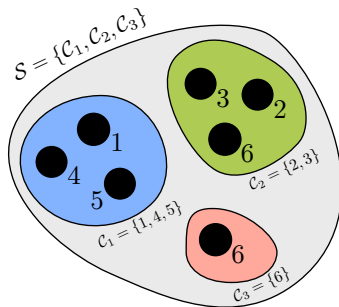


Figure 4.1. Example of a coalition structure \mathcal{S} when $\mathcal{I} = \{1, 2, 3, 4, 5, 6\}$. The BSs are represented by the black dots, and the coalitions are represented by the coloured areas.

4.1.1 Long Term

The long-term time scale is determined by the coherence time of the CSI statistics (i.e. $\{\gamma_{i,k,j}\}_{i \in \mathcal{I}, k \in \mathcal{K}_i, j \in \mathcal{I}}$), which is dominated by large-scale factors such as path loss and shadowing (see Section 2.1.2). We assume that all MSs can estimate their local CSI statistics (i.e. $\{\gamma_{i,k,j}\}_{j \in \mathcal{I}}$ for MS i_k) without any associated cost, and that the feedback of this information to the serving BS also is cost-free. When the CSI statistics have been acquired at the BSs, coalition formation is performed (see Section 2.1.3).

4.1.2 Short Term

The short-term time scale is determined by the coherence time of the CSI (i.e. $\{\mathbf{H}_{i,k,j}\}_{i \in \mathcal{I}, k \in \mathcal{K}_i, j \in \mathcal{I}}$), which is dominated by the small-scale fading. This coherence time is denoted L_c , and we call this a *coherence block* (see Section 2.1.2). In each coherence block, the CSI is perfectly estimated at the MSs through pilot transmissions from the BSs such that $\{\mathbf{H}_{i,k,j}\}_{j \in \mathcal{I}}$ is obtained by MS i_k . MS i_k then feeds back $\{\mathbf{H}_{i,k,j}\}_{j \in \mathcal{S}(i)}$ to its serving BS i , which in its turn shares the information over the backhaul network with the BSs in its coalition $\mathcal{S}(i)$. Using the acquired intra-coalition CSI, precoder optimization is performed independently by the coalitions. A final training stage is then performed, where the MSs estimate their effective channels² from all the BSs, thus allowing them to form a receive filter accounting for the effective intercoalition interference.

At the end of a coherence block, the CSI changes abruptly and must be estimated again. A schematic of the system operation (cf. Section 2.1.3) can be seen in Figure 4.2 on the next page. For clarity, we summarize how the CSI is shared within each coalition in the following definition.

²An effective channel is a channel multiplied by a precoder, e.g. $\mathbf{H}_{i,k,j} \mathbf{V}_{j_l}$.

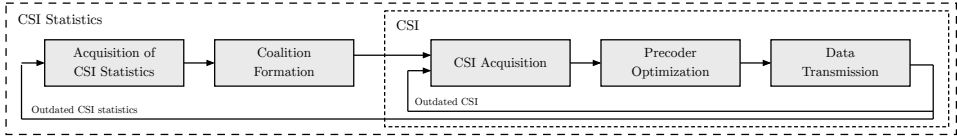


Figure 4.2. Block diagram of proposed system. Note that the acquisition of the CSI statistics does not necessarily need to be a discrete block, but could be performed concurrently with the other system operation. As a rough approximation for intermediate MS mobility, the CSI statistics must be re-estimated on the order of seconds, whereas the actual CSI must be re-estimated on the order of milliseconds.

Definition 4.1 (Intracoalition CSI Sharing). *The cells in a coalition \mathcal{C}_s share their local intracoalition CSI over the backhaul, such that all cells in \mathcal{C}_s have access to $\{\mathbf{H}_{i_k j}\}_{i \in \mathcal{C}_s, k \in \mathcal{K}_i, j \in \mathcal{C}_s}$. The cells in \mathcal{C}_s also have access to the full intercoalition and intracoalition CSI statistics, i.e. $\{\gamma_{i_k j}\}_{i \in \mathcal{C}_s, k \in \mathcal{K}_i, j \in \mathcal{I}}$.*

We assume that the channel training is performed orthogonally over all cells. This is to ensure that the MSs can estimate their channels with high quality. However, this puts a cap on the size of networks which can be supported; for sufficiently large networks the entire coherence time would be consumed by CSI acquisition (see e.g. [LHA13]). For very large networks, the techniques proposed herein could however be extended by combining them with frequency reuse techniques.

4.1.3 Management of Intercoalition Interference

Given a coalition structure, the *intracoalition* interference can be spatially mitigated since the intracoalition CSI is available to all members of the coalition (cf. Definition 4.1). The *intercoalition* interference cannot be spatially mitigated however, due to the lack of intercoalition CSI. We therefore propose two phases, in which this spatially unmitigated interference will be handled differently.

Phase 1: Time Sharing

In phase 1, the coalitions are temporally separated (cf. [PH12]), such that no intercoalition interference is received between coalitions. With this approach, the rate is high but the temporal resources are not used maximally.

Phase 2: Spectrum Sharing

In phase 2, the coalitions are spatially separated (cf. [CC14]), such that—ideally—only distant BSs contribute unmitigated intercoalition interference. With this approach, the rate is lower than in phase 1 due to the unmitigated intercoalition interference, but the temporal resources are maximally used.

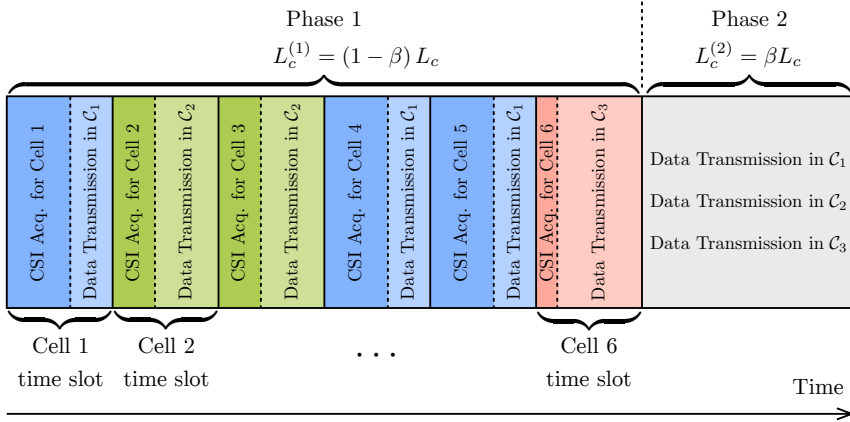


Figure 4.3. Schematic of proposed frame structure for the coalition structure in Figure 4.1. Note that the total CSI acquisition in phase 1 grows quadratically with the coalition size (cf. Example 4.3). Full frequency reuse is applied in phase 2.

Frame Structure

A frame structure parameter³ $0 \leq \beta < 1$ determines the temporal allocation between the two phases. See Figure 4.3 for a schematic of the frame structure. Phase 1 will generally deliver higher throughputs when the SNR is high and any unmitigated interference is detrimental, whereas phase 2 will generally deliver higher throughputs when the intercoalition interference is negligible compared to the thermal noise. (A deeper comparison is given in Section 4.2.4.) Since the CSI acquisition is performed orthogonally between coalitions, we assume that the phase 1 time allocation is partially used for CSI acquisition and partially used for data transmission.

4.2 Long-Term Throughput Model

The total long-term throughput of MS i_k is written as a sum of the throughputs in phase 1 and phase 2. In each phase, we model the throughput as a product of a pre-log factor α and a long-term rate \bar{r} , giving the total throughput as

$$\begin{aligned} \bar{t}_{i_k}(\mathcal{S}(i)) &= \mathbb{E}_{\{\mathbf{H}_{i_k j}\}_{j \in \mathcal{I}}}(t_{i_k}(\mathcal{S}(i))) \cdot \mathbb{F}(\mathcal{S}(i)) \\ &= \left(\alpha_i^{(1)}(\mathcal{S}(i)) \bar{r}_{i_k}^{(1)} + \alpha_i^{(2)} \bar{r}_{i_k}^{(2)}(\mathcal{S}(i)) \right) \cdot \mathbb{F}(\mathcal{S}(i)), \end{aligned} \quad (4.1)$$

where $\mathbb{F}(\mathcal{S}(i)) = \mathbb{F}_{\text{IIA}}(\mathcal{S}(i)) \cdot \mathbb{F}_{\text{CSI}}(\mathcal{S}(i))$ is a product of feasibility tests, as defined in Definition 4.2 on the next page and Definition 4.3 on page 66.

³Due to the lack of a central controller in the network, we let β be static and fixed. All cells have a priori knowledge of the value of β .

In the model for the long-term throughput of MS i_k in (4.1), the pre-log factors $\alpha_i^{(1)}(\mathcal{S}(i))$ and $\alpha_i^{(2)}$ describe the temporal degrees of freedom available for data transmission in phase 1 and phase 2, respectively. The long-term rates $\bar{r}_{i_k}^{(1)}$ and $\bar{r}_{i_k}^{(2)}(\mathcal{S}(i))$ depend on the signal, interference, and noise powers experienced. In this section we provide a model for how these quantities depend on the coalition structure \mathcal{S} .

4.2.1 Fundamental Assumptions

In order to model the rates $\bar{r}_{i_k}^{(1)}$ and $\bar{r}_{i_k}^{(2)}(\mathcal{S}(i))$, we assume that every coalition performs *intracoalition interference alignment* (IIA):

Assumption 4.1 (Intracoalition Interference Alignment). *For a coalition $\mathcal{C}_s \in \mathcal{S}$, the precoders $\{\mathbf{V}_{i_k}\}_{i \in \mathcal{C}_s, k \in \mathcal{K}_i}$ and receive filters $\{\mathbf{U}_{i_k}\}_{i \in \mathcal{C}_s, k \in \mathcal{K}_i}$ satisfy*

$$\mathbf{U}_{i_k}^H \mathbf{H}_{i_k j} \mathbf{V}_{j_l} = \mathbf{0}, \quad \forall j \in (\mathcal{S}(i) \setminus \{i\}), l \in \mathcal{K}_i, \quad (4.2)$$

$$\mathbf{U}_{i_k}^H \mathbf{H}_{i_k i} \mathbf{V}_{i_l} = \mathbf{0}, \quad \forall l \in (\mathcal{K}_i \setminus \{k\}), \quad (4.3)$$

$$\text{rank}(\mathbf{U}_{i_k}^H \mathbf{H}_{i_k i} \mathbf{V}_{i_k}) = d_{i_k}. \quad (4.4)$$

Equation (4.2) ensures that all intracoalition intercell interference is cancelled, whereas equation (4.3) ensures that all intracoalition intracell interference is cancelled. Finally, equation (4.4) ensures that the effective desired channel does not lose rank, thus enabling the transmission of the allocated data streams.

Since the rates $\bar{r}_{i_k}^{(1)}$ and $\bar{r}_{i_k}^{(2)}(\mathcal{S}(i))$ will not have any operational meaning unless IIA is feasible, we multiply the throughputs in (4.1) with the *IIA feasibility test* as defined by:

Definition 4.2 (IIA Feasibility Test).

$$\mathbb{F}_{\text{IIA}}(\mathcal{C}_s) = \begin{cases} 1 & \text{if IIA is feasible a.s.}, \\ 0 & \text{otherwise.} \end{cases} \quad (4.5)$$

Note that although we study the case of IA in coalitions, since there is no coordination between coalitions, the IIA results in [YGJK10, RSL12, LY13] can be applied directly.⁴ For a symmetric network, an example of an IIA feasibility test is given by:

Example 4.1 (IIA Feasibility Test in Symmetric Networks). *For a coalition $\mathcal{C}_s \in \mathcal{S}$ in a symmetric network, a necessary and sufficient condition on a.s. IIA feasibility is [LY13, Section V-A]:*

$$\mathbb{F}_{\text{IIA}}(\mathcal{C}_s) = \begin{cases} 1 & \text{if } |\mathcal{C}_s| \leq \frac{M+N-d}{Kd}, \\ 0 & \text{otherwise.} \end{cases} \quad (4.6)$$

⁴Given an IIA feasible coalition, full intracoalition CSI (as available by Definition 4.1 on page 60) is generally needed in order to find a solution to the conditions in (4.2)–(4.4) [CJ08].

For tractability in the long-term throughput model, we further make some assumptions on the IIA solution:

Assumption 4.2 (Properties of IIA Solution). *For an IIA solution satisfying Assumption 4.1, the following additional properties hold for all $i \in \mathcal{I}, k \in \mathcal{K}_i$:*

- A. \mathbf{U}_{i_k} is a semi-unitary matrix, i.e. $\mathbf{U}_{i_k}^H \mathbf{U}_{i_k} = \mathbf{I}_{d_{i_k}}$
- B. \mathbf{V}_{i_k} is a matrix with orthogonal columns and uniform power allocation, i.e. $\mathbf{V}_{i_k}^H \mathbf{V}_{i_k} = \frac{P_i}{K_i d_{i_k}} \mathbf{I}_{d_{i_k}}$
- C. $\mathbf{u}_{i_k,n}$ is statistically independent of $\mathbf{H}_{i_k i} \mathbf{v}_{i_k,n}$ and is selected such that $\mathbf{u}_{i_k,n}^H \mathbf{H}_{i_k i} \mathbf{v}_{i_k,m} = 0$ for all $m \neq n$
- D. \mathbf{V}_{i_k} is statistically independent of $\mathbf{H}_{i_k i}$
- E. Both \mathbf{U}_{i_k} and \mathbf{V}_{i_k} are statistically independent of $\mathbf{H}_{i_k j}$ for all $j \in \mathcal{S}^\perp(i)$

The interpretation of these assumptions is that the precoders are used for intracell zero-forcing precoding, and the receive filters are used for intrauser inter-stream zero-forcing receive filtering. These assumptions are similar to the assumptions in [EALH12, Lemma 1], but generalized to the *cellular* case with *clustered* cells. The existence of a solution to (4.2)–(4.4) is not restricted by the assumptions, as given by the following novel result:

Theorem 4.1. *If an IIA solution satisfying Assumption 4.1 exists, there exists an IIA solution satisfying both Assumption 4.1 and Assumption 4.2.*

Proof: The proof is given in Appendix 4.A. ■

For the modelling of $\bar{r}_{i_k}^{(1)}$ and $\bar{r}_{i_k}^{(2)}(\mathcal{S}(i))$, we now provide a characterization of the effective channels:

Lemma 4.1. *For an IIA solution satisfying Assumption 4.2, the effective desired channel for the n th stream of MS i_k is*

$$f_{i_k,n} = \mathbf{u}_{i_k,n}^H \mathbf{H}_{i_k i} \mathbf{v}_{i_k,n} \sim \mathcal{CN} \left(0, \gamma_{i_k i} \frac{P_i}{K_i d_{i_k}} \right). \quad (4.7)$$

The effective intercoalition interfering channel between the m th stream intended for MS j_l to the n th stream of MS i_k , where $j \in \mathcal{S}^\perp(i)$, is

$$g_{i_k j_l, nm} = \mathbf{u}_{i_k,n}^H \mathbf{H}_{i_k j} \mathbf{v}_{j_l,m} \sim \mathcal{CN} \left(0, \gamma_{i_k j} \frac{P_j}{K_j d_{j_l}} \right). \quad (4.8)$$

Proof: Due to the bi-unitary invariance of $\mathbf{H}_{i_k i}$ [TV04], together with Assumptions 4.2-B and 4.2-D, each element of $\mathbf{H}_{i_k i} \mathbf{v}_{i_k,n}$ is i.i.d. $\mathcal{CN}(0, \gamma_{i_k i} P_i / d_{i_k})$. Due to Assumption 4.2-C together with the bi-unitary invariance of $\mathbf{H}_{i_k i} \mathbf{v}_{i_k,n}$, the result in (4.7) follows. The result for (4.8) follows similarly, except that Assumption 4.2-E is used for the independence. ■

4.2.2 Phase 1: Time Sharing for Intercoalition Interference

In phase 1, the intercoalition interference is handled by time sharing and the intra-coalition interference is handled by IIA (see Assumption 4.1). The received filtered signal for MS i_k is thus modelled as

$$\hat{\mathbf{x}}_{i_k}^{(1)} = \underbrace{\mathbf{U}_{i_k}^H \mathbf{H}_{i_k i} \mathbf{V}_{i_k} \mathbf{x}_{i_k}}_{\text{desired signal}} + \underbrace{\sum_{\substack{j \in \mathcal{S}(i), l \in \mathcal{K}_j \\ (j,l) \neq (i,k)}} \mathbf{U}_{i_k}^H \mathbf{H}_{i_k j} \mathbf{V}_{j_l} \mathbf{x}_{j_l}}_{\text{intra-coalition interference}} + \underbrace{\mathbf{U}_{i_k}^H \mathbf{z}_{i_k}}_{\text{filtered thermal noise}}. \quad (4.9)$$

Note the absence of intercoalition interference due to the time sharing.

Pre-Log Factor

The total time allocated to phase 1 is $L_c^{(1)} = (1 - \beta)L_c$. For fairness, we allot $1/I$ fraction of this time to each cell.⁵ When several cells form a coalition $\mathcal{C}_s \in \mathcal{S}$ they each contribute their fraction of time to the coalition, such that the total time available is $|\mathcal{C}_s|/I$. Assuming that the number of symbols needed for CSI acquisition is $L_t(\mathcal{C}_s)$, the fraction of time used for CSI acquisition is thus $\frac{L_t(\mathcal{C}_s)}{\frac{|\mathcal{C}_s|}{I} L_c^{(1)}}$.

For cell i , we therefore model the pre-log factor as

$$\begin{aligned} \alpha_i^{(1)}(\mathcal{S}(i)) &= (1 - \beta) \frac{|\mathcal{S}(i)|}{I} \left(1 - \frac{L_t(\mathcal{S}(i))}{\frac{|\mathcal{S}(i)|}{I} L_c^{(1)}} \right) \\ &= (1 - \beta) \left(\frac{|\mathcal{S}(i)|}{I} - \frac{L_t(\mathcal{S}(i))}{L_c^{(1)}} \right). \end{aligned} \quad (4.10)$$

The relation in (4.10) depends on the specifics of $L_t(\mathcal{C}_s)$, which is a function of the CSI acquisition method used. For the case of pilot-assisted channel training and analog feedback, we have the following example:

Example 4.2 (CSI Acquisition with Analog Feedback [MBGB15]). *Assume that pilot-assisted channel training and analog feedback [EAH12] is used for the CSI acquisition in an FDD mode system. Further assume that $M_j \geq N_{i_k}$ for all $j \in \mathcal{I}, i \in \mathcal{I}, k \in \mathcal{K}_i$. A model for the minimum⁶ number of symbols needed for CSI acquisition [MBGB15] in a coalition $\mathcal{C}_s \in \mathcal{S}$ is then given by*

$$L_t(\mathcal{C}_s) = \sum_{i \in \mathcal{C}_s} \left(\underbrace{M_i}_{\text{DL training for all MSs}} + \sum_{k \in \mathcal{K}_i} \left(\underbrace{N_{i_k}}_{\text{UL training for this MS}} + \underbrace{d_{i_k}}_{\text{Effective DL training for this MS}} + \underbrace{\sum_{j \in \mathcal{C}_s} M_j}_{\text{Analog feedback for all intra-coalition channels}} \right) \right) \quad (4.11)$$

⁵Generalizing to an unequal static allotment over cells is straightforward.

⁶This model is simplistic, since it assumes *perfect* channel estimation with *minimum* training length.

In Example 4.2, the term corresponding to the analog feedback is quadratic in the coalition size $|\mathcal{C}_s|$, thus growing large for large coalitions. The terms corresponding to the channel training are linear in the size of the coalition, in virtue of the broadcast nature of the wireless channel. For symmetric networks, Example 4.2 simplifies to the following:

Example 4.3 (CSI Acquisition with Analog Feedback in Symmetric Networks). *For a coalition $\mathcal{C}_s \in \mathcal{S}$ in a symmetric network, the minimum number of symbols needed for CSI acquisition as given by (4.11) simplifies to*

$$L_t(\mathcal{C}_s) = (M + K(N + d)) |\mathcal{C}_s| + KM |\mathcal{C}_s|^2. \quad (4.12)$$

In equation (4.10), note that larger coalitions benefit by having a large fraction of time available for transmission (cf. (4.10)), but are at a disadvantage since the number of symbols needed for CSI acquisition $L_t(\mathcal{C}_s)$ is an increasing function in the coalition size $|\mathcal{C}_s|$. If a coalition were to grow too large, there would not be enough time for the required CSI acquisition. The model would then again (cf. IIA feasibility) lose its operational meaning, and we therefore multiply the throughputs in (4.1) with the *CSI feasibility test* as defined by:

Definition 4.3 (CSI Acquisition Feasibility Test).

$$\mathbb{F}_{\text{CSI}}(\mathcal{C}_s) = \begin{cases} 1 & \text{if } \frac{|\mathcal{C}_s|}{I} \geq \frac{L_t(\mathcal{C}_s)}{L_c^{(1)}}, \\ 0 & \text{otherwise.} \end{cases} \quad (4.13)$$

Rate

Under Assumption 4.2, the received filtered signal for the n th stream of MS i_k in phase 1 (see (4.9) and (4.7)) can be simplified to

$$\hat{x}_{i_k,n}^{(1)} = f_{i_k,n} x_{i_k,n} + \mathbf{u}_{i_k}^H \mathbf{z}_{i_k}. \quad (4.14)$$

The rate of (4.14) is then given by:

Theorem 4.2. *For an IIA solution satisfying Assumption 4.2, the long-term rate in phase 1 for the n th stream of MS i_k is*

$$\bar{r}_{i_k,n}^{(1)} = \mathbb{E} \left(\ln \left(1 + |f_{i_k,n}|^2 / \sigma_{i_k}^2 \right) \right) = e^{1/\varrho_{i_k}^{(1)}} E_1 \left(1/\varrho_{i_k}^{(1)} \right), \quad (4.15)$$

where $\varrho_{i_k}^{(1)} = \frac{\gamma_{i_k} P_{i_k}/d_{i_k}}{\sigma_{i_k}^2}$ is the average per-stream SNR and $E_1(\xi) = \int_{\xi}^{\infty} t^{-1} e^{-t} dt$ is the exponential integral.⁷

⁷ $E_1(\xi)$ can be calculated numerically, e.g. by summing its truncated power series expansion [AS65, 5.1.11]. In Matlab [MAT15], it is available as `expint` (ξ).

Proof: Given a realization of $f_{i_k,n}$, equation (4.14) describes a complex Gaussian channel with rate $\ln \left(1 + |f_{i_k,n}|^2 / \sigma_{i_k}^2 \right)$ [CT06, Chapter 9.1]. The result then follows by applying Lemma 4.1 and performing integration by parts on the expectation integral; see e.g. [OSW94]. ■

Summing up the d_{i_k} streams, we thus write the long-term rate for MS i_k in phase 1 as the constant:

$$\bar{r}_{i_k}^{(1)} = d_{i_k} e^{1/\rho_{i_k}^{(1)}} E_1 \left(1/\rho_{i_k}^{(1)} \right). \quad (4.16)$$

4.2.3 Phase 2: Spectrum Sharing for Intercoalition Interference

In phase 2, the whole network operates using spectrum sharing, such that the received filtered signal for MS i_k is given by

$$\begin{aligned} \hat{\mathbf{x}}_{i_k}^{(2)} &= \underbrace{\mathbf{U}_{i_k}^H \mathbf{H}_{i_k i} \mathbf{V}_{i_k} \mathbf{x}_{i_k}}_{\text{desired signal}} \\ &+ \underbrace{\sum_{\substack{j \in \mathcal{S}(i), l \in \mathcal{K}_j \\ (j,l) \neq (i,k)}} \mathbf{U}_{i_k}^H \mathbf{H}_{i_k j} \mathbf{V}_{j_l} \mathbf{x}_{j_l}}_{\text{intracoalition interference}} + \underbrace{\sum_{j \in \mathcal{S}^\perp(i), l \in \mathcal{K}_j} \mathbf{U}_{i_k}^H \mathbf{H}_{i_k j} \mathbf{V}_{j_l} \mathbf{x}_{j_l}}_{\text{intercoalition interference}} \\ &+ \underbrace{\mathbf{U}_{i_k}^H \mathbf{z}_{i_k}}_{\text{filtered thermal noise}}. \end{aligned} \quad (4.17)$$

Pre-Log Factor

Since all cells share the same time slot in phase 2, the pre-log factor is the constant

$$\alpha^{(2)} = \beta. \quad (4.18)$$

Rate

Under Assumption 4.2, the received filtered signal for the n th stream of MS i_k in phase 2 (see (4.17) and (4.8)) can be simplified to

$$\hat{x}_{i_k,n}^{(1)} = f_{i_k,n} x_{i_k,n} + \sum_{j \in \mathcal{S}^\perp(i), l \in \mathcal{K}_j} \sum_{m=1}^{d_{j_l}} g_{i_k j_l, nm} x_{j_l, m} + \mathbf{u}_{i_k,n}^H \mathbf{z}_{i_k} \quad (4.19)$$

The rate of (4.19) is then given by the following theorem.

Theorem 4.3. *For an IIA solution satisfying Assumption 4.2 and assuming that the intercoalition interference is treated as additional thermal noise in the decoder, the long-term rate in phase 2 for the n th stream of MS i_k is*

$$\bar{r}_{i_k,n}^{(2)}(\mathcal{S}(i)) = \mathbb{E} \left(\ln \left(1 + \frac{|f_{i_k,n}|^2}{\sum_{j \in \mathcal{S}^\perp(i), l \in \mathcal{K}_j} \sum_{m=1}^{d_{j_l}} \mathbb{E} \left(|g_{i_k j_l, nm}|^2 \right) + \sigma_{i_k}^2} \right) \right) \quad (4.20)$$

$$= e^{1/\rho_{i_k}^{(2)}(\mathcal{S}(i))} E_1 \left(1/\rho_{i_k}^{(2)}(\mathcal{S}(i)) \right), \quad (4.21)$$

where $\rho_{i_k}^{(2)}(\mathcal{S}(i)) = \frac{\gamma_{i_k} P_{i_k}/d_{i_k}}{\sigma_{i_k}^2 + \sum_{j \in \mathcal{S}^\perp(i)} \gamma_{i_k j} P_j}$ is the average per-stream SINR.

Proof: Under Definition 4.1, the realization of $f_{i_k,n}$ is known to MS i_k , but $\{g_{i_k j_l, nm}\}_{j \in \mathcal{S}^\perp(i), l \in \mathcal{K}_j, n=1, \dots, d_{i_k}, m=1, \dots, d_{j_l}}$ are unknown. Due to the construction of the decoder, the intercoalition interference plays the role of additional Gaussian noise [Lap96]. This gives the form of the instantaneous rate as given inside the expectation operator. The result then follows by applying Lemma 4.1 and performing integration by parts on the expectation integral. ■

Summing up the d_{i_k} streams, we thus write the long-term rate for MS i_k in phase 2 as:

$$\bar{r}_{i_k}^{(2)}(\mathcal{S}(i)) = d_{i_k} e^{1/\rho_{i_k}^{(2)}(\mathcal{S}(i))} E_1 \left(1/\rho_{i_k}^{(2)}(\mathcal{S}(i)) \right). \quad (4.22)$$

4.2.4 Comparison of phase 1 and phase 2

The rate of phase 1 is noise-limited (see (4.16)), since all interference is mitigated through either IIA or time sharing. Due to the time sharing, the temporal resources (see (4.10)) are not efficiently employed however. Overall, this makes phase 1 suitable for data transmission in high-SNR scenarios, where any unmitigated interference is the main limiting factor in the throughput. The rate of phase 2 is interference-limited (see (4.22)), since the intercoalition interference is not mitigated. The temporal resources (see (4.18)) are maximally used however. Overall, this makes phase 2 suitable for intermediate-SNR scenarios, where the CSI acquisition overhead is more important than the unmitigated interference.

The coalition structure \mathcal{S} affects the pre-log factors of phase 1 (but not the corresponding rates), and the rates of phase 2 (but not the corresponding pre-log factors).

Depending on the scenario, for each MS the data transmission in either phase 1 or phase 2 will be the most efficient. Given a coalition structure \mathcal{S} , the selection of β could thus be optimized. Since we are considering a distributed system, we however assume that the β is fixed and selected offline.

4.3 Coalition Formation

It is now our goal to design an algorithm which finds a good coalition structure \mathcal{S} , but with low complexity and a distributed structure. We consider this problem from the perspective of coalitional games [SHD⁺09], which is a suitable framework for studying the formation of coalitions of intelligent and rational *players*, when such formation leads to mutual benefits in terms of the players' *utilities*. In our system, the cells are the players and the corresponding utilities are related to the long-term cell sum throughputs, such that the utility of player i (i.e. cell i) in the game is defined as

$$\tilde{t}_i(\mathcal{S}; \mathcal{H}_i, \eta_i) = \begin{cases} \sum_{k \in \mathcal{K}_i} \bar{t}_{ik}(\mathcal{S}(i)) & \text{if } (\mathcal{S}(i) \notin \mathcal{H}_i \text{ or } |\mathcal{S}(i)| = 1) \text{ and } \eta_i \leq b_i, \\ 0 & \text{otherwise.} \end{cases} \quad (4.23)$$

The utility depends on a *history set* $\mathcal{H}_i \subseteq \{\mathcal{E} \in 2^{\mathcal{I}} \mid i \in \mathcal{E}\}$ and a *search budget* $b_i \in \mathbb{N}$, which are introduced for stabilization and complexity reduction, respectively.⁸ The history set \mathcal{H}_i stores the coalitions which player i has been part of before and the quantity $\eta_i \in \mathbb{N}$ denotes the number of times that the player has communicated with other coalitions during the coalition formation. The interpretation of (4.23) is that the utility of player i is the sum of the long-term throughputs of the MSs in cell i , with the restriction that the player never benefits from joining a coalition that it has been a member of before—unless it is the singleton—and the restriction that a player does not benefit if the search budget has been exhausted. Given the utility model, the game associated with our setting is

$$\langle \mathcal{I}, \{\tilde{t}_i\}_{i \in \mathcal{I}}, \{b_i\}_{i \in \mathcal{I}} \rangle. \quad (4.24)$$

The throughputs of the MSs in a particular cell only depend on what other cells participate in the corresponding coalition, and the game is therefore *hedonic* [DG80, BJ02]. A player is not able to share its achieved utility with other players in its coalition, and the utilities are therefore *non-transferable*. Due to the history set and the design of the utilities, i.e. the fact that a player never benefits from joining a coalition that it has been a member of before, the coalition formation algorithm to be proposed will be convergent [SHZ⁺12].⁹

For the proposed game we now study *coalition formation*, which is the dynamics that lead to stable coalition structures. We will detail the three main components [SHD⁺09] needed in order to describe the coalition formation.

⁸The notion of a history set has previously been used in e.g. [SHZ⁺12], and a search budget was previously used in e.g. [MBB15].

⁹For the simpler case of additively separable utilities, the existence of an individually stable coalition structure for hedonic games—without the introduction of a history set—was shown in [BJ02].

4.3.1 Components of Coalition Formation

An individual deviation¹⁰ is when a player $i \in \mathcal{I}$ leaves its current coalition $\mathcal{S}(i)$ to join another coalition $\mathcal{T} \in (\mathcal{S} \setminus \mathcal{S}(i)) \cup \{\emptyset\}$. We propose two types of deviations:

Definition 4.4 (Attach Deviation). *In an attach deviation, which we capture with the notation $\mathcal{S} \xrightarrow{i} \mathcal{S}_{\mathcal{T}}$, player i simply attaches itself to a coalition \mathcal{T} such that the coalition structure changes to $\mathcal{S}_{\mathcal{T}} = (\mathcal{S} \setminus \mathcal{S}(i)) \cup \{\mathcal{S}(i) \setminus \{i\}, \mathcal{T} \cup \{i\}\}$.*

Definition 4.5 (Supplant Deviation). *In a supplant deviation, which we capture with the notation $\mathcal{S} \xrightarrow{i \Leftarrow q} \mathcal{S}_{\mathcal{T}}$, player i supplants another player $q \in \mathcal{T}$ (the outcast), expelling it to a singleton coalition, such that the coalition structure changes to $\mathcal{S}_{\mathcal{T}} = (\mathcal{S} \setminus \mathcal{S}(i)) \cup \{\mathcal{S}(i) \setminus \{i\}, (\mathcal{T} \setminus \{q\}) \cup \{i\}, \{q\}\}$.*

In the literature, the attach deviation is common (see e.g. [SHZ⁺12, MBB15, DG80]). By letting the players either attach, or supplant, (i.e. an *attach-or-supplant* deviation), we allow for a more flexible deviation model, however. This leads to more efficient solutions in some operating regimes (see Section 4.4.2), than if only the attach deviation was allowed.

Visual examples of the two deviations are shown in Figures 4.4 and 4.5.

Definition 4.6 (Admissible Deviation). *For player $i \in \mathcal{I}$, a deviation is admissible only if $\tilde{t}_i(\mathcal{S}_{\mathcal{T}}; \mathcal{H}_i, \eta_i) > \tilde{t}_i(\mathcal{S}; \mathcal{H}_i, \eta_i)$.*

An attach deviation $\mathcal{S} \xrightarrow{i} \mathcal{S}_{\mathcal{T}}$ is then admissible if and only if $\tilde{t}_j(\mathcal{S}_{\mathcal{T}}; \mathcal{H}_j, \eta_j) \geq \tilde{t}_j(\mathcal{S}; \mathcal{H}_j, \eta_j)$, for all players $j \in \mathcal{T}$.

A supplant deviation $\mathcal{S} \xrightarrow{i \Leftarrow q} \mathcal{S}_{\mathcal{T}}$ is then admissible if and only if $\tilde{t}_j(\mathcal{S}_{\mathcal{T}}; \mathcal{H}_j, \eta_j) \geq \tilde{t}_j(\mathcal{S}; \mathcal{H}_j, \eta_j)$, for all players $j \in \mathcal{T} \setminus \{q\}$.

In the attach case, if any existing member of the coalition that is being joined by player i decreases its utility, the player will not be allowed to join. In the supplant case, all members in the coalition being joined, except the outcast q , must agree to allow the player i to supplant player q . The rational players pursue any admissible deviations, until stability has been reached:

Definition 4.7 (Individual Stability). *A coalition structure \mathcal{S} is individually stable if there exists no player $i \in \mathcal{I}$ and coalition structure $\mathcal{S}_{\mathcal{T}}$ such that $\mathcal{S} \xrightarrow{i} \mathcal{S}_{\mathcal{T}}$, or $\mathcal{S} \xrightarrow{i \Leftarrow q} \mathcal{S}_{\mathcal{T}}$ for all potential outcasts $q \in \mathcal{T} \setminus \{i\}$, are admissible.*

When an individually stable coalition structure has been reached, no player benefits from deviating.

¹⁰For complexity reasons, we only consider individual deviations where a single player deviates at a time, as inspired by [DG80, BJ02].

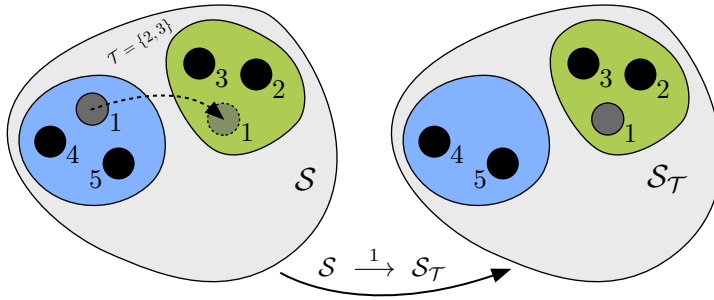


Figure 4.4. Example of an attach deviation.

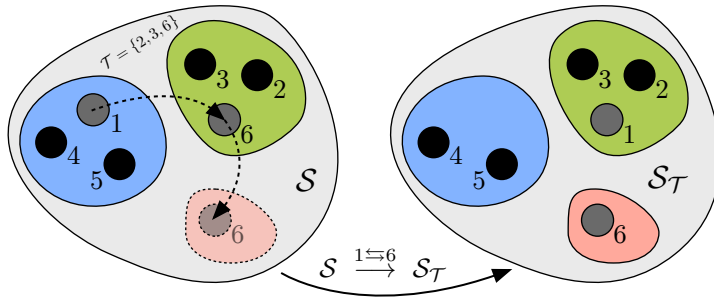


Figure 4.5. Example of a supplant deviation.

4.3.2 Coalition Formation Algorithm

Based on the provided concepts in the previous section, we formulate the coalition formation algorithm in Algorithm 4.1 on the facing page. The initial coalition structure can be arbitrarily selected, but we choose the set of singletons $\mathcal{S}^{\text{singletons}} = \{\{1\}, \dots, \{I\}\}$ for simplicity. One at a time, according to the sequence $1, \dots, I$, the players initiate deviations.

Given its turn, player i forms the set $\mathcal{D}_i = (\mathcal{S} \setminus \mathcal{S}(i)) \cup \{\emptyset\}$ of all possible coalitions that it could possibly deviate to. It further forms the set

$$\Lambda_i(\mathcal{S}) = \{\mathcal{T} \in \mathcal{D}_i \mid \tilde{t}_i(\mathcal{S}_{\mathcal{T}}; \mathcal{H}_i, \eta_i) > \tilde{t}_i(\mathcal{S}; \mathcal{H}_i, \eta_i), \mathcal{S} \xrightarrow{i} \mathcal{S}_{\mathcal{T}}\}, \quad (4.25)$$

of all coalitions in attach deviations benefiting itself, and

$$\Delta_i(\mathcal{S}) = \{(\mathcal{T}, q) \in \mathcal{D}_i \times \mathcal{I} \mid \tilde{t}_i(\mathcal{S}_{\mathcal{T}}; \mathcal{H}_i, \eta_i) > \tilde{t}_i(\mathcal{S}; \mathcal{H}_i, \eta_i), q \in \mathcal{T}, \mathcal{S} \xrightarrow{i \leftarrow q} \mathcal{S}_{\mathcal{T}}\}, \quad (4.26)$$

the set of all coalition-outcast pairs in supplant deviations benefiting itself. The entries of $\Lambda_i(\mathcal{S})$ and $\Delta_i(\mathcal{S})$ are then sorted in decreasing order of the utility of player i , such that the player will try to deviate to the coalitions which benefits it the most first. For a coalition $\mathcal{T} \in \Lambda_i(\mathcal{S})$ that player i wants to attach to, it sends a deviation *proposal* to all members of \mathcal{T} . Each player in \mathcal{T} then communicates its *decision* back to player i , based on the admissibility criterion in Definition 4.6. If all members of \mathcal{T} allow player i to attach, it stores its old coalition $\mathcal{S}(i)$ to the history set and joins \mathcal{T} . For a coalition-outcast pair $(\mathcal{T}, q) \in \Delta_i(\mathcal{S})$, the same protocol can be used as for the attach deviation, except that only the decisions of the non-outcasts $\mathcal{T} \setminus \{q\}$ matter (cf. Definition 4.6). Note that it is up to the deviating player to propose to treat player $q \in \mathcal{T}$ as the outcast to the rest of the members of \mathcal{T} . If the outcast $q \in \mathcal{T}$ is expelled from \mathcal{T} , it receives this message from the other members of \mathcal{T} . For each deviation proposal, player i increments its search count η_i by one. The coalition formation continues until no deviations are admissible.

Remark 4.1. *A state where no deviations are admissible necessarily happens eventually, as given by [SHZ⁺12, Proof of Thm. 1]. This result is due to the restriction imposed by the history set: since only a finite number of possible coalition structures exist, and each coalition structure appears at most once in the iterations due to the history set restriction, convergence is guaranteed.*

Since each player i can only change coalitions a maximum of b_i times, the worst case number of iterations is limited by the by the number of partitions of \mathcal{I} , which is \mathbb{B}_I , and $\sum_{i \in \mathcal{I}} b_i$. Note that the search budgets in themselves guarantee convergence of the algorithm, although we only explicitly use them for complexity reduction.

4.3.3 Distributed Implementation

Due to the availability of full local CSI statistics (cf. Definition 4.1), the players can calculate their own utility for all possible deviations. The only message exchange

Algorithm 4.1 Coalition Formation for Base Station Clustering

Initialize: $\mathcal{S} = \mathcal{S}^{\text{singletons}}$, $\mathcal{H}_i = \emptyset$, $\eta_i = 0$, $\forall i \in \mathcal{I}$

- 1: **repeat**
- 2: **loop** over $i \in \mathcal{I}$ in lexicographic order
- 3: **loop** over $\mathcal{T} \in \Lambda_i(\mathcal{S})$ and $(\mathcal{T}, q) \in \Delta_i(\mathcal{S})$
 in decreasing order of $\tilde{t}_i(\mathcal{S}_{\mathcal{T}}; \mathcal{H}_i, \eta_i)$
- 4: Increment search factor $\eta_i = \eta_i + 1$
- 5: **if** deviation $\mathcal{S} \xrightarrow{i(\leftrightarrow q)} \mathcal{S}_{\mathcal{T}}$ is admissible **then**
- 6: Replace \mathcal{H}_i with $\mathcal{H}_i \cup \mathcal{S}(i)$
- 7: Replace \mathcal{S} with $\mathcal{S}_{\mathcal{T}}$
- 8: Go to line 2
- 9: **end if**
- 10: **end loop**
- 11: **end loop**
- 12: **until** no player deviated

that is needed is to communicate the deviation proposals (from the deviating player to the members of the new coalition) and the deviation decisions (from the members of the new coalition to the deviator and the potential outcast).

The history set provides the guarantee of convergence of the algorithm. However, for large number of cells I , the size of the history set could grow large. For the particular case of bounded coalition sizes (e.g. due to the IIA feasibility in Definition 4.2 or due to the CSI feasibility in Definition 4.3), the maximum size of the history set is however polynomial in I :

Lemma 4.2. *If all formed coalitions \mathcal{C}_s satisfy $|\mathcal{C}_s| \leq \check{C}$, for some constant $\check{C} \in \mathbb{N}$, then $|\mathcal{H}_i| = O(I^{\check{C}-1})$.*

Proof: The cardinality of the history set for player i is upper bounded by the total number of coalitions that can form which have player i as a member. Thus,

$$|\mathcal{H}_i| \leq \sum_{c=0}^{\check{C}-1} \binom{I}{c} \leq 1 + \sum_{c=1}^{\check{C}-1} \frac{I^c}{c!} \leq \check{C} \cdot I^{\check{C}-1}, \quad (4.27)$$

which gives the result. ■

4.4 Performance Evaluation

The performance of the proposed system is studied through numerical simulations. The simulation scenario is a large-scale deployment of macro BSs which includes effects like path loss, shadow fading, and small-scale fading. The parameters are generally inspired by 3GPP Case 2 [3GP06, A.2.1.1], except for the small-scale fading modelling where we choose i.i.d. Rayleigh fading for simplicity (cf. Section 2.1.2).

Scenario

We consider a symmetric network where $I = 12$ BSs each serve $K = 2$ MSs with $d = 1$ stream each. The BSs have $M = 8$ antennas each and the MSs have $N = 2$ antennas each. The IIA feasibility test and CSI acquisition overhead are given by Example 4.1 and Example 4.3, respectively.¹¹ Since base station clustering is more challenging in asymmetric geographies, instead of the typical hexagonal cells, we randomly drop the BSs in a square. The area of the square is selected such that the average cell size is identical to the case of hexagonal cells with an inter site distance of 500 m, as mandated by 3GPP Case 2. For simplicity, we let the K served MSs be placed uniformly at random at a circle around the serving BS at a distance of 150 m. We study the performance averaged over 250 drops of the BSs and MSs, and for each drop we generate 10 small-scale fading realizations. As given by 3GPP Case 2, we consider a carrier frequency of 2 GHz, giving the path loss as $15.3 + 37.6 \log_{10}(\text{distance [m]})$ in decibels. The shadow fading is i.i.d. log-normal with 8 dB standard deviation. All antennas are omnidirectional with antenna gain 0 dB. Unless otherwise noted, we let $\beta = 0.5$, $\text{SNR} = \frac{P_{i_k}}{\sigma_{i_k}^2} = 20$ dB and the MS speed is 30 km/h. The coherence bandwidth is set as $W_c = 300$ kHz. As the system-level objective, we use the sum throughput over all served MSs.

Benchmarks

For benchmarking of the coalition formation algorithm, we compare to the optimal coalition structure as generated by Algorithm 3.1 on page 55. We also compare to the case of singleton coalitions $\mathcal{S}^{\text{singletons}} = \{\{1\}, \dots, \{I\}\}$, as well as the grand coalition $\mathcal{S}^{\text{grand}} = \{\mathcal{I}\}$. We also compare to the heuristic grouping method of [PH12], which has been slightly modified to always serve all MSs with equal number of data streams.

4.4.1 Example Coalition Structure

First we give an example of a typical network realization, together with the correspondingly generated coalition structure from the coalition formation algorithm with attach-or-supplant deviations; see Figure 4.6. The geographic proximity of cells is important in the distance-dependent path loss, leading to grouping of nearby cells.

¹¹Note that we consider a symmetric network for simplicity, but the proposed algorithms are not limited to symmetric networks in general.

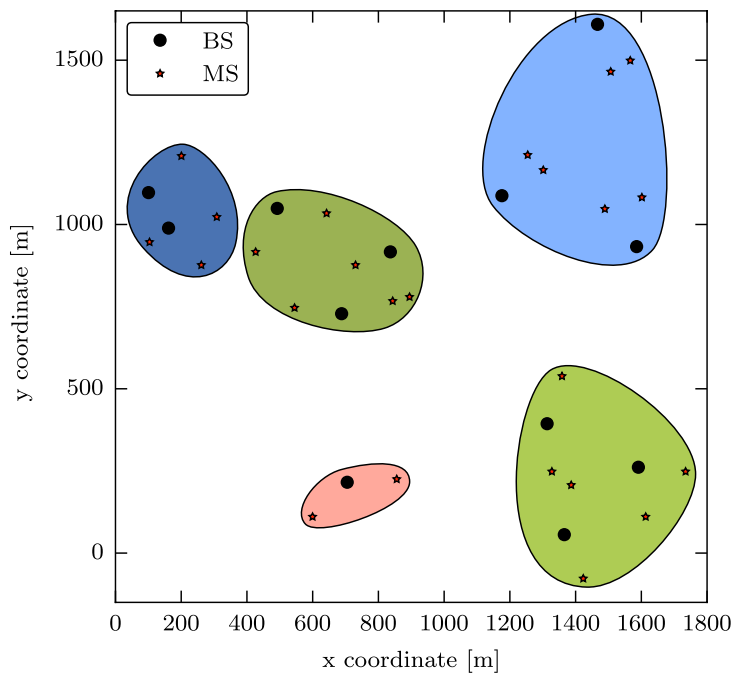


Figure 4.6. Example of network realization and coalition structure generated by the coalition formation algorithm. The MSs are dropped 150 m from their serving BS, and with high probability the serving BS is the closest BS.

4.4.2 Coherence Block Length

The length of the coherence block L_c directly affects performance in the proposed frame structure and long-term throughput model. In the simulations, we use a simple model (see [JL10] for details) that maps the MS speed into an integer L_c .¹² Varying the MS speed—thus varying L_c —we show the sum throughputs in Figure 4.7 and the corresponding average coalition size in Figure 4.8. As the MS speed increases, L_c decreases, leading to lower performance. The plateauing effects in Figure 4.7 and Figure 4.8 are due to the CSI acquisition overhead limiting the size of the coalitions. The coalition formation algorithms are able to track the global optimum, significantly outperforming the case of singleton coalitions. The long-term throughput of the grand coalition is constantly zero, as the grand coalition is not IIA feasible. In the low MS speed regime, the limiting factor of the coalitions is the IIA feasibility and not the CSI acquisition overhead. The coalition formation algorithm with only attach deviations could thus easily get stuck, since there generally is little benefit from going from a larger coalition to a smaller one—an action which might be necessary for efficiency under the hard constraints of IIA feasibility. By allowing for the attach-or-supplant deviation however, more dynamism is allowed, leading to improved sum throughput in the low MS speed regime. In the following, we therefore use the attach-or-supplant version.

4.4.3 Selection of Frame Structure Parameter β

The frame structure parameter β determines the temporal resource allocation between phase 1 and phase 2. Depending on the SNR, the sum throughput optimal value of β will either be $\beta^{(1),*} = 0$ (in the high-SNR regime), or close to $\beta^{(2),*} = \max_{\mathbb{F}_{\text{CSI}}(c_s)=1, \forall c_s \in \mathcal{S}} \beta = 0.65$ (in the intermediate SNR regime). To find the boundary between these two regimes, we plot the IIA throughput for the case of $\beta \in \{0, 0.5, 0.65\}$ in Figure 4.9 on page 78. For the proposed coalition formation, the intersection of the three curves is at an SNR of 42 dB. With an SNR lower than 42 dB, it is beneficial to maximize the time in phase 2 (i.e. selecting $\beta = 0.65$). With an SNR higher than 42 dB, it is beneficial to maximize the time in phase 1, (i.e. selecting $\beta = 0$). A good trade-off is achieved by selecting $\beta = 0.5$. The grouping heuristic of [PH12] performs well for $\beta = 0$, which is the setting it was developed for. Its lacklustre performance for $\beta \in \{0.5, 0.65\}$ is due to the fact that only the coalition *sizes* matter in the grouping heuristic, and not the actual members of the coalitions. This leads to poor performance in phase 2.

¹²This is done by showing that the achievable rate with pilot-assisted training is identical between continuous fading with rectangular Doppler spectrum and block fading if $f_D = 1/(2L_c)$, where $f_D = L_s v/\lambda$ is the Doppler frequency, L_s is the symbol period and λ is the carrier wavelength.

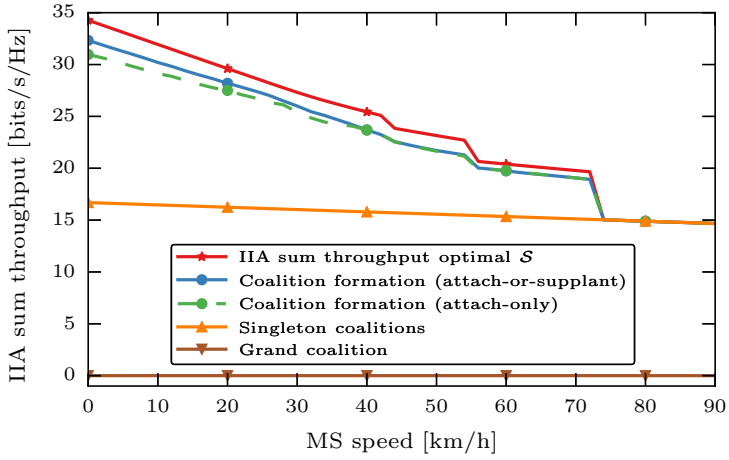


Figure 4.7. Long-term sum throughput when implicitly varying L_c through the proxy of MS speed.

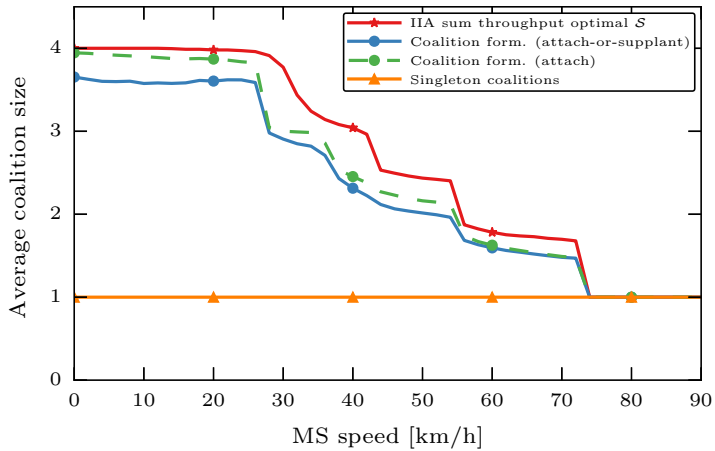


Figure 4.8. Average coalition size when implicitly varying L_c .

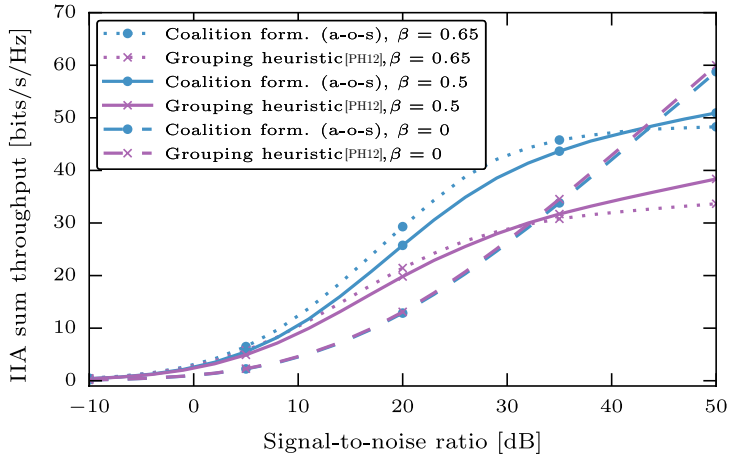


Figure 4.9. Long-term sum throughput for $\beta \in \{0, 0.5, 0.65\}$ and varying SNR.

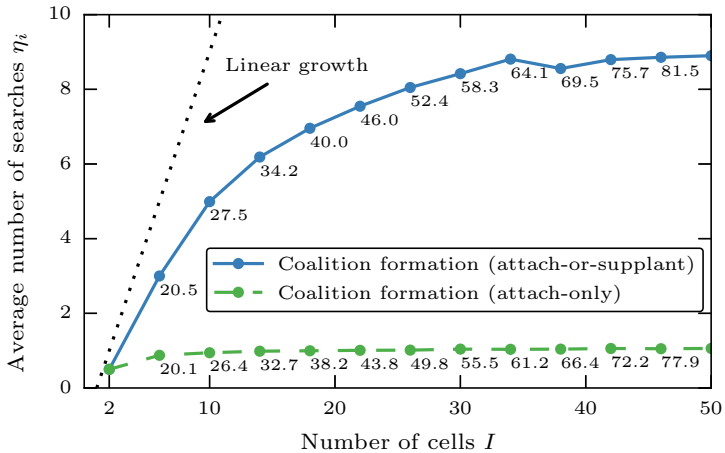


Figure 4.10. Coalition formation complexity and achieved long-term sum throughput (numbers below curves, [bits/s/Hz]) when varying the number of cells I .

4.4.4 Coalition Formation Complexity for Large Networks

We now consider a network of I cells randomly placed in a square whose sides give the same average cell size as before. In order to accommodate large networks, we let the MS speed be 3 km/h. The average number of searches in the coalition formation is given in Figure 4.10 on the preceding page, together with the achieved long-term sum throughput. The coalition formation with attach-or-supplant deviations has a higher complexity than the coalition formation with attach-only deviations. In absolute terms, both algorithms have very low complexities however. The higher complexity of the attach-or-supplant version does pay off in terms of higher sum throughputs.

4.5 Conclusions

Based on first principles, we have derived a specific throughput model for clustered multicell networks. By employing concepts from the field of coalitional games, we have further designed a distributed clustering heuristic with low complexity. In the numerical study, the performance of the coalition formation algorithm is promising.

4.A Proof of Theorem 4.1

Let $d_i = \sum_{k \in \mathcal{K}_i} d_{i_k}$ be the total number of data streams transmitted in cell i . For all $i \in \mathcal{I}$, let $\mathbf{V}_i \in \mathbb{C}^{M_i \times d_i}$ be the horizontal stacking of $\{\mathbf{V}_{i_k}\}_{k \in \mathcal{K}_i}$, i.e. $\mathbf{V}_i = \begin{pmatrix} \mathbf{V}_{i_1} & \mathbf{V}_{i_2} & \cdots & \mathbf{V}_{i_{K_i}} \end{pmatrix}$. Now study the relaxed system of equations given by

$$\mathbf{U}_{i_k}^H \mathbf{H}_{i_k j} \mathbf{V}_j = \mathbf{0}, \quad \forall j \in (\mathcal{S}(i) \setminus \{i\}), \quad (4.28)$$

$$\text{rank}(\mathbf{U}_{i_k}) = d_{i_k}, \quad (4.29)$$

$$\text{rank}(\mathbf{V}_i) = d_i, \quad (4.30)$$

for all $i \in \mathcal{I}, k \in \mathcal{K}_i$. If a solution exists to the original system of equations in (4.2)–(4.4), then there must also exist a solution to the relaxed system of equations in (4.28)–(4.30). Denote such a partial IIA solution as $\{\tilde{\mathbf{U}}_{i_k}, \tilde{\mathbf{V}}_{i_k}\}_{i \in \mathcal{I}, k \in \mathcal{K}_i}$. We now constructively proceed by forming a full IIA solution $\{\mathbf{U}_{i_k}, \mathbf{V}_{i_k}\}_{i \in \mathcal{I}, k \in \mathcal{K}_i}$ that will satisfy both the original system of equations in (4.2)–(4.4) as well as Assumption 4.2.

For all $i \in \mathcal{I}$, let $\mathbf{A}_i \in \mathbb{C}^{M_i \times \sum_{j \in (\mathcal{S}(i) \setminus \{i\})} d_j}$ be the horizontal stacking of $\{\mathbf{H}_{j_i}^H \tilde{\mathbf{U}}_{j_l}\}_{j \in (\mathcal{S}(i) \setminus \{i\}), l \in \mathcal{K}_j}$. The intracoalition interference cancellation conditions in (4.28) can now be written as

$$\mathbf{A}_i^H \tilde{\mathbf{V}}_i = \mathbf{0}, \quad \forall i \in \mathcal{I}. \quad (4.31)$$

From (4.30), we have that $\text{rank}(\tilde{\mathbf{V}}_i) = d_i$ for all $i \in \mathcal{I}$. Thus, in order for (4.31) to hold, we necessarily have that $\text{rank}(\mathbf{A}_i) \leq M_i - d_i$. For MS i_k , we can now form a matrix $\mathbf{B}_{i_k} \in \mathbb{C}^{M_i \times (\sum_{j \in \mathcal{I}} d_j - d_{i_k})}$ whose column space spans the space that \mathbf{V}_{i_k} is restricted from in order to satisfy (4.2)–(4.3):

$$\mathbf{B}_{i_k} = \begin{pmatrix} \mathbf{H}_{i_1 i}^H \tilde{\mathbf{U}}_{i_1} & \cdots & \mathbf{H}_{i_{k-1} i}^H \tilde{\mathbf{U}}_{i_{k-1}} & \mathbf{H}_{i_{k+1} i}^H \tilde{\mathbf{U}}_{i_{k+1}} & \cdots & \mathbf{H}_{i_{K_i} i}^H \tilde{\mathbf{U}}_{i_{K_i}} & \mathbf{A}_i \end{pmatrix} \quad (4.32)$$

Thus, since $\text{rank}(\mathbf{B}_{i_k}) \leq M_i - d_{i_k}$, by solving

$$\mathbf{B}_{i_k}^H \mathbf{V}_{i_k} = \mathbf{0}, \quad \forall i \in \mathcal{I}, k \in \mathcal{K}_i, \quad (4.33)$$

a new partial IIA solution $\{\tilde{\mathbf{U}}_{i_k}, \mathbf{V}_{i_k}\}_{i \in \mathcal{I}, k \in \mathcal{K}_i}$ is found such that (4.2)–(4.3) as well as Assumptions 4.2-B and 4.2-D are satisfied.

We will use the same reasoning in order to form $\{\mathbf{U}_{i_k}\}_{i \in \mathcal{I}, k \in \mathcal{K}_i}$ satisfying Assumption 4.2-A and 4.2-C. For MS i_k , let $\mathbf{C}_{i_k} \in \mathbb{C}^{N_{i_k} \times \sum_{j \in (\mathcal{S}(i) \setminus \{i\})} d_j}$ be the horizontal stacking of $\{\mathbf{H}_{i_k j} \mathbf{V}_j\}_{j \in (\mathcal{S}(i) \setminus \{i\}), l \in \mathcal{K}_j}$ and note that we necessarily have that $\text{rank}(\mathbf{C}_{i_k}) \leq N_{i_k} - d_{i_k}$ due to the intercoalition interference alignment condition in (4.2) satisfied by $\{\tilde{\mathbf{U}}_{i_k}, \mathbf{V}_{i_k}\}_{i \in \mathcal{I}, k \in \mathcal{K}_i}$. For the n th stream of MS i_k , we can then form a matrix $\mathbf{D}_{i_k, n} \in \mathbb{C}^{N_{i_k} \times (\sum_{j \in \mathcal{I}} d_j - 1)}$ whose column space span the space that

$\mathbf{u}_{i_k, n}$ is restricted from in order to satisfy (4.2)–(4.3) and the zero-forcing constraint in Assumption 4.2-C:

$$\mathbf{D}_{i_k, n} = \left(\mathbf{H}_{i_k i} \mathbf{V}_{i_k, 1} \quad \cdots \quad \mathbf{H}_{i_k i} \mathbf{V}_{i_k, n-1} \quad \mathbf{H}_{i_k i} \mathbf{V}_{i_k, n+1} \quad \cdots \quad \mathbf{H}_{i_k i} \mathbf{V}_{i_k, d_{i_k}} \quad \mathbf{C}_{i_k} \right) \quad (4.34)$$

We see that $\text{rank}(\mathbf{D}_{i_k, n}) \leq N_{i_k} - 1$, and thus by solving

$$\mathbf{D}_{i_k, n}^H \mathbf{u}_{i_k, n} = \mathbf{0}, \quad \forall i \in \mathcal{I}, k \in \mathcal{K}_i, n \in \{1, \dots, d_{i_k}\}, \quad (4.35)$$

we obtain a solution $\{\mathbf{U}_{i_k}, \mathbf{V}_{i_k}\}_{i \in \mathcal{I}, k \in \mathcal{K}_i}$ that satisfies (4.2)–(4.3) and Assumptions 4.2-A to 4.2-D. We can w.l.o.g. assume that the rank constraint in (4.4) holds a.s. due to the full rank of the involved filters and the genericness of the channel under our channel model. Finally, we can further w.l.o.g. assume that Assumption 4.2-E holds since no $\mathbf{H}_{i_k j}$ for any $j \in \mathcal{S}^\perp(i)$ appeared in the derivations above. Thus, we have constructed a full IIA solution $\{\mathbf{U}_{i_k}, \mathbf{V}_{i_k}\}_{i \in \mathcal{I}, k \in \mathcal{K}_i}$ that satisfies both Assumption 4.1 and Assumption 4.2, which concludes the proof. ■

Part II

Coordinated Precoding

Coordinated Precoding with Intercluster Interference

In Chapter 4, intracluster interference alignment (IIA) was assumed for the precoding, which led to a tractable statistical characterization of the long-term throughputs. IIA may not be throughput optimal in general however, which in particular can be seen for the transmissions in phase 2, where the unaligned intercluster interference limited the degrees of freedom of the network (see Figure 4.9 on page 78).

In this chapter, we therefore propose an alternative precoding algorithm, which given (short-term) CSI and a clustering (e.g. from any of the algorithms in Chapters 3 and 4) optimally accounts for the unknown intercluster interference. We only consider the precoding in phase 2. For the precoding in phase 1, any existing precoding method (see e.g. [SSB⁺13]) can be used as there is no intercluster interference due to the time sharing.

Our algorithm is based on the WMMSE algorithm of [SRLH11] (see Appendix 2.B), but altered to be robust against intercluster interference, given only knowledge of the intercluster CSI statistics and some filter norms. The robustness is achieved by applying an optimal level of diagonal loading [CZO87] to the precoders and receive filters. The algorithm is distributed over the cells, but requires some limited message exchange between clusters.

5.1 Throughput Bound

Recall that the received signal in phase 2 for MS i_k in the clustered network is given by (4.17) on page 67, which we for clarity reiterate here:

$$\hat{\mathbf{x}}_{i_k} = \mathbf{U}_{i_k}^H \mathbf{H}_{i_k i} \mathbf{V}_{i_k} \mathbf{x}_{i_k} + \sum_{\substack{j \in \mathcal{S}(i), l \in \mathcal{K}_j \\ (j,l) \neq (i,k)}} \mathbf{U}_{i_k}^H \mathbf{H}_{i_k j} \mathbf{V}_{j_l} \mathbf{x}_{j_l} + \sum_{j \in \mathcal{S}^\perp(i), l \in \mathcal{K}_j} \mathbf{U}_{i_k}^H \mathbf{H}_{i_k j} \mathbf{V}_{j_l} \mathbf{x}_{j_l} + \mathbf{U}_{i_k}^H \mathbf{z}_{i_k}. \quad (5.1)$$

The third term corresponds to intercluster channels, which are unknown (see Section 4.1) and thus contribute intercluster interference. It is here our goal to handle this intercluster interference as well as we can.

The first step in the algorithm design is formulating an optimization problem where we bound the impact of the unknown intercluster interference. For simplicity, we only consider per-stream decoding in this chapter, which means that we model the rate in phase 2 as:

$$r_{i_k,n} = \log_2 \left(1 + \frac{|\mathbf{u}_{i_k,n}^H \mathbf{H}_{i_k,i} \mathbf{v}_{i_k,n}|^2}{\sum_{\substack{j \in \mathcal{I}, l \in \mathcal{K}_j, \\ m \in \{1, \dots, d_{j_l}\}, \\ (j,l,m) \neq (i,k,n)}} |\mathbf{u}_{i_k,n}^H \mathbf{H}_{i_k,j} \mathbf{v}_{j_l,m}|^2 + \|\mathbf{u}_{i_k,n}\|_2^2 \sigma_{i_k}^2} \right). \quad (5.2)$$

After the precoder design has finished, a final effective CSI training stage is performed where all MSs (perfectly) estimate their incoming effective channels from all the BSs (cf. Sections 2.1.3 and 4.1.2). Due to this training stage, the rate in (5.2) is indeed achievable, given the normal assumptions of long codewords and optimal decoding. The explicit intercluster CSI is however never estimated.

Original Optimization Problem

Since the intercluster CSI is unknown, we formulate an optimization problem where the sum throughput¹ performance, averaged w.r.t. the unknown channels, is maximized:

$$\begin{aligned} & \underset{\{\mathbf{U}_{i_k}\}, \{\mathbf{V}_{i_k}\}}{\text{maximize}} && \sum_{\substack{i \in \mathcal{I}, k \in \mathcal{K}_j \\ n=1, \dots, d_{i_k}}} \omega_{i_k} \mathbb{E}_{\{\mathbf{H}_{i_k,j}\}_{j \in \mathcal{S}^\perp(i)}} [r_{i_k,n}] \\ & \text{subject to} && \sum_{k \in \mathcal{K}_i} \|\mathbf{V}_{i_k}\|_{\mathbb{F}}^2 \leq P_i, \quad i \in \mathcal{I}. \end{aligned} \quad (5.3)$$

By applying the WMMSE procedure, we will find a stationary point to a bounded version of the optimization problem in (5.3).

Bounded Optimization Problem

The first step is defining the per-stream MSE as

$$\begin{aligned} e_{i_k,n} &= \mathbb{E} \left(|x_{i_k,n} - \mathbf{u}_{i_k,n}^H \mathbf{y}_{i_k}|^2 \right) \\ &= 1 - 2\text{Re} \left(\mathbf{u}_{i_k,n}^H \mathbf{H}_{i_k,i} \mathbf{v}_{i_k,n} \right) + \mathbf{u}_{i_k,n}^H \mathbf{\Phi}_{i_k} \mathbf{u}_{i_k,n}, \end{aligned} \quad (5.4)$$

¹Note that the pre-log factor in phase 2, $\alpha^{(2)} = \beta$ is constant, and thus omitted.

where we recall that the received signal covariance matrix (see (2.3)) is

$$\Phi_{i_k} = \sum_{j \in \mathcal{I}, l \in \mathcal{K}_j} \mathbf{H}_{i_k j} \mathbf{V}_{j l} \mathbf{V}_{j l}^H \mathbf{H}_{i_k j}^H + \sigma_{i_k}^2 \mathbf{I}_{N_{i_k}}. \quad (5.5)$$

We further recall the relation between the rate and the minimum MSE (see (2.21)):

$$\max_{\mathbf{u}_{i_k, n}} r_{i_k, n} = \max_{\mathbf{u}_{i_k, n}} \log_2 (1/e_{i_k, n}). \quad (5.6)$$

Next, we apply Jensen's inequality [Jen05] to note that

$$\mathbb{E}_{\{\mathbf{H}_{i_k j}\}_{j \in \mathcal{S}^\perp(i)}} \left[\log_2 (e_{i_k, n}) \right] \leq \log_2 \left(\mathbb{E}_{\{\mathbf{H}_{i_k j}\}_{j \in \mathcal{S}^\perp(i)}} \left[e_{i_k, n} \right] \right). \quad (5.7)$$

We then calculate the averaged per-stream MSE as

$$\bar{e}_{i_k, n} = \mathbb{E}_{\{\mathbf{H}_{i_k j}\}_{j \in \mathcal{S}^\perp(i)}} \left[e_{i_k, n} \right] = 1 - 2\text{Re} \left(\mathbf{u}_{i_k, n}^H \mathbf{H}_{i_k i} \mathbf{v}_{i_k, n} \right) + \mathbf{u}_{i_k, n}^H \bar{\Phi}_{i_k} \mathbf{u}_{i_k, n}, \quad (5.8)$$

with averaged received signal covariance

$$\begin{aligned} \bar{\Phi}_{i_k} &= \mathbb{E}_{\{\mathbf{H}_{i_k j}\}_{j \in \mathcal{S}^\perp(i)}} \left[\Phi_{i_k} \right] \\ &= \sum_{j \in \mathcal{S}(i), l \in \mathcal{K}_j} \mathbf{H}_{i_k j} \mathbf{V}_{j l} \mathbf{V}_{j l}^H \mathbf{H}_{i_k j}^H + \\ &\quad \sum_{j \in \mathcal{S}^\perp(i), l \in \mathcal{K}_j} \mathbb{E}_{\{\mathbf{H}_{i_k j}\}_{j \in \mathcal{S}^\perp(i)}} \left[\mathbf{H}_{i_k j} \mathbf{V}_{j l} \mathbf{V}_{j l}^H \mathbf{H}_{i_k j}^H \right] + \sigma_{i_k}^2 \mathbf{I}_{N_{i_k}} \\ &= \sum_{j \in \mathcal{S}(i), l \in \mathcal{K}_j} \mathbf{H}_{i_k j} \mathbf{V}_{j l} \mathbf{V}_{j l}^H \mathbf{H}_{i_k j}^H + \sum_{j \in \mathcal{S}^\perp(i), l \in \mathcal{K}_j} \gamma_{i_k j} \|\mathbf{V}_{j l}\|_F^2 \mathbf{I}_{N_{i_k}} + \sigma_{i_k}^2 \mathbf{I}_{N_{i_k}}. \end{aligned} \quad (5.9)$$

Now by applying the relation in (5.6) and the bound in (5.7) to the optimization problem in (5.3), we write a bounded optimization problem as

$$\begin{aligned} &\underset{\{\mathbf{u}_{i_k}\}, \{\mathbf{v}_{i_k}\}}{\text{minimize}} \quad \sum_{\substack{i \in \mathcal{I}, k \in \mathcal{K}_j \\ n=1, \dots, d_{i_k}}} \omega_{i_k} \log_2(\bar{e}_{i_k, n}) \\ &\text{subject to} \quad \sum_{k \in \mathcal{K}_i} \|\mathbf{v}_{i_k}\|_F^2 \leq P_i, \quad i \in \mathcal{I}. \end{aligned} \quad (5.10)$$

By assuming that the decoder of MS i_k is oblivious to the statistical distribution of the intercluster interference and simply treats it as Gaussian noise with the same power [Lap96], the quantity $-\min_{\mathbf{u}_{i_k, n}} \log_2(\bar{e}_{i_k, n})$ in (5.10) can be interpreted as a per-stream achievable rate (cf. Theorem 4.3).

Linearized Optimization Problem

The final optimization problem is now obtained by linearizing the logarithms and including the reciprocals of the linearization points as optimization variables $\{w_{i_k,n}\}_{n=1}^{d_{i_k}}$ (see Appendix 2.B for the full details):

$$\begin{aligned} & \underset{\substack{\{\mathbf{U}_{i_k}\}, \{\mathbf{V}_{i_k}\} \\ \{w_{i_k,n}\}}} & \log_2(e) \sum_{\substack{i \in \mathcal{I}, k \in \mathcal{K}_j \\ n=1, \dots, d_{i_k}}} \omega_{i_k} (w_{i_k,n} \bar{e}_{i_k,n} - \ln(w_{i_k,n}) - 1) \\ \text{subject to} & \sum_{k \in \mathcal{K}_i} \|\mathbf{V}_{i_k}\|_{\mathbb{F}}^2 \leq P_i, \quad i \in \mathcal{I}. \end{aligned} \quad (5.11)$$

5.2 Distributed WMMSE Algorithm

Following the steps described in Appendix 2.B for the original WMMSE algorithm, we can now derive a distributed and iterative coordinated precoding algorithm that finds a stationary point of the optimization problem in (5.11). We briefly summarize the required steps.

The optimality condition for the receive filter of MS i_k is

$$\mathbf{U}_{i_k} = (\bar{\Phi}_{i_k})^{-1} \mathbf{H}_{i_k} \mathbf{V}_{i_k}, \quad (5.12)$$

with resulting optimal MSE weight for the corresponding n th stream:

$$w_{i_k,n} = 1/\bar{e}_{i_k,n}. \quad (5.13)$$

For brevity, we store the MSE weights in a diagonal² matrix

$$\mathbf{W}_{i_k} = \text{diag}(\{w_{i_k,n}\}_{n=1}^{d_{i_k}}) \in \mathbb{R}^{d_{i_k} \times d_{i_k}}. \quad (5.14)$$

The precoder for MS i_k is then given by

$$\mathbf{V}_{i_k} = \sqrt{\omega_{i_k}} (\bar{\Gamma}_i + \mu_i \mathbf{I}_{M_i})^{-1} \mathbf{H}_{i_k}^H \mathbf{U}_{i_k} \mathbf{W}_{i_k}, \quad (5.15)$$

where $\bar{\Gamma}_i$ is an virtual uplink covariance matrix for BS i :

$$\bar{\Gamma}_i = \sum_{j \in \mathcal{S}(i), l \in \mathcal{K}_j} \omega_{j_l} \mathbf{H}_{j_l}^H \mathbf{U}_{j_l} \mathbf{W}_{j_l} \mathbf{U}_{j_l}^H \mathbf{H}_{j_l} + \sum_{j \in \mathcal{S}^+(i), l \in \mathcal{K}_j} \omega_{j_l} \gamma_{j_l} \text{Tr}(\mathbf{U}_{j_l} \mathbf{W}_{j_l} \mathbf{U}_{j_l}^H) \mathbf{I}_{M_i}. \quad (5.16)$$

The Lagrange multiplier $\mu_i \geq 0$ is found by bisection at BS i such that

$$\sum_{k \in \mathcal{K}_i} \|\mathbf{V}_{i_k}\|_{\mathbb{F}}^2 \leq P_i. \quad (5.17)$$

²This can be compared to the non-diagonal MSE weight matrix in Appendix 2.B. The difference here is that we are optimizing the *per-stream decoding* rate expression, whereas the algorithm in Appendix 2.B optimizes the *multi-stream decoding* rate expression. There is always a per-stream optimal solution whose sum throughput is identical to that of the multi-stream optimal solution [KTJ13].

Algorithm 5.1 Robust Intracluster WMMSE Algorithm for Phase 2 Precoding

- 1: **Initialization:** $\{\mathbf{V}_{i_k}\}_{i \in \mathcal{I}, k \in \mathcal{K}_i}$
 - 2: **repeat**
 - 3: For MS i_k , update \mathbf{U}_{i_k} in (5.12) and \mathbf{W}_{i_k} in (5.14)
 - 4: For BS i , find $\mu_i \geq 0$ such that $\sum_{k=1}^{K_i} \|\mathbf{V}_{i_k}\|_{\mathbb{F}}^2 \leq P_i$
 - 5: For MS i_k , update \mathbf{V}_{i_k} in (5.15)
 - 6: **until** convergence
-

Notice that the last term in (5.16) corresponds to a diagonal loading of the precoder in (5.15). The amount of diagonal loading is proportional to the statistical channel strength of the unknown intercluster channels from BS i .

The full algorithm now consists of consecutively updating the receive filters in (5.12), then updating the MSE weights in (5.14), and then updating the precoders in (5.15). The algorithm is summarized in Algorithm 5.1.

Theorem 5.1. *Algorithm 5.1 converges to a stationary point of the bounded optimization problem in (5.10).*

Proof: This can be shown using the same technique as Theorem 3 of [SRLH11]. ■

Remark 5.1. *When there is no intercluster interference, the proposed algorithm is identical to the original WMMSE algorithm in [SRLH11]. Thus, Algorithm 5.1 could directly be used for maximizing the phase 1 sum throughput as well.*

5.2.1 Distributed Implementation

In order to form $\bar{\Phi}_{i_k}$ in (5.9) and $\bar{\Gamma}_i$ in (5.16), intracluster CSI is needed, together with intercluster CSI statistics. This information is available as per Definition 4.1 on page 60. BS i also requires knowledge of $\{\|\mathbf{V}_{j_l}\|_{\mathbb{F}}^2\}_{j \in \mathcal{S}^\perp(i)}$ and $\{\text{Tr}(\mathbf{U}_{j_l} \mathbf{W}_{j_l} \mathbf{U}_{j_l}^H)\}_{j \in \mathcal{S}^\perp(i)}$. These values must therefore be communicated between clusters in each iteration.³ In order to completely avoid the message exchange between clusters, the bound in (5.7) could be further upper bounded by completely disregarding the intercluster interference. This would completely separate the computation between clusters, but would also lead to performance degradations since no robustification would take place.

With the rate definition in (5.2), the final training stage mentioned in Sections 2.1.3 and 4.1.2 is necessary. Without this final training stage, the rates described by the right hand side of (5.7) would be the achieved rates instead [Lap96].

³Note that this differs from the IIA precoding used in Chapter 4, where no communication between clusters was needed.

5.3 Performance Evaluation

We study the performance of the proposed algorithm in the same simulation environment as described in Section 4.4. We still let $\beta = 0.5$, and use the proposed robust WMMSE algorithm for the precoder design in both phases (see Remark 5.1 on the previous page). We perform sufficiently many iterations to reach a relative convergence of 10^{-3} of the sum throughput. We choose the initial precoder for MS i_k as the d_{i_k} strongest right singular vectors of $\mathbf{H}_{i_k i}$.

As naive precoding algorithm benchmarks, we use the original WMMSE algorithm from [SRLH11] and the original MaxSINR algorithm from [GCJ11]. These algorithms are oblivious of the intercluster interference. As a robust precoding algorithm benchmark, we use the robustified MaxSINR algorithm from [CC14], which is diagonally loaded (similar to our proposed robust WMMSE algorithm) to handle the unknown intercluster interference.

5.3.1 Coherence Block Length

In Figure 5.1 on the facing page, we show the WMMSE sum throughputs for different clustering algorithms as a function of the MS speed. When compared to the long-term IIA sum throughputs in Figure 4.7 on page 77, a large performance gain can be seen due to the mitigation of the intercluster interference. Since the robust WMMSE algorithm performs power allocation, IIA feasibility is not strictly necessary in order to reach good performance. This can be seen for low MS speeds, where the grand coalition is outperforming the methods relying on the long-term IIA throughput model. By heuristically modifying the throughputs used in the coalition formation to ignore the IIA feasibility (“Coalition form. (a-o-s, ignoring IA feas.)” in the legend), the resulting WMMSE sum throughput follows that of the grand coalition.

5.3.2 Comparison with Benchmarks

In Figure 5.2a on page 92, we compare different clustering algorithms in terms of their WMMSE throughput when varying the SNR. The coalition formation algorithm from Chapter 4 outperforms all other clustering algorithms, except the IIA throughput optimal clustering from Chapter 3. The coalition formation algorithm performance is however very close to the IIA throughput optimal clustering algorithm performance. The grouping heuristic of [PH12], which is designed for the $\beta = 0$ case, is still better than the singleton cluster structure. Although the k -means algorithm of [CC14] is the best algorithm in [CC14], its performance is underwhelming in our context. This may be due to the fact that we are studying the cellular case, as the same implementation of the algorithm has been verified to perform well in the interference channel setting [BMB15, Figure 4].

In Figure 5.2b on page 92, we compare our proposed robust WMMSE algorithm with the precoding algorithm benchmarks. Our proposed robust WMMSE

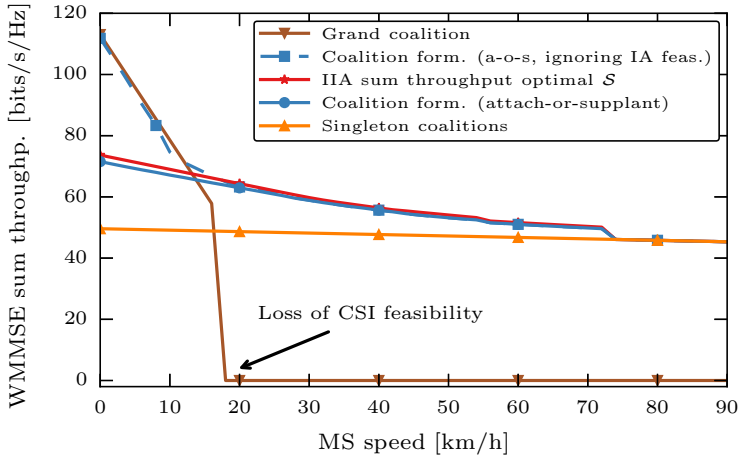
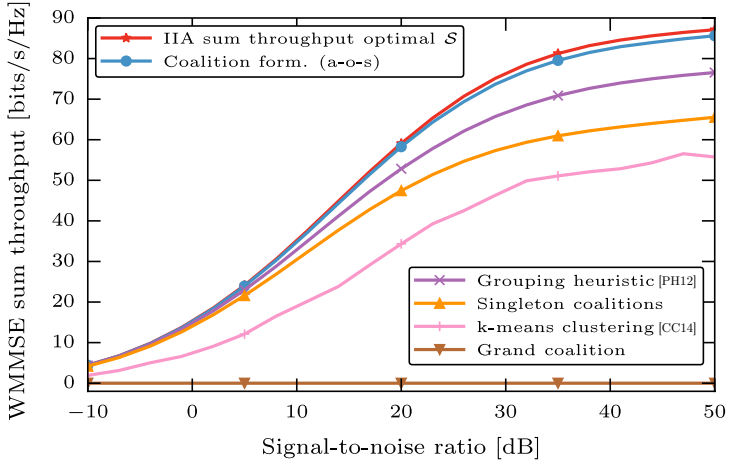


Figure 5.1. WMMSE sum throughput for different clustering algorithms when implicitly varying L_c through the proxy of MS speed.

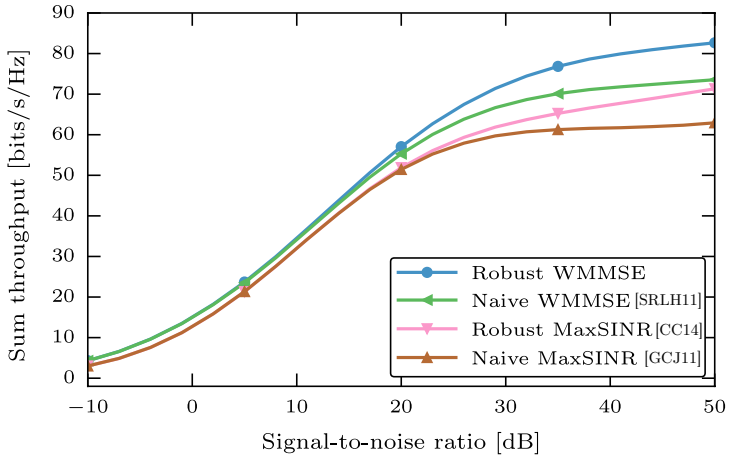
algorithm is superior to existing robust MaxSINR approach. Our method outperforms the benchmarks by between 10–25% at high SNR.

5.4 Conclusions

Although the assumption of intercluster interference alignment was useful for the derivation of the long-term throughput model in Chapter 4, in this chapter we have shown that a properly derived robust WMMSE algorithm can give further increases in sum throughputs. This comes at the cost of some intercluster message passing during the precoder design iterations however.



(a) Comparing clustering methods.



(b) Comparing precoding methods.

Figure 5.2. Comparison of methods when varying SNR.

Coordinated Precoding with Imperfect Channel State Information

In the previous chapters, we have been concerned with the clustering problem and how to design a robust coordinated precoding algorithm for a clustered multicell network. One major assumption in that line of work was the availability of CSI at the MSs and BSs. In order to focus on the core issues of clustering and CSI acquisition overhead, we did not consider the details of how the CSI was acquired. In this chapter, we instead consider the issue of CSI acquisition and robust coordinated precoding under CSI imperfections. We assume that the multicell network is not clustered, such that all BSs can coordinate with all other BSs.

The WMMSE algorithm (see Appendix 2.B), seems to be a good foundation for implementing a robust distributed coordinated precoding algorithm. As the first step in this chapter, we will therefore succinctly describe what local CSI is required by the nodes of the network to perform one iteration of the WMMSE algorithm. Many approaches can be imagined for obtaining this necessary CSI, e.g. using various combinations of channel estimation, feedback, signalling, backhaul usage, etc. Corresponding to different tradeoffs between these techniques, we will propose three different CSI acquisition methods with different levels of distributedness.

Given the acquired CSI, we will show that naively applying the original WMMSE algorithm leads to poor performance. This is because it was not designed with robustness against imperfect CSI in mind. We will therefore propose a robustified WMMSE algorithm, which retains the distributedness of the original algorithm. We will derive the local worst-case WMMSE optimization problems, and show that their solution structure is that of diagonal loading [CZO87]. The optimal amount of diagonal loading unfortunately depends on an unknown quantity. Therefore we propose alternate ways of selecting the diagonal loading levels; at the transmitters we introduce a transmit power scaling procedure, whereas at the receivers we enforce an invariant onto the receive filters and MSE weights.

6.1 Uplink/Downlink Model

The system model for the downlink transmissions in this chapter is the IBC from (2.2) on page 12:

$$\mathbf{y}_{i_k} = \mathbf{H}_{i_k i} \mathbf{V}_{i_k} \mathbf{x}_{i_k} + \sum_{\substack{j \in \mathcal{I}, l \in \mathcal{K}_j \\ (j,l) \neq (i,k)}} \mathbf{H}_{i_k j} \mathbf{V}_{j_l} \mathbf{x}_{j_l} + \mathbf{z}_{i_k}. \quad (6.1)$$

The CSI $\{\mathbf{H}_{i_k j}\}_{i \in \mathcal{I}, k \in \mathcal{K}_i, j \in \mathcal{I}}$ is not known a priori at the transceivers, and it must therefore be estimated before the coordinated precoding and data transmission can take place. The user weight¹ $\omega_{i_k} \in [0, 1]$ for MS i_k is however known at BS i .

In addition to the downlink transmission, communication also takes place in the uplink. Since the downlink is described by the IBC, the uplink is described by the *interfering multiple access channel* (IMAC). We will in the following assume that the system operates in a perfectly time-synchronized TDD mode, and that the corresponding radio hardware is perfectly calibrated [GSK05, RBP⁺14]. Under this assumption, the cascade of transmit hardware, wireless channel, and receiver hardware is reciprocal and the uplink channel from MS j_l to BS i is² $\overleftarrow{\mathbf{H}}_{j_l i} = \mathbf{H}_{j_l i}^T$. Let $\overleftarrow{\mathbf{s}}_{i_k}^* \sim \mathcal{CN}(\mathbf{0}, \overleftarrow{\mathbf{\Xi}}_{i_k})$ be the uplink transmitted signal from MS i_k and $\overleftarrow{\mathbf{z}}_i^* \sim \mathcal{CN}(\mathbf{0}, \varsigma_i^2 \mathbf{I}_{M_i})$ be the receiver noise at BS i . The received uplink signal at BS i is then modelled as

$$\overleftarrow{\mathbf{y}}_i^* = \sum_{k \in \mathcal{K}_i} \mathbf{H}_{i_k i}^T \overleftarrow{\mathbf{s}}_{i_k}^* + \sum_{\substack{j \in \mathcal{I} \setminus \{i\} \\ l \in \mathcal{K}_j}} \mathbf{H}_{j_l i}^T \overleftarrow{\mathbf{s}}_{j_l}^* + \overleftarrow{\mathbf{z}}_i^*. \quad (6.2)$$

For convenience, we will work with the complex conjugate version of the received signal in (6.2). The model we will use for the uplink is thus

$$\overleftarrow{\mathbf{y}}_i = (\overleftarrow{\mathbf{y}}_i^*)^* = \sum_{k \in \mathcal{K}_i} \mathbf{H}_{i_k i}^H \overleftarrow{\mathbf{s}}_{i_k} + \sum_{\substack{j \in \mathcal{I} \setminus \{i\} \\ l \in \mathcal{K}_j}} \mathbf{H}_{j_l i}^H \overleftarrow{\mathbf{s}}_{j_l} + \overleftarrow{\mathbf{z}}_i. \quad (6.3)$$

We will assume that the MSs have individual sum power constraints such that

$$\mathbb{E} \left(\|\overleftarrow{\mathbf{s}}_{i_k}\|_{\mathbb{F}}^2 \right) = \text{Tr} \left(\overleftarrow{\mathbf{\Xi}}_{i_k} \right) \leq \overleftarrow{\mathcal{P}}_{i_k}, \quad \forall i \in \mathcal{I}, k \in \mathcal{K}_i \quad (6.4)$$

holds on average per transmitted symbol. For the model in (6.3), the uplink signal-plus-interference covariance matrix for BS i is

$$\mathbf{\Gamma}_i = \sum_{j \in \mathcal{I}, l \in \mathcal{K}_j} \mathbf{H}_{j_l i}^H \overleftarrow{\mathbf{\Xi}}_{j_l} \mathbf{H}_{j_l i}. \quad (6.5)$$

¹In this chapter, the requirement that $0 \leq \omega_{i_k} \leq 1$ simplifies the power scaling in the uplink/downlink transmissions. The general case of unconstrained non-negative user weights can easily be transformed to this case, without loss of generality.

²The arrow $\overleftarrow{\cdot}$ denotes uplink quantities.

Table 6.1. Summary of CSI shorthands

Downlink	$\mathbf{F}_{i_k} = \mathbf{H}_{i_k i} \mathbf{V}_{i_k}$ $\Phi_{i_k} = \mathbf{F}_{i_k} \mathbf{F}_{i_k}^H + \Phi_{i_k}^{i+n}$ $\Phi_{i_k}^{i+n} = \sum_{\substack{j \in \mathcal{I}, l \in \mathcal{K}_j \\ (j,l) \neq (i,k)}} \mathbf{H}_{i_k j} \mathbf{V}_{j l} \mathbf{V}_{j l}^H \mathbf{H}_{i_k j}^H + \sigma_{i_k}^2 \mathbf{I}$
Uplink	$\mathbf{G}_{i_k} = \mathbf{H}_{i_k i}^H \mathbf{A}_{i_k}$ $\Gamma_i = \Gamma_i^{s+i} = \sum_{j \in \mathcal{I}, l \in \mathcal{K}_j} \mathbf{H}_{j l i}^H \mathbf{A}_{j l} \mathbf{A}_{j l}^H \mathbf{H}_{j l i}$

The MSs will estimate their local CSI using downlink pilot transmissions from the BSs, which then is used to form the MMSE receive filters and MSE weights. Conversely, the BSs will estimate their local CSI using uplink pilot transmissions from the MSs. Due to the assumed perfect reciprocity of the channel, this will provide the BSs with the information they need to form the precoders.

For the resource allocation, the WMMSE algorithm (see Algorithm 2.1 on page 43) will be used. As will be shown below, the WMMSE algorithm is an example of a distributed resource allocation method, which only requires local CSI at the participating nodes. Since we are assuming unclustered operation in this chapter, we disregard the pre-log factors $\{\alpha_{i_k}\}_{i \in \mathcal{I}, k \in \mathcal{K}_i}$ by letting them be set to unity for all users.

6.1.1 Adapted Notation for the WMMSE Algorithm

In order to lighten the forthcoming exposition, we first introduce some shorthands for the quantities involved in the WMMSE algorithm. For MS i_k , we define a *weighted receive filter* as $\mathbf{A}_{i_k} = \sqrt{\omega_{i_k}} \mathbf{U}_{i_k} \mathbf{W}_{i_k}^{1/2}$ and denote the *effective downlink channel* as $\mathbf{F}_{i_k} = \mathbf{H}_{i_k i} \mathbf{V}_{i_k}$. The *receive filter* can then be written as $\mathbf{U}_{i_k} = \Phi_{i_k}^{-1} \mathbf{F}_{i_k}$. Similarly, at BS i serving MS i_k , we have the *precoder* $\mathbf{V}_{i_k} = \sqrt{\omega_{i_k}} \mathbf{B}_{i_k} \mathbf{W}_{i_k}^{1/2}$ and the *effective uplink channel* $\mathbf{G}_{i_k} = \mathbf{H}_{i_k i}^H \mathbf{A}_{i_k}$. Finally, we have the *component precoder* $\mathbf{B}_{i_k} = (\Gamma_i + \mu_i \mathbf{I})^{-1} \mathbf{G}_{i_k}$. The CSI shorthands are summarized in Table 6.1. With these shorthands, we restate the WMMSE algorithm in Algorithm 6.1 on the next page.

It is obvious from Algorithm 6.1 that the WMMSE algorithm operates in two stages: one in which the MSs form their receive filters and MSE weights, and one in which the BSs form the precoders for their served MSs. In both stages, only local CSI is required at the corresponding nodes. The MSs need estimates of Φ_{i_k} and \mathbf{F}_{i_k} to form their filters. Similarly, the BSs need estimates of Γ_i , and estimates of \mathbf{G}_{i_k} for their correspondingly served MSs. The local CSI requirements are summarized in Table 6.2 on the following page. Assuming that this information is available, the filters can be formed in parallel over all MSs. The same goes for the precoders

Algorithm 6.1 WMMSE Algorithm [SRLH11] (Adapted to notation in Chapter 6)

- 1: **repeat**
 - At MS i_k :
 - 2: $\mathbf{W}_{i_k} = (\mathbf{I} - \mathbf{F}_{i_k}^H \Phi_{i_k}^{-1} \mathbf{F}_{i_k})^{-1}$
 - 3: $\mathbf{U}_{i_k} = \Phi_{i_k}^{-1} \mathbf{F}_{i_k}$, $\mathbf{A}_{i_k} = \sqrt{\omega_{i_k}} \mathbf{U}_{i_k} \mathbf{W}_{i_k}^{1/2}$
 - At BS i :
 - 4: Find μ_i which satisfies $\sum_{k \in \mathcal{K}_i} \|\mathbf{V}_{i_k}\|_F^2 \leq P_i$
 - 5: $\mathbf{B}_{i_k} = (\Gamma_i + \mu_i \mathbf{I})^{-1} \mathbf{G}_{i_k}$, $\mathbf{V}_{i_k} = \sqrt{\omega_{i_k}} \mathbf{B}_{i_k} \mathbf{W}_{i_k}^{1/2}$, $k \in \mathcal{K}_i$
 - 6: **until** convergence criterion met, or fixed number of iterations
-

Table 6.2. CSI needed at each network node to perform one iteration of the WMMSE algorithm

	Covariance matrix	Effective channel(s)	MSE weights
MS i_k	Φ_{i_k}	\mathbf{F}_{i_k}	—
BS i	Γ_i	$\{\mathbf{G}_{i_k}\}_{k \in \mathcal{K}_i}$	$\{\mathbf{W}_{i_k}^{1/2}\}_{k \in \mathcal{K}_i}$

at the BSs; no direct coordination is needed between them, and the precoders can be formed in parallel over BSs. Given local CSI, the WMMSE algorithm is thus an example of a distributed resource allocation method. The details of how the estimation will be performed will be described next.

6.2 Distributed CSI Acquisition

According to Table 6.2, MS i_k needs to know its effective channel from its serving BS \mathbf{F}_{i_k} as well as its signal-plus-interference-and-noise covariance matrix Φ_{i_k} . BS i needs to know the effective uplink channels $\{\mathbf{G}_{i_k}\}_{k \in \mathcal{K}_i}$ to the MSs it serves, the corresponding MSE weights $\{\mathbf{W}_{i_k}\}_{k \in \mathcal{K}_i}$, and the uplink signal-plus-interference covariance matrix Γ_i . There might be several methods useful for acquiring this local CSI. In this section, we will propose an estimation framework that can be used for the CSI acquisition. The estimation will be based on pilot transmissions in both the downlink and the uplink. Due to the assumed reciprocity of the network, the BSs will then be able to obtain their local CSI from the uplink pilot transmissions.

As the effective channels $\{\mathbf{F}_{i_k}\}_{i \in \mathcal{I}, k \in \mathcal{K}_i}$ and $\{\mathbf{G}_{i_k}\}_{i \in \mathcal{I}, k \in \mathcal{K}_i}$ change between iterations in the WMMSE algorithm, a training phase needs to be performed in between each WMMSE iteration. A simple schematic of the TDD transmission subframes that we envision can be seen in Figure 6.1 on the next page. The subframe is split between pilot transmission and data transmission, in both the uplink and downlink. Note that we assume data transmissions in all subframes.³ An illustration of the

³Before the iterative algorithm has converged, the data rates that are achievable in the down-

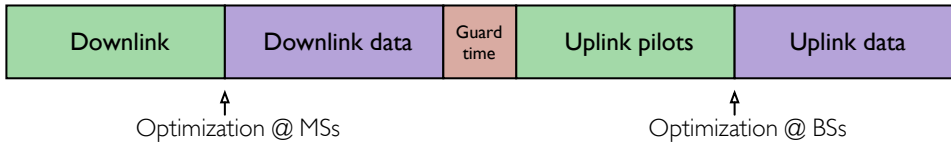


Figure 6.1. Schematic drawing of a subframe.

downlink/uplink CSI estimation process is shown in Figure 6.2 on the following page.

We will only focus on the downlink transmission optimization, but the proposed method can in principle be used for uplink transmission optimization as well. The training intervals would then need to be doubled, accommodating the corresponding uplink optimization training symbols.

6.2.1 Global Sharing of a Common Scale Factor

We will present three CSI acquisition schemes of varying levels of distributedness. All schemes require some form of coordination between the BSs, but the MSs only need to coordinate with their serving BSs. The scheme presented in this particular section is almost fully distributed over the participating nodes. The only level of coordination that is needed is the joint selection of a common power scaling parameter for the uplink pilot transmissions.

When a priori statistical information about the channel to be estimated is available, the MMSE estimator [BG06] is often used. In our case, we are interested in estimating effective channels, i.e. the product of the channel and a transmit filter. It is complicated to obtain a statistical characterization of the effective channels, and therefore we choose not to assign a prior distribution to the quantities to be estimated. That is, for the estimation we regard the effective channels as deterministic but unknown. With this perspective from classical estimation theory, it is easy to find the minimum variance unbiased (MVU) estimator.

Downlink Estimation

First, we will show how to estimate the effective downlink channel $\mathbf{F}_{i_k} = \mathbf{H}_{i_k i} \mathbf{V}_{i_k}$ using synchronous pilot transmissions. First, define orthogonal pilot sequences $\mathbf{P}_{i_k} \in \mathbb{C}^{d_{i_k} \times L_p}$, such that

$$\mathbf{P}_{i_k} \mathbf{P}_{j_l}^H = \begin{cases} L_p \mathbf{I}_{d_{i_k}} & (i, k) = (j, l) \\ \mathbf{0}_{d_{i_k} \times d_{j_l}} & (i, k) \neq (j, l) \end{cases}. \quad (6.6)$$

In order to fulfill the orthogonality requirement, $L_p \geq \sum_{j \in \mathcal{I}, l \in \mathcal{K}_j} d_{j_l}$ must hold. In the downlink training phase, BS i then transmits $\mathbf{s}_i = \sum_{k \in \mathcal{K}_i} \mathbf{V}_{i_k} \mathbf{P}_{i_k}$ such that the link data transmission phase may be low, but not negligible, as shown by numerical results in Section 6.5.

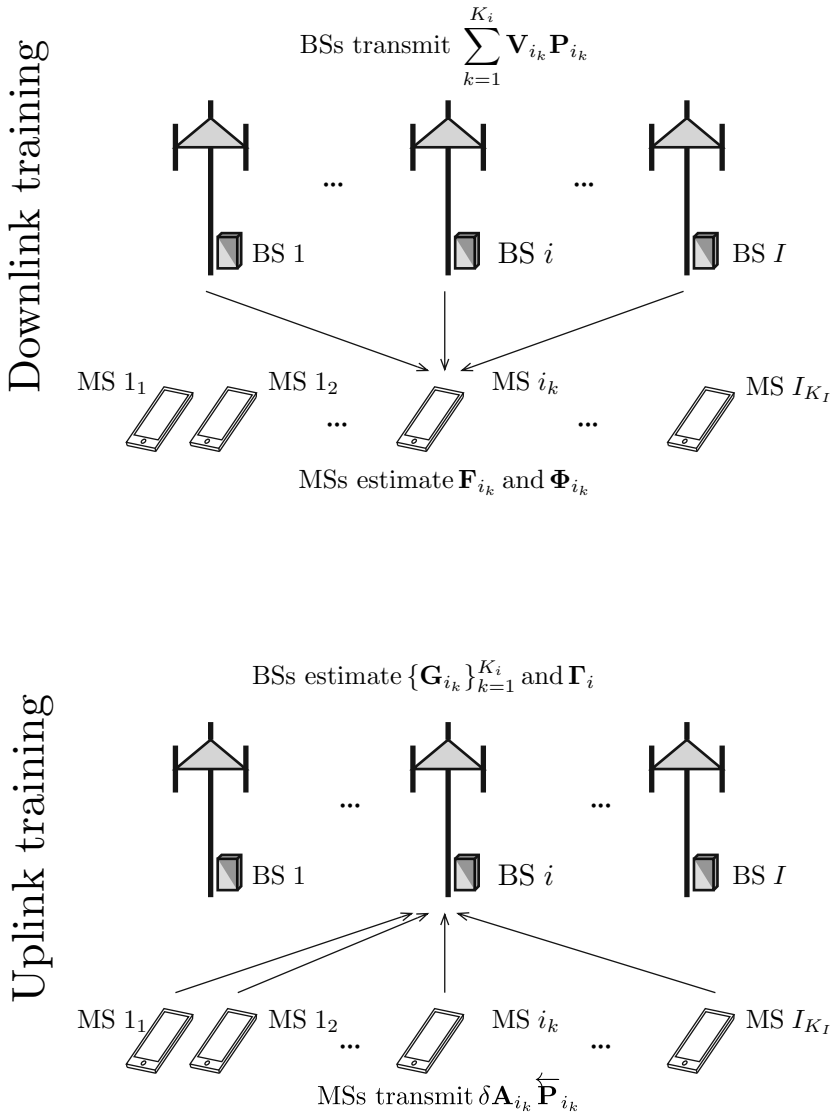


Figure 6.2. CSI estimation in one subframe (see Figure 6.1 on the preceding page). In each subframe, the downlink channels are estimated using pilots from the BSs. Later, the uplink channels are estimated using pilots from the MSs. Additionally, the MSs feed back their MSE weights to their serving BSs.

received signal at MS i_k is

$$\mathbf{Y}_{i_k} = \mathbf{H}_{i_k i} \mathbf{V}_{i_k} \mathbf{P}_{i_k} + \sum_{\substack{j \in \mathcal{I}, l \in \mathcal{K}_j \\ (j, l) \neq (i, k)}} \mathbf{H}_{i_k j} \mathbf{V}_{j l} \mathbf{P}_{j l} + \mathbf{Z}_{i_k}. \quad (6.7)$$

Notice that the power allocated to the pilots in (6.7) is the same as the power allocated to the data symbols in (2.2) on page 12. This is intentional, and will enable distributed and unbiased estimation of Φ_{i_k} . This type of pilot transmissions are called *MS-specific reference signals* in the LTE standard [DPS11].

Assuming that MS i_k knows its designated pilot \mathbf{P}_{i_k} , the problem of estimating \mathbf{F}_{i_k} is a deterministic parameter estimation problem in Gaussian noise. The MVU estimator is then [BG06]:

$$\hat{\mathbf{F}}_{i_k} = \frac{1}{L_p} \mathbf{Y}_{i_k} \mathbf{P}_{i_k}^H = \mathbf{H}_{i_k i} \mathbf{V}_{i_k} + \frac{1}{L_p} \mathbf{Z}_{i_k} \mathbf{P}_{i_k}^H. \quad (6.8)$$

The MVU estimator is an unbiased, efficient, and asymptotically consistent (in L_p) estimator of \mathbf{F}_{i_k} .

In addition to knowing \mathbf{F}_{i_k} , MS i_k also needs knowledge of Φ_{i_k} . This can be obtained from the sample covariance estimator:

$$\begin{aligned} \hat{\Phi}_{i_k} &= \frac{1}{L_p} \mathbf{Y}_{i_k} \mathbf{Y}_{i_k}^H \\ &= \sum_{j \in \mathcal{I}, l \in \mathcal{K}_j} (\mathbf{H}_{i_k j} \mathbf{V}_{j l} \mathbf{V}_{j l}^H \mathbf{H}_{i_k j}^H) + \frac{1}{L_p} \mathbf{Z}_{i_k} \mathbf{Z}_{i_k}^H \\ &\quad + \frac{1}{L_p} \sum_{j \in \mathcal{I}, l \in \mathcal{K}_j} (\mathbf{H}_{i_k j} \mathbf{V}_{j l} \mathbf{P}_{j l} \mathbf{Z}_{i_k}^H + \mathbf{Z}_{i_k} \mathbf{P}_{j l}^H \mathbf{V}_{j l}^H \mathbf{H}_{i_k j}^H). \end{aligned} \quad (6.9)$$

Note that the pilots $\{\mathbf{P}_{j l}\}_{j \in \mathcal{I}, l \in \mathcal{K}_j}$ are deterministic, and the channels $\{\mathbf{H}_{i_k j}\}_{i \in \mathcal{I}, k \in \mathcal{K}_i, j \in \mathcal{I}}$ are also treated as deterministic. Since the only stochastic component of \mathbf{Y}_{i_k} is \mathbf{Z}_{i_k} , the estimator in (6.9) is unbiased.

Uplink Estimation

The uplink estimation is performed in a similar fashion as the downlink estimation. Now the MSs each transmit a signal $\overleftarrow{\mathbf{S}}_{i_k} = \delta \mathbf{A}_{i_k} \overleftarrow{\mathbf{P}}_{i_k}$, where $\overleftarrow{\mathbf{P}}_{i_k} \in \mathbb{C}^{d_{i_k} \times \overleftarrow{L}_p}$ are orthogonal pilots, such that

$$\overleftarrow{\mathbf{P}}_{i_k} \overleftarrow{\mathbf{P}}_{j l}^H = \begin{cases} \overleftarrow{L}_p \mathbf{I}_{d_{i_k}} & (i, k) = (j, l) \\ \mathbf{0}_{d_{i_k} \times d_{j l}} & (i, k) \neq (j, l) \end{cases}. \quad (6.10)$$

In order to fulfill the orthogonality requirement, $\overleftarrow{L}_p \geq \sum_{j \in \mathcal{I}, l \in \mathcal{K}_j} d_{j l}$ must hold. As will be shown in Theorem 6.1 on page 113, for MS i_k it holds that

$$\|\mathbf{A}_{i_k}\|_{\mathbf{F}}^2 = \omega_{i_k} \left\| \mathbf{U}_{i_k} \mathbf{W}_{i_k}^{1/2} \right\|_{\mathbf{F}}^2 \leq \omega_{i_k} \frac{d_{i_k}}{\sigma_{i_k}^2}. \quad (6.11)$$

Based on this fact, the common scale factor δ can be set to make sure that the uplink transmit power constraints are satisfied for all MSs. We let

$$\delta_{i_k} = \sqrt{\frac{\overleftarrow{P}_{i_k} \sigma_{i_k}^2}{\omega_{i_k} d_{i_k}}}, \quad \forall i \in \mathcal{I}, k \in \mathcal{K}_i, \quad (6.12)$$

and set the common scale factor as $\delta = \min_{i_k} \delta_{i_k}$. The sum power constraint for MS i_k is then satisfied since

$$\begin{aligned} \|\overleftarrow{\mathbf{S}}_{i_k}\|_{\mathbb{F}}^2 &= \delta^2 \|\mathbf{A}_{i_k} \overleftarrow{\mathbf{P}}_{i_k}\|_{\mathbb{F}}^2 = \overleftarrow{L}_p \delta^2 \|\mathbf{A}_{i_k}\|_{\mathbb{F}}^2 \\ &= \overleftarrow{L}_p \min_{j_l} \left(\frac{\overleftarrow{P}_{j_l} \sigma_{j_l}^2}{\omega_{j_l} d_{j_l}} \right) \|\mathbf{A}_{i_k}\|_{\mathbb{F}}^2 \\ &\stackrel{(6.11)}{\leq} \overleftarrow{L}_p \min_{j_l} \left(\frac{\overleftarrow{P}_{j_l} \sigma_{j_l}^2}{\omega_{j_l} d_{j_l}} \right) \omega_{i_k} \frac{d_{i_k}}{\sigma_{i_k}^2} \\ &\leq \overleftarrow{L}_p \left(\frac{\overleftarrow{P}_{i_k} \sigma_{i_k}^2}{\omega_{i_k} d_{i_k}} \right) \omega_{i_k} \frac{d_{i_k}}{\sigma_{i_k}^2} = \overleftarrow{L}_p \overleftarrow{P}_{i_k}. \end{aligned} \quad (6.13)$$

MS i_k will only use its full power if it has equality in (6.11) and if $\delta = \delta_{i_k}$. For heterogenous scenarios, due to the minimization in δ , potentially only one MS will use its full power. This is the price to pay for enabling distributed estimation of $\mathbf{\Gamma}_i$ in the uplink.

Remark 6.1. *In order to determine δ , each MS can estimate its own δ_{i_k} and feed it back to its serving BS. The BSs can then jointly determine $\delta = \min_{i_k} \delta_{i_k}$. After the selected δ has been shared to the MSs from their serving BS, no more explicit coordination is needed. For static scenarios, where the data stream allocation and transmit and noise powers do not change, δ only needs to be computed once in a transmission interval. For symmetric scenarios, where $\delta = \delta_{i_k}, \forall i_k$, no coordination is necessary, and the CSI acquisition can be performed in a fully distributed manner.*

Assuming synchronized pilot transmissions from the MSs, the received signal at BS i during the uplink training phase is

$$\overleftarrow{\mathbf{Y}}_i = \delta \sum_{k \in \mathcal{K}_i} \mathbf{H}_{i_k i}^H \mathbf{A}_{i_k} \overleftarrow{\mathbf{P}}_{i_k} + \delta \sum_{\substack{j \in \mathcal{I} \setminus \{i\} \\ l \in \mathcal{K}_j}} \mathbf{H}_{j_l i}^H \mathbf{A}_{j_l} \overleftarrow{\mathbf{P}}_{j_l} + \overleftarrow{\mathbf{Z}}_i. \quad (6.14)$$

Similarly to the downlink, the uplink effective channel MVU estimator is

$$\widehat{\mathbf{G}}_{i_k} = \frac{1}{\delta \overleftarrow{L}_p} \overleftarrow{\mathbf{Y}}_i \overleftarrow{\mathbf{P}}_{i_k}^H = \mathbf{H}_{i_k i}^H \mathbf{A}_{i_k} + \frac{1}{\delta \overleftarrow{L}_p} \overleftarrow{\mathbf{Z}}_i \overleftarrow{\mathbf{P}}_{i_k}^H. \quad (6.15)$$

Furthermore, the signal-plus-interference-and-(scaled-)noise covariance matrix is estimated using the sample covariance method:

$$\begin{aligned}\widehat{\mathbf{\Gamma}}_i^{s+i+n} &= \frac{1}{\delta^2} \frac{1}{L_p} \overleftarrow{\mathbf{Y}}_i \overleftarrow{\mathbf{Y}}_i^H \\ &= \sum_{j \in \mathcal{I}, l \in \mathcal{K}_j} (\mathbf{H}_{jli}^H \mathbf{A}_{jl} \mathbf{A}_{jl}^H \mathbf{H}_{jli}) + \frac{1}{\delta^2} \frac{1}{L_p} \overleftarrow{\mathbf{Z}}_i \overleftarrow{\mathbf{Z}}_i^H \\ &\quad + \frac{1}{\delta} \frac{1}{L_p} \sum_{j \in \mathcal{I}, l \in \mathcal{K}_j} \left(\mathbf{H}_{jli}^H \mathbf{A}_{jl} \overleftarrow{\mathbf{P}}_{jl} \overleftarrow{\mathbf{Z}}_i^H + \overleftarrow{\mathbf{Z}}_i \overleftarrow{\mathbf{P}}_{jl}^H \mathbf{A}_{jl}^H \mathbf{H}_{jli} \right).\end{aligned}\tag{6.16}$$

Unless $\delta = 1$, this is a biased estimator of the signal-plus-interference-and-noise covariance matrix in the uplink. The WMMSE algorithm however needs an estimate of $\mathbf{\Gamma}_i = \mathbf{\Gamma}_i^{s+i}$, without the noise covariance part of $\mathbf{\Gamma}_i^{s+i+n}$. In Section 6.3.3, we resolve this issue by modifying the WMMSE algorithm.

MSE Weight Feedback

According to Algorithm 6.1 on page 96, the precoders are formed as

$$\mathbf{V}_{i_k} = \sqrt{\omega_{i_k}} \mathbf{B}_{i_k} \mathbf{W}_{i_k}^{1/2} = \omega_{i_k} (\mathbf{\Gamma}_i + \mu_i \mathbf{I})^{-1} \mathbf{H}_{i_k i}^H \mathbf{U}_{i_k} \mathbf{W}_{i_k}, \quad \forall i \in \mathcal{I}, k \in \mathcal{K}_i, \tag{6.17}$$

at the BSs, assuming perfect CSI. To form the precoders as in (6.17), the product $\omega_{i_k} \mathbf{H}_{i_k i}^H \mathbf{U}_{i_k} \mathbf{W}_{i_k} = \sqrt{\omega_{i_k}} \mathbf{G}_{i_k} \mathbf{W}_{i_k}^{1/2}$ is needed. This quantity is however not directly provided by the proposed estimation scheme. It could be independently estimated in a second uplink estimation phase, but instead we let MS i_k explicitly feed back \mathbf{W}_{i_k} to its serving BS i . Together with $\widehat{\mathbf{G}}_{i_k}$ in (6.15), BS i can then form $\widehat{\mathbf{G}}_{i_k} \mathbf{W}_{i_k}^{1/2}$ and use that in⁴ (6.17). The reason for this procedure is to avoid *signal cancellation* [Cox73], where a small mismatch between the estimate of $\mathbf{G}_{i_k} \mathbf{W}_{i_k}^{1/2}$ and the estimate of $\mathbf{\Gamma}_i$ can have a large detrimental impact on performance. If \mathbf{G}_{i_k} and $\mathbf{\Gamma}_i$ are estimated using the same pilot transmissions, as in (6.15) and (6.16), we can decompose

$$\widehat{\mathbf{\Gamma}}_i^{s+i+n} = \widehat{\mathbf{\Gamma}}_i^{i+n} + \widehat{\mathbf{G}}_{i_k} \widehat{\mathbf{G}}_{i_k}^H. \tag{6.18}$$

Then, there is no mismatch between $\widehat{\mathbf{G}}_{i_k}$ and $\widehat{\mathbf{\Gamma}}_i$ and consequently no mismatch between $\widehat{\mathbf{G}}_{i_k} \mathbf{W}_{i_k}^{1/2}$ and $\widehat{\mathbf{\Gamma}}_i$. Therefore, signal cancellation does not occur [Cox73].

Note that $r_{i_k} = \log_2 \det(\mathbf{W}_{i_k}) = \sum_{n=1}^{d_{i_k}} \log_2(\lambda_n(\mathbf{W}_{i_k}))$. Thus, feedback of \mathbf{W}_{i_k} implicitly constitutes a *rate request* for each stream for MS i_k , describing what rate that stream can handle under the current network conditions.

Remark 6.2. *The CSI acquisition proposed in this section is fully distributed, except for the selection of δ . Due to the channel reciprocity, all nodes are able to estimate their local CSI from the pilot transmissions. MS i_k feeds back \mathbf{W}_{i_k} to its serving BS, but the BSs do not need to share the MSE weights over the backhaul.*

⁴Recall that ω_{i_k} is assumed a priori known at BS i .

6.2.2 Global Sharing of Individual Scale Factors

In the previous section, an almost fully distributed CSI acquisition scheme was proposed. In order to perform the estimation of $\mathbf{\Gamma}_i$ in a fully distributed manner at the BSs, all MSs had to use a common power scaling δ . For heterogenous settings, with different δ_{i_k} over the different MSs, that meant that some MSs might not satisfy their uplink pilot power constraint with equality, meaning decreased estimation performance. In this section, we relax the requirement of fully distributed estimation of $\mathbf{\Gamma}_i$ at the BSs in order to improve the estimation SNRs. We keep the distributed downlink pilot transmission phase the same as in Section 6.2, as well as the MSE weight feedback, but modify the uplink pilot transmission phase.

Uplink Estimation

Letting $\hat{\mathbf{S}}_{i_k} = \frac{\sqrt{\hat{P}_{i_k}}}{\|\mathbf{A}_{i_k}\|_F} \mathbf{A}_{i_k} \hat{\mathbf{P}}_{i_k}$, the uplink sum power constraint in (6.4) on page 94 is met with equality for MS i_k . The received signal at BS i is then

$$\hat{\mathbf{Y}}_i = \sum_{k \in \mathcal{K}_i} \frac{\sqrt{\hat{P}_{i_k}}}{\|\mathbf{A}_{i_k}\|_F} \mathbf{H}_{i_k}^H \mathbf{A}_{i_k} \hat{\mathbf{P}}_{i_k} + \sum_{j \in \mathcal{I} \setminus \{i\}, l \in \mathcal{K}_j} \frac{\sqrt{\hat{P}_{j_l}}}{\|\mathbf{A}_{j_l}\|_F} \mathbf{H}_{j_l}^H \mathbf{A}_{j_l} \hat{\mathbf{P}}_{j_l} + \hat{\mathbf{Z}}_i. \quad (6.19)$$

Assuming that the individual scale factors $\left\{ \frac{\|\mathbf{A}_{i_k}\|_F}{\sqrt{\hat{P}_{i_k}}} \right\}_{i \in \mathcal{I}, k \in \mathcal{K}_i}$ are fed back from the MSs to their serving BSs and then globally shared over the BS backhaul, BS i can estimate the effective channels from MS j_l as

$$\hat{\mathbf{G}}_{j_l i} = \frac{\|\mathbf{A}_{j_l}\|_F}{\sqrt{\hat{P}_{j_l}}} \hat{\mathbf{Y}}_i \hat{\mathbf{P}}_{j_l}^H = \mathbf{H}_{j_l}^H \mathbf{A}_{j_l} + \frac{\|\mathbf{A}_{j_l}\|_F}{\sqrt{\hat{P}_{j_l}}} \hat{\mathbf{Z}}_i \hat{\mathbf{P}}_{j_l}^H. \quad (6.20)$$

Since the scaled pilots effectively all have the same weight, the sample covariance estimator of $\mathbf{\Gamma}_i$ in (6.16) cannot be used. Instead, we rely on the biased estimator

$$\begin{aligned} \hat{\mathbf{\Gamma}}_i^{s+i+n} &= \sum_{j \in \mathcal{I}, l \in \mathcal{K}_j} \hat{\mathbf{G}}_{j_l i} \hat{\mathbf{G}}_{j_l i}^H \\ &= \sum_{j \in \mathcal{I}, l \in \mathcal{K}_j} (\mathbf{H}_{j_l}^H \mathbf{A}_{j_l} \mathbf{A}_{j_l}^H \mathbf{H}_{j_l}^i) + \frac{1}{\hat{L}_p} \hat{\mathbf{Z}}_i \left(\frac{1}{\hat{L}_p} \sum_{j \in \mathcal{I}, l \in \mathcal{K}_j} \frac{\|\mathbf{A}_{j_l}\|_F^2}{\hat{P}_{j_l}} \hat{\mathbf{P}}_{j_l}^H \hat{\mathbf{P}}_{j_l} \right) \hat{\mathbf{Z}}_i^H \\ &\quad + \frac{1}{\hat{L}_p} \sum_{j \in \mathcal{I}, l \in \mathcal{K}_j} \frac{\|\mathbf{A}_{j_l}\|_F}{\sqrt{\hat{P}_{j_l}}} \left(\mathbf{H}_{j_l}^H \mathbf{A}_{j_l} \hat{\mathbf{P}}_{j_l} \hat{\mathbf{Z}}_i^H + \hat{\mathbf{Z}}_i \hat{\mathbf{P}}_{j_l}^H \mathbf{A}_{j_l}^H \mathbf{H}_{j_l}^i \right). \end{aligned} \quad (6.21)$$

The bias is determined by the individual scale factors $\left\{ \frac{\|\mathbf{A}_{j_l}\|_F^2}{\hat{P}_{j_l}} \right\}_{j \in \mathcal{I}, l \in \mathcal{K}_j}$ and the pilots length \hat{L}_p .

This estimation scheme is similar to one proposed in [KTJ13]. There, a scaled version of \mathbf{U}_{i_k} was used as the uplink precoder. Then, the MSE weights \mathbf{W}_{i_k} can be calculated at the serving BSs and do not need to be fed back. However, in order for the BSs to estimate $\tilde{\mathbf{F}}_i^{s+i+n}$ in that estimation scheme, they must exchange the MSE weights for their corresponding MSs over the backhaul. In essence, reduced over-the-air feedback has been traded for more backhaul use.

Remark 6.3. *The CSI acquisition proposed in this section is fully distributed over the MSs, but not over the BSs. Each BS needs knowledge of the individual scale factors for all MSs.*

6.2.3 Global Sharing of Filters

Finally, we present a CSI acquisition scheme which relies even further on feedback and backhaul. Here, only the underlying channels are estimated exploiting the reciprocity, but the receive filters, MSE weights, and precoders are fed back. With the subframe structure in Figure 6.1 on page 97, this means that consecutive training phases can be used to monotonically improve the channel estimates in one coherence block of the channel.⁵

Downlink Estimation

Let $\mathbf{P}_j \in \mathbb{C}^{M_j \times L_p}$ be orthogonal pilots sent from BS j such that

$$\mathbf{P}_i \mathbf{P}_j^H = \begin{cases} L_p \mathbf{I}_{M_i} & i = j \\ \mathbf{0}_{M_i \times M_j} & i \neq j \end{cases}. \quad (6.22)$$

As usual, $L_p \geq \sum_{i \in \mathcal{I}} M_i$ is needed for orthogonality reasons. For the downlink, with a transmitted signal $\mathbf{s}_i = \mathbf{P}_i$ at BS i , the received training signal at MS i_k would be

$$\mathbf{Y}_{i_k} = \sqrt{\frac{P_i}{K_i M_i}} \mathbf{H}_{i_k i} \mathbf{P}_i + \sum_{\substack{j \in \mathcal{I}, l \in \mathcal{K}_j \\ (j,l) \neq (i,k)}} \sqrt{\frac{P_j}{K_j M_j}} \mathbf{H}_{i_k j} \mathbf{P}_j + \mathbf{Z}_{i_k}. \quad (6.23)$$

This type of pilot transmissions are called *cell-specific reference signals* in the LTE standard [DPS11].

The precoder is assumed to be fed back to the MSs, and the goal is therefore only to estimate the channels. We can therefore use Bayesian methods for the estimation. For example, assuming i.i.d. Rayleigh fading such that

$$\text{vec}(\mathbf{H}_{i_k j}) \sim \mathcal{CN}\left(0, \mathbf{I}_{N_{i_k} \times M_j}\right), \quad (6.24)$$

⁵This can be done using iterative techniques, see e.g. [Kay93, Chapter 12.6].

the MMSE estimator of the channel from BS j to MS i_k is [BG06]

$$\widehat{\mathbf{H}}_{i_k j} = \frac{\sqrt{\frac{P_j}{K_j M_j}}}{L_p \frac{P_j}{K_j M_j} + \sigma_{i_k}^2} \mathbf{Y}_{i_k} \mathbf{P}_{j_l}^H. \quad (6.25)$$

Then, assuming that all precoders $\{\mathbf{V}_{j_l}\}_{j \in \mathcal{I}, l \in \mathcal{K}_j}$ have been fed back to MS i_k , and that $\sigma_{i_k}^2$ is known, it can form

$$\widehat{\mathbf{F}}_{i_k} = \widehat{\mathbf{H}}_{i_k i} \mathbf{V}_{i_k}, \quad (6.26)$$

$$\widehat{\mathbf{\Phi}}_{i_k} = \sum_{j \in \mathcal{I}, l \in \mathcal{K}_j} \widehat{\mathbf{H}}_{i_k j} \mathbf{V}_{j_l} \mathbf{V}_{j_l}^H \widehat{\mathbf{H}}_{i_k j}^H + \sigma_{i_k}^2 \mathbf{I}. \quad (6.27)$$

Uplink Estimation

A similar procedure is used in the uplink. The weighted receive filters and MSE weights from MS i_k is fed back to BS i , and the BSs then share their information over the backhaul.

Let $\overleftarrow{\mathbf{P}}_{j_l} \in \mathbb{C}^{N_{i_k} \times \overleftarrow{L}_p}$ be orthogonal pilots, assuming $\overleftarrow{L}_p \geq \sum_{j \in \mathcal{I}, l \in \mathcal{K}_j} N_{j_l}$, such that

$$\overleftarrow{\mathbf{P}}_{i_k} \overleftarrow{\mathbf{P}}_{j_l}^H = \begin{cases} \overleftarrow{L}_p \mathbf{I}_{N_{i_k}} & (i, k) = (j, l) \\ \mathbf{0}_{N_{i_k} \times N_{j_l}} & (i, k) \neq (j, l) \end{cases}. \quad (6.28)$$

Given a transmitted signal $\overleftarrow{\mathbf{s}}_{i_k} = \overleftarrow{\mathbf{P}}_{i_k}$ from MS i_k , the received signal at BS i in the uplink training phase is then

$$\overleftarrow{\mathbf{Y}}_i = \sum_{k \in \mathcal{K}_i} \sqrt{\frac{\overleftarrow{P}_{i_k}}{N_{i_k}}} \mathbf{H}_{i_k i}^H \overleftarrow{\mathbf{P}}_{i_k} + \sum_{j \in \mathcal{I} \setminus \{i\}, l \in \mathcal{K}_j} \sqrt{\frac{\overleftarrow{P}_{j_l}}{N_{j_l}}} \mathbf{H}_{j_l i}^H \overleftarrow{\mathbf{P}}_{j_l} + \overleftarrow{\mathbf{Z}}_i. \quad (6.29)$$

The MMSE estimator of the uplink channel from MS j_l to BS i is

$$\widehat{\mathbf{H}}_{j_l i}^H = \frac{\sqrt{\frac{\overleftarrow{P}_{j_l}}{N_{j_l}}}}{\overleftarrow{L}_p \frac{\overleftarrow{P}_{j_l}}{N_{j_l}} + \varsigma_i^2} \overleftarrow{\mathbf{Y}}_i \overleftarrow{\mathbf{P}}_{j_l}^H. \quad (6.30)$$

With the estimated uplink channels, together with perfect knowledge of all weighted receive filters $\{\mathbf{A}_{j_l}\}_{j \in \mathcal{I}, l \in \mathcal{K}_j}$, BS i can form

$$\widehat{\mathbf{G}}_{i_k} = \widehat{\mathbf{H}}_{i_k i}^H \mathbf{A}_{i_k}, \quad \forall k \in \mathcal{K}_i \quad (6.31)$$

$$\widehat{\mathbf{\Gamma}}_i = \sum_{j \in \mathcal{I}, l \in \mathcal{K}_j} \widehat{\mathbf{H}}_{j_l i}^H \mathbf{A}_{j_l} \mathbf{A}_{j_l}^H \widehat{\mathbf{H}}_{j_l i}. \quad (6.32)$$

The estimation procedure presented in this section requires significant feedback and signalling of filters among BSs and MSs in every subframe in order to form the

effective channels and covariance matrices. This method is still important however, since the state-of-the-art robust WMMSE algorithms in [NGS12, SM12, LKY13, RBCL13] require this type of channel estimation.

Remark 6.4. *The CSI acquisition proposed in this section is centralized. It requires significant feedback and sharing of filters among BSs and MSs in every subframe. In terms of estimating the underlying channels $\{\mathbf{H}_{i_k,j}\}$, it is however distributed over the BSs and MSs.*

6.2.4 Feedback Requirements and Complexity

The proposed CSI acquisition schemes in Section 6.2.1 to Section 6.2.3 have vastly different feedback loads. We compare these in Table 6.4 on the following page.

The computational complexities [TB97] of forming the channel estimates are given in Table 6.3. For simplicity, the expressions are shown for a symmetric network. The $NMI(L_p + \overleftarrow{L}_p)$ term in the Section 6.2.3 estimation method flop count dominates all other terms when the number of pilots is large. An illustration of this will be given in the numerical results of Section 6.5.

Table 6.3. Total estimation complexity, per iteration and MS

Method	Approximate number of flops
Section 6.2.1	$(Nd + N^2)L_p + Md\overleftarrow{L}_p + M^2\overleftarrow{L}_p/K$
Section 6.2.2	$(Nd + N^2)L_p + (Md\overleftarrow{L}_p + M^2d + M^2)I$
Section 6.2.3	$NMI(L_p + \overleftarrow{L}_p) + (NMc + N^2d + N^2)K + (NMc + M^2d + M^2)I$

6.2.5 Quantized Feedback of MSE Weights

In the proposed CSI acquisition schemes in Section 6.2.1 and Section 6.2.2, feedback of the MSE weights is needed. In practical applications, quantized feedback should be employed to reduce the overhead of the feedback. Since \mathbf{W}_{i_k} is positive definite, it has an eigenvalue decomposition, which can be quantized and fed back to the serving BS. The eigenvectors can e.g. be quantized using Grassmannian subspace packing [LH05]. For the quantization of the eigenvalues, we have the following helpful lemma:

Lemma 6.1. *The eigenvalues of the MSE weight for MS i_k are bounded as $1 \leq \lambda_n(\mathbf{W}_{i_k}) \leq 1 + \frac{P_i s_{max}^2(\mathbf{H}_{i_k,i})}{\sigma_{i_k}^2}$, $\forall n \in \{1, \dots, d_{i_k}\}$, where $s_{max}(\cdot)$ is the largest singular value of the matrix argument.*

Table 6.4. Feedback and estimation needed for the different methods

Method	Globally shared common scale parameter (Section 6.2.1)	Globally shared individual scale parameters (Section 6.2.2)	Globally shared filters (Section 6.2.3)
Estimated at MS i_k	$\Phi_{i_k}, \mathbf{F}_{i_k}$	$\Phi_{i_k}, \mathbf{F}_{i_k}$	$\{\mathbf{H}_{i_k j}\}_{j \in \mathcal{I}}^{(a)}$
BS i feedback to served MS i_k	$\omega_{i_k}^{(b)}$	$\omega_{i_k}^{(b)}$	$\omega_{i_k}^{(b)},$ $\{\mathbf{V}_{j_l}\}_{j \in \mathcal{I}, l \in \mathcal{K}_j}$
Estimated at BS i	$\Gamma_i, \{\mathbf{G}_{i_k}\}_{k \in \mathcal{K}_i}$	$\{\mathbf{G}_{j_l i}\}_{j \in \mathcal{I}, l \in \mathcal{K}_j}$	$\{\mathbf{H}_{j_l i}^H\}_{j \in \mathcal{I}, l \in \mathcal{K}_j}^{(a)}$
MS i_k feedback to serving BS i	$\mathbf{W}_{i_k}, \delta_{i_k}$	$\ \mathbf{A}_{i_k}\ _F, \mathbf{W}_{i_k}$	$\mathbf{A}_{i_k}, \mathbf{W}_{i_k}$
Shared over BS backhaul	$\{\delta_{j_l}\}_{j \in \mathcal{I}, l \in \mathcal{K}_j}^{(c)}$	$\left\{ \frac{\sqrt{P_{j_l}}}{\ \mathbf{A}_{j_l}\ _F} \right\}_{j \in \mathcal{I}, l \in \mathcal{K}_j}^{(d)}$	$\{\mathbf{A}_{j_l}\}_{j \in \mathcal{I}, l \in \mathcal{K}_j}^{(d)}$ $\{\mathbf{V}_{j_l}\}_{j \in \mathcal{I}, l \in \mathcal{K}_j}^{(d)}$

(a) The estimated quantities for the method in Section 6.2.3 do not change within one coherence block, and can therefore be improved upon in every iteration. This is contrary to the the estimated quantities for the methods in Section 6.2.1 and Section 6.2.2, which depend on the precoders and receive filters and therefore must be re-estimated in every iteration.

(b) The user priorities only need to be fed back if/when they are changed.

(c) The quantities $\delta_{j_l} = \sqrt{\frac{P_{j_l} \sigma_{j_l}^2}{\omega_{j_l} d_{j_l}}}$ only need to be shared among BSs whenever some of the involved variables change. For static conditions, they only need to be shared once.

(d) These quantities must be shared over the BS backhaul in each iteration.

Proof: For MS i_k it holds that $\Phi_{i_k}^{i+n} \succeq \sigma_{i_k}^2 \mathbf{I}$, with equality if the MS does not experience any interference. Thus, the MSE weight for that MS satisfies

$$\mathbf{W}_{i_k} = \mathbf{I} + \mathbf{V}_{i_k}^H \mathbf{H}_{i_k}^H (\Phi_{i_k}^{i+n})^{-1} \mathbf{H}_{i_k} \mathbf{V}_{i_k}, \quad (6.33)$$

$$\preceq \mathbf{I} + \frac{1}{\sigma_{i_k}^2} \mathbf{V}_{i_k}^H \mathbf{H}_{i_k}^H \mathbf{H}_{i_k} \mathbf{V}_{i_k}. \quad (6.34)$$

Now introduce the spectral norm $\|\mathbf{D}\|_2 = \max_{\mathbf{c}} \frac{\|\mathbf{D}\mathbf{c}\|_2}{\|\mathbf{c}\|_2} = s_{\max}(\mathbf{D})$, where $s_{\max}(\mathbf{D})$ is the largest singular value of \mathbf{D} . Then, for all \mathbf{c}_{i_k} such that $\|\mathbf{c}_{i_k}\|_2 = 1$, we have that

$$\begin{aligned} \mathbf{c}_{i_k}^H \mathbf{V}_{i_k}^H \mathbf{H}_{i_k}^H \mathbf{H}_{i_k} \mathbf{V}_{i_k} \mathbf{c}_{i_k} &\leq \|\mathbf{V}_{i_k} \mathbf{c}_{i_k}\|_2^2 \cdot \lambda_{\max}(\mathbf{H}_{i_k}^H \mathbf{H}_{i_k}) \\ &= \|\mathbf{V}_{i_k} \mathbf{c}_{i_k}\|_2^2 \cdot s_{\max}^2(\mathbf{H}_{i_k}) \leq \|\mathbf{V}_{i_k}\|_2^2 \cdot \|\mathbf{c}_{i_k}\|_2^2 \cdot s_{\max}^2(\mathbf{H}_{i_k}) \\ &= \|\mathbf{V}_{i_k}\|_2^2 \cdot s_{\max}^2(\mathbf{H}_{i_k}) \leq \|\mathbf{V}_{i_k}\|_F^2 \cdot s_{\max}^2(\mathbf{H}_{i_k}) \leq P_i s_{\max}^2(\mathbf{H}_{i_k}). \end{aligned} \quad (6.35)$$

Thus, $\lambda_{\max}(\mathbf{V}_{i_k}^H \mathbf{H}_{i_k}^H \mathbf{H}_{i_k} \mathbf{V}_{i_k}) \leq P_i s_{\max}^2(\mathbf{H}_{i_k})$, and the upper bound then directly follows from (6.34). For the lower bound, note that

$$\mathbf{I} \preceq \mathbf{I} + \mathbf{V}_{i_k}^H \mathbf{H}_{i_k}^H (\Phi_{i_k}^{i+n})^{-1} \mathbf{H}_{i_k} \mathbf{V}_{i_k} = \mathbf{W}_{i_k}. \quad (6.36)$$

■

The consequence of Lemma 6.1 is that the eigenvalues of \mathbf{W}_{i_k} can be suitably quantized over

$$\left[1, 1 + \frac{P_i s_{\max}^2(\mathbf{H}_{i_k})}{\sigma_{i_k}^2} \right]. \quad (6.37)$$

We however leave the details of how to design such quantizers for future work.

As mentioned in Section 6.2.1, $r_{i_k} = \sum_n \log_2(\lambda_n(\mathbf{W}_{i_k}))$ can be seen as the data rate (summed over data streams) for MS i_k . Quantizing $\lambda_n(\mathbf{W}_{i_k})$ therefore corresponds to making a set of discrete rates available to the MS, corresponding to e.g. a set of different modulation and coding schemes. For a further treatment of this subject, see Chapter 8.

6.3 Inherent and Enforced Robustness

In this section, we propose some modifications to the original WMMSE algorithm that lead to an algorithm which is robustified against CSI estimation errors.

6.3.1 Naive WMMSE Algorithm with Estimated CSI

It is straightforward to naively feed the WMMSE algorithm the estimated CSI from one of the presented CSI acquisition methods. An example⁶ of the resulting

⁶The simulation settings are described in detail in Section 6.5.1.

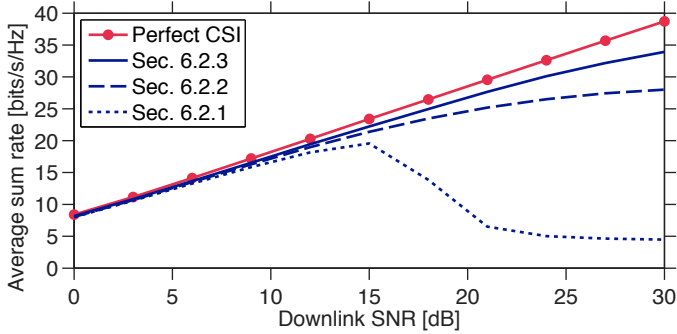


Figure 6.3. Sum rate performance when naively applying the WMMSE algorithm together with the proposed CSI acquisition schemes. The scenario was a symmetric IBC with $I = 3$, $K = 2$, $M = 4$, $N = 2$, and $d = 1$. The channels were i.i.d. Rayleigh fading, and the uplink SNR was set as $\overleftarrow{\text{SNR}} = \overleftarrow{P}/\zeta^2 = 10$ dB for all links. Note that the downlink SNR $= P/\sigma^2$ affects both the power constraint in the WMMSE algorithm, as well as the estimation performance in the downlink estimation, since the downlink pilots are precoded with the same precoders as used in the data transmission (see (6.7)).

performance can be seen in Figure 6.3. It is clear that the naive application of the WMMSE algorithm works moderately well for the centralized CSI acquisition schemes, but the performance for the fully distributed CSI acquisition scheme catastrophically deteriorates at high SNR. Thus, some form of robustification against CSI estimation errors is necessary.

6.3.2 General Worst-Case Robustness WMMSE Problem

One approach to robustifying the WMMSE optimization problem in (2.23) on page 41 is to minimize the objective function⁷ under the worst-case error conditions:

$$\begin{aligned}
 & \underset{\substack{\{\mathbf{U}_{i_k}\} \\ \{\mathbf{W}_{i_k} \succ \mathbf{0}\} \\ \{\mathbf{V}_{i_k}\}}} \text{minimize} & & \max_{\{\text{uncertainty}\}} & \sum_{i \in \mathcal{I}, k \in \mathcal{K}_i} \omega_{i_k} (\text{Tr}(\mathbf{W}_{i_k} \mathbf{E}_{i_k}) - \ln \det(\mathbf{W}_{i_k})) \\
 & \text{subject to} & & \sum_{k \in \mathcal{K}_i} \|\mathbf{V}_{i_k}\|_{\text{F}}^2 \leq P_i, \forall i \in \mathcal{I}.
 \end{aligned} \tag{6.38}$$

The proposed CSI acquisition methods provide estimates both of the downlink effective channels, as well as of the uplink effective channels. Due to the definition of these effective channels however, the general uncertainty set in (6.38) cannot be explicitly defined in terms of the uplink and downlink estimation errors simultaneously. For example, one of the terms in the objective function of (6.38) is

⁷Here we drop all constant terms for brevity.

$\omega_{i_k} \mathbf{W}_{i_k} \mathbf{U}_{i_k}^H \mathbf{H}_{i_k} \mathbf{V}_{i_k} = \sqrt{\omega_{i_k}} \mathbf{W}_{i_k}^{1/2} \mathbf{G}_{i_k}^H \mathbf{V}_{i_k} = \omega_{i_k} \mathbf{W}_{i_k} \mathbf{U}_{i_k}^H \mathbf{F}_{i_k}$, which cannot be written in terms of \mathbf{G}_{i_k} and \mathbf{F}_{i_k} simultaneously. In the forthcoming block coordinate descent, we will therefore solve (6.38) with the CSI uncertainty relating to the particular block of variables for which (6.38) is solved for. That is, for the precoders the CSI uncertainty at the BSs will be considered, whereas for the receive filters and MSE weights, the CSI uncertainty at the MSs will be considered. We now detail the block coordinate descent solutions for the three blocks of (6.38).

6.3.3 Precoder Robustness

First we fix $\{\mathbf{U}_{i_k}, \mathbf{W}_{i_k}\}_{i \in \mathcal{I}, k \in \mathcal{K}_i}$ and solve (6.38) with respect to the precoders $\{\mathbf{V}_{i_k}\}_{i \in \mathcal{I}, k \in \mathcal{K}_i}$. The optimization problem can then be interpreted as a local optimization problem at each BS, given that the CSI uncertainty in (6.38) comes from the uplink channel estimation phase. We let the estimation errors for BS i be $\tilde{\mathbf{\Gamma}}_i = \mathbf{\Gamma}_i - \hat{\mathbf{\Gamma}}_i^{\text{s}+i}$ and $\tilde{\mathbf{G}}_{i_k} = \mathbf{G}_{i_k} - \hat{\mathbf{G}}_{i_k}$, $\forall k \in \mathcal{K}_i$. For the local uncertainty set at BS i , we assume that the errors are norm bounded as $\|\tilde{\mathbf{\Gamma}}_i\|_{\text{F}} \leq \varepsilon_i^{(\text{BS})}$ and $\|\tilde{\mathbf{G}}_{i_k} \mathbf{W}_{i_k}^{1/2}\|_{\text{F}} \leq \xi_{i_k}^{(\text{BS})}$, $\forall k \in \mathcal{K}_i$. Note that $\xi_{i_k}^{(\text{BS})}$ depends on \mathbf{W}_{i_k} , which is fixed at BS i . The local worst-case optimization problem for BS i is then:

$$\begin{aligned} & \underset{\{\mathbf{V}_{i_k}\}_{k \in \mathcal{K}_i}}{\text{minimize}} && \max_{\substack{\|\tilde{\mathbf{\Gamma}}_i\|_{\text{F}} \leq \varepsilon_i^{(\text{BS})} \\ \|\tilde{\mathbf{G}}_{i_k} \mathbf{W}_{i_k}^{1/2}\|_{\text{F}} \leq \xi_{i_k}^{(\text{BS})}}} \sum_{k \in \mathcal{K}_i} \text{Tr} \left(\mathbf{v}_{i_k}^H \left(\hat{\mathbf{\Gamma}}_i^{\text{s}+i} + \tilde{\mathbf{\Gamma}}_i \right) \mathbf{v}_{i_k} \right) \\ & && - 2\sqrt{\omega_{i_k}} \text{Re} \left(\text{Tr} \left(\mathbf{W}_{i_k}^{1/2} \left(\hat{\mathbf{G}}_{i_k} + \tilde{\mathbf{G}}_{i_k} \right)^H \mathbf{v}_{i_k} \right) \right) \\ & \text{subject to} && \sum_{k \in \mathcal{K}_i} \|\mathbf{V}_{i_k}\|_{\text{F}}^2 \leq P_i, \forall i \in \mathcal{I}. \end{aligned} \quad (6.39)$$

The solution to the inner optimization problem of (6.39) can be found by extending the results of [SGLW03, ZSGL05] to the multiuser matrix case. By upper bounding the optimal value of the inner optimization problem using the triangle inequality⁸ and the submultiplicativity of the Frobenius norm, the (pessimistic) robust optimal precoder for MS i_k is

$$\mathbf{V}_{i_k}^{\text{rob}} = \sqrt{\omega_{i_k}} \left(\hat{\mathbf{\Gamma}}_i^{\text{s}+i} + \left(\varepsilon_i^{(\text{BS})} + \frac{\xi_{i_k}^{(\text{BS})}}{\|\mathbf{V}_{i_k}^{\text{rob}}\|_{\text{F}}} + \mu_i^{\text{rob}} \right) \mathbf{I} \right)^{-1} \hat{\mathbf{G}}_{i_k} \mathbf{W}_{i_k}^{1/2}. \quad (6.40)$$

As before, μ_i^{rob} is the Lagrange multiplier for the sum power constraint. Note that the robust precoder in (6.40) is *diagonally loaded* by a constant factor $\varepsilon_i^{(\text{BS})}$, a

⁸This relaxes the problem such that $\tilde{\mathbf{\Gamma}}_i$ is the worst for each MS simultaneously. This is equivalent to replacing the existing covariance constraint with $\|\tilde{\mathbf{\Gamma}}_{i_k}\|_{\text{F}} \leq \varepsilon_i^{(\text{BS})}$, $\forall k \in \mathcal{K}_i$, and changing the objective accordingly.

data dependent factor $\xi_{i_k}^{(\text{BS})} / \|\mathbf{V}_{i_k}^{\text{rob}}\|_{\text{F}}$, and the Lagrange multiplier μ_i^{rob} . Diagonal loading is well known to robustify beamformers in various settings, and a large body of literature has studied its robustifying effects; see e.g. [CZO87, Car88, WBM96, LSW03, VGL03, SGLW03, ZSGL05].

In order to construct the robust precoder in (6.40), the parameters $\varepsilon_i^{(\text{BS})}$ and $\xi_{i_k}^{(\text{BS})}$ must be known. For the fully distributed CSI estimation in Section 6.2.1, the effective channel error $\tilde{\mathbf{G}}_{i_k}$ follows a zero-mean Gaussian distribution with known covariance, and $\xi_{i_k}^{(\text{BS})}$ can thus be selected such that $\|\tilde{\mathbf{G}}_{i_k} \mathbf{W}_{i_k}^{1/2}\|_{\text{F}} \leq \xi_{i_k}^{(\text{BS})}$ holds with some probability. The statistics of the covariance error $\tilde{\mathbf{\Gamma}}_i$ however depend on the filters $\{\mathbf{U}_{j_l}\}_{j \in \mathcal{I}, l \in \mathcal{K}_j}$, which are unknown at BS i . Since the optimal amount of diagonal loading therefore is unknown, we subsequently propose to disregard $\varepsilon_i^{(\text{BS})}$ and $\xi_{i_k}^{(\text{BS})}$, and let the factor μ_i^{rob} handle all the diagonal loading. To compensate for the missing $\varepsilon_i^{(\text{BS})}$ and $\xi_{i_k}^{(\text{BS})}$, we implicitly amplify μ_i^{rob} using a scaling procedure.

Implicitly Selecting the Diagonal Loading Parameter

When applying diagonal loading for robustness, a heuristic often used in the literature [ZSGL05] is to select a fixed loading level around 10 dB over the noise level. Instead, we propose a data dependent method for selecting the diagonal loading parameter implicitly. We note that, given estimates $\hat{\mathbf{\Gamma}}_i^{\text{s}+i+\text{n}}$, $\hat{\mathbf{G}}_{i_k}$ and fed back \mathbf{W}_{i_k} , the precoders in the WMMSE algorithm are formed like

$$\mathbf{V}_{i_k} = \sqrt{\omega_{i_k}} \left(\hat{\mathbf{\Gamma}}_i^{\text{s}+i+\text{n}} + \mu_i \mathbf{I} \right)^{-1} \hat{\mathbf{G}}_{i_k} \mathbf{W}_{i_k}^{1/2}. \quad (6.41)$$

The form of (6.41) and (6.40) are similar, and it can therefore be concluded that μ_i alone acts as the diagonal loading for the naive WMMSE precoder in (6.41). The factor μ_i therefore robustifies the solution, and the amount of diagonal loading is determined by $\hat{\mathbf{\Gamma}}_i^{\text{s}+i+\text{n}}$, $\hat{\mathbf{G}}_{i_k} \mathbf{W}_{i_k}^{1/2}$ and P_i .

In order to artificially amplify the factor μ_i , we now introduce a scaling procedure. We let $0 \leq \vartheta \leq 1$ be a transmit power scale factor, and modify the WMMSE algorithm as follows:

1. In the precoder optimization at BS i (step 4 in Algorithm 6.1), let the sum power constraint be ϑP_i . The resulting precoders from (6.41) are denoted $\{\mathbf{V}_{i_k}^{(\vartheta)}\}_{i \in \mathcal{I}, k \in \mathcal{K}_i}$, and will have equal or higher diagonal loading level than the original precoder in (6.41), since μ_i is nonincreasing in the sum power constraint value.
2. Form scaled precoders $\mathbf{V}_{i_k} = \frac{1}{\sqrt{\vartheta}} \mathbf{V}_{i_k}^{(\vartheta)}$, $\forall i_k$, and use these for downlink pilot and data transmission. This scaling ensures that the correct transmit power is used.

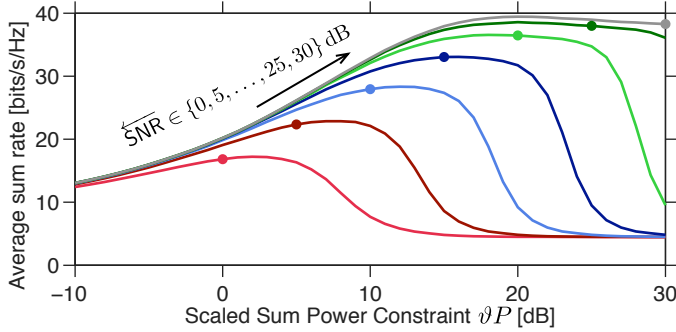


Figure 6.4. Sum rate performance when varying ϑ and $\overline{\text{SNR}} = \overline{P}/\zeta^2$, for fixed $P = 1000$ and $\sigma^2 = 1$. The solid markers represent the performance for $\vartheta = \min\left(\frac{\overline{P}/\zeta^2}{P/\sigma^2}, 1\right)$. The scenario is the same as in Figure 6.3 on page 108.

3. At the MSs, perform the estimation given the precoders $\{\mathbf{V}_{i_k}\}_{i \in \mathcal{I}, k \in \mathcal{K}_i}$, giving $\{\widehat{\mathbf{F}}_{i_k}^{(\vartheta)}\}_{i \in \mathcal{I}, k \in \mathcal{K}_i}$ and $\{\widehat{\Phi}_{i_k}^{(\vartheta)}\}_{i \in \mathcal{I}, k \in \mathcal{K}_i}$.
4. Scale the estimates as $\widehat{\Phi}_{i_k} = \vartheta \widehat{\Phi}_{i_k}^{(\vartheta)}$, $\widehat{\mathbf{F}}_{i_k} = \sqrt{\vartheta} \widehat{\mathbf{F}}_{i_k}^{(\vartheta)}$, $\forall i_k$, and use $\{\widehat{\Phi}_{i_k}\}_{i \in \mathcal{I}, k \in \mathcal{K}_i}$ and $\{\widehat{\mathbf{F}}_{i_k}\}_{i \in \mathcal{I}, k \in \mathcal{K}_i}$ to form receive filters and MSE weights. This scaling is necessary in order for the WMMSE algorithm at the MSs to be aware of what the original precoders $\{\mathbf{V}_{i_k}^{(\vartheta)}\}_{i \in \mathcal{I}, k \in \mathcal{K}_i}$ were.

The same scaling ϑ is used at all BSs, and therefore the signal-to-interference ratios of the interfering links are not affected. In Figure 6.4, we plot the impact of selecting different ϑ . A simple selection that appears to work well is $\vartheta = \min\left(\frac{\overline{P}/\zeta^2}{P/\sigma^2}, 1\right)$.

Removing the Noise Component of $\widehat{\Gamma}_i^{\text{s}+i+n}$

Comparing (6.41) with (6.17), it can be noted that the covariance matrix should be $\widehat{\Gamma}_i^{\text{s}+i}$, and not $\widehat{\Gamma}_i^{\text{s}+i+n}$. For the fully distributed CSI acquisition, the noise portion of $\widehat{\Gamma}_i^{\text{s}+i+n}$ will on average be $\frac{\zeta^2}{\delta^2} \mathbf{I}_{M_i}$, but simply subtracting that might make the resulting matrix indefinite. Instead, we modify μ_i to allow for *negative* values; this is the same as seeing μ_i as the difference of a non-negative Lagrange multiplier with an estimate of the noise power. Specifically, we allow $\mu_i \geq -\min\left(\frac{\zeta^2}{\delta^2}, \lambda_{\min}\left(\widehat{\Gamma}_i^{\text{s}+i+n}\right) - \zeta\right)$ where ζ is some constant value determining how close to singular $\widehat{\Gamma}_i^{\text{s}+i+n} + \mu_i \mathbf{I}$ can be.

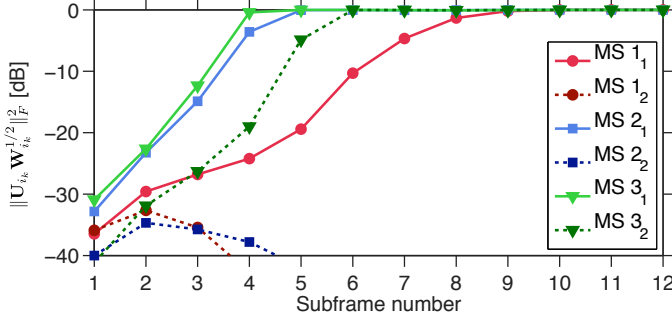


Figure 6.5. Example of convergence of $\left\| \mathbf{U}_{i_k} \mathbf{W}_{i_k}^{1/2} \right\|_{\text{F}}^2$ for $I = 3, K = 2, \text{SNR} = 30 \text{ dB}, d = d_{i_k} = 1, \forall i_k, \sigma^2 = \sigma_{i_k}^2 = 1, \forall i_k$. Note how 4 MSs get close to achieving the bound, and how the remaining 2 MSs are effectively turned off.

6.3.4 Receive Filter and MSE Weight Robustness

With similar notation and assumptions as the optimization problem in (6.39), the local worst-case optimization problem for the receive filter at MS i_k is

$$\begin{aligned} \underset{\mathbf{U}_{i_k}}{\text{minimize}} \quad & \max_{\substack{\left\| \tilde{\Phi}_{i_k} \right\|_{\text{F}} \leq \varepsilon_i^{(\text{MS})} \\ \left\| \tilde{\mathbf{F}}_{i_k} \mathbf{W}_{i_k}^{1/2} \right\|_{\text{F}} \leq \xi_{i_k}^{(\text{MS})}}} \text{Tr} \left(\mathbf{W}_{i_k} \left(\mathbf{I} + \mathbf{U}_{i_k}^{\text{H}} \left(\hat{\Phi}_{i_k} + \tilde{\Phi}_{i_k} \right) \mathbf{U}_{i_k} \right) \right) \\ & - 2 \text{Re} \left(\text{Tr} \left(\mathbf{W}_{i_k} \left(\hat{\mathbf{F}}_{i_k} + \tilde{\mathbf{F}}_{i_k} \right)^{\text{H}} \mathbf{U}_{i_k} \right) \right), \end{aligned} \quad (6.42)$$

whose (pessimistic) solution [ZSGL05] is

$$\mathbf{U}_{i_k}^{\text{rob}} = \left(\hat{\Phi}_{i_k} + \left(\varepsilon_i^{(\text{MS})} + \frac{\xi_{i_k}^{(\text{MS})}}{\left\| \mathbf{U}_{i_k}^{\text{rob}} \mathbf{W}_{i_k}^{1/2} \right\|_{\text{F}}} \right) \mathbf{I} \right)^{-1} \hat{\mathbf{F}}_{i_k}. \quad (6.43)$$

Finally, the corresponding (pessimistic) robust MSE weight is

$$\mathbf{W}_{i_k}^{\text{rob}} = \left(\mathbf{I} - \hat{\mathbf{F}}_{i_k}^{\text{H}} \left(\hat{\Phi}_{i_k} + \left(\varepsilon_i^{(\text{MS})} + \frac{\xi_{i_k}^{(\text{MS})}}{\left\| \mathbf{U}_{i_k}^{\text{rob}} \mathbf{W}_{i_k}^{1/2} \right\|_{\text{F}}} \right) \mathbf{I} \right)^{-1} \hat{\mathbf{F}}_{i_k} \right)^{-1}. \quad (6.44)$$

Again, the optimal level of diagonal loading is unknown. This is because $\varepsilon_i^{(\text{MS})}$ depends on the statistics of the covariance error $\tilde{\Phi}_{i_k} = \Phi_{i_k} - \hat{\Phi}_{i_k}$, which in turn depends on the unknown precoders $\{\mathbf{V}_{j_l}\}_{j \in \mathcal{I}, l \in \mathcal{K}_j}$. We therefore propose to indirectly apply diagonal loading at the MSs instead, based on the following observation:

Theorem 6.1. *The receive filter \mathbf{U}_{i_k} and MSE weight \mathbf{W}_{i_k} obtained in the MS side optimization of the WMMSE algorithm with perfect CSI satisfy $\|\mathbf{U}_{i_k} \mathbf{W}_{i_k}^{1/2}\|_{\text{F}}^2 = \text{Tr}\left(\left(\Phi_{i_k}^{i+n}\right)^{-1} - \Phi_{i_k}^{-1}\right) \leq d_{i_k}/\sigma_{i_k}^2$. If the effective channel is fully contained in an interference-free subspace of dimension $\tilde{d}_{i_k} \leq d_{i_k}$, then asymptotically $\|\mathbf{U}_{i_k} \mathbf{W}_{i_k}^{1/2}\|_{\text{F}}^2 \rightarrow \tilde{d}_{i_k}/\sigma_{i_k}^2$ as the SNR grows large.*

Proof: The proof is given in Appendix 6.A. ■

The first part of this theorem has an important connection to the uplink training stage in the fully distributed estimation scheme (Section 6.2.1). Since $\delta \mathbf{A}_{i_k} = \sqrt{\sqrt{P_{i_k}} \sigma_{i_k}^2 / d_{i_k} \sqrt{\omega_{i_k}}} \mathbf{U}_{i_k} \mathbf{W}_{i_k}^{1/2}$ is acting as the uplink training stage precoder, the factor $\|\mathbf{U}_{i_k} \mathbf{W}_{i_k}^{1/2}\|_{\text{F}}^2$ determines the effective MS transmit power, and hence the uplink estimation SNR. The second part of the theorem shows that $\|\mathbf{U}_{i_k} \mathbf{W}_{i_k}^{1/2}\|_{\text{F}}^2$ also indicates whether *perfect interference alignment* is achieved for MS i_k .

An example of how $\|\mathbf{U}_{i_k} \mathbf{W}_{i_k}^{1/2}\|_{\text{F}}^2$ converges, as a function of subframe number (i.e. WMMSE iteration), can be seen in Figure 6.5 on the facing page.

Enforcing Theorem 6.1 onto WMMSE Solutions with Imperfect CSI

Theorem 6.1 relates to perfect CSI, but the inequality may not hold for the naive solutions in (2.19) and (2.27) on page 42 with imperfect CSI. In order to robustify the algorithm, we therefore explicitly impose the constraint on the MS side optimization problem with imperfect CSI. The problems still decouple over users, and the problem that MS i_k should solve is

$$\begin{aligned} & \underset{\mathbf{U}_{i_k}, \mathbf{W}_{i_k} \succ \mathbf{0}}{\text{minimize}} && \text{Tr}\left(\mathbf{W}_{i_k} \left(\mathbf{I} + \mathbf{U}_{i_k}^{\text{H}} \widehat{\Phi}_{i_k} \mathbf{U}_{i_k}\right)\right) - 2\text{Re}\left(\mathbf{W}_{i_k} \widehat{\mathbf{F}}_{i_k}^{\text{H}} \mathbf{U}_{i_k}\right) - \ln \det\left(\mathbf{W}_{i_k}\right) \\ & \text{subject to} && \|\mathbf{U}_{i_k} \mathbf{W}_{i_k}^{1/2}\|_{\text{F}}^2 \leq d_{i_k}/\sigma_{i_k}^2. \end{aligned} \quad (6.45)$$

Theorem 6.2. *The solution to the optimization problem in (6.45) is*

$$\mathbf{U}_{i_k}^* = \left(\widehat{\Phi}_{i_k} + \nu_{i_k}^* \mathbf{I}\right)^{-1} \widehat{\mathbf{F}}_{i_k} \quad (6.46)$$

$$\mathbf{W}_{i_k}^* = \left(\mathbf{I} - \widehat{\mathbf{F}}_{i_k}^{\text{H}} \left(\widehat{\Phi}_{i_k} + \nu_{i_k}^* \mathbf{I}\right)^{-1} \widehat{\mathbf{F}}_{i_k}\right)^{-1}. \quad (6.47)$$

If $\|\mathbf{U}_{i_k}^* \left(\mathbf{W}_{i_k}^*\right)^{1/2}\|_{\text{F}}^2 \leq d_{i_k}/\sigma_{i_k}^2$ holds for $\nu_{i_k}^* = 0$, the constraint is not active and the solution has the same form as the original solution in Algorithm 2.1. Otherwise, $\nu_{i_k}^*$ can be found by bisection over $(0, \sigma_{i_k}^2]$ such that $\|\mathbf{U}_{i_k}^* \left(\mathbf{W}_{i_k}^*\right)^{1/2}\|_{\text{F}}^2 = d_{i_k}/\sigma_{i_k}^2$.

Proof: The proof is given in Appendix 6.B. ■

Interestingly, explicitly imposing Theorem 6.1 as a constraint in the optimization problem in (6.45) corresponds to diagonal loading of the receive filter $\mathbf{U}_{i_k}^*$,

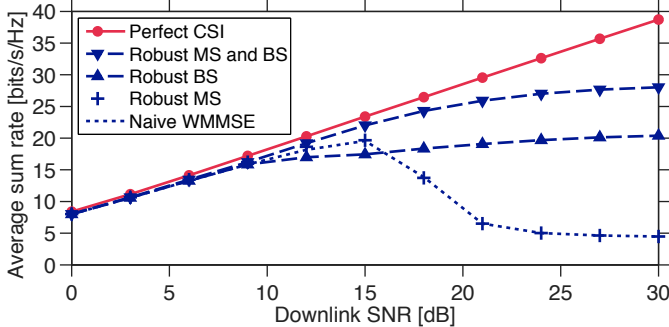


Figure 6.6. Sum rate performance when selectively applying the robustifying measures in Section 6.3, together with the fully distributed CSI acquisition in Section 6.2.1. For comparison purposes, the scenario is the same as in Figure 6.3.

giving it the same form as $\mathbf{U}_{i_k}^{\text{rob}}$ in (6.43). Likewise, $\mathbf{W}_{i_k}^*$ has the same form as $\mathbf{W}_{i_k}^{\text{rob}}$ in (6.44). The important difference is that $\mathbf{U}_{i_k}^*$ and $\mathbf{W}_{i_k}^*$ do not depend on unknown parameters, whereas $\mathbf{U}_{i_k}^{\text{rob}}$ and $\mathbf{W}_{i_k}^{\text{rob}}$ do. Thus, $\mathbf{U}_{i_k}^*$ and $\mathbf{W}_{i_k}^*$ can be applied as realizable proxies for the unrealizable $\mathbf{U}_{i_k}^{\text{rob}}$ and $\mathbf{W}_{i_k}^{\text{rob}}$ in the robust WMMSE algorithm to be proposed.

By increasing $\nu_{i_k}^*$, the requested rate $\ln \det(\mathbf{W}_{i_k}^*)$ is decreased. A large $\nu_{i_k}^*$ would occur when there are obvious discrepancies in the estimated CSI, such that $\|\mathbf{U}_{i_k} \mathbf{W}_{i_k}^{1/2}\|_{\text{F}}^2 \leq d_{i_k}/\sigma_{i_k}^2$ is far from being fulfilled without the diagonal loading.

We visualize the combined robustifying effects in Figure 6.6. The robustifying measures are effective, and result in up to a factor 5 sum rate gain over the naive WMMSE algorithm.

6.4 Robust and Distributed WMMSE Algorithm

We now combine the diagonal loading robustifications in Section 6.3.3 and Section 6.3.4 to form a *RoBustified WMMSE algorithm* (RB-WMMSE); see Algorithm 6.2 on the next page. This algorithm can be combined with any of the channel estimation procedures outlined in Section 6.2, and the joint system is fully distributed if the CSI acquisition is distributed.

The existing robust WMMSE algorithms in [NGS12, SM12, LKY13, RBCL13] also gain their robustness from diagonal loading, obtained by optimizing a lower bound on performance. Although not being directly tailored for TDD channel estimation, these algorithms can be applied together with the centralized CSI acquisition method⁹ proposed in Section 6.2.3. In doing so, an implicit assumption on

⁹The algorithms in [NGS12, SM12, LKY13, RBCL13] need the statistics of the CSI uncertainty, which is very complicated to derive for the CSI acquisition methods in Section 6.2.1 and

Algorithm 6.2 RB-WMMSE Algorithm (Estimated CSI)

-
- 1: **repeat**
 - At MSs:
 - 2: Pilot transmission from BSs: estimate $\widehat{\mathbf{\Phi}}_{i_k}^{(\vartheta)}$ and $\widehat{\mathbf{F}}_{i_k}^{(\vartheta)}$ using one of the methods in Section 6.2.
 - 3: Rescale $\widehat{\mathbf{\Phi}}_{i_k} = \vartheta \widehat{\mathbf{\Phi}}_{i_k}^{(\vartheta)}$, $\widehat{\mathbf{F}}_{i_k} = \sqrt{\vartheta} \widehat{\mathbf{F}}_{i_k}^{(\vartheta)}$
 - 4: Find ν_{i_k} to satisfy $\left\| \mathbf{U}_{i_k} \mathbf{W}_{i_k}^{1/2} \right\|_{\text{F}}^2 \leq d_{i_k} / \sigma_{i_k}^2$
 - 5: $\mathbf{W}_{i_k} = \left(\mathbf{I} - \widehat{\mathbf{F}}_{i_k}^{\text{H}} \left(\widehat{\mathbf{\Phi}}_{i_k} + \nu_{i_k} \mathbf{I} \right)^{-1} \widehat{\mathbf{F}}_{i_k} \right)^{-1}$
 - 6: $\mathbf{U}_{i_k} = \left(\widehat{\mathbf{\Phi}}_{i_k} + \nu_{i_k} \mathbf{I} \right)^{-1} \widehat{\mathbf{F}}_{i_k}$, $\mathbf{A}_{i_k} = \sqrt{\omega_{i_k}} \mathbf{U}_{i_k} \mathbf{W}_{i_k}^{1/2}$
 - At BSs:
 - 7: Pilot transmission from MSs: estimate $\widehat{\mathbf{\Gamma}}_i^{\text{s}+i+n}$ and $\widehat{\mathbf{G}}_{i_k}$ using one of the methods in Section 6.2.
 - 8: Obtain $\mathbf{W}_{i_k}^{1/2}$ through feedback.
 - 9: Find $\mu_i \geq -\min \left(\frac{\zeta^2}{\delta^2}, \lambda_{\min} \left(\widehat{\mathbf{\Gamma}}_i^{\text{s}+i+n} \right) - \zeta \right)$ to satisfy $\sum_{k \in \mathcal{K}_i} \left\| \mathbf{V}_{i_k}^{(\vartheta)} \right\|_{\text{F}}^2 \leq \vartheta P_i$
 - 10: $\mathbf{B}_{i_k}^{(\vartheta)} = \left(\widehat{\mathbf{\Gamma}}_i^{\text{s}+i+n} + \mu_i \mathbf{I} \right)^{-1} \widehat{\mathbf{G}}_{i_k}$, $\mathbf{V}_{i_k}^{(\vartheta)} = \sqrt{\omega_{i_k}} \mathbf{B}_{i_k}^{(\vartheta)} \mathbf{W}_{i_k}^{1/2}$
 - 11: Scale $\mathbf{V}_{i_k} = \frac{1}{\sqrt{\vartheta}} \mathbf{V}_{i_k}^{(\vartheta)}$
 - 12: **until** fixed number of iterations
-

the channel estimation errors in the uplink and downlink is made however. Since these algorithms only have a notion of *downlink* channel estimation errors, they are unaware of the *uplink* channel estimation errors in the TDD channel estimation. Thus, the implicit assumption that the channel estimation errors in the downlink and uplink are *identical* is made.

6.5 Performance Evaluation

Performance of the proposed system is evaluated by means of numerical simulations. Two scenarios are studied:

1. A *canonical IBC*, without large-scale fading. This model is relevant in local environments where the intercell interference power levels are on par with the desired power levels.
2. A *large-scale 3-cell network*, with path loss, shadow fading, and small-scale fading. This models a possible large-scale deployment scenario, where only cell-edge users are significantly affected by intercell interference.

Section 6.2.2 since those methods estimate the *effective channels*.

In both scenarios, we studied a symmetric network with $I = 3$ BSs, each serving K users with $d = 1$ data streams each. The BSs had $M = 4$ antennas each, and the MSs had $N = 2$ antennas each. We let the transmit powers be P and \overleftarrow{P} for the BSs and MSs, respectively. The noise powers were σ^2 and ζ^2 for the BSs and MSs, respectively. Unless otherwise stated, the RB-WMMSE BS power scaling was set as $\vartheta = \min\left(\frac{\overleftarrow{P}/\zeta^2}{P/\sigma^2}, 1\right)$, based on the findings in Figure 6.4 on page 111. For numerical stability, we let the constant $\zeta = 10^{-10}$ such that $\lambda_{\min}\left(\widehat{\Gamma}_i^{\text{s+i+n}} + \mu_i \mathbf{I}\right) \geq 10^{-10}$, $\forall i \in \mathcal{I}$, in the RB-WMMSE algorithm. The user weights were $\omega_{i_k} = 1$ for all MSs. Truncated discrete Fourier transform (DFT) matrices of appropriate dimensions were used for the pilot matrices \mathbf{P}_{i_k} and \mathbf{P}_i , as well as for the initial precoders. Since we do not model the CSI acquisition overhead, the pre-log factors are $\alpha_{i_k} = 1$ for all MSs.

As a baseline performance measure, we used single-user eigenprecoding and waterfilling with channels estimated by the MMSE estimator in Section 6.2.3. With the single-user processing, we show the performance under TDMA, as well as under nonorthogonal concurrent transmissions from all BSs simultaneously (i.e. uncoordinated transmission).

6.5.1 Canonical IBC

For the simulations with the canonical channel the channel model was i.i.d. Rayleigh fading on all antenna-pairs in the system such that $[\mathbf{H}_{i_k j}]_{mn} \sim \mathcal{CN}(0, 1)$. This models a setting where each interfering link on average is equally strong as the desired channel. We assume a sufficiently long coherence interval such that the channels do not change between WMMSE iterations. We let each BS serve $K = 2$ MSs, a setting which is feasible for interference alignment [LY13]. For fairness when comparing estimation schemes, we let $L_p = IM$ and $\overleftarrow{L}_p = IKN$. The results were averaged over 1 000 independent Monte Carlo realizations.

Convergence

First, we investigate the average convergence behaviour of the RB-WMMSE algorithm with $\text{SNR} = P/\sigma^2 = 20$ dB and $\overleftarrow{\text{SNR}} = \overleftarrow{P}/\zeta^2 = 10$ dB.

The results in Figure 6.7 on the next page, indicate that the RB-WMMSE algorithm needs on the order of 1 000 iterations to converge, which is consistent with the findings of [SSB⁺13]. We do however note that a significant fraction of the final performance is achieved after just 10 to 20 iterations. In the following, we therefore let the algorithms run for 20 iterations.

Sum Rate vs. Signal-to-Noise Ratio

Next, we study the sum rate when the downlink and uplink SNRs are varied. Recall that the downlink SNR affects both the downlink data transmission, as well as the

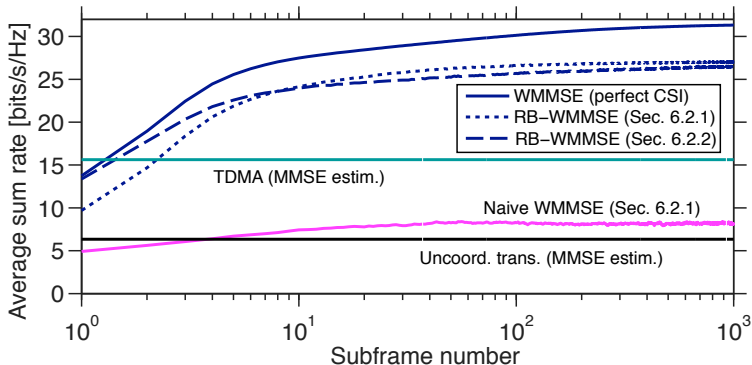


Figure 6.7. Convergence comparison of the different methods for $I = 3, K = 2, M = 4, N = 2, d = 1, \text{SNR} = 20 \text{ dB}$ and $\hat{\text{SNR}} = 10 \text{ dB}$.

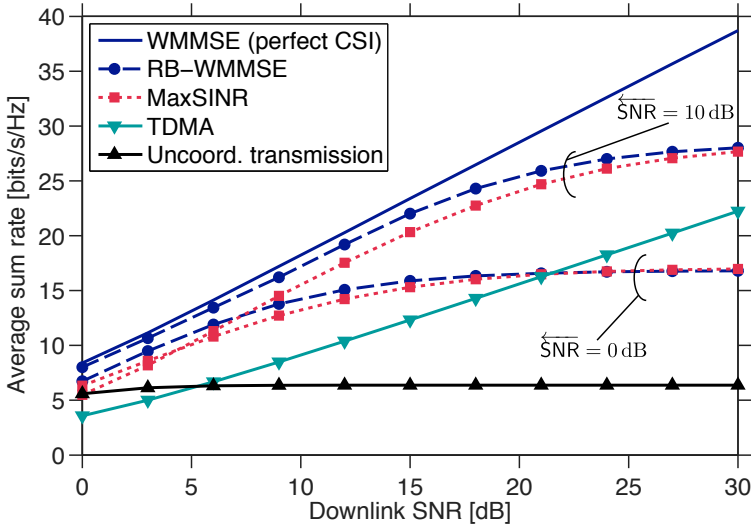
downlink estimation performance (see Section 6.2.1). The uplink SNR only affects the uplink estimation performance. We compare with MaxSINR [GCJ11], for which we actively turn off two users in order not to overload the algorithm.

The results for the fully distributed CSI acquisition (Section 6.2.1) are shown in Figure 6.8a on the following page. The RB-WMMSE algorithm consistently performs better than MaxSINR, and better than TDMA for sufficiently high uplink SNR.

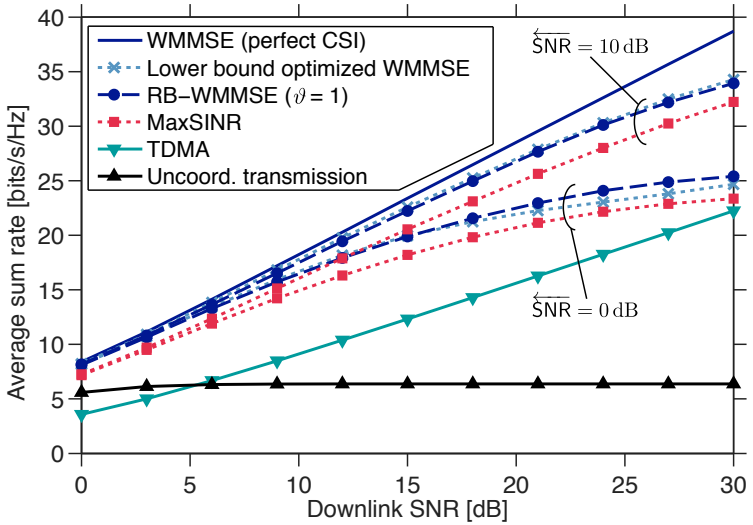
The results for the CSI acquisition with global sharing of filters and MSE weights (Section 6.2.3) are shown in Figure 6.8b on the next page. Here we also compare with the lower bound optimization method of [NGS12, SM12, LKY13, RBCL13], which *requires* this form of centralized CSI estimation. We relax their requirement of downlink and uplink estimation errors being identical (see Section 6.4). In Figure 6.8b, it can be seen that the RB-WMMSE algorithm exhibits similar performance as the lower bound optimization method of [NGS12, SM12, LKY13, RBCL13]. The sum rates in Figure 6.8b are higher than the corresponding sum rates in Figure 6.8a. This is because the improved channel estimation performance, due to the perfect feedback of filters, and that the estimates of the channels are improved in every iteration, as described in Section 6.2.3.

Sum Rate and Complexity vs. Flop Count

For the case with $\text{SNR} = 20 \text{ dB}$, and $\hat{\text{SNR}} = 10 \text{ dB}$, we vary the number of pilots $L_p = \overleftarrow{L}_p$ and study the resulting performance and complexity of the system. The results can be seen in Figure 6.9 on page 119. The more complex CSI acquisition methods perform slightly better in the sum rate sense. The centralized CSI acquisition from Section 6.2.3 requires particularly many flops, since it estimates all interfering channels.



(a) Fully distributed CSI acquisition (Section 6.2.1)



(b) CSI acquisition with globally shared filters and MSE weights (Section 6.2.3)

Figure 6.8. Sum rate after the 20th iteration for canonical IBC with $I = 3, K = 2, M = 4, N = 2$, and $d = 1$.

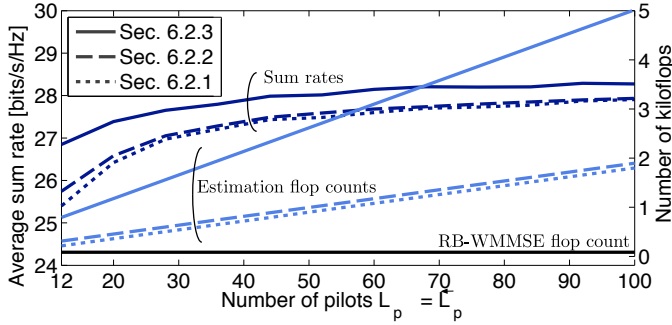


Figure 6.9. Comparison of complexity and sum rate performance after the 20th iteration for $I = 3, K = 2, M = 4, N = 2$ canonical IBC with $d = 1$, $\text{SNR} = 20$ dB, and $\overleftarrow{\text{SNR}} = 10$ dB.

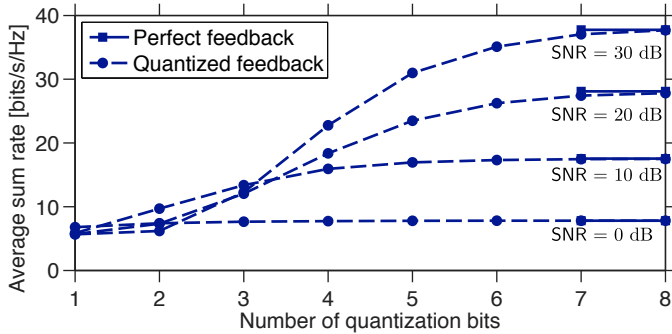


Figure 6.10. Sum rate as a function of quantization accuracy for $I = 3, K = 2, M = 4, N = 2$ canonical IBC with $d = 1$ and $\overleftarrow{\text{SNR}} = 30$ dB.

Quantized MSE Weight Feedback

So far, the feedback of the MSE weights was assumed to be perfect. We now study performance of the system, using quantized MSE weights, while varying the number of feedback bits used. For the case with fixed uplink $\overleftarrow{\text{SNR}} = 30$ dB, we vary the downlink SNR and the number of quantization bits. Each MS had an individual codebook with weights uniformly quantized on $\left[0, 10 \log_{10} \left(1 + \frac{P_i s_{\max}^2 \langle \mathbf{H}_{i_k i} \rangle}{\sigma^2}\right)\right]$ dB. The performance is shown in Figure 6.10. For higher downlink SNR, more bits are needed for good performance. For high resolution quantization, the performance is equal to that of perfect feedback.

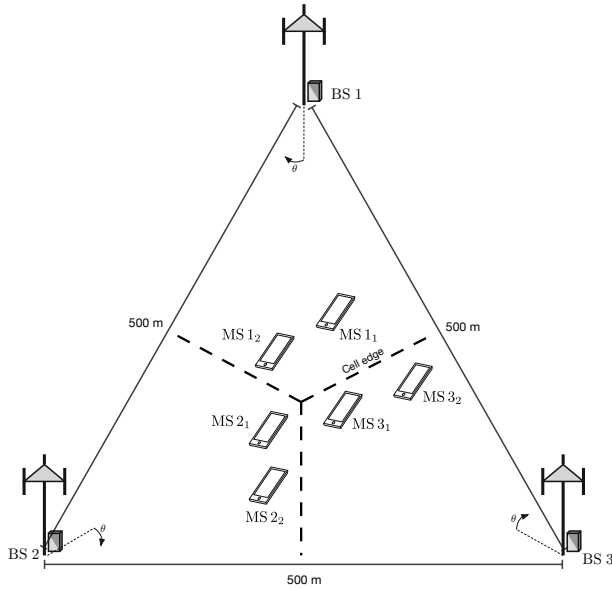


Figure 6.11. Cell layout for large-scale 3-cell network, here displayed with $K = 2$ MSs per cell.

6.5.2 Large scale 3-cell network

The results presented so far describe the performance in a setting where the desired signal and interfering signals had equal average power levels. In realistic deployments, e.g. macrocell setups, large-scale fading such as path loss and shadow fading are present however, leading to a more heterogeneous setting. In order to investigate the performance for such a setting, we study a scenario where the BSs are located at the vertices of an equilateral triangle, and the antenna boresights are aimed towards the centre of the triangle (see Figure 6.11). This scenario models three interfering sectors in a larger hexagonal macrocell deployment. In particular, we assume a setup where fractional frequency reuse is combined with coordinated precoding, such that cell centre and cell edge users are served on orthogonal subbands [WY11]. Since the cell centre users typically have very high signal-to-interference ratios (SIRs), they can be served well using single-cell techniques. The cell edge users experience low SIRs however, and thus multicell coordinated precoding is a fruitful transmission strategy for these users. Since our focus is on coordinated precoding, our simulations only study the performance of the cell edge users. The simulation parameters (see Table 6.5 on the next page) can be described as a simplified version of the 3GPP Case 1 [3GP06, 3GP10], where the small scale-fading is i.i.d. Rayleigh fading, and where we only study one subcarrier.

The purpose of the simulation study is to investigate the impact on sum rate

Table 6.5. Simulation parameters for large-scale 3-cell network (Adapted from 3GPP Case 1 [3GP06, 3GP10])

Inter site distance	500 m
Max. distance, MS to cell edge	50 m
Path loss	$15.3 + 37.6 \log_{10}(\text{distance [m]})$ dB
Penetration loss	20 dB
BS antenna gain	$-\min\left(12\left(\frac{\theta}{35^\circ}\right)^2, 23\right)$ dB [3GP12]
MS antenna gain	0 dB
Shadow fading	Lognormal with std. dev. 8 dB
Small scale fading	i.i.d. $\mathcal{CN}(0, 1)$
Bandwidth [†]	15 kHz
BS transmit power [†]	$P = 18.2$ dBm
MS receiver noise power [†]	$\sigma^2 = -123.2$ dBm (9 dB NF)
MS transmit power [†]	$P = -4.8$ dBm
BS receiver noise power [†]	$\zeta^2 = -127.2$ dBm (5 dB NF)

[†] We only study one subcarrier in a 10 MHz system with 600 subcarriers. The total transmit powers are thus $P^{\text{tot}} = 46$ dBm and $\overline{P}^{\text{tot}} = 23$ dBm.

performance, when the number of cell edge users per cell K is varied. For each of the two simulations to be described, we generated 500 independent user drops, where the MSs were dropped uniformly at random in the cell, but never farther than 50 m from the cell edge. For each user drop, 5 independent small-scale fading realizations were generated. We used the fully distributed estimation method in Section 6.2.1 for channel estimation in the RB-WMMSE algorithm and MaxSINR, and we assumed perfect feedback for the MSE weights. In order to have the same estimation performance regardless of K , we fixed $L_p = \overline{L}_p = 3 \cdot 10 \cdot 1 = 30$.

We used the same baseline methods as described in Section 6.5.1. For large K , all baseline methods would perform poorly due to the high interference levels experienced at the cell edge. We therefore coupled the baseline methods with a user selection procedure that determined which MSs to serve. Before describing the main results of the simulation study, we first detail the user selection procedure performance.

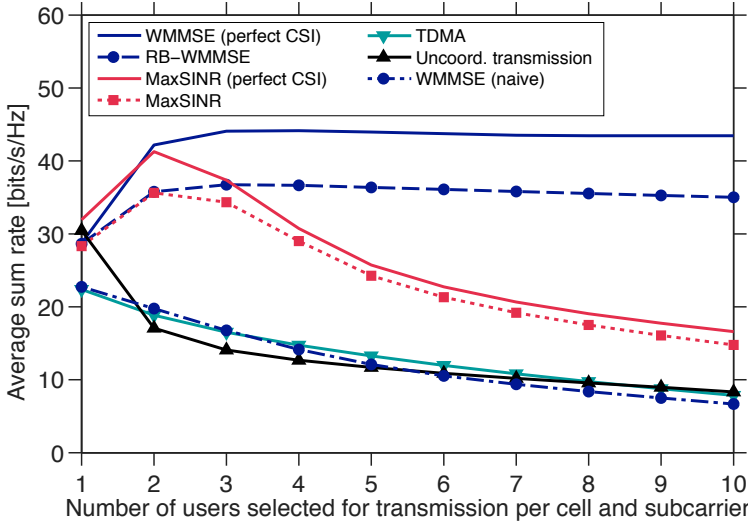
Sum Rate vs. Number of Users Selected for Transmission

In order to study how many users to select for transmission for the baseline methods, we performed simulations where $K = 10$ users were dropped per cell, and the number of users selected for transmission was varied. The user selection was based solely on the channel strength to the serving BS. The results are plotted in Figure 6.12a on the facing page. It can be seen that performance for MaxSINR is maximized when 2 users are selected for transmission. For TDMA and uncoordinated transmission, performance is maximized when only a single user is selected for transmission in each cell. The performance of the RB-WMMSE algorithm is the highest when 3 users are selected for transmission in each cell, but performance only slightly drops as more users are selected. This is because the RB-WMMSE algorithm, just like the WMMSE algorithm, is able to implicitly perform user selection—through power allocation—in the iterations. The fact that the performance is almost constant when more than 3 users are selected for transmission in each cell suggests that the RB-WMMSE algorithm is able to find a good local solution to the weighted sum rate problem.

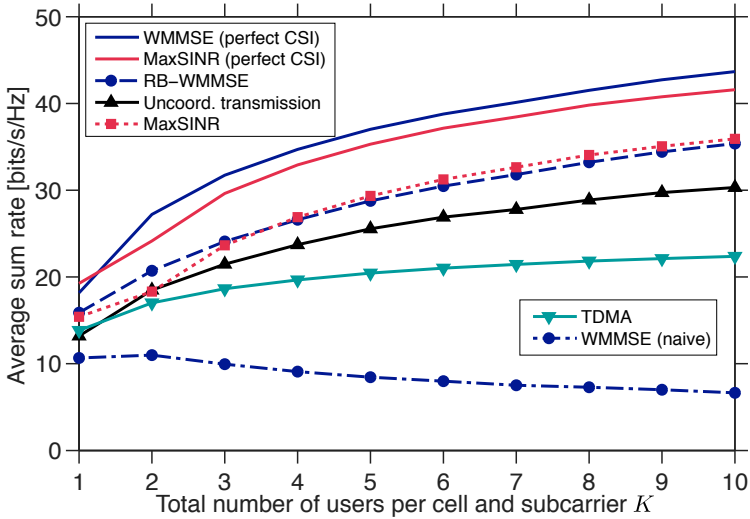
Sum Rate vs. Total Number of Users per Cell

We now study system performance as a function of the total number of users per cell K . Given the results in the previous section, we select at most 2 users for transmission per cell for MaxSINR. Similarly for TDMA and uncoordinated transmission, disregarding the obvious unfairness of such a strategy, we only select 1 user per cell. For the RB-WMMSE and WMMSE algorithms, we do not explicitly perform any user selection, but rather let the algorithms perform their own implicit user selection in the iterations. The results of the simulation can be seen in Figure 6.12b on the next page. For the baselines with user selection, the improved performance with K is due to the increased multiuser diversity. The RB-WMMSE algorithm is also able to harness this increase in multiuser diversity. The large gap between the perfect CSI case, and the RB-WMMSE algorithm with fully distributed CSI acquisition (Section 6.2.1) is due to the low uplink SNR in this scenario¹⁰. The RB-WMMSE algorithm performs slightly worse than the MaxSINR with user selection, for large K . It has however been verified that this gap can be closed by combining the RB-WMMSE algorithm together with explicit user selection, serving at most 3 users per cell (see Figure 6.12a). Here we however show the results without explicit user selection, in order to display the self-reliant performance of the algorithm. The uncoordinated transmission strategy works fairly well in terms of sum rate, but as noted earlier, corresponds to a highly unfair situation where only one user is served per cell.

¹⁰Along the cell edge, the average uplink SNR ranges between -4.9 dB and -11.8 dB. The corresponding average downlink SNR ranges between 7.2 dB and 14.1 dB. Note that the average SNRs are determined both by the distance to the BS, as well as the angle to the antenna bore sight.



(a) Varying the number of users selected for transmission, given $K = 10$ users per cell.



(b) Varying the total number of users per cell K . At most 2 users per cell were served by MaxSINR. For TDMA and uncoordinated transmission, only 1 user per cell was served.

Figure 6.12. Sum rate after the 20th iteration for the large-scale scenario with fully distributed CSI acquisition (Section 6.2.1).

6.6 Conclusions

In this chapter, we focused directly on solving the weighted sum rate problem. In order to find a practical solution, we sought a distributed and robust coordinated precoding method. In that venture, first three CSI acquisition schemes of varying level of distributedness were proposed. The most distributed method only required joint selection of one real-valued parameter. When this parameter was fixed, all further steps could be performed in a fully distributed manner. Directly using the estimates into the WMMSE algorithm developed for perfect CSI, was shown to yield inferior performance. Instead, robustifying measures at both the BS as well as the MS sides were proposed. At the MS side, enforcing some properties of the solutions with perfect CSI, to the solutions with imperfect CSI, resulted in diagonally loaded receive filters. At the BS side, some diagonal loading was provided by the sum power constraint. This effect was amplified using a common power scaling parameter.

6.A Proof of Theorem 6.1

Decompose $\Phi_{i_k} = \mathbf{F}_{i_k} \mathbf{F}_{i_k}^H + \Phi_{i_k}^{i+n}$ and let $\mathbf{C}_{i_k} = \mathbf{F}_{i_k}^H (\Phi_{i_k}^{i+n})^{-1} \mathbf{F}_{i_k}$ and $\mathbf{D}_{i_k} = \mathbf{F}_{i_k}^H (\Phi_{i_k}^{i+n})^{-2} \mathbf{F}_{i_k}$. We have that $\mathbf{U}_{i_k} = \Phi_{i_k}^{-1} \mathbf{F}_{i_k}$ and $\mathbf{W}_{i_k} = \mathbf{I} + \mathbf{C}_{i_k}$. Plugging in,

$$\left\| \mathbf{U}_{i_k} \mathbf{W}_{i_k}^{1/2} \right\|_{\mathbf{F}}^2 = \text{Tr} (\mathbf{U}_{i_k} \mathbf{W}_{i_k} \mathbf{U}_{i_k}^H) = \text{Tr} (\mathbf{U}_{i_k}^H \mathbf{U}_{i_k} \mathbf{W}_{i_k}) = \text{Tr} (\mathbf{F}_{i_k}^H \Phi_{i_k}^{-2} \mathbf{F}_{i_k} (\mathbf{I} + \mathbf{C}_{i_k})).$$

Applying the matrix inversion lemma to $\Phi_{i_k}^{-1}$, it can be shown that

$$\mathbf{F}_{i_k}^H \Phi_{i_k}^{-2} \mathbf{F}_{i_k} = (\mathbf{I} + \mathbf{C}_{i_k})^{-1} \mathbf{D}_{i_k} (\mathbf{I} + \mathbf{C}_{i_k})^{-1} \quad (6.48)$$

after simplifications. Thus,

$$\left\| \mathbf{U}_{i_k} \mathbf{W}_{i_k}^{1/2} \right\|_{\mathbf{F}}^2 = \text{Tr} \left((\mathbf{I} + \mathbf{C}_{i_k})^{-1} \mathbf{D}_{i_k} \right) \quad (6.49)$$

$$= \text{Tr} \left(\left(\Phi_{i_k}^{i+n} \right)^{-1} \mathbf{F}_{i_k} \left(\mathbf{I} + \mathbf{F}_{i_k}^H \left(\Phi_{i_k}^{i+n} \right)^{-1} \mathbf{F}_{i_k} \right)^{-1} \mathbf{F}_{i_k}^H \left(\Phi_{i_k}^{i+n} \right)^{-1} \right) \quad (6.50)$$

$$= \text{Tr} \left(\left(\Phi_{i_k}^{i+n} \right)^{-1} - \Phi_{i_k}^{-1} \right), \quad (6.51)$$

where the last equality comes from applying the matrix inversion lemma backwards. Further,

$$\left\| \mathbf{U}_{i_k} \mathbf{W}_{i_k}^{1/2} \right\|_{\mathbf{F}}^2 = \text{Tr} \left((\mathbf{I} + \mathbf{C}_{i_k})^{-1} \mathbf{D}_{i_k} \right) \stackrel{(c)}{\leq} \text{Tr} (\mathbf{C}_{i_k}^{-1} \mathbf{D}_{i_k}) \quad (6.52)$$

$$= \text{Tr} \left(\left(\mathbf{F}_{i_k}^H \left(\Phi_{i_k}^{i+n} \right)^{-1} \mathbf{F}_{i_k} \right)^{-1} \mathbf{F}_{i_k}^H \left(\Phi_{i_k}^{i+n} \right)^{-2} \mathbf{F}_{i_k} \right) \quad (6.53)$$

$$= \left[\text{Let } \tilde{\mathbf{F}}_{i_k} = \left(\Phi_{i_k}^{i+n} \right)^{-1/2} \mathbf{F}_{i_k} \right] \quad (6.54)$$

$$= \text{Tr} \left(\left(\tilde{\mathbf{F}}_{i_k}^H \tilde{\mathbf{F}}_{i_k} \right)^{-1} \tilde{\mathbf{F}}_{i_k}^H \left(\Phi_{i_k}^{i+n} \right)^{-1} \tilde{\mathbf{F}}_{i_k} \right) \quad (6.55)$$

$$= \text{Tr} \left(\left(\Phi_{i_k}^{i+n} \right)^{-1} \tilde{\mathbf{F}}_{i_k} \left(\tilde{\mathbf{F}}_{i_k}^H \tilde{\mathbf{F}}_{i_k} \right)^{-1} \tilde{\mathbf{F}}_{i_k}^H \right) \quad (6.56)$$

$$\stackrel{(d)}{\leq} \max_{\text{rank}(\mathbf{\Pi}_{i_k})=d_{i_k}} \text{Tr} \left(\left(\Phi_{i_k}^{i+n} \right)^{-1} \mathbf{\Pi}_{i_k} \right) \quad (6.57)$$

$$= \sum_{n=1}^{d_{i_k}} \lambda_n \left(\left(\Phi_{i_k}^{i+n} \right)^{-1} \right) = \sum_{n=1}^{d_{i_k}} \frac{1}{\lambda_{N_{i_k}-n+1} \left(\Phi_{i_k}^{i+n} \right)} \stackrel{(a)}{\leq} \frac{d_{i_k}}{\sigma_{i_k}^2} \quad (6.58)$$

where $\mathbf{\Pi}_{i_k}$ is a rank- d_{i_k} projection matrix. The inequality (a) is due to the trace being an increasing function on the cone of positive definite matrices and the fact that $\mathbf{D}_{i_k}^{1/2} (\mathbf{I} + \mathbf{C}_{i_k})^{-1} \mathbf{D}_{i_k}^{1/2} \preceq \mathbf{D}_{i_k}^{1/2} \mathbf{C}_{i_k}^{-1} \mathbf{D}_{i_k}^{1/2}$. The inequality (b) holds since

$\tilde{\mathbf{F}}_{i_k} \left(\tilde{\mathbf{F}}_{i_k}^H \tilde{\mathbf{F}}_{i_k} \right)^{-1} \tilde{\mathbf{F}}_{i_k}^H$ is a rank- d_{i_k} projection matrix. The inequality (d) is due to the fact that $\Phi_{i_k}^{i+n} \succeq \sigma_{i_k}^2 \mathbf{I}$.

Now assume that there are $\tilde{d}_{i_k} \leq d_{i_k}$ interference-free dimensions, and that the effective channel is fully contained in those. Let the eigenvalues of Φ_{i_k} be $\{\tau_{i_k,n}^{s+i+n}\}$ and the eigenvalues of $\Phi_{i_k}^{i+n}$ be $\{\tau_{i_k,n}^{i+n}\}$. Let the eigenvalues be ordered such that

$$\tau_{i_k,n}^{s+i+n} = \begin{cases} \tau_{i_k,n}^{i+n}, & n \in \{1, \dots, N_{i_k} - \tilde{d}_{i_k}\} \\ \tau_{i_k,n}^s + \sigma_{i_k}^2, & n \in \{N_{i_k} - \tilde{d}_{i_k} + 1, \dots, N_{i_k}\} \end{cases}, \quad (6.59)$$

where the first $N_{i_k} - \tilde{d}_{i_k}$ eigenvalues are for the interference subspace, and the remaining eigenvalues are for the interference-free subspace. The $\{\tau_{i_k,n}^s\}$ are the signal powers of the effective channel in the interference-free subspace. Further, note that $\tau_{i_k,n}^{i+n} = \sigma_{i_k}^2$ for all $n \in \{N_{i_k} - \tilde{d}_{i_k} + 1, \dots, N_{i_k}\}$. Then,

$$\text{Tr} \left((\Phi_{i_k}^{i+n})^{-1} - \Phi_{i_k}^{-1} \right) = \sum_{n=1}^{N_{i_k}} \left(\frac{1}{\tau_{i_k,n}^{i+n}} - \frac{1}{\tau_{i_k,n}^{s+i+n}} \right) \quad (6.60)$$

$$= \underbrace{\sum_{n=1}^{N_{i_k} - \tilde{d}_{i_k}} \left(\frac{1}{\tau_{i_k,n}^{i+n}} - \frac{1}{\tau_{i_k,n}^{s+i+n}} \right)}_{\text{Interference dimensions}} + \underbrace{\sum_{n=N_{i_k} - \tilde{d}_{i_k} + 1}^{N_{i_k}} \left(\frac{1}{\sigma_{i_k}^2} - \frac{1}{\tau_{i_k,n}^s + \sigma_{i_k}^2} \right)}_{\text{Interference-free dimensions}} \quad (6.61)$$

$$= \sum_{n=N_{i_k} - \tilde{d}_{i_k} + 1}^{N_{i_k}} \frac{\tau_{i_k,n}^s}{\sigma_{i_k}^2 (\tau_{i_k,n}^s + \sigma_{i_k}^2)} \rightarrow \sum_{n=N_{i_k} - \tilde{d}_{i_k} + 1}^{N_{i_k}} \frac{1}{\sigma_{i_k}^2} = \frac{\tilde{d}_{i_k}}{\sigma_{i_k}^2} \quad (6.62)$$

as the $\{\tau_{i_k,n}^s\}$ grow large w.r.t. $\sigma_{i_k}^2$. ■

6.B Proof of Theorem 6.2

We first denote the objective function as $g_0(\mathbf{U}_{i_k}, \mathbf{W}_{i_k})$ and the constraint function as $g_1(\mathbf{U}_{i_k}, \mathbf{W}_{i_k})$ such that

$$g_0(\mathbf{U}_{i_k}, \mathbf{W}_{i_k}) = \text{Tr} \left(\left(\mathbf{I} - \mathbf{U}_{i_k}^H \widehat{\mathbf{F}}_{i_k} - \widehat{\mathbf{F}}_{i_k}^H \mathbf{U}_{i_k} + \mathbf{U}_{i_k}^H \widehat{\mathbf{\Phi}}_{i_k} \mathbf{U}_{i_k} \right) \mathbf{W}_{i_k} \right) - \ln \det(\mathbf{W}_{i_k}), \quad (6.63)$$

$$g_1(\mathbf{U}_{i_k}, \mathbf{W}_{i_k}) = \left\| \mathbf{U}_{i_k} \mathbf{W}_{i_k}^{1/2} \right\|_{\text{F}}^2 - \frac{d_{i_k}}{\sigma_{i_k}^2} = \text{Tr}(\mathbf{U}_{i_k} \mathbf{W}_{i_k} \mathbf{U}_{i_k}^H) - \frac{d_{i_k}}{\sigma_{i_k}^2}. \quad (6.64)$$

For future convenience, we also note that the complex partial gradients [HG07] of the functions are

$$\nabla_{\mathbf{U}_{i_k}^*} g_0(\mathbf{U}_{i_k}, \mathbf{W}_{i_k}) = \widehat{\mathbf{\Phi}}_{i_k} \mathbf{U}_{i_k} \mathbf{W}_{i_k} - \widehat{\mathbf{F}}_{i_k} \mathbf{W}_{i_k}, \quad (6.65)$$

$$\nabla_{\mathbf{W}_{i_k}^*} g_0(\mathbf{U}_{i_k}, \mathbf{W}_{i_k}) = \mathbf{I} - \mathbf{U}_{i_k}^H \widehat{\mathbf{F}}_{i_k} - \widehat{\mathbf{F}}_{i_k}^H \mathbf{U}_{i_k} + \mathbf{U}_{i_k}^H \widehat{\mathbf{\Phi}}_{i_k} \mathbf{U}_{i_k} - \mathbf{W}_{i_k}^{-1}, \quad (6.66)$$

$$\nabla_{\mathbf{U}_{i_k}^*} g_1(\mathbf{U}_{i_k}, \mathbf{W}_{i_k}) = \mathbf{U}_{i_k} \mathbf{W}_{i_k}, \quad (6.67)$$

$$\nabla_{\mathbf{W}_{i_k}^*} g_1(\mathbf{U}_{i_k}, \mathbf{W}_{i_k}) = \mathbf{U}_{i_k}^H \mathbf{U}_{i_k}. \quad (6.68)$$

The full gradients $\nabla(\cdot) = \nabla_{\mathbf{U}_{i_k}^*, \mathbf{W}_{i_k}^*}(\cdot)$ are the partial gradients stacked row-wise.

Any regular stationary point $(\mathbf{U}_{i_k}^*, \mathbf{W}_{i_k}^*)$ of the optimization problem in (6.45) must satisfy the KKT conditions [Ber06, Chapter 3.3.1],

$$\nabla g_0(\mathbf{U}_{i_k}^*, \mathbf{W}_{i_k}^*) + \nu_{i_k}^* \nabla g_1(\mathbf{U}_{i_k}^*, \mathbf{W}_{i_k}^*) = \mathbf{0}, \quad (6.69)$$

$$\mathbf{W}_{i_k} \succ \mathbf{0}, \quad (6.70)$$

$$g_1(\mathbf{U}_{i_k}^*, \mathbf{W}_{i_k}^*) \leq 0, \quad (6.71)$$

$$\nu_{i_k}^* \geq 0, \quad (6.72)$$

$$\nu_{i_k}^* g_1(\mathbf{U}_{i_k}^*, \mathbf{W}_{i_k}^*) = 0. \quad (6.73)$$

For the single-constraint problem at hand, a feasible point $(\mathbf{U}_{i_k}, \mathbf{W}_{i_k})$ is said to be *regular* if [Ber06, Chapter 3.3.1],

$$g_1(\mathbf{U}_{i_k}, \mathbf{W}_{i_k}) < 0, \quad \text{or} \quad \begin{cases} g_1(\mathbf{U}_{i_k}, \mathbf{W}_{i_k}) = 0 \\ \nabla g_1(\mathbf{U}_{i_k}, \mathbf{W}_{i_k}) \neq \mathbf{0} \end{cases}. \quad (6.74)$$

To find a potentially irregular point $(\mathbf{U}_{i_k}^0, \mathbf{W}_{i_k}^0)$, we note that since

$$\nabla g_1(\mathbf{U}_{i_k}^0, \mathbf{W}_{i_k}^0) = \begin{pmatrix} \mathbf{U}_{i_k}^0 \mathbf{W}_{i_k}^0 \\ \mathbf{U}_{i_k}^{0,H} \mathbf{U}_{i_k}^0 \end{pmatrix}, \quad (6.75)$$

and $\mathbf{W}_{i_k}^0 \succ \mathbf{0}$, we must have $\mathbf{U}_{i_k}^0 \mathbf{W}_{i_k}^0 = \mathbf{0}$ in order to have $\nabla g_1(\mathbf{U}_{i_k}^0, \mathbf{W}_{i_k}^0) = \mathbf{0}$. From the rank-nullity theorem [HJ85], we know that

$$\text{nullity}(\mathbf{U}_{i_k}^0) = d_{i_k} - \text{rank}(\mathbf{U}_{i_k}^0), \quad (6.76)$$

and since $\mathbf{U}_{i_k}^0 \mathbf{W}_{i_k}^0 = \mathbf{0}$ requires nullity $(\mathbf{U}_{i_k}^0) \geq d_{i_k}$, we then must have $\text{rank}(\mathbf{U}_{i_k}^0) = 0$ for our potentially irregular point. The only point satisfying this is $\mathbf{U}_{i_k}^0 = \mathbf{0}$, and since $g_1(\mathbf{0}, \mathbf{W}_{i_k}) = -d_{i_k}/\sigma_{i_k}^2 < 0$, this is a regular point according to (6.74). Concluding, all feasible points are regular for this problem, and therefore the global minimizer is among the points described by the KKT conditions in (6.69)–(6.73).

We now venture to solve the KKT conditions. From (6.69), together with the fact that $\mathbf{W}_{i_k} \succ \mathbf{0}$, we get the expressions

$$\mathbf{U}_{i_k}^* = \left(\widehat{\Phi}_{i_k} + \nu_{i_k}^* \mathbf{I} \right)^{-1} \widehat{\mathbf{F}}_{i_k} \quad (6.77)$$

$$\mathbf{W}_{i_k}^* = \left(\mathbf{I} - \widehat{\mathbf{F}}_{i_k}^H \left(\widehat{\Phi}_{i_k} + \nu_{i_k}^* \mathbf{I} \right)^{-1} \widehat{\mathbf{F}}_{i_k} \right)^{-1} \quad (6.78)$$

$$= \mathbf{I} + \widehat{\mathbf{F}}_{i_k}^H \left(\widehat{\Phi}_{i_k}^{i+n} + \nu_{i_k}^* \mathbf{I} \right)^{-1} \widehat{\mathbf{F}}_{i_k}, \quad (6.79)$$

where the last equality is due to the matrix inversion lemma [HJ85]. It now remains to find the optimal $\nu_{i_k}^* \geq 0$. If the constraint is satisfied for $\nu_{i_k}^* = 0$, the problem is solved and the form is identical to the solutions in (2.19) and (2.27).

Otherwise, let $\widehat{\Phi}_{i_k} = \mathbf{L}_{i_k} \mathbf{\Lambda}_{i_k} \mathbf{L}_{i_k}^H$ and $\widehat{\Phi}_{i_k}^{i+n} = \mathbf{L}_{i_k}^{i+n} \mathbf{\Lambda}_{i_k}^{i+n} \mathbf{L}_{i_k}^{i+n,H}$ be eigenvalue decompositions. Then, as can be seen in (6.82), $\left\| \mathbf{U}_{i_k} \mathbf{W}_{i_k}^{1/2} \right\|_{\mathbb{F}}^2$ is decreasing in ν_{i_k} , and the $\nu_{i_k}^*$ which satisfies the inequality constraint with equality can be found by bisection. A natural starting point for the lower value in the bisection is $\nu_{i_k}^{\text{lower}} = 0$. Using the same argument as in the proof for Theorem 6.1, we have that

$$\left\| \mathbf{U}_{i_k} \mathbf{W}_{i_k}^{1/2} \right\|_{\mathbb{F}}^2 \leq \frac{d_{i_k}}{\lambda_{\min} \left(\widehat{\Phi}_{i_k}^{i+n} + \nu_{i_k} \mathbf{I} \right)} \quad (6.80)$$

and we can thus enforce

$$\left\| \mathbf{U}_{i_k} \mathbf{W}_{i_k}^{1/2} \right\|_{\mathbb{F}}^2 \Big|_{\nu_{i_k} = \nu_{i_k}^{\text{upper}}} \leq \frac{d_{i_k}}{\sigma_{i_k}^2} \quad (6.81)$$

with $\nu_{i_k}^{\text{upper}} = \sigma_{i_k}^2$. The optimal $\nu_{i_k}^*$ can now be found using bisection on (6.82) on the facing page, given the bounds. With $\nu_{i_k}^*$ found, the minimizer can be identified as unique. The fact that $(\mathbf{U}_{i_k}^*, \mathbf{W}_{i_k}^*)$ is indeed a minimizer is clear, since each variable minimizes the objective function when the other variable is kept fixed. ■

$$\begin{aligned}
& \left\| \mathbf{U}_{i_k} \mathbf{W}_{i_k}^{1/2} \right\|_{\mathbb{F}}^2 = \text{Tr} \left(\mathbf{U}_{i_k} \mathbf{W}_{i_k} \mathbf{U}_{i_k}^{\text{H}} \right) \\
& = \text{Tr} \left(\widehat{\mathbf{F}}_{i_k}^{\text{H}} \left(\widehat{\mathbf{\Phi}}_{i_k} + \nu_{i_k} \mathbf{I} \right)^{-2} \widehat{\mathbf{F}}_{i_k} \left(\mathbf{I} + \widehat{\mathbf{F}}_{i_k}^{\text{H}} \left(\widehat{\mathbf{\Phi}}_{i_k}^{i+n} + \nu_{i_k} \mathbf{I} \right)^{-1} \widehat{\mathbf{F}}_{i_k} \right) \right) = \\
& \text{Tr} \left(\mathbf{L}_{i_k}^{\text{H}} \widehat{\mathbf{F}}_{i_k} \widehat{\mathbf{F}}_{i_k}^{\text{H}} \mathbf{L}_{i_k} \left(\mathbf{\Lambda}_{i_k} + \nu_{i_k} \mathbf{I} \right)^{-2} \right. \\
& \left. + \left(\mathbf{\Lambda}_{i_k}^{i+n} + \nu_{i_k} \mathbf{I} \right)^{-1/2} \mathbf{L}_{i_k}^{i+n, \text{H}} \widehat{\mathbf{F}}_{i_k} \widehat{\mathbf{F}}_{i_k}^{\text{H}} \mathbf{L}_{i_k} \left(\mathbf{\Lambda}_{i_k} + \nu_{i_k} \mathbf{I} \right)^{-2} \mathbf{L}_{i_k}^{\text{H}} \widehat{\mathbf{F}}_{i_k} \widehat{\mathbf{F}}_{i_k}^{\text{H}} \mathbf{L}_{i_k}^{i+n} \left(\mathbf{\Lambda}_{i_k}^{i+n} + \nu_{i_k} \mathbf{I} \right)^{-1/2} \right) \\
& = \sum_{n=1}^{N_{i_k}} \frac{\left[\mathbf{L}_{i_k}^{\text{H}} \widehat{\mathbf{F}}_{i_k} \widehat{\mathbf{F}}_{i_k}^{\text{H}} \mathbf{L}_{i_k} \right]_{nn}}{\left(\left[\mathbf{\Lambda}_{i_k} \right]_{nn} + \nu_{i_k} \right)^2} + \left\| \left(\mathbf{\Lambda}_{i_k} + \nu_{i_k} \mathbf{I} \right)^{-1} \mathbf{L}_{i_k}^{\text{H}} \widehat{\mathbf{F}}_{i_k} \widehat{\mathbf{F}}_{i_k}^{\text{H}} \mathbf{L}_{i_k}^{i+n} \left(\mathbf{\Lambda}_{i_k}^{i+n} + \nu_{i_k} \mathbf{I} \right)^{-1/2} \right\|_{\mathbb{F}}^2 \\
& = \sum_{n=1}^{N_{i_k}} \frac{\left[\mathbf{L}_{i_k}^{\text{H}} \widehat{\mathbf{F}}_{i_k} \widehat{\mathbf{F}}_{i_k}^{\text{H}} \mathbf{L}_{i_k} \right]_{nn}}{\left(\left[\mathbf{\Lambda}_{i_k} \right]_{nn} + \nu_{i_k} \right)^2} \\
& + \sum_{n=1}^{N_{i_k}} \sum_{p=1}^{N_{i_k}} \frac{1}{\left(\left[\mathbf{\Lambda}_{i_k} \right]_{nn} + \nu_{i_k} \right)^2} \frac{1}{\left(\left[\mathbf{\Lambda}_{i_k}^{i+n} \right]_{pp} + \nu_{i_k} \right)} \left| \left[\mathbf{L}_{i_k}^{\text{H}} \widehat{\mathbf{F}}_{i_k} \widehat{\mathbf{F}}_{i_k}^{\text{H}} \mathbf{L}_{i_k}^{i+n} \right]_{np} \right|^2
\end{aligned} \tag{6.82}$$

Coordinated Precoding with Hardware Impairments

So far in this thesis, a major assumption has been that the radio hardware was ideal, meaning that it would not emit spurious emissions. In this chapter, we relax this assumption, and investigate coordinated precoding under imperfect hardware. In order to fully focus on this effect, we assume unclustered operation and perfect CSI acquisition.

7.1 Distortion Noise Model

We consider a wideband system, where OFDM is used to transform the wideband channel into a set of orthogonal narrowband subcarriers; see the discussion in Section 2.1.2. The subcarriers are orthogonal, and for simplicity we only consider one subcarrier. The multiuser interaction in the downlink is described by the IBC in (2.2) on page 12, but we will augment the model with some transceiver distortion noises coming from the hardware impairments. At a given subcarrier, the received signal at MS i_k will be

$$\mathbf{y}_{i_k} = \mathbf{H}_{i_k i} \mathbf{V}_{i_k} \mathbf{x}_{i_k} + \sum_{\substack{j \in \mathcal{I}, l \in \mathcal{K}_j \\ (j,l) \neq (i,k)}} \mathbf{H}_{i_k j} \mathbf{V}_{j_l} \mathbf{x}_{j_l} + \sum_{j \in \mathcal{I}} \mathbf{H}_{i_k j} \mathbf{z}_j^{(\text{BS})} + \mathbf{z}_{i_k}^{(\text{MS})}. \quad (7.1)$$

As before, the received signal contains terms for the desired signal, as well as the received interference. The two last terms in (7.1) are however new compared to the model in (2.2). They represent the additive transmitter distortion noises, $\mathbf{z}_j^{(\text{BS})}$, as well as the additive receiver distortion noise $\mathbf{z}_{i_k}^{(\text{MS})}$. We assume that the system uses compensation techniques [Sch08] for the hardware impairments, and thus $\mathbf{z}_j^{(\text{BS})}$ and $\mathbf{z}_{i_k}^{(\text{MS})}$ are the distortion noises coming from the *residual* hardware impairments. The compensation techniques applied are necessarily imperfect, and the hardware

impairments can therefore not be completely eliminated. Our goal is thus to design robust precoders, taking into consideration the effect of the hardware impairments.

In the model with ideal hardware in (2.2), the *desired* transmitted signal of BS i is $\mathbf{s}_i = \sum_{k \in \mathcal{K}_i} \mathbf{V}_{i_k} \mathbf{x}_{i_k}$. Under the residual hardware impairments however, the *actual* transmitted signal of BS i is $\tilde{\mathbf{s}}_i = \sum_{k \in \mathcal{K}_i} \mathbf{V}_{i_k} \mathbf{x}_{i_k} + \mathbf{z}_i^{(\text{BS})}$.¹

With the extended system model in (7.1), the goal is now to solve the corresponding weighted sum rate problem. In order to formulate that problem, we will introduce models for the transceiver distortion noises. We will use a model proposed in [BJ13, Chapter 4.3], where the distortion noises are modelled as zero-mean circularly symmetric complex Gaussian random variables. The rationale for this modelling assumption is the fact that there are generally many residual hardware impairments. Their sum, after compensation, will then behave as Gaussian [Sch08, SWB10]. This fact applies to both transmitters and receivers, and has been verified using measurements on a wireless testbed [SWB10].

7.1.1 Transmitter Distortions

With the Gaussian assumption of the transmitter distortions, it now remains to find the mean and covariance of the signal. The mean is assumed to be zero, otherwise further compensation could be applied that reduces the power of the distortions.

In modelling the covariance, the distortion noises are assumed to be uncorrelated over the antennas. This is a reasonable assumption for systems where the antennas are served with individual RF chains, if the transmitted signal is independent over the antennas. The point of the precoding is however to introduce correlations between the transmitted signals at different antennas. The effect on the cross-correlations of the corresponding transmitter distortion noises was studied in [MZHH12], for a 3rd order non-linear memoryless system. The analysis showed that the cross-correlation coefficient between the distortion noises scaled as the cross-correlation coefficient between desired transmitted signals, to the 3rd power. The correlation of the distortion noises is thus small, and in the forthcoming modelling we will approximate it as zero, for tractability. Concluding, the model for the transmitter distortion noise at BS i is

$$\mathbf{z}_i^{(\text{BS})} \sim \mathcal{CN}(\mathbf{0}, \mathbf{C}_i^{(\text{BS})}), \quad \mathbf{C}_i^{(\text{BS})} = \text{diag}\left(c_{i,1}^{(\text{BS}),2}, \dots, c_{i,M_i}^{(\text{BS}),2}\right). \quad (7.2)$$

The transmitter distortion noise $\mathbf{z}_i^{(\text{BS})}$ is further assumed to be independent of the desired transmitted signal \mathbf{s}_i . If the compensation schemes are reasonably effective, any distortion noises from the residual hardware impairments should be independent of the desired transmitted signal, and this motivates our independence assumption. The *power* of $\mathbf{z}_i^{(\text{BS})}$ will however be a function of the *power* of \mathbf{s}_i . To

¹Not all hardware impairments can be described using the model in (7.1). For example, the common phase error due to phase noise can be seen as a rotation of the perceived channel [Sch08], and should thus appear as a multiplicative error.

allow for a large class of relations between these powers, we model the power of the transmitter distortion noise at the m th antenna branch of BS i as

$$c_{i,m}^{(\text{BS}),2} = \eta_i^2 \left(\sqrt{\sum_{k \in \mathcal{K}_i} \|\mathbf{V}_{i_k}]_{m,:}\|_{\mathbb{F}}^2} \right), \quad (7.3)$$

where $\sum_{k \in \mathcal{K}_i} \|\mathbf{V}_{i_k}]_{m,:}\|_{\mathbb{F}}^2$ is the power of the desired signal allocated to antenna m . In this model, the transmitter *impairment functions* $\eta_i(\cdot)$ are convex, nonnegative, and nondecreasing functions describing how the magnitude of the desired signal maps to the magnitude of the distortions. These assumptions cover a large class of functions, and crucially, will enable the optimization in Section 7.2.

In the literature, the level of distortion noises in a radio transmitter is typically measured using the *error vector magnitude* (EVM) metric. In essence, this metric describes the relation of the distortion noise power, to the desired signal power. For the proposed model, the EVM at transmitter antenna m at BS i is

$$\text{EVM}_{i,m}^{(\text{BS})} \triangleq \sqrt{\frac{c_{i,m}^{(\text{BS}),2}}{\sum_{k \in \mathcal{K}_i} \|\mathbf{V}_{i_k}]_{m,:}\|_{\mathbb{F}}^2}} = \frac{\eta_i \left(\sqrt{\sum_{k \in \mathcal{K}_i} \|\mathbf{V}_{i_k}]_{m,:}\|_{\mathbb{F}}^2} \right)}{\sqrt{\sum_{k \in \mathcal{K}_i} \|\mathbf{V}_{i_k}]_{m,:}\|_{\mathbb{F}}^2}}. \quad (7.4)$$

The first equality defines the transmitter EVM as the square root of the distortion noise power relative to the desired signal power. The second equality shows how $\eta_i(\cdot)$ affects the EVM.

Depending on the required spectral efficiency, a typical maximum transmit-EVM range in the 3GPP LTE standard [HT11] is [0.08, 0.175].

7.1.2 Receiver Distortions

The modelling of the receiver distortion noises is performed in a similar manner. Again, we base our model on the one proposed in [BJ13, Chapter 4.3]. That model however only considered single-antenna receivers. Here we extend the model in a simple way to allow for multi-antenna receivers. The receiver distortion noises are assumed to be uncorrelated over the antennas, for the same reason as given for the transmitter distortion noises. The receiver distortion noise at MS i_k can then be modelled as

$$\mathbf{z}_{i_k}^{(\text{MS})} \sim \mathcal{CN}(\mathbf{0}, \mathbf{C}_{i_k}^{(\text{MS})}), \quad \mathbf{C}_{i_k}^{(\text{MS})} = \text{diag}(c_{i_k,1}^{(\text{MS}),2}, \dots, c_{i_k,N_{i_k}}^{(\text{MS}),2}). \quad (7.5)$$

Assuming reasonably effective compensation schemes for the receiver hardware impairments, the distortion noise $\mathbf{z}_{i_k}^{(\text{MS})}$ is assumed to be independent of the received signal $\sum_{j \in \mathcal{I}, l \in \mathcal{K}_j} \mathbf{H}_{i_k j} \mathbf{V}_{j l} \mathbf{x}_{j l}$. Again, the *power* of the receiver distortion noise will

however depend on the power of the received signal. This is modelled as

$$c_{i_k,n}^{(\text{MS}),2} = \sigma_{i_k}^2 + \zeta_{i_k}^2 \left(\sqrt{\sum_{j \in \mathcal{I}, l \in \mathcal{K}_j} \left\| [\mathbf{H}_{i_k j} \mathbf{V}_{j l}]_{n,:} \right\|_{\mathbb{F}}^2} \right). \quad (7.6)$$

where $\sum_{j \in \mathcal{I}, l \in \mathcal{K}_j} \left\| [\mathbf{H}_{i_k j} \mathbf{V}_{j l}]_{n,:} \right\|_{\mathbb{F}}^2$ is the power of the received signal² at antenna n . The receiver impairment functions $\zeta_{i_k}(\cdot)$ are convex, nonnegative, and nondecreasing functions describing how the magnitude of the received signal maps to the magnitude of the receiver distortions. The $\sigma_{i_k}^2$ represents the power of the thermal noise, as a part of the total receiver distortion noise.

As in the transmitter case, we define a receiver EVM. We choose to define it in terms of the receiver distortion noise, excluding the thermal noise, relative to the desired received signal. At receive antenna m at MS i_k , it is

$$\text{EVM}_{i_k,n}^{(\text{MS})} \triangleq \frac{\zeta_{i_k} \left(\sqrt{\sum_{j \in \mathcal{I}, l \in \mathcal{K}_j} \left\| [\mathbf{H}_{i_k j} \mathbf{V}_{j l}]_{m,:} \right\|_{\mathbb{F}}^2} \right)}{\sqrt{\sum_{j \in \mathcal{I}, l \in \mathcal{K}_j} \left\| [\mathbf{H}_{i_k j} \mathbf{V}_{j l}]_{m,:} \right\|_{\mathbb{F}}^2}} \quad (7.7)$$

Received Signal Covariance Matrices

With the proposed model for the distortion noises, the covariance matrix of the received signal in (7.1) can be formed. In order to distinguish it from the covariance matrix for the IBC (without hardware-impairments) in (2.3) on page 14, we denote it as $\tilde{\Phi}_{i_k}$ for MS i_k . It is defined as

$$\begin{aligned} \tilde{\Phi}_{i_k} &= \mathbb{E}(\mathbf{y}_{i_k} \mathbf{y}_{i_k}^{\text{H}}) \\ &= \underbrace{\mathbf{H}_{i_k i} \mathbf{V}_{i_k} \mathbf{V}_{i_k}^{\text{H}} \mathbf{H}_{i_k}^{\text{H}}}_{\text{desired signal}} + \underbrace{\sum_{\substack{j \in \mathcal{I}, l \in \mathcal{K}_j \\ (j,l) \neq (i,k)}} \mathbf{H}_{i_k j} \mathbf{V}_{j l} \mathbf{V}_{j l}^{\text{H}} \mathbf{H}_{i_k}^{\text{H}}}_{\text{intercell and intracell interference}} \\ &+ \underbrace{\sum_{j \in \mathcal{I}} \mathbf{H}_{i_k j} \mathbf{C}_j^{(\text{BS})} \mathbf{H}_{i_k}^{\text{H}}}_{\text{impact of transmitter distortions}} + \underbrace{\mathbf{C}_{i_k}^{(\text{MS})}}_{\text{receiver thermal noise and distortions}}. \end{aligned} \quad (7.8)$$

²Note that we neglect the received transmitter distortion noises here. In any well-designed system, the part of the receiver distortion noise power which is directly dependent on the received transmitter distortion noise power should be small. Because of this model simplification, some expressions will simplify in the impending exposition.

The corresponding interference-plus-distortions covariance matrix is then

$$\begin{aligned}\tilde{\Phi}_{i_k}^{\text{i+d}} &= \tilde{\Phi}_{i_k} - \mathbf{H}_{i_k i} \mathbf{V}_{i_k} \mathbf{V}_{i_k}^H \mathbf{H}_{i_k i}^H \\ &= \sum_{\substack{j \in \mathcal{I}, l \in \mathcal{K}_j \\ (j,l) \neq (i,k)}} \mathbf{H}_{i_k j} \mathbf{V}_{j l} \mathbf{V}_{j l}^H \mathbf{H}_{i_k j}^H + \sum_{j \in \mathcal{I}} \mathbf{H}_{i_k j} \mathbf{C}_j^{(\text{BS})} \mathbf{H}_{i_k j}^H + \mathbf{C}_{i_k}^{(\text{MS})}.\end{aligned}\quad (7.9)$$

7.2 Semi-Distributed WMMSE Algorithm

Given the model of the transceiver distortion noises, the goal is now to maximize the weighted sum rate. First, we must modify our definition of the user rates to take into account the distortion noises. Assuming that the receivers treat the received distortion noises as additive Gaussian noise in the decoder, the rate for MS i_k is

$$\tilde{r}_{i_k} = \log_2 \det \left(\mathbf{I} + \mathbf{V}_{i_k}^H \mathbf{H}_{i_k i}^H \left(\tilde{\Phi}_{i_k}^{\text{i+d}} \right)^{-1} \mathbf{H}_{i_k i} \mathbf{V}_{i_k} \right).\quad (7.10)$$

We now want to solve the weighted sum rate problem³ with hardware-impaired transceivers

$$\begin{aligned}& \underset{\{\mathbf{V}_{i_k}\}}{\text{maximize}} && \sum_{i \in \mathcal{I}, k \in \mathcal{K}_i} \omega_{i_k} \tilde{r}_{i_k} \\ & \text{subject to} && \text{Tr} \left(\mathbf{C}_i^{(\text{BS})} \right) + \sum_{k \in \mathcal{K}_i} \|\mathbf{V}_{i_k}\|_{\text{F}}^2 \leq P_i, \quad \forall i \in \mathcal{I},\end{aligned}\quad (7.11)$$

where we assume that the transmitted distortion noises count towards the total power budget of a BS.

7.2.1 Weighted MMSE Minimization

The weighted sum rate problem with hardware-impaired transceivers in (7.11) is non-convex since (7.10) is non-convex in $\{\mathbf{V}_{i_k}\}_{i \in \mathcal{I}, k \in \mathcal{K}_i}$. We will therefore apply the WMMSE approach [SRLH11] as described in Appendix 2.B. With linear receive filters $\{\mathbf{U}_{i_k}\}_{i \in \mathcal{I}, k \in \mathcal{K}_i}$ at all MSs, the MSE matrix for MS i_k is

$$\begin{aligned}\tilde{\mathbf{E}}_{i_k} &= \mathbb{E} \left((\mathbf{x}_{i_k} - \hat{\mathbf{x}}_{i_k}) (\mathbf{x}_{i_k} - \hat{\mathbf{x}}_{i_k})^H \right) = \mathbb{E} \left((\mathbf{x}_{i_k} - \mathbf{U}_{i_k}^H \mathbf{y}_{i_k}) (\mathbf{x}_{i_k} - \mathbf{U}_{i_k}^H \mathbf{y}_{i_k})^H \right) \\ &= \mathbf{I} - \mathbf{U}_{i_k}^H \mathbf{H}_{i_k i} \mathbf{V}_{i_k} - \mathbf{V}_{i_k}^H \mathbf{H}_{i_k i}^H \mathbf{U}_{i_k} + \mathbf{U}_{i_k}^H \tilde{\Phi}_{i_k} \mathbf{U}_{i_k}.\end{aligned}\quad (7.12)$$

Notice the similarity to the MSE matrix in (2.18) on page 40 for the system without hardware impairments. The impact of the distortion noises appear inside $\tilde{\Phi}_{i_k}$, and

³We are assuming unity pre-log factors in this chapter, and the weighted sum rate problem is thus identical to the weighted sum throughput problem.

therefore the WMMSE approach can be applied directly. Next, we seek the MMSE receiver

$$\mathbf{U}_{i_k}^{\text{MMSE}} = \arg \min_{\mathbf{U}_{i_k}} \text{Tr} \left(\tilde{\mathbf{E}}_{i_k} \right) = \tilde{\mathbf{\Phi}}_{i_k}^{-1} \mathbf{H}_{i_k i} \mathbf{V}_{i_k} \quad (7.13)$$

and note that

$$\begin{aligned} \tilde{\mathbf{E}}_{i_k}^{\text{MMSE}} &= \tilde{\mathbf{E}}_{i_k} \left(\mathbf{U}_{i_k}^{\text{MMSE}} \right) = \mathbf{I} - \mathbf{V}_{i_k}^{\text{H}} \mathbf{H}_{i_k i}^{\text{H}} \tilde{\mathbf{\Phi}}_{i_k}^{-1} \mathbf{H}_{i_k i} \mathbf{V}_{i_k} \\ &= \left(\mathbf{I} + \mathbf{V}_{i_k}^{\text{H}} \mathbf{H}_{i_k i}^{\text{H}} \left(\tilde{\mathbf{\Phi}}_{i_k}^{\dagger+d} \right)^{-1} \mathbf{H}_{i_k i} \mathbf{V}_{i_k} \right)^{-1}. \end{aligned} \quad (7.14)$$

The last equality in (7.14) is due to the matrix inversion lemma. By applying the WMMSE approach (see Appendix 2.B), we arrive at the weighted MMSE problem for hardware-impaired transceivers,

$$\begin{aligned} &\underset{\substack{\{\mathbf{V}_{i_k}\}, \{\mathbf{U}_{i_k}\} \\ \{\mathbf{W}_{i_k} \succ \mathbf{0}\}}}{\text{minimize}} \quad \log_2(e) \sum_{i \in \mathcal{I}, k \in \mathcal{K}_i} \omega_{i_k} \left(\text{Tr} \left(\mathbf{W}_{i_k} \tilde{\mathbf{E}}_{i_k} \right) - \ln \det \left(\mathbf{W}_{i_k} \right) - d_{i_k} \right) \\ &\text{subject to} \quad \text{Tr} \left(\mathbf{C}_i^{(\text{BS})} \right) + \sum_{k \in \mathcal{K}_i} \|\mathbf{V}_{i_k}\|_{\text{F}}^2 \leq P_i, \quad \forall i \in \mathcal{I}. \end{aligned} \quad (7.15)$$

Comparing to the WMMSE problem for unimpaired transceivers in (2.23) on page 41, it can be seen that the two problems have the same structure, but different MSE matrices. In a similar vein as the WMMSE algorithm without hardware impairments, we can thus try to find a local optimum to (7.15) using block coordinate descent.

7.2.2 Optimality Conditions

Before applying block coordinate descent to (7.15), we derive the first-order necessary optimality conditions [Ber06] for two of the blocks of variables. These are found by setting the partial complex gradients [HG07] of the objective function to zero.

Since $\mathbf{W}_{i_k} \succ \mathbf{0}$, the first-order optimality conditions for the receive filters are

$$\tilde{\mathbf{\Phi}}_{i_k} \mathbf{U}_{i_k} = \mathbf{H}_{i_k i} \mathbf{V}_{i_k}, \quad \forall i \in \mathcal{I}, k \in \mathcal{K}_i. \quad (7.16)$$

The first-order optimality conditions for the MSE weights are

$$\left(\mathbf{W}_{i_k} \right)^{-1} = \tilde{\mathbf{E}}_{i_k}, \quad \forall i \in \mathcal{I}, k \in \mathcal{K}_i. \quad (7.17)$$

We will now show that (7.15) has the same global solutions as (7.11). This follows analogously to the problem considered in [SRLH11], but we show the steps here for completeness.

Substituting the necessary conditions in (7.17) into (7.15) and changing the base of the logarithm, the resulting equivalent optimization problem is

$$\begin{aligned} & \underset{\{\mathbf{V}_{i_k}\}, \{\mathbf{U}_{i_k}\}}{\text{minimize}} && \sum_{i \in \mathcal{I}, k \in \mathcal{K}_i} \omega_{i_k} \log_2 \det \left(\tilde{\mathbf{E}}_{i_k}^{-1} \right) \\ & \text{subject to} && \text{Tr} \left(\mathbf{C}_i^{(\text{BS})} \right) + \sum_{k \in \mathcal{K}_i} \|\mathbf{V}_{i_k}\|_{\text{F}}^2 \leq P_i, \quad \forall i \in \mathcal{I}. \end{aligned} \quad (7.18)$$

Then further substituting (7.16) into (7.18), using (7.14), the resulting equivalent optimization problem is

$$\begin{aligned} & \underset{\{\mathbf{V}_{i_k}\}}{\text{maximize}} && \sum_{i \in \mathcal{I}, k \in \mathcal{K}_i} \omega_{i_k} \log_2 \det \left(\mathbf{I} + \mathbf{V}_{i_k}^{\text{H}} \mathbf{H}_{i_k}^{\text{H}} \left(\tilde{\Phi}_{i_k}^{i+d} \right)^{-1} \mathbf{H}_{i_k} \mathbf{V}_{i_k} \right) \\ & \text{subject to} && \text{Tr} \left(\mathbf{C}_i^{(\text{BS})} \right) + \sum_{k \in \mathcal{K}_i} \|\mathbf{V}_{i_k}\|_{\text{F}}^2 \leq P_i, \quad \forall i \in \mathcal{I}. \end{aligned} \quad (7.19)$$

Clearly, (7.19) is identical to (7.11), and thus (7.15) and (7.11) have the same globally optimal solutions.

Furthermore, it can be shown using [SRLH11, Theorem 3] that (7.15) and (7.11) have the same locally optimal solutions as well. This is done by noting that the stationarity condition of the optimization problem in (7.15) w.r.t. $\{\mathbf{V}_{i_k}\}_{i \in \mathcal{I}, k \in \mathcal{K}_i}$, for optimal $\{\mathbf{U}_{i_k}^*, \mathbf{W}_{i_k}^*\}_{i \in \mathcal{I}, k \in \mathcal{K}_i}$, is the same as the stationarity condition of the optimization problem in (7.11).

7.2.3 Block Coordinate Descent

Although we have shown that the optimization problems in (7.15) and (7.11) have the same global optima, we will only be able to constructively find local optima. In order to do that, we now apply block coordinate descent to the optimization problem in (7.15). The blocks we will optimize over are $\{\mathbf{U}_{i_k}\}_{i \in \mathcal{I}, k \in \mathcal{K}_i}$, $\{\mathbf{W}_{i_k}\}_{i \in \mathcal{I}, k \in \mathcal{K}_i}$ and $\{\mathbf{V}_{i_k}\}_{i \in \mathcal{I}, k \in \mathcal{K}_i}$.

Subproblem Solutions

By fixing $\{\mathbf{W}_{i_k}, \mathbf{V}_{i_k}\}_{i \in \mathcal{I}, k \in \mathcal{K}_i}$, the remaining unconstrained optimization problem is convex in $\{\mathbf{U}_{i_k}\}_{i \in \mathcal{I}, k \in \mathcal{K}_i}$. The first-order necessary condition in (7.16) is thus both necessary and sufficient, and the solution for MS i_k is

$$\mathbf{U}_{i_k}^* = \tilde{\Phi}_{i_k}^{-1} \mathbf{H}_{i_k} \mathbf{V}_{i_k} = \mathbf{U}_{i_k}^{\text{MMSE}}, \quad (7.20)$$

where the last equality is identified from (7.13). Similarly, fixing $\{\mathbf{U}_{i_k}, \mathbf{V}_{i_k}\}_{i \in \mathcal{I}, k \in \mathcal{K}_i}$, the remaining optimization problem is convex in $\{\mathbf{W}_{i_k}\}_{i \in \mathcal{I}, k \in \mathcal{K}_i}$. The necessary and sufficient first-order condition in (7.17) then gives the solution for MS i_k as

$$\mathbf{W}_{i_k}^* = \left(\tilde{\mathbf{E}}_{i_k} \right)^{-1} = \mathbf{I} + \mathbf{V}_{i_k}^{\text{H}} \mathbf{H}_{i_k}^{\text{H}} \left(\tilde{\Phi}_{i_k}^{i+d} \right)^{-1} \mathbf{H}_{i_k} \mathbf{V}_{i_k}, \quad (7.21)$$

where the last equality is from substituting (7.20) and (7.14). Since $\mathbf{W}_{i_k}^* \succ \mathbf{0}$, this is indeed the solution.

Finally, we fix $\{\mathbf{U}_{i_k}, \mathbf{W}_{i_k}\}_{i \in \mathcal{I}, k \in \mathcal{K}_i}$ and optimize over $\{\mathbf{V}_{i_k}\}_{i \in \mathcal{I}, k \in \mathcal{K}_i}$. By dropping constant terms, and rearranging the remaining terms using properties of the trace, the following problem should be solved:

$$\begin{aligned} \underset{\{\mathbf{V}_{i_k}\}}{\text{minimize}} \quad & \sum_{i \in \mathcal{I}} \left[\text{Tr} \left(\mathbf{\Gamma}_i \mathbf{C}_i^{(\text{BS})} \right) + \sum_{k \in \mathcal{K}_i} \left[\text{Tr} \left(\mathbf{V}_{i_k}^H \mathbf{\Gamma}_i \mathbf{V}_{i_k} \right) \right. \right. \\ & \left. \left. - 2\omega_{i_k} \text{Re} \left(\text{Tr} \left(\mathbf{W}_{i_k} \mathbf{U}_{i_k}^H \mathbf{H}_{i_k i} \mathbf{V}_{i_k} \right) \right) + \omega_{i_k} \text{Tr} \left(\mathbf{U}_{i_k} \mathbf{W}_{i_k} \mathbf{U}_{i_k}^H \mathbf{C}_{i_k}^{(\text{MS})} \right) \right] \right] \\ \text{subject to} \quad & \text{Tr} \left(\mathbf{C}_i^{(\text{BS})} \right) + \sum_{k \in \mathcal{K}_i} \|\mathbf{V}_{i_k}\|_F^2 \leq P_i, \quad \forall i \in \mathcal{I}. \end{aligned} \quad (7.22)$$

Here $\mathbf{\Gamma}_i = \sum_{j \in \mathcal{I}, l \in \mathcal{K}_j} \omega_{j_l} \mathbf{H}_{j_l i}^H \mathbf{U}_{j_l} \mathbf{W}_{j_l} \mathbf{U}_{j_l}^H \mathbf{H}_{j_l i}$ is the signal-plus-interference covariance matrix for a virtual uplink.⁴ Compared to the optimization problem in (2.29) on page 42, there are two additional terms. The term $\text{Tr} \left(\mathbf{\Gamma}_i \mathbf{C}_i^{(\text{BS})} \right)$ describes the impact of the transmitter distortion noises generated by BS i on the total performance. Similarly, the term $\omega_{i_k} \text{Tr} \left(\mathbf{U}_{i_k} \mathbf{W}_{i_k} \mathbf{U}_{i_k}^H \mathbf{C}_{i_k}^{(\text{MS})} \right)$ describes the impact of the receiver distortion noises generated by MS i_k on the total performance.

Note that $\mathbf{C}_i^{(\text{BS})}$ and $\mathbf{C}_{i_k}^{(\text{MS})}$ are functions of $\{\mathbf{V}_{i_k}\}_{i \in \mathcal{I}, k \in \mathcal{K}_i}$, and since $\eta_i^2(\cdot)$ and $\zeta_{i_k}^2(\cdot)$ are convex, the problem in (7.22) is convex in $\{\mathbf{V}_{i_k}\}$. For the general case, it can thus be solved efficiently using general interior-point methods [BV04, Chapter 11].

Semi-Distributed Algorithm

The block coordinate descent procedure now consists of iteratively applying (7.20), (7.21), and solving (7.22). The resulting algorithm is presented in Algorithm 7.1. The iterations continue until convergence, or until a fixed number of steps is reached.

⁴In this chapter, we do not assume reciprocal channels, and $\mathbf{\Gamma}_i$ may therefore be a quantity which is not related to the true uplink.

Algorithm 7.1 WMMSE Algorithm for Hardware-Impaired Transceivers

1: **repeat**

 At MS i_k :

2: Find MSE weights: $\mathbf{W}_{i_k} = \mathbf{I} + \mathbf{V}_{i_k}^H \mathbf{H}_{i_k i}^H \left(\tilde{\mathbf{\Phi}}_{i_k}^{i+d} \right)^{-1} \mathbf{H}_{i_k i} \mathbf{V}_{i_k}$

3: Find MMSE receive filters: $\mathbf{U}_{i_k} = \tilde{\mathbf{\Phi}}_{i_k}^{-1} \mathbf{H}_{i_k i} \mathbf{V}_{i_k}$

 At Central BS Unit:

4: Find precoders as solution to the optimization problem in (7.22)

5: **until** convergence criterion met, or fixed number of iterations

Theorem 7.1. *The block coordinate descent of (7.15) monotonically converges. Every limit point of the block coordinate descent iterates is a stationary point of the optimization problem in (7.11) on page 135.*

Proof: In each substep, solving for either $\{\mathbf{U}_{i_k}\}_{i \in \mathcal{I}, k \in \mathcal{K}_i}$, $\{\mathbf{W}_{i_k}\}_{i \in \mathcal{I}, k \in \mathcal{K}_i}$, or $\{\mathbf{V}_{i_k}\}_{i \in \mathcal{I}, k \in \mathcal{K}_i}$, the objective value of (7.15) can never increase. Since the objective function of (7.15) can be lower-bounded, the objective value monotonically converges.

It now remains to show that the block coordinate descent iterates reach a stationary point of the problem. If any of the $c_{i,m}^{(\text{BS}),2}$ or $c_{i_k,n}^{(\text{MS}),2}$ are non-differentiable w.r.t. $\{\mathbf{V}_{i_k}\}_{i \in \mathcal{I}, k \in \mathcal{K}_i}$, introduce auxiliary optimization variables $d_{i,m}^{(\text{BS})}$ and $d_{i_k,n}^{(\text{MS})}$ to (7.15). Replace $c_{i,m}^{(\text{BS}),2} \rightarrow d_{i,m}^{(\text{BS})}$, $c_{i_k,n}^{(\text{MS}),2} \rightarrow d_{i_k,n}^{(\text{MS})}$ and introduce inequality constraints

$$c_{i,m}^{(\text{BS}),2} = \eta_i^2 \left(\sqrt{\sum_k \|\llbracket \mathbf{V}_{i_k} \rrbracket_{m,:}\|_{\text{F}}^2} \right) \leq d_{i,m}^{(\text{BS})}, \quad \forall i, m$$

$$c_{i_k,n}^{(\text{MS}),2} = \sigma_{i_k}^2 + \zeta_{i_k}^2 \left(\sqrt{\sum_{j \in \mathcal{I}, l \in \mathcal{K}_j} \|\llbracket \mathbf{H}_{i_k j} \mathbf{V}_{j l} \rrbracket_{n,:}\|_{\text{F}}^2} \right) \leq d_{i_k,n}^{(\text{MS})}, \quad \forall i_k, n$$

to (7.15), in order to get the squared impairment functions on epigraph form. For this equivalent problem, the objective function is continuously differentiable and the extended feasible set is convex. Then, since the subproblem for $\{\mathbf{U}_{i_k}\}_{i \in \mathcal{I}, k \in \mathcal{K}_i}$ is strictly convex, [GS00, Prop. 5] gives that every limit point of the block coordinate descent iterates is a stationary point of (7.15). That this is also a stationary point of (7.11) follows directly from the proof of Theorem 3 in [SRLH11]. ■

7.3 Distributed Implementation for Constant-EVM Transceivers

One interesting special case is that of *constant-EVM* transceivers. For these, the EVMs are

$$\text{EVM}_{i,m}^{(\text{BS})} = \kappa_i^{(\text{BS})}, \quad \forall i, m \quad (7.23)$$

$$\text{EVM}_{i_k,n}^{(\text{MS})} = \kappa_{i_k}^{(\text{MS})}, \quad \forall i_k, n. \quad (7.24)$$

which for our model with impairment functions corresponds to

$$\eta_i(x) = \kappa_i^{(\text{BS})} x, \quad \forall i, \quad (7.25)$$

$$\zeta_{i_k}(x) = \kappa_{i_k}^{(\text{MS})} x, \quad \forall i_k. \quad (7.26)$$

With these impairment functions, the distortion noise covariance matrices are

$$\mathbf{C}_i^{(\text{BS})} = \left(\kappa_i^{(\text{BS})}\right)^2 \sum_{k=1}^{K_i} \text{Diag}(\mathbf{V}_{i_k} \mathbf{V}_{i_k}^H), \quad \forall i, \quad (7.27)$$

$$\mathbf{C}_{i_k}^{(\text{MS})} = \sigma_{i_k}^2 \mathbf{I} + \left(\kappa_{i_k}^{(\text{MS})}\right)^2 \sum_{j \in \mathcal{I}, l \in \mathcal{K}_j} \text{Diag}(\mathbf{H}_{i_k j} \mathbf{V}_{j l} \mathbf{V}_{j l}^H \mathbf{H}_{i_k j}^H), \quad \forall i_k, \quad (7.28)$$

where the $\text{Diag}(\cdot)$ operator retains the diagonal elements and lets the non-diagonal elements be zero.

Two features of this special case is that the proposed semi-distributed WMMSE algorithm in Algorithm 7.1 will become distributed over the BSs, and that we can propose a modified version of the well-known MaxSINR algorithm from [GCJ11].

7.3.1 Distributed WMMSE Algorithm

Algorithm 7.1 on page 138 is naturally distributed over the MSs, but the BS side optimization problem in (7.22) on page 138 must in general be solved in a centralized fashion. The optimization problem can only be solved in parallel over the BSs if the term

$$\sum_{i \in \mathcal{I}, k \in \mathcal{K}_i} \omega_{i_k} \text{Tr}(\mathbf{U}_{i_k} \mathbf{W}_{i_k} \mathbf{U}_{i_k}^H \mathbf{C}_{i_k}^{(\text{MS})}) \quad (7.29)$$

decomposes, which indeed is the case for the constant-EVM transceivers.

It can easily be shown that $\text{Tr}(\mathbf{F} \text{Diag}(\mathbf{G})) = \text{Tr}(\text{Diag}(\mathbf{F}) \mathbf{G})$, for arbitrary square matrices \mathbf{F} and \mathbf{G} . Using this fact, together with the covariance matrix in (7.28), we can rewrite (7.29) as

$$\begin{aligned} \sum_{i \in \mathcal{I}, k \in \mathcal{K}_i} \omega_{i_k} \text{Tr}(\mathbf{U}_{i_k} \mathbf{W}_{i_k} \mathbf{U}_{i_k}^H \mathbf{C}_{i_k}^{(\text{MS})}) = \\ \sum_{i \in \mathcal{I}, k \in \mathcal{K}_i} \left(\text{Tr}(\mathbf{V}_{i_k}^H \bar{\mathbf{\Gamma}}_i \mathbf{V}_{i_k}) + \omega_{i_k} \sigma_{i_k}^2 \text{Tr}(\mathbf{U}_{i_k} \mathbf{W}_{i_k} \mathbf{U}_{i_k}^H) \right), \end{aligned} \quad (7.30)$$

where

$$\bar{\mathbf{\Gamma}}_i = \sum_{j \in \mathcal{I}, l \in \mathcal{K}_j} \omega_{j l} \left(\kappa_{j l}^{(\text{MS})}\right)^2 \mathbf{H}_{j l}^H \text{Diag}(\mathbf{U}_{j l} \mathbf{W}_{j l} \mathbf{U}_{j l}^H) \mathbf{H}_{j l} i. \quad (7.31)$$

Using the same trick, we can show that

$$\text{Tr}(\mathbf{\Gamma}_i \mathbf{C}_i^{(\text{BS})}) = \left(\kappa_i^{(\text{BS})}\right)^2 \sum_{k \in \mathcal{K}_i} \text{Tr}(\mathbf{V}_{i_k}^H \text{Diag}(\mathbf{\Gamma}_i) \mathbf{V}_{i_k}). \quad (7.32)$$

Substituting (7.30) and (7.32) into the optimization problem in (7.22), an equivalent problem is obtained as

$$\begin{aligned} & \underset{\{\mathbf{V}_{i_k}\}}{\text{minimize}} && \sum_{i \in \mathcal{I}, k \in \mathcal{K}_i} \left[\text{Tr} \left(\mathbf{V}_{i_k}^H \left(\mathbf{\Gamma}_i + \bar{\mathbf{\Gamma}}_i + \left(\kappa_i^{(\text{BS})} \right)^2 \text{Diag}(\mathbf{\Gamma}_i) \right) \mathbf{V}_{i_k} \right) \right. \\ & && \left. - 2\omega_{i_k} \text{Re} \left(\text{Tr} \left(\mathbf{W}_{i_k} \mathbf{U}_{i_k}^H \mathbf{H}_{i_k i} \mathbf{V}_{i_k} \right) \right) \right] \\ & \text{subject to} && \text{Tr} \left(\mathbf{C}_i^{(\text{BS})} \right) + \sum_{k \in \mathcal{K}_i} \|\mathbf{V}_{i_k}\|_{\text{F}}^2 \leq P_i, \quad \forall i \in \mathcal{I}. \end{aligned} \quad (7.33)$$

The problem in (7.33) decomposes over BSs, and the optimal precoder for MS i_k is

$$\mathbf{V}_{i_k}^* = \omega_{i_k} \left(\mathbf{\Gamma}_i + \bar{\mathbf{\Gamma}}_i + \left(\kappa_i^{(\text{BS})} \right)^2 \text{Diag}(\mathbf{\Gamma}_i) + \tilde{\mu}_i^* \mathbf{I} \right)^{-1} \mathbf{H}_{i_k i}^H \mathbf{U}_{i_k} \mathbf{W}_{i_k}. \quad (7.34)$$

If the optimal Lagrange multiplier for BS i is $\tilde{\mu}_i^* = 0$, the solution is given. Otherwise, $\tilde{\mu}_i^* > 0$ can be found by bisection such that

$$\left(1 + \left(\kappa_i^{(\text{BS})} \right)^2 \right) \sum_{k=1}^{K_i} \|\mathbf{V}_{i_k}^*\|_{\text{F}}^2 = P_i. \quad (7.35)$$

The distributed algorithm for the constant-EVM transceivers is described in Algorithm 7.2.

Algorithm 7.2 Distributed WMMSE Algorithm for Constant-EVM Transceivers

1: **repeat**

 At MS i_k :

2: Find MSE weights: $\mathbf{W}_{i_k} = \mathbf{I} + \mathbf{V}_{i_k}^H \mathbf{H}_{i_k i}^H \left(\tilde{\mathbf{\Phi}}_{i_k}^{i+d} \right)^{-1} \mathbf{H}_{i_k i} \mathbf{V}_{i_k}$

3: Find MMSE receive filters: $\mathbf{U}_{i_k} = \tilde{\mathbf{\Phi}}_{i_k}^{-1} \mathbf{H}_{i_k i} \mathbf{V}_{i_k}$

 At BS i :

4: Find $\tilde{\mu}_i$ which satisfies $\left(1 + \left(\kappa_i^{(\text{BS})} \right)^2 \right) \sum_{k \in \mathcal{K}_i} \|\mathbf{V}_{i_k}\|_{\text{F}}^2 \leq P_i$

5: Find precoders:

$$\mathbf{V}_{i_k} = \omega_{i_k} \left(\mathbf{\Gamma}_i + \bar{\mathbf{\Gamma}}_i + \left(\kappa_i^{(\text{BS})} \right)^2 \text{Diag}(\mathbf{\Gamma}_i) + \tilde{\mu}_i \mathbf{I} \right)^{-1} \mathbf{H}_{i_k i}^H \mathbf{U}_{i_k} \mathbf{W}_{i_k}, \quad k \in \mathcal{K}_i$$

6: **until** convergence criterion met, or fixed number of iterations

7.3.2 Distributed MaxSINDR Algorithm

For the case of constant-EVM transceivers, with the covariances in (7.27) and (7.28), a MaxSINDR algorithm can also be devised. This is done by modifying the original MaxSINR [GCJ11], by taking into account the constant-EVM distortions.

First, we define the virtual uplink signal for the MaxSINDR algorithm as

$$\mathbf{r}_i = \sum_{j \in \mathcal{I}, l \in \mathcal{K}_j} \omega_{j_l} \mathbf{H}_{i_k j}^H \mathbf{U}_{j_l} \mathbf{U}_{j_l}^H \mathbf{H}_{i_k j}, \quad (7.36)$$

and a corresponding “diagonalized” signal-plus-interference covariance matrix

$$\tilde{\mathbf{r}}_i = \sum_{j \in \mathcal{I}, l \in \mathcal{K}_j} \omega_{j_l} \left(\kappa_{j_l}^{(\text{MS})} \right)^2 \mathbf{H}_{j_l i}^H \text{Diag} \left(\mathbf{U}_{j_l} \mathbf{U}_{j_l}^H \right) \mathbf{H}_{j_l i}. \quad (7.37)$$

Receive Filter Optimization

At the MSs, the receive filters $\{\mathbf{U}_{i_k}\}_{i \in \mathcal{I}, k \in \mathcal{K}_I}$ are found on a per-stream basis, such that the instantaneous per-stream signal-to-interference-distortions-and-noise ratio (SINDR) is maximized. The columns of the receive filters are then given by

$$\begin{aligned} \mathbf{u}_{i_k, n}^* &= \arg \max_{\mathbf{u}_{i_k, n}^H \mathbf{u}_{i_k, n} = 1} \frac{\mathbf{u}_{i_k, n}^H \mathbf{H}_{i_k i} \mathbf{v}_{i_k, n} \mathbf{v}_{i_k, n}^H \mathbf{H}_{i_k i}^H \mathbf{u}_{i_k, n}}{\mathbf{u}_{i_k, n}^H \tilde{\mathbf{\Phi}}_{i_k}^{i+d} \mathbf{u}_{i_k, n}} \\ &= \frac{\left(\tilde{\mathbf{\Phi}}_{i_k}^{i+d} \right)^{-1} \mathbf{H}_{i_k i} \mathbf{v}_{i_k, n}}{\left\| \left(\tilde{\mathbf{\Phi}}_{i_k}^{i+d} \right)^{-1} \mathbf{H}_{i_k i} \mathbf{v}_{i_k, n} \right\|_2} \\ &= \frac{\tilde{\mathbf{\Phi}}_{i_k}^{-1} \mathbf{H}_{i_k i} \mathbf{v}_{i_k, n}}{\left\| \tilde{\mathbf{\Phi}}_{i_k}^{-1} \mathbf{H}_{i_k i} \mathbf{v}_{i_k, n} \right\|_2}, \quad \forall i_k, n \end{aligned} \quad (7.38)$$

where the last equality is due to the matrix inversion lemma. The receive filters can be found in parallel over the MSs, and even in parallel over the streams for each MS.

Precoder Optimization

At the BSs, the precoders $\{\mathbf{V}_{i_k}\}_{i \in \mathcal{I}, k \in \mathcal{K}_I}$ are also found on a per-stream basis. These are however selected to maximize a metric which is related to the ratio between the received desired signal power due to the per-stream beamformer, and the received interference and distortion signal power due to the per-stream precoder. We call this metric a “quasi-SINDR”. The intuition is that each beamformer $\mathbf{v}_{i_k, n}$ creates a desired signal at MS i_k , but it will also create interference at all other MSs, as well as distortions at all MSs. The per-stream beamformers should thus be

selected to balance the positive and detrimental effects. In order to find the per-stream beamformer for stream n to MS i_k , we first note that the weighted received desired signal power can be written as

$$\omega_{i_k} \left| \mathbf{u}_{i_k,n}^H \mathbf{H}_{i_k i} \mathbf{v}_{i_k,n} \right|^2 = \omega_{i_k} \mathbf{v}_{i_k,n}^H \mathbf{H}_{i_k i}^H \mathbf{u}_{i_k,n} \mathbf{u}_{i_k,n}^H \mathbf{H}_{i_k i} \mathbf{v}_{i_k,n}. \quad (7.39)$$

This quantity will end up in the numerator of the quasi-SINDR.

We now study the quantities that will end up in the denominator of the quasi-SINDR. The total weighted interference power due to $\mathbf{v}_{i_k,n}$ is

$$\begin{aligned} & \sum_{j \in \mathcal{I}, l \in \mathcal{K}_j} \omega_{j_l} \text{Tr} \left(\mathbf{U}_{j_l}^H \mathbf{H}_{j_l i} \mathbf{v}_{i_k,n} \mathbf{v}_{i_k,n}^H \mathbf{H}_{j_l i}^H \mathbf{U}_{j_l} \right) - \omega_{i_k} \left| \mathbf{u}_{i_k,n}^H \mathbf{H}_{i_k i} \mathbf{v}_{i_k,n} \right|^2 \\ & = \mathbf{v}_{i_k,n}^H \left(\mathbf{\Upsilon}_i - \omega_{i_k} \mathbf{H}_{i_k i} \mathbf{u}_{i_k,n} \mathbf{u}_{i_k,n}^H \mathbf{H}_{i_k i}^H \right) \mathbf{v}_{i_k,n}. \end{aligned} \quad (7.40)$$

For the constant-EVM transmitters, the transmitter distortion power is linear in the power of the per-stream beamformers (see (7.27)). Therefore, the total weighted (received) transmitter distortion power due to $\mathbf{v}_{i_k,n}$ is

$$\left(\kappa_i^{(\text{BS})} \right)^2 \text{Tr} \left(\mathbf{\Upsilon}_i \text{Diag} \left(\mathbf{v}_{i_k,n} \mathbf{v}_{i_k,n}^H \right) \right) = \left(\kappa_i^{(\text{BS})} \right)^2 \mathbf{v}_{i_k,n}^H \text{Diag} \left(\mathbf{\Upsilon}_i \right) \mathbf{v}_{i_k,n}. \quad (7.41)$$

Finally, using a similar relation as in (7.30) on page 140, the total weighted receiver distortion power due to $\mathbf{v}_{i_k,n}$ is

$$\mathbf{v}_{i_k,n}^H \tilde{\mathbf{\Upsilon}}_i \mathbf{v}_{i_k,n}. \quad (7.42)$$

Putting together the desired signal power with the interference and distortion terms in (7.40), (7.41), and (7.42), the quasi-SINDR to optimize is

$$\frac{\omega_{i_k} \mathbf{v}_{i_k,n}^H \mathbf{H}_{i_k i}^H \mathbf{u}_{i_k,n} \mathbf{u}_{i_k,n}^H \mathbf{H}_{i_k i} \mathbf{v}_{i_k,n}}{\mathbf{v}_{i_k,n}^H \left(\mathbf{\Upsilon}_i - \omega_{i_k} \mathbf{H}_{i_k i} \mathbf{u}_{i_k,n} \mathbf{u}_{i_k,n}^H \mathbf{H}_{i_k i}^H + \tilde{\mathbf{\Upsilon}}_i + \left(\kappa_i^{(\text{BS})} \right)^2 \text{Diag} \left(\mathbf{\Upsilon}_i \right) + \frac{\sigma_{i_k}^2 K_i}{P_i} \mathbf{I} \right) \mathbf{v}_{i_k,n}}. \quad (7.43)$$

Notice that a white term relating to the SNR of MS i_k was also added to the denominator. This term is needed at low SNR, since the interference is negligible then.

Concluding, the per-stream beamformers are now given by

$$\begin{aligned}
\mathbf{v}_{i_k, n}^* &= \arg \max_{\mathbf{v}_{i_k, n}^H = \frac{P_i}{K_i d_{i_k}}} \text{quasi-SINDR}_{i_k, n} \quad \text{in (7.43)} \\
&= \sqrt{\frac{P_i}{K_i d_{i_k}}} \frac{\sqrt{\omega_{i_k}} \left(\mathbf{\Upsilon}_i - \omega_{i_k} \mathbf{H}_{i_k i} \mathbf{u}_{i_k, n} \mathbf{u}_{i_k, n}^H \mathbf{H}_{i_k i}^H + \tilde{\mathbf{\Upsilon}}_i + (\kappa_i^{(\text{BS})})^2 \text{Diag}(\mathbf{\Upsilon}_i) + \frac{\sigma_{i_k}^2 K_i}{P_i} \mathbf{I} \right)^{-1} \mathbf{H}_{i_k i}^H \mathbf{u}_{i_k, n}}{\left\| \sqrt{\omega_{i_k}} \left(\mathbf{\Upsilon}_i - \omega_{i_k} \mathbf{H}_{i_k i} \mathbf{u}_{i_k, n} \mathbf{u}_{i_k, n}^H \mathbf{H}_{i_k i}^H + \tilde{\mathbf{\Upsilon}}_i + (\kappa_i^{(\text{BS})})^2 \text{Diag}(\mathbf{\Upsilon}_i) + \frac{\sigma_{i_k}^2 K_i}{P_i} \mathbf{I} \right)^{-1} \mathbf{H}_{i_k i}^H \mathbf{u}_{i_k, n} \right\|_2} \\
&= \sqrt{\frac{P_i}{K_i d_{i_k}}} \frac{\sqrt{\omega_{i_k}} \left(\mathbf{\Upsilon}_i + \tilde{\mathbf{\Upsilon}}_i + (\kappa_i^{(\text{BS})})^2 \text{Diag}(\mathbf{\Upsilon}_i) + \frac{\sigma_{i_k}^2 K_i}{P_i} \mathbf{I} \right)^{-1} \mathbf{H}_{i_k i}^H \mathbf{u}_{i_k, n}}{\left\| \sqrt{\omega_{i_k}} \left(\mathbf{\Upsilon}_i + \tilde{\mathbf{\Upsilon}}_i + (\kappa_i^{(\text{BS})})^2 \text{Diag}(\mathbf{\Upsilon}_i) + \frac{\sigma_{i_k}^2 K_i}{P_i} \mathbf{I} \right)^{-1} \mathbf{H}_{i_k i}^H \mathbf{u}_{i_k, n} \right\|_2}, \quad \forall i_k, n
\end{aligned} \tag{7.44}$$

where the last equality is due to the matrix inversion lemma. The full algorithm is summarized in Algorithm 7.3. Since the algorithm does not optimize a single global objective, it is unclear whether it is guaranteed to converge or not. A pragmatic approach is therefore to perform a predetermined fixed number of iterations before quitting.

Algorithm 7.3 MaxSINDR Algorithm for Hardware-Impaired Transceivers

1: **repeat**

At MS i_k :

2: $\mathbf{u}_{i_k, n} = \frac{\tilde{\mathbf{\Phi}}_{i_k}^{-1} \mathbf{H}_{i_k i} \mathbf{v}_{i_k, n}}{\left\| \tilde{\mathbf{\Phi}}_{i_k}^{-1} \mathbf{H}_{i_k i} \mathbf{v}_{i_k, n} \right\|_2}, \quad \forall n = 1, \dots, d_{i_k}$

3: $\mathbf{U}_{i_k} = \begin{pmatrix} \mathbf{u}_{i_k, 1} & \mathbf{u}_{i_k, 2} & \cdots & \mathbf{u}_{i_k, d_{i_k}} \end{pmatrix}$

At BS i :

4: $\mathbf{v}_{i_k, n} = \frac{\sqrt{\omega_{i_k}} \left(\mathbf{\Upsilon}_i + \tilde{\mathbf{\Upsilon}}_i + (\kappa_i^{(\text{BS})})^2 \text{Diag}(\mathbf{\Upsilon}_i) + \frac{\sigma_{i_k}^2 K_i}{P_i} \mathbf{I} \right)^{-1} \mathbf{H}_{i_k i}^H \mathbf{u}_{i_k, n}}{\left\| \sqrt{\omega_{i_k}} \left(\mathbf{\Upsilon}_i + \tilde{\mathbf{\Upsilon}}_i + (\kappa_i^{(\text{BS})})^2 \text{Diag}(\mathbf{\Upsilon}_i) + \frac{\sigma_{i_k}^2 K_i}{P_i} \mathbf{I} \right)^{-1} \mathbf{H}_{i_k i}^H \mathbf{u}_{i_k, n} \right\|_2}$
 $\quad \forall k \in \mathcal{K}_i, \forall n = 1, \dots, d_{i_k}$

5: $\mathbf{V}_{i_k} = \sqrt{\frac{P_i}{K_i d_{i_k}}} \begin{pmatrix} \mathbf{v}_{i_k, 1} & \mathbf{v}_{i_k, 2} & \cdots & \mathbf{v}_{i_k, d_{i_k}} \end{pmatrix}, \quad \forall k \in \mathcal{K}_i$

6: **until** fixed number of iterations

7.4 Performance Evaluation

We study the performance of the proposed method using numerical simulation. In the simulation study, we let the impairment functions be

$$\eta_i(x) = \kappa_t x \left(1 + \left(\frac{x}{\kappa^{(\text{NL})}} \right)^2 \right), \quad \forall i, \quad (7.45)$$

$$\zeta_{i_k}(x) = \kappa_r x, \quad \forall i_k. \quad (7.46)$$

The receivers are thus constant-EVM receivers (with constant EVM of κ_r), and the transmitters have a 3rd order non-linearity. For low transmit powers, the EVM of the transmitters is κ_t . At a transmit power of $\kappa^{(\text{NL})}$, the EVM has doubled. With this choice of impairment functions, the covariance matrices $\mathbf{C}_{i_k}^{(\text{MS})}$ and $\mathbf{C}_i^{(\text{BS})}$ are differentiable w.r.t. $\{\mathbf{V}_{i_k}\}_{i \in \mathcal{I}, k \in \mathcal{K}_I}$. We use the modelling language YALMIP [LÖ4] together with the Gurobi solver [Gur14] to solve the optimization problem in (7.22).

Scenario

We study a symmetric scenario with $I = 3$ BSs, each serving $K = 2$ MSs. The BSs have $M = 4$ antennas each. The MSs have $N = 2$ antennas each, and the user priorities are $\omega_{i_k} = 1$ for all MSs. The BSs are located at the corner of an equilateral triangle with an inter-site distance of 500 m, and their antenna boresights are aimed towards the center of the triangle (see Figure 7.1 on the following page). For each Monte Carlo realization of the network, the MSs were dropped with uniform probability in the cells belonging to their serving BS. They were however never closer than 35 m to their serving BS. The remaining simulation parameters are described in Table 7.1 on the next page.

Benchmarks

We compare the performance of the proposed Algorithm 7.1 to the case of impairments-ignoring BSs and MSs using the original WMMSE algorithm (i.e. Algorithm 2.1 on page 43). We also compare it to the case of having impairments-aware MSs which use the impairments-aware MMSE receiver in (7.13), but impairments-ignoring BSs which solve the BS subproblem of Algorithm 2.1. The case of having aware MSs but ignorant BSs could occur if the MSs estimate their covariances $\tilde{\Phi}_{i_k}$ over the air (using e.g. the techniques in Section 6.2), without having a specific model for the impairments. The impact of the distortions is then picked up by the MSs, and that knowledge is implicitly distributed to the BSs in the WMMSE iterations. Effectively, the ignorant BSs let $\mathbf{C}_i^{(\text{BS})} = \mathbf{0}$ and $\mathbf{C}_{i_k}^{(\text{MS})} = \mathbf{0}$ in their optimization of (7.22).

As baselines, we use the proposed MaxSINDR algorithm (see Algorithm 7.3), as well as TDMA. MaxSINDR is only aware of the linear impairments, and is thus unaware of the non-linearity in $\eta_i(x)$. For TDMA, we use Algorithm 7.1 to find the impairments-aware precoders. For TDMA with impairments-ignoring BSs and MSs, we use eigenprecoding with water filling.

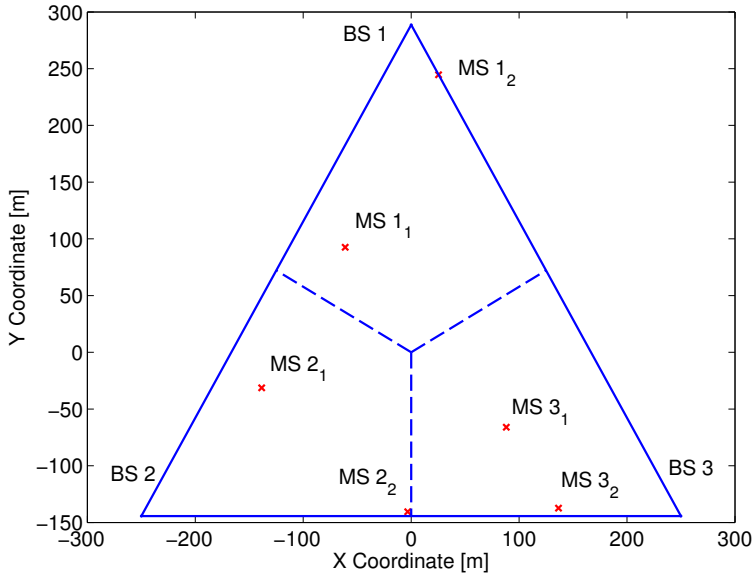


Figure 7.1. User geography for the convergence simulation in Figure 7.2 on the next page.

Table 7.1. Simulation parameters

Path loss	$PL_{\text{dB}} = 15.3 + 37.6 \log_{10}(\text{distance [m]})$
Shadow fading	Not used
Penetration loss	20 dB
BS antenna gain	$12 \left(\frac{\theta}{35^\circ}\right)^2$ dB
MS antenna gain	0 dB
Small scale fading	i.i.d. $\mathcal{CN}(0, 1)$
Bandwidth	15 kHz
Transmit power	$P = P_i, \forall i$
Noise power	$\sigma^2 = \sigma_{i_k}^2 = -127$ dBm, $\forall i_k$

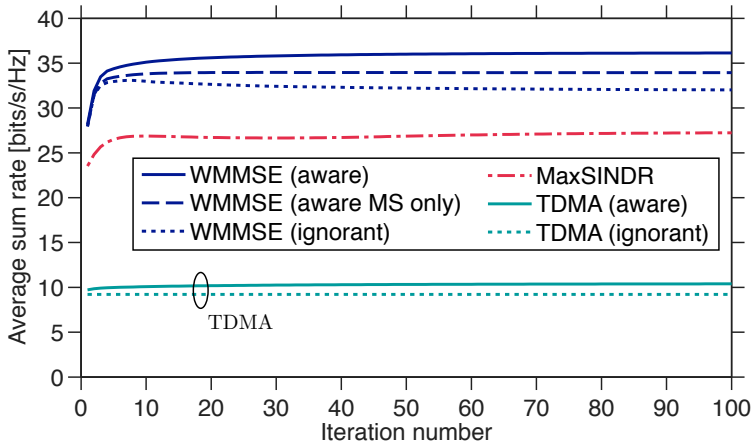


Figure 7.2. Sum rate evolution (one realization) for $P = 18.2$ dBm, $\kappa_t = \kappa_r = \frac{10}{100}$ and $20 \log_{10}(\kappa^{(NL)}) = 15.2$ dBm.

7.4.1 Convergence

First we investigate the convergence behaviour of the proposed algorithms. We generate one user drop, and show sum rate performance as a function of iteration number. The specific user geography for this user drop is shown in Figure 7.1 on the preceding page.

We let $d = 2$ for Algorithm 7.1 and $d = 1$ for Algorithm 7.3.⁵ The power constraint per BS is $P = 18.2$ dBm and the impairments parameters are $\kappa_t = \kappa_r = \frac{10}{100}$ and $20 \log_{10}(\kappa^{(NL)}) = 15.2$ dBm. The sum rate evolution for these parameters is shown in Figure 7.2. The proposed impairments-aware WMMSE converges within a couple of tens of iterations. Interestingly, the WMMSE algorithm with impairments-aware MSs but impairments-ignoring BSs also seems to converge, but to a lower sum rate performance. The performance of the impairments-ignoring WMMSE algorithm actually slowly deteriorates as the number of iterations grow large. This shows that it is clearly important to take the hardware impairments into account when performing the resource allocation. Finally, the MaxSINDR also seems to converge, but to a sum rate around 25 % lower than the proposed WMMSE algorithm.

⁵Using $d = 2$ for Algorithm 7.3 decreased performance.

7.4.2 Varying Impairment Levels

Next, we study sum rate performance when varying the levels of impairments. We fix the transmit power at $P = 18.2$ dBm. We generated 100 user drops, and 10 small scale-fading realizations per user drop. The iterative methods were run with a stopping criterion of 10^{-3} relative difference in increased sum rate. The sum rate results, averaged over Monte Carlo realizations, are presented in Figure 7.3 on the facing page. Clearly, the fully impairments-aware Algorithm 7.1 performs the best, but performance drops as the severity of the impairments increases. The same trend holds for the WMMSE algorithm with and without impairments-aware MSs. MaxSINDR performs significantly worse than all other methods.

7.4.3 Varying Transmit Powers

Lastly, we study performance as a function of available transmit power. In order to have a reasonable simulation scenario, we specialize to $\eta(x) = \kappa_t x$ and vary $\kappa_t = \kappa_r$ and the transmit power P . The sum rate results, averaged over Monte Carlo realizations, can be seen in Figure 7.4 on the next page. The sum rates saturate at high transmit powers, due to the residual hardware impairments. Clearly, the high-SNR scaling of the curves are zero, but the gain for coordinated precoding over TDMA is significant, as predicted by [BZBO12]. Interestingly, in this case the WMMSE algorithm with impairments-ignoring BSs performs almost equally well as Algorithm 7.1. For TDMA, there is barely any difference in taking the hardware impairments into account or not.

7.5 Conclusions

The studies in earlier chapters assumed ideal hardware, but in this chapter we studied the weighted sum rate optimization problem with hardware-impaired transceivers. Applying the WMMSE approach to the weighted sum rate problem, a block coordinate descent technique was proposed. Convergence of the algorithm was shown, and sum rate performance was evaluated using numerical methods. These showed that the high-SNR scaling was zero due to the hardware impairments. However, the relative gain in performance for coordinated precoding over TDMA was still large.

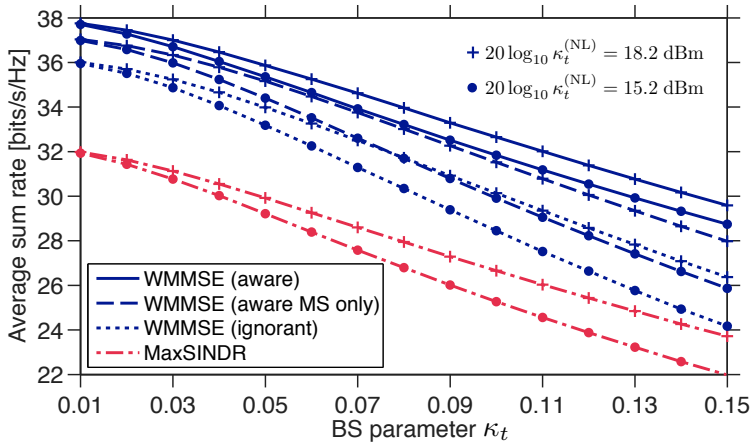


Figure 7.3. Sum rate for $P = 18.2$ dBm when varying impairment parameters. Note the scale of the vertical axis.

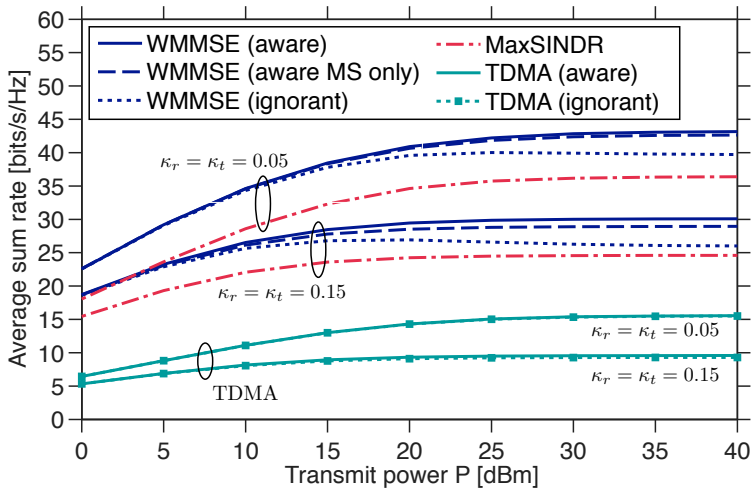


Figure 7.4. Sum rate for $\eta(x) = \kappa_t x$ when varying transmit power and impairment parameters.

Joint Coordinated Precoding and Discrete Rate Selection

A major assumption in the thesis so far has been the fact that the user rate is given by the Shannon formula (see e.g. (2.13) on page 25). This formula describes the rate that can be achieved with vanishingly low error probabilities using long codewords. This is an optimistic model, which further assumes optimal decoders and modulation constellations with infinite granularity. Practical wireless communications systems typically have none of these however. Instead, these systems are often adhering to the bit-interleaved coded modulation (BICM) paradigm [Mad08, Chapter 7.4.1], where the transmit rate is determined by the selection of a channel code and a modulation constellation size. The discrete combinations of codes and constellations are called the modulation and coding schemes (MCSs). Given an SINR at the receiver, the highest discrete rate that achieves some acceptable block error rate is then used for the transmissions.

In this chapter, we therefore consider the case of joint precoder design and discrete rate selection. We assume unclustered operation, perfect CSI acquisition, and perfect radio hardware. We aim to maximize the weighted sum rate while using minimal amount of power. Since the optimization problem is both combinatorial and non-convex, we first rewrite it using some discontinuous rate functions. These are then bounded by their concave envelopes, in some domain which can be selected by the system designer. After a linearization step, block coordinate descent [Ber06, Chapter 2.7] is applied, resulting in a convergent algorithm which is distributed over the mobile stations.

8.1 Discrete Rate Model

We no longer assume that the transmitted signal $\mathbf{x}_{i_k} \in \mathbb{C}^{d_{i_k}}$ is drawn from a Gaussian distribution, but we still assume that the signal has zero mean, unit per-stream power, and is i.i.d. over the streams. For simplicity, we also assume

single-stream decoding in the receivers, such that the n th receive filtered stream at MS i_k is given by (cf. (2.2) on page 12):

$$\hat{x}_{i_k,n} = \mathbf{u}_{i_k,n}^H \mathbf{H}_{i_k i} \mathbf{v}_{i_k,n} x_{i_k,n} + \mathbf{u}_{i_k,n}^H \sum_{\substack{j \in \mathcal{I}, l \in \mathcal{K}_j \\ m=1, \dots, d_{j_l}}} \mathbf{H}_{i_k j} \mathbf{v}_{j_l,m} x_{j_l,m} + \mathbf{u}_{i_k,n}^H \mathbf{z}_{i_k}. \quad (8.1)$$

The corresponding per-stream SINR is then given by

$$\text{SINR}_{i_k,n}(\mathbf{u}_{i_k,n}, \{\mathbf{V}_{j_l}\}) = \frac{|\mathbf{u}_{i_k,n}^H \mathbf{H}_{i_k i} \mathbf{v}_{i_k,n}|^2}{\sum_{(j,l,m) \neq (i,k,n)} |\mathbf{u}_{i_k,n}^H \mathbf{H}_{i_k j} \mathbf{v}_{j_l,m}|^2 + \sigma_{i_k}^2 \|\mathbf{u}_{i_k,n}\|^2}. \quad (8.2)$$

Discrete Rates

The discrete rates that are available to MS i_k are described by the set

$$\mathcal{Q}_{i_k} = \left\{ q_{i_k}^{(0)}, \dots, q_{i_k}^{(|\mathcal{Q}_{i_k}|-1)} \right\} \subset \mathbb{R}^+, \quad (8.3)$$

and we assume without loss of generality that $0 = q_{i_k}^{(0)} < q_{i_k}^{(1)} < \dots < q_{i_k}^{(|\mathcal{Q}_{i_k}|-1)} < \infty$. We include the zero rate in order to ensure feasibility in the optimization problem to be formulated. Due to its inclusion, our optimization formulation will also perform implicit user selection. Different MSs may belong to different terminal classes, corresponding to the discrete rates they can decode, and the sets $\{\mathcal{Q}_{i_k}\}_{i \in \mathcal{I}, k \in \mathcal{K}_i}$ need thus not be identical. Some examples of discrete rate sets are:

Example 8.1 (Discrete rates in WiFi). *In the IEEE 802.11ac WiFi standard, channel code rates between 1/2 and 5/6 are combined with constellations ranging from BPSK to 256-QAM [BKP13]. The corresponding MCSs give the discrete rate set as $\mathcal{Q} = \{0, 0.5, 1, 1.5, 2, 3, 4, 4.5, 5, 6, 6.67\}$ [bits/s/Hz].*

Example 8.2 (Discrete rates in cellular communication). *In the 3GPP LTE standard, channel code rates between 1/8 to 4/5 are combined with constellations ranging from QPSK to 64-QAM [STB09, Sec. 22.4.4.1]. The corresponding MCSs give the discrete rate set as $\mathcal{Q} = \{0, 0.25, 0.4, 0.5, 0.67, 1, 1.33, 1.5, 1.6, 2, 2.67, 3, 3.2, 4, 4.5, 4.8\}$ [bits/s/Hz].*

We assume that a discrete rate is achievable when the achieved SINR exceeds a corresponding pre-determined threshold:

Definition 8.1 (Achievable discrete rate). *The discrete rate for the n th stream of MS i_k , $s_{i_k,n} \in \mathcal{Q}_{i_k}$, is achievable if and only if the SINR for that stream satisfies*

$$\text{SINR}_{i_k,n}(\mathbf{u}_{i_k,n}, \{\mathbf{V}_{j_l}\}) \geq \beta_{i_k}(s_{i_k,n}), \quad (8.4)$$

where $\beta_{i_k} : \mathbb{R}^+ \rightarrow \mathbb{R}^+$ is a function that maps a discrete rate to its required minimum SINR.

For a rate $q_{i_k}^{(p)} \in \mathcal{Q}_{i_k}$, the required SINR $\beta_{i_k}(q_{i_k}^{(p)})$ is typically selected such that the corresponding block error rate (BLER) at the receiver is lower than some $\epsilon_{i_k}^{(p)} > 0$. An example is given by:

Example 8.3 (Receiver with constant implementation margin). *Given a BLER target of ϵ , assume that the receiver needs a factor $\bar{\beta} \geq 1$ higher SINR than the theoretical minimum.¹ The discrete rate then satisfies the Shannon formula $s = \log_2(1 + \beta(s)/\bar{\beta})$ and the corresponding minimum SINR is $\beta(s) = \bar{\beta}(2^s - 1)$.*

Original Optimization Problem

Our goal is now to optimize the network utility, given the model for the discrete rates. We consider the weighted sum rate as the system-level objective function.² Since any excess power used will increase the interference in the network, we maximize the weighted sum rate subject to a power regularization term:

$$\begin{aligned} & \underset{\{\mathbf{U}_{i_k}\}, \{\mathbf{V}_{i_k}\}, \{s_{i_k, n}\}}{\text{maximize}} && \sum_{\substack{i \in \mathcal{I}, k \in \mathcal{K}_i \\ n=1, \dots, d_{i_k}}} \omega_{i_k} s_{i_k, n} - g_\kappa(\{\mathbf{V}_{j_l}\}) \\ & \text{subject to} && s_{i_k, n} \in \mathcal{Q}_{i_k}, \quad \forall i_k, n \\ & && \text{SINR}_{i_k, n}(\mathbf{u}_{i_k, n}, \{\mathbf{V}_{j_l}\}) \geq \beta_{i_k}(s_{i_k, n}), \quad \forall i_k, n \\ & && \sum_{k \in \mathcal{K}_i} \|\mathbf{V}_{i_k}\|_{\mathbb{F}}^2 \leq P_i, \quad \forall i \in \mathcal{I}, \end{aligned} \tag{8.5}$$

where $g_\kappa(\{\mathbf{V}_{j_l}\}) = \kappa \sum_{i \in \mathcal{I}, k \in \mathcal{K}_i} \|\mathbf{V}_{i_k}\|_{\mathbb{F}}^2$. The regularization parameter κ is selected according to the following theorem, as inspired by Claim 1 in [MSLT08]:

Theorem 8.1. *Define $f(\{s_{i_k, n}\}) = \sum_{\substack{i \in \mathcal{I}, k \in \mathcal{K}_i \\ n=1, \dots, d_{i_k}}} \omega_{i_k} s_{i_k, n}$ and*

$$\delta = \min_{\{s_{i_k, n}\}, \{\check{s}_{i_k}\}, \{s_{i_k, n}\} \neq \{\check{s}_{i_k, n}\}} |f(\{s_{i_k, n}\}) - f(\{\check{s}_{i_k, n}\})|.$$

If $\kappa = \delta / (\sum_{i \in \mathcal{I}} P_i + 1)$, the optimal solution to the optimization problem in (8.5) simultaneously gives the maximum achievable weighted sum rate and the corresponding minimum sum power precoders.

Proof: See Appendix 8.A. ■

With this selection of κ , no loss in the objective due to selecting a smaller discrete rate for some MS can be made up for by the corresponding decrease in used power. Therefore, the optimization problem in (8.5) simultaneously gives the maximum weighted sum rate and the corresponding minimum sum power precoders. The proof for this hinges on the fact that the weighted sum rate only takes on discrete values and that the sum power is bounded; a related discussion is given in [MSLT08].

¹This is called the *SINR gap approximation* [HKB11, Chapter 9.2.2], or the *implementation margin* [STB09, Chapter 22.4.4].

²For each MS, we sum the discrete rates over all data streams. We do not model the CSI acquisition overhead and thus assume unity pre-log factors.

Reformulation with Discontinuous Rate Functions

The optimization problem in (8.5) on the preceding page is both combinatorial (due to the selection of the discrete rates) and non-concave (due to the non-concavity of $\text{SINR}_{i_k,n}(\mathbf{u}_{i_k,n}, \{\mathbf{V}_{j_l}\})$). As posed, it is thus difficult to solve. We will therefore reformulate the problem into one with a discontinuous objective function, which we will then bound. After the reformulation and bounding, we will apply ideas similar to WMMSE minimization (see Appendix 2.B) in order to get a semi-distributed optimization algorithm.

The first step in the reformulation is the introduction of the MSE of the n th stream of MS i_k :

$$e_{i_k,n}(\mathbf{u}_{i_k,n}, \{\mathbf{V}_{j_l}\}) = \mathbb{E} \left(|x_{i_k,n} - \hat{x}_{i_k,n}|^2 \right) = \quad (8.6)$$

$$1 - 2\text{Re}(\mathbf{u}_{i_k,n}^H \mathbf{H}_{i_k} \mathbf{v}_{i_k,n}) + \mathbf{u}_{i_k,n}^H \mathbf{\Phi}_{i_k}(\{\mathbf{V}_{j_l}\}) \mathbf{u}_{i_k,n},$$

where the received signal covariance matrix for MS i_k as usual is

$$\mathbf{\Phi}_{i_k}(\{\mathbf{V}_{j_l}\}) = \sum_{j \in \mathcal{I}, l \in \mathcal{K}_j} \mathbf{H}_{i_k j} \mathbf{V}_{j_l} \mathbf{V}_{j_l}^H \mathbf{H}_{i_k j}^H + \sigma_{i_k}^2 \mathbf{I}. \quad (8.7)$$

Assuming finite-power precoders, together with the unit-power symbols, we have that $0 < e_{i_k,n}(\mathbf{u}_{i_k,n}, \{\mathbf{V}_{j_l}\}) \leq 1, \forall i_k, n$.

The next step in the formulation is rewriting the SINR constraint as a general quality of service (QoS) constraint, which is a function of the MSE. The QoS domain is given by:

Definition 8.2 (QoS domain). *Let $\eta: \mathbb{R}_+ \rightarrow \mathbb{R}_+$ be a concave and strictly increasing function. It describes the mapping from the MSE domain to another QoS domain.*

Definition 8.3 (Discontinuous rate function). *Given a fixed receive filter $\mathbf{u}_{i_k,n}$, fixed precoders $\{\mathbf{V}_{j_l}\}_{j \in \mathcal{I}, l \in \mathcal{K}_j}$, and a QoS domain represented by $\eta(\cdot)$, the discrete rate for the n th stream of MS i_k is given by the discontinuous rate function*

$$g_\eta(e_{i_k,n}(\mathbf{u}_{i_k,n}, \{\mathbf{V}_{j_l}\})) = \quad (8.8)$$

$$\begin{aligned} & \text{maximize } q \\ & q \in \mathcal{Q}_{i_k} \\ & \text{subject to } \eta(e_{i_k,n}(\mathbf{u}_{i_k,n}, \{\mathbf{V}_{j_l}\})) \leq \eta\left(\frac{1}{1 + \beta_{i_k}(q)}\right). \end{aligned}$$

In the reformulated optimization problem to be described, this discontinuous function will be bounded by a continuous function. The purpose of introducing the QoS domain of Definition 8.2 into the optimization problem in (8.8) is to provide a degree of freedom in designing this bound.

Given the discontinuous rate function in Definition 8.3, we now reformulate the optimization problem in (8.5) on page 153 as:

$$\begin{aligned} & \underset{\{\mathbf{U}_{i_k}\}, \{\mathbf{V}_{i_k}\}}{\text{maximize}} && \sum_{\substack{i \in \mathcal{I}, k \in \mathcal{K}_i \\ n=1, \dots, d_{i_k}}} \omega_{i_k} g_\eta(e_{i_k, n}(\mathbf{u}_{i_k, n}, \{\mathbf{V}_{j_l}\})) - g_\kappa(\{\mathbf{V}_{j_l}\}) \\ & \text{subject to} && \sum_{k \in \mathcal{K}_i} \|\mathbf{V}_{i_k}\|_{\mathbb{F}}^2 \leq P_i, \quad \forall i \in \mathcal{I}. \end{aligned} \quad (8.9)$$

The discrete rates are now implicitly selected by the discontinuous rate function $g_\eta(\cdot)$, and the problem is no longer combinatorial. The objective function has however become discontinuous. There is no loss in optimality due to this reformulation though, since it holds that

$$\min_{\mathbf{u}_{i_k, n}} e_{i_k, n}(\mathbf{u}_{i_k, n}, \{\mathbf{V}_{j_l}\}) = \min_{\mathbf{u}_{i_k, n}} \frac{1}{1 + \text{SINR}_{i_k, n}(\mathbf{u}_{i_k, n}, \{\mathbf{V}_{j_l}\})}.$$

Upper Bounding the Discontinuous Rate Functions

We will now bound the objective function in (8.9) by bounding the discontinuous rate function by its concave envelope.³ Given $\mathcal{P}_{i_k} \subset \mathbb{N}$ and $\{c_{i_k}^{(p)}\}_{p \in \mathcal{P}_{i_k}}, \{m_{i_k}^{(p)}\}_{p \in \mathcal{P}_{i_k}}$ which are uniquely defined slopes and offsets,⁴ the concave envelope is given by the following piecewise linear function:

$$g_\eta^{\text{conc}}(e) = \min_{p \in \mathcal{P}_{i_k}} \left\{ c_{i_k}^{(p)} \eta(e) + m_{i_k}^{(p)} \right\} \geq g_\eta(e). \quad (8.10)$$

Some examples of concave envelopes are given in Figure 8.1 on the following page, for three different QoS domains. This figure illustrates two key properties of our model. First, note that different QoS domains give bounds with different tightness. In the MSE domain (i.e. $\eta(e) = e$), the concave envelope is a loose bound since the discontinuous rate function “looks convex” in this domain. In the continuous rate domain (i.e. $\eta(e) = \log_2(e)$) on the other hand, the concave envelope is a tight bound. This is because the discrete rates satisfy $s = \log_2(1 + \beta(s))$ in this example, i.e. they “look linear” in the continuous rate domain and are therefore well approximated by a piecewise linear function. The second property to note is that our model accounts for the maximum discrete rate that is achievable. That is, there is no point in reducing the MSE past the maximum value which achieves the largest discrete rate.⁵ In Figure 8.1, this is seen by the curves having slope zero for sufficiently small MSEs.

³The concave envelope is the “smallest” concave function which majorizes the function. It is thus the best concave approximation available.

⁴These are uniquely determined by \mathcal{Q}_{i_k} and $\beta_{i_k}(\cdot)$, see examples in Figure 8.1.

⁵By reducing the MSE further, the performance at the corresponding MS would not increase but all other MSs might receive stronger interference, which is detrimental for the system-level performance.

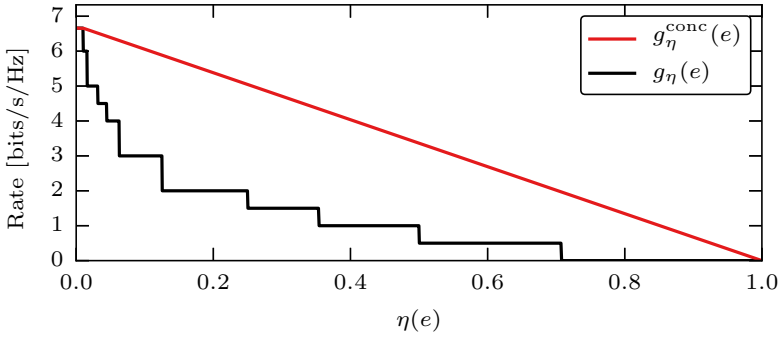
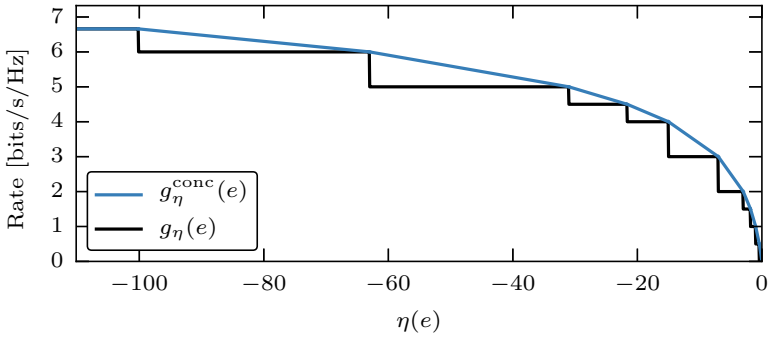
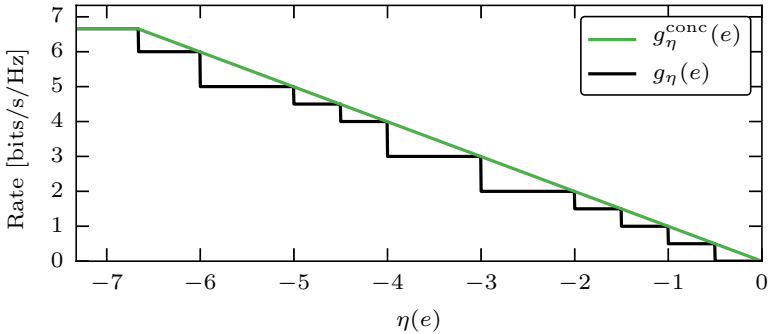
(a) MSE domain, $\eta(e) = e$ (b) SINR domain, $\eta(e) = 1 - 1/e$ (c) Continuous rate domain, $\eta(e) = \log_2(e)$

Figure 8.1. Discontinuous rate functions together with their concave envelopes in different QoS domains. Note the poor fit of the bound in (a), compared to the bounds in (b) and (c). The discrete rates were taken from Example 8.1, with required SINRs from Example 8.3 where we let $\bar{\beta} = 1$.

By bounding the discontinuous rate functions by their concave envelopes, we now get the following bounded optimization problem:

$$\begin{aligned} & \underset{\{\mathbf{U}_{i_k}\}, \{\mathbf{V}_{i_k}\}}{\text{maximize}} && \sum_{\substack{i \in \mathcal{I}, k \in \mathcal{K}_i \\ n=1, \dots, d_{i_k}}} \omega_{i_k} g_{\eta}^{\text{conc}}(e_{i_k, n}(\mathbf{u}_{i_k, n}, \{\mathbf{V}_{j_l}\})) - g_{\kappa}(\{\mathbf{V}_{j_l}\}) \\ & \text{subject to} && \sum_{k \in \mathcal{K}_i} \|\mathbf{V}_{i_k}\|_{\mathbb{F}}^2 \leq P_i, \quad \forall i \in \mathcal{I}. \end{aligned} \quad (8.11)$$

This step introduces some non-optimality, since we are upper bounding the objective of a maximization problem. The benefit is that the problem no longer is discontinuous however.

Linearizing the QoS Domain Function

Finally, in order to get the objective on a form which is amenable for block coordinate descent, we will now linearize the QoS domain function. By Taylor expanding the $\eta(\cdot)$ function around a point $1/w_{i_k, n}$, we thus get

$$\begin{aligned} & g_{\eta}^{\text{conc}}(e_{i_k, n}(\mathbf{u}_{i_k, n}, \{\mathbf{V}_{j_l}\}), w_{i_k, n}) = \\ & \min_{p \in \mathcal{P}_{i_k}} \left\{ c_{i_k}^{(p)} \left(\eta \left(\frac{1}{w_{i_k, n}} \right) + \eta' \left(\frac{1}{w_{i_k, n}} \right) \left(e_{i_k, n}(\mathbf{u}_{i_k, n}, \{\mathbf{V}_{j_l}\}) - \frac{1}{w_{i_k, n}} \right) \right) + m_{i_k}^{(p)} \right\} \\ & \leq g_{\eta}^{\text{conc}}(e_{i_k, n}(\mathbf{u}_{i_k, n}, \{\mathbf{V}_{j_l}\})) \end{aligned} \quad (8.12)$$

The last inequality holds since $c_{i_k}^{(p)} \eta(\cdot)$ is a convex function⁶ and the fact that the first-order Taylor expansion of a convex function is a global underestimator [BV04, Chapter 3.1.3]. By introducing the linearization points as optimization variables, we get the final optimization problem as:

$$\begin{aligned} & \underset{\substack{\{\mathbf{U}_{i_k}\}, \{\mathbf{V}_{i_k}\}, \\ \{w_{i_k, n}\}}} {\text{maximize}} && \sum_{\substack{i \in \mathcal{I}, k \in \mathcal{K}_i \\ n=1, \dots, d_{i_k}}} \omega_{i_k} g_{\eta}^{\text{conc}}(e_{i_k, n}(\mathbf{u}_{i_k, n}, \{\mathbf{V}_{j_l}\}), w_{i_k, n}) - g_{\kappa}(\{\mathbf{V}_{j_l}\}) \\ & \text{subject to} && \sum_{k \in \mathcal{K}_i} \|\mathbf{V}_{i_k}\|_{\mathbb{F}}^2 \leq P_i, \quad \forall i \in \mathcal{I}. \end{aligned} \quad (8.13)$$

It can easily be shown that $\max_{w_{i_k, n}} g_{\eta}^{\text{conc}}(\cdot, w_{i_k, n}) = g_{\eta}^{\text{conc}}(\cdot)$, and the linearization in (8.12) is therefore tight at optimality. The optimization problems in (8.11) and (8.13) therefore have the same optimal value.

8.2 Semi-Distributed Algorithm

The final optimization problem in (8.13) still has a jointly non-concave objective function, but it has the desired structure that the objective is concave in each block

⁶By construction, it holds that $c_{i_k}^{(p)} \leq 0, \forall p \in \mathcal{P}_{i_k}$.

of variables when the two other blocks are held fixed. By applying block coordinate descent [Ber06, Chapter 2.7], we will thus be able to find an iterative resource allocation algorithm. When the algorithm has converged, the implicitly selected discrete rates can be extracted using e.g. the condition in Definition 8.1.

Optimality Conditions

First, we fix $\{\mathbf{V}_{j_l}\}_{j \in \mathcal{I}, l \in \mathcal{K}_j}$ and $\{w_{j_l, m}\}_{j \in \mathcal{I}, l \in \mathcal{K}_j, m=1, \dots, d_{j_l}}$ and solve the optimization problem in (8.13) w.r.t. to $\{\mathbf{U}_{i_k}\}_{i \in \mathcal{I}, k \in \mathcal{K}_i}$. It can easily be shown that the problem decomposes over the MSSs, and that an optimal receive filter is the MMSE filter

$$\mathbf{U}_{i_k}^* = (\Phi_{i_k}(\{\mathbf{V}_{j_l}\}))^{-1} \mathbf{H}_{i_k} \mathbf{V}_{i_k}, \quad \forall i_k. \quad (8.14)$$

Second, we fix $\{\mathbf{U}_{j_l}\}_{j \in \mathcal{I}, l \in \mathcal{K}_j}$ and $\{\mathbf{V}_{j_l}\}_{j \in \mathcal{I}, l \in \mathcal{K}_j}$ and solve the optimization problem in (8.13) w.r.t. to $\{w_{i_k, n}\}_{i \in \mathcal{I}, k \in \mathcal{K}_i, n=1, \dots, d_{i_k}}$. The optimal linearization weights are then

$$w_{i_k, n}^* = 1/e_{i_k, n}(\mathbf{u}_{i_k, n}^*, \{\mathbf{V}_{j_l}\}), \quad \forall i_k, n. \quad (8.15)$$

Finally, the optimal precoders $\{\mathbf{V}_{i_k}^*\}_{i \in \mathcal{I}, k \in \mathcal{K}_i}$ are given by the solution to the optimization problem

$$\begin{aligned} & \underset{\{\mathbf{V}_{i_k}\}}{\text{maximize}} && \sum_{\substack{i \in \mathcal{I}, k \in \mathcal{K}_i \\ n=1, \dots, d_{i_k}}} \omega_{i_k} g_{\eta^{\text{lin}}}^{\text{conc}}(e_{i_k, n}(\mathbf{u}_{i_k, n}, \{\mathbf{V}_{j_l}\}), w_{i_k, n}) - g_{\mathcal{R}}(\{\mathbf{V}_{j_l}\}) \\ & \text{subject to} && \sum_{k \in \mathcal{K}_i} \|\mathbf{V}_{i_k}\|_{\mathbb{F}}^2 \leq P_i, \quad \forall i \in \mathcal{I}. \end{aligned} \quad (8.16)$$

This is a strongly concave maximization problem whose unique solution can be found using, e.g., interior-point methods [BV04, Chapter 11].

Block Coordinate Descent

Block coordinate descent now amounts to sequentially solving for each block, while keeping the two other blocks fixed. This results in an iterative algorithm, which we summarize in Algorithm 8.1 on the next page. As can be seen from (8.14) and (8.15), the optimal receive filters and linearization weights can be found distributedly over the MSSs, whereas solving for the optimal precoders in (8.16) must be done centrally at the BSs.

Theorem 8.2. *The sequence of objective values obtained from Algorithm 8.1 converges.*

Proof: The sequence of objective values is nondecreasing, since in each step of the algorithm, the objective function is maximized. The sequence is further bounded above by the finite optimal value of the optimization problem in (8.13). The sequence thus converges [Rud76, Thm. 3.14]. \blacksquare

Algorithm 8.1 Heuristic WMMSE Algorithm for Discrete Weighted Sum Rate Maximization

- 1: **repeat**
 - At MS i_k :
 - 2: Find MSE weights: $w_{i_k,n} = 1/e_{i_k,n}(\mathbf{u}_{i_k,n}^*, \{\mathbf{V}_{j_l}\})$, $\forall n = 1, \dots, d_{i_k}$
 - 3: Find MMSE receive filters: $\mathbf{U}_{i_k} = (\Phi_{i_k}(\{\mathbf{V}_{j_l}\}))^{-1} \mathbf{H}_{i_k} \mathbf{V}_{i_k}$
 - At Central BS Unit:
 - 4: Find precoders as solution to the optimization problem in (8.13)
 - 5: **until** convergence criterion met, or fixed number of iterations
-

8.3 Performance Evaluation

We evaluate the performance of the proposed algorithm using numerical simulations.

Scenario

We let $I = 3$ BSs be placed equidistant along the centre line of a 120×20 [m] office corridor. Each BS serves $K = 2$ randomly placed MSs with $d = 2$ data streams. The BSs have $M = 4$ antennas each and the MSs have $N = 2$ antennas each. The large-scale fading is given by the ITU-R InH model [IR09, Table A1-2], but we model the small-scale fading as i.i.d. Rayleigh fading. We use the discrete rates from the IEEE 802.11ac standard without any implementation margin, as given by Examples 8.1 and 8.3 with $\beta = 1$. We draw 100 i.i.d. Monte Carlo realizations, and average the results. The proposed algorithm is run until the relative difference between subsequently achieved objective values is less than 10^{-3} . We consider the unweighted case, where $\omega_{i_k} = 1$ for all MSs.

Benchmarks

We compare our proposed algorithm to the per-stream WMMSE algorithm [KTJ13] and the MaxSINR algorithm [GCJ11], which both are well-known to perform well for the continuous rate⁷ case [SSB⁺13].⁸ We also consider intercell and intracell time-division multiple access (TDMA), where the precoders are selected as the strongest singular vectors of the desired channel.

8.3.1 Convergence

In Figure 8.2 on the following page, we show the convergence of our heuristic algorithm for the case of $\eta(e) = \log(e)$ and a fixed transmit power of 21 dBm.

⁷We define the continuous rate as $\log_2(1 + \text{SINR})$.

⁸The existing work in [WJN13, WLM13, CP15] cannot handle the MIMO case, which we consider here, and are consequently not included as benchmarks.

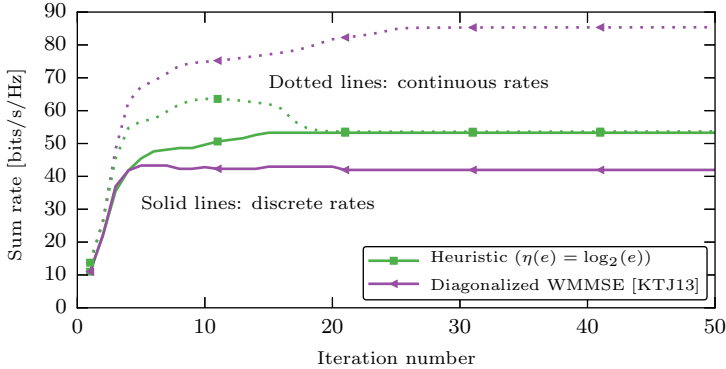


Figure 8.2. Example of convergence of the algorithms for one realization.

Instead of showing the evolution of the objective values (which are guaranteed to converge monotonically as per Theorem 8.2), we instead show the achieved discrete and continuous sum rates. Mathematically, the discrete sum rate is

$$\sum_{\substack{i \in \mathcal{I}, k \in \mathcal{K}_i \\ n=1, \dots, d_{i_k}}} s_{i_k, n}, \quad (8.17)$$

where $s_{i_k, n}$ is the maximum achievable discrete rate, given the final receive filters and precoders. The continuous sum rate is

$$\sum_{\substack{i \in \mathcal{I}, k \in \mathcal{K}_i \\ n=1, \dots, d_{i_k}}} \log_2(1 + \text{SINR}_{i_k, n}(\mathbf{u}_{i_k, n}, \{\mathbf{V}_{j_l}\})). \quad (8.18)$$

Neither of these are guaranteed to be monotonic, since neither of these are directly optimized.

The continuous and discrete sum rates achieved by our algorithm meets after about 20 iterations in Figure 8.2. This indicates that no excess power is used, since otherwise the continuous rate would be larger than the discrete rate. The power regularization in the optimization problem in (8.5) thus clearly works as intended. The per-stream WMMSE algorithm of [KTJ13] achieves significantly higher continuous rates than our algorithm, but the discrete rate performance is relatively abysmal. This is because this algorithm allocates too much power to some streams which have already reached the maximum discrete rate available.

8.3.2 Varying the Transmit Power

In Figure 8.3, we compare the performance for different QoS domains as we vary the transmit power. The rate and SINR domains (see Figure 8.1 on page 156)

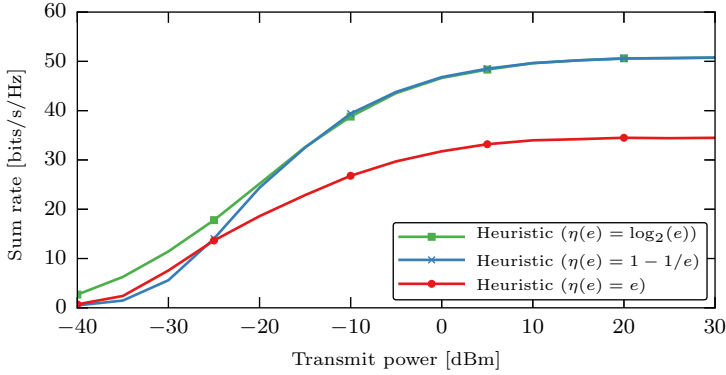


Figure 8.3. Comparing different QoS domains.

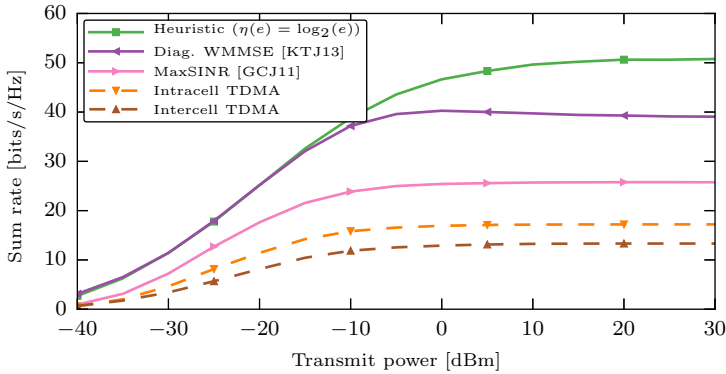


Figure 8.4. Comparing the proposed algorithm to the benchmarks.

perform identically at high transmit powers, whereas the MSE domain is unable to perform as well. This may be due to the poor bound tightness in the MSE domain, as shown in Figure 8.1a.

In Figure 8.4, we compare our heuristic algorithm to the benchmarks as we vary the transmit power. For low transmit powers, there is little to gain from using our algorithm. At high transmit powers however, the necessity of modelling the discrete rates is shown. The WMMSE algorithm actually performs worse for sufficiently high transmit power. Neither the MaxSINR algorithm, nor the traditional TDMA methods, are competitive.

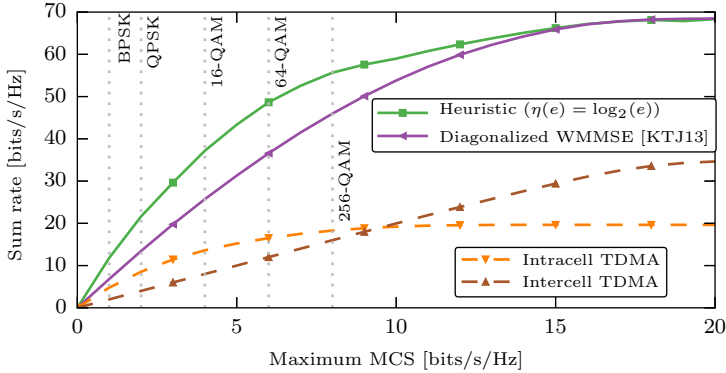


Figure 8.5. Sum rate when varying the maximum discrete rate. The rates of uncoded QAM-constellations are shown as grey dotted lines.

8.3.3 Varying the Maximum MCS

In Figure 8.5, we compare the performance when varying the number of available discrete rates at a fixed transmit power of 21 dBm. We consider discrete rates from the set $\mathcal{Q} = \{1, 2, \dots, q^{\max}\}$, where we sweep q^{\max} in steps of 1 bits/s/Hz. When there are few discrete rates to select from, our proposed method is by far the best. As there are more discrete rates to choose from however, eventually the WMMSE algorithm catches up. Note that this only happens for very large constellation sizes.

8.4 Conclusion

Since most practical wireless communications systems have a finite number of discrete rates available, it is reasonable to adapt the precoding methodology to this constraint. By appropriately selecting the QoS domain, we have shown that large performance gains can be achieved using our heuristic coordinated algorithm, as compared to the existing algorithms which approximate the set of discrete rates by the continuous rate function.

8.A Proof of Theorem 8.1

The proof follows along the lines of the proof of Claim 1 in [MSLT08], from where we get our inspiration. First we show by contradiction that the optimal solution maximizes the weighted sum rate. Second, we show that the sum power of the corresponding precoders is simultaneously minimized.

Let $(\{s'_{i_k,n}\}, \{\mathbf{U}'_{i_k}\}, \{\mathbf{V}'_{i_k}\})$ be an optimal solution to the optimization problem in (8.5) on page 153. Further, assume that $(\{s''_{i_k,n}\}, \{\mathbf{U}''_{i_k}\}, \{\mathbf{V}''_{i_k}\})$ is another feasible point such that $f(\{s''_{i_k,n}\}) > f(\{s'_{i_k,n}\})$. Given our definition of δ , this can equivalently be written as

$$f(\{s''_{i_k,n}\}) \geq f(\{s'_{i_k,n}\}) + \delta. \quad (8.19)$$

Since $\{\mathbf{V}''_{i_k}\}$ is feasible, it further holds that

$$\sum_{i \in \mathcal{I}, k \in \mathcal{K}_i} \|\mathbf{V}''_{i_k}\|_{\mathbb{F}}^2 \leq \sum_{i \in \mathcal{I}} P_i. \quad (8.20)$$

Under the assumption in (8.19) and the fact in (8.20), we therefore have that

$$\begin{aligned} & f(\{s''_{i_k,n}\}) - \kappa \sum_{i \in \mathcal{I}, k \in \mathcal{K}_i} \|\mathbf{V}''_{i_k}\|_{\mathbb{F}}^2 \\ & \stackrel{(a)}{\geq} f(\{s'_{i_k,n}\}) + \delta - \kappa \sum_{i \in \mathcal{I}, k \in \mathcal{K}_i} \|\mathbf{V}''_{i_k}\|_{\mathbb{F}}^2 \\ & \stackrel{(b)}{\geq} f(\{s'_{i_k,n}\}) + \delta - \kappa \sum_{i \in \mathcal{I}} P_i \\ & \stackrel{(c)}{=} f(\{s'_{i_k,n}\}) + \delta \left(1 - \frac{\sum_{i \in \mathcal{I}} P_i}{\sum_{i \in \mathcal{I}} P_i + 1}\right) \\ & \stackrel{(d)}{>} f(\{s'_{i_k,n}\}) \\ & \stackrel{(e)}{\geq} f(\{s'_{i_k,n}\}) - \kappa \sum_{i \in \mathcal{I}, k \in \mathcal{K}_i} \|\mathbf{V}'_{i_k}\|_{\mathbb{F}}^2, \end{aligned} \quad (8.21)$$

where (a) holds due to (8.19), (b) holds due to (8.20), (c) is due to the definition of κ , (d) holds since the removed term is positive, and (e) holds since the added term is non-positive. The inequalities in (8.21) contradict the optimality of $(\{s'_{i_k,n}\}, \{\mathbf{U}'_{i_k}\}, \{\mathbf{V}'_{i_k}\})$, thus showing that the optimal solution $(\{s'_{i_k,n}\}, \{\mathbf{U}'_{i_k}\}, \{\mathbf{V}'_{i_k}\})$ necessarily maximizes $f(\{s'_{i_k,n}\})$.

Given the set of weighted sum rate optimal discrete rates $\{s'_{i_k,n}\}$, the term $f(\{s'_{i_k,n}\})$ in the objective of the optimization problem in (8.5) is constant. It thus

remains to solve the optimization problem

$$\begin{aligned}
 & \underset{\{\mathbf{U}_{i_k}\}, \{\mathbf{V}_{i_k}\}}{\text{minimize}} && \kappa \sum_{i \in \mathcal{I}, k \in \mathcal{K}_i} \|\mathbf{V}_{i_k}\|_{\mathbb{F}}^2 \\
 & \text{subject to} && \text{SINR}_{i_k, n}(\mathbf{u}_{i_k, n}, \{\mathbf{v}_{j_l}\}) \geq \beta_{i_k}(s_{i_k, n}), \quad \forall i_k, n \\
 & && \sum_{k \in \mathcal{K}_i} \|\mathbf{V}_{i_k}\|_{\mathbb{F}}^2 \leq P_i, \quad \forall i \in \mathcal{I}.
 \end{aligned}$$

which yields optimal receive filters and optimal precoders with minimum sum power. This concludes the proof. \blacksquare

Conclusions

Due to the increasing traffic in wireless networks, capacity improvements are direly needed. In this thesis, we considered solutions to this problem using tools from multicell coordination. In particular, we studied the problem domains of base station clustering and coordinated precoding.

In intermediate-sized networks, we showed that base station clustering is a useful technique for reducing the CSI acquisition overhead, while still maintaining a sufficient interference mitigation ability. By formulating a bound on the throughput given a partial clustering, we provided an algorithm that finds the optimal base station clustering. The algorithm was found useful for the benchmarking of more practical base station clustering schemes. One such practical scheme was developed based on coalitional game theory. By modelling the base stations as players in a game, we derived a low complexity distributed base station clustering scheme, which was numerically shown to perform well compared to the optimum.

Given a base station clustering, we then proposed coordinated precoding algorithms for several types of problems. We first considered intercluster interference and proposed an algorithm which exploited statistical information about the unknown interfering links to achieve robustness. Assuming a reciprocal channel, we then described how the CSI acquisition can be performed in a distributed fashion. The acquired CSI will necessarily be imperfect, and we therefore provided a distributed coordinated precoding algorithm which employed diagonal loading to achieve robustness against the imperfections. Another problem considered was that of imperfect radio hardware, where we used a general model for the distortion noises coming from the hardware impairments. We provided an algorithm, and showed that for the special case of constant-EVM transceivers, the algorithm can be implemented in a distributed fashion. We concluded the technical contributions of the thesis by modelling the modulation and coding schemes of a practical wireless communications system as a discrete rate selection problem. Based on reformulation and bounding steps, we provided a heuristic algorithm for the joint coordinated

precoding and discrete rate selection problem.

Altogether, we have provided several important building blocks for the implementation and benchmarking of a distributed base station clustering and coordinated precoding system. The numerical simulations that have been performed alongside the theoretical developments of this thesis have shown the viability of the proposed approaches.

Future Research

There are several directions for future research based on the direction set out by the contributions of this thesis. We highlight some of these directions below:

- For tractability, we only considered disjoint base station-centric clustering of the base stations. Other approaches to handle the CSI acquisition overhead includes user-centric grouping and link-centric grouping, where the groups possibly are overlapping. It would be interesting to compare these techniques to our disjoint base station-centric clustering.
- It would be relevant to generalize the throughput model of Chapter 4 to the case of imperfect CSI acquisition and non-orthogonal training. This would widen the applicability of the model to very large networks, which under the current model have zero sum throughputs due to the orthogonal training.
- The coalition formation algorithm in Chapter 4 performed well in the numerical simulations. Yet, the only analytical performance guarantee that was derived was that of it reaching a state of individual stability. It would be interesting with a more general performance analysis of the algorithm.
- The robust coordinated precoding algorithm in Chapter 6 relied on heuristics for the robustification. Although these were shown to work well in the numerical experiments, it would be interesting to explore more rigorously derived robustifying measures that would still work well in the distributed setting.
- In the hardware distortion noise model of Chapter 7, we optimized a single subcarrier, although part of the distortions were due to the transmissions at other subcarriers. It would be interesting to formulate the joint optimization problem describing precoding on all subcarriers, and their respective impact on distortions at other subcarriers.
- It would be interesting to provide further benchmarks of the algorithm in Chapter 8. For example, the max-min WMMSE algorithm of [RHL13b] could be used as a pseudo feasibility check and combined with branch and bound or exhaustive search over the possible rate combinations in the network.
- In each of the Chapters 5–8, a coordinated precoding technique was derived which was robust against some specific issue with a multicell MIMO systems.

In practice, all of these issues (intercluster interference, CSI imperfections, hardware imperfections, discrete rates, ...) need to be accounted for simultaneously. It should be possible to combine the techniques proposed into one big algorithm, and the design and evaluation of such a system would be an interesting applied research topic.

Bibliography

- [3GP06] 3GPP. TR 25.814, Physical layer aspects for evolved universal terrestrial radio access (Release 7). Technical report, 3GPP, 2006.
- [3GP10] 3GPP. TR 36.814, Further advancements for E-UTRA physical layer aspects (Release 9). Technical report, 3GPP, 2010.
- [3GP12] 3GPP. TR 25.996, Spatial channel model for multiple input multiple output (MIMO) simulations (Release 11). Technical report, 3GPP, 2012.
- [ABB⁺07] P. Almers, E. Bonek, A. Burr, N. Czink, M. Debbah, V. Degli-Esposti, H. Hofstetter, P. Kyösti, D. Laurenson, G. Matz, C. Oestges, and H. Özcelik. Survey of channel and radio propagation models for wireless MIMO systems. *EURASIP J. Wireless Commun. Netw.*, 2007.
- [AS65] M. Abramowitz and I. Stegun. *Handbook of Mathematical Functions*. Dover Publications, 1965.
- [BAB12] R. Brandt, H. Asplund, and M. Bengtsson. Interference alignment in frequency – a measurement based performance analysis. In *Proc. Int. Conf. Systems, Signals and Image Process.*, pages 227–230, 2012.
- [BB11] R. Brandt and M. Bengtsson. Wideband MIMO channel diagonalization in the time domain. In *Proc. IEEE Int. Symp. Indoor, Mobile Radio Commun.*, pages 1958–1962, 2011.
- [BB15] R. Brandt and M. Bengtsson. Fast-convergent distributed coordinated precoding for TDD multicell MIMO systems. In *Proc. IEEE Int. Workshop Computational Advances in Multi-Sensor Adaptive Process.*, pages 457–460, 2015.

- [BB16a] R. Brandt and M. Bengtsson. Distributed CSI acquisition and coordinated precoding for TDD multicell MIMO systems. *IEEE Trans. Veh. Technol.*, 2016. Accepted in Apr. 2015.
- [BB16b] R. Brandt and M. Bengtsson. Joint coordinated precoding and discrete rate selection in multicell MIMO networks. *IEEE Signal Process. Lett.*, 2016. Submitted in Mar. 2016.
- [BBB14] R. Brandt, E. Björnson, and M. Bengtsson. Weighted sum rate optimization for multicell MIMO systems with hardware-impaired transceivers. In *Proc. IEEE Conf. Acoust., Speech, and Signal Process.*, pages 479–483, 2014.
- [BCT14] G. Bresler, D. Cartwright, and D. Tse. Feasibility of interference alignment for the MIMO interference channel. *IEEE Trans. Inf. Theory*, 60(9):5573–5586, 2014.
- [Ber06] D. Bertsekas. *Nonlinear programming*. Athena Scientific, 2006.
- [BG06] M. Biguesh and A. B. Gershman. Training-based MIMO channel estimation: a study of estimator tradeoffs and optimal training signals. *IEEE Trans. Signal Process.*, 54(3), 2006.
- [BHL⁺14] H. Baligh, M. Hong, W. C. Liao, Z. Q. Luo, M. Razaviyayn, M. Sanjabi, and R. Sun. Cross-layer provision of future cellular networks: A WMMSE-based approach. *IEEE Signal Process. Mag.*, 31(6):56–68, 2014.
- [BJ02] A. Bogomolnaia and M. O. Jackson. The stability of hedonic coalition structures. *Games Econ. Behav.*, 38(2):201–230, 2002.
- [BJ13] E. Björnson and E. Jorswieck. Optimal resource allocation in coordinated multi-cell systems. *Foundations Trends Commun. Inform. Theory*, 9(2-3):113–381, 2013.
- [BKP13] O. Bejarano, E. W. Knightly, and M. Park. IEEE 802.11ac: From channelization to multi-user MIMO. *IEEE Commun. Mag.*, pages 84–90, 2013.
- [BMB15] R. Brandt, R. Mochaourab, and M. Bengtsson. Interference alignment-aided base station clustering using coalition formation. In *Proc. Asilomar Conf. Signals, Systems, Computers*, pages 1087–1091, 2015.
- [BMB16a] R. Brandt, R. Mochaourab, and M. Bengtsson. Distributed long-term base station clustering in cellular networks using coalition formation. *IEEE Trans. Signal Inf. Process. Netw.*, 2016. Submitted in Dec. 2015, revised in Feb. 2016.

- [BMB16b] R. Brandt, R. Mochaourab, and M. Bengtsson. Globally optimal base station clustering in interference alignment-based multicell networks. *IEEE Signal Process. Lett.*, 23(4):512–516, 2016.
- [Bra11] R. Brandt. Matlab simulation environment for wideband MIMO channel diagonalization in the time domain, 2011. Accessible at: https://github.com/rasmusbrandt/pimrc2011_polynomial_svd.
- [Bra14a] R. Brandt. *Coordinated Precoding for Multicell MIMO Networks*. Tech. lic. thesis, KTH Royal Institute of Technology, 2014.
- [Bra14b] R. Brandt. Matlab simulation environment for weighted sum rate optimization for multicell MIMO systems with hardware-impaired transceivers, 2014. Accessible at: https://github.com/rasmusbrandt/icassp2014_transceiver_impairments.
- [Bra15a] R. Brandt. Julia simulation environment for fast-convergent distributed coordinated precoding for TDD multicell MIMO systems, 2015. Accessible at: <https://github.com/rasmusbrandt/FastConvergentCoordinatedPrecoding.jl>.
- [Bra15b] R. Brandt. Julia simulation environment for interference alignment-aided base station clustering using coalition formation, 2015. Accessible at: <https://github.com/rasmusbrandt/DistributedBaseStationClustering.jl>.
- [Bra16a] R. Brandt. Julia simulation environment for globally optimal base station clustering in interference alignment-based multicell networks, 2016. Accessible at: <https://github.com/rasmusbrandt/OptimalBaseStationClustering.jl>.
- [Bra16b] R. Brandt. Matlab simulation environment for distributed CSI acquisition and coordinated precoding for TDD multicell MIMO systems, 2016. Accessible at: https://github.com/rasmusbrandt/tvt2015_distributed_CSI_acquisition.
- [Bru09] R. A. Brualdi. *Introductory Combinatorics*. Pearson, 2009.
- [BT09] H. Bölcskei and J. Thukral. Interference alignment with limited feedback. In *Proc. IEEE Int. Symp. Inform. Theory*, pages 1759–1763, 2009.
- [BT10] D. Berend and T. Tassa. Improved bounds on Bell numbers and on moments of sums of random variables. *Prob. and Math. Stat.*, 30(2):185–205, 2010.
- [BV04] S. Boyd and L. Vandenberghe. *Convex Optimization*. Cambridge University Press, 2004.

- [BZB12] E. Björnson, P. Zetterberg, and M. Bengtsson. Optimal coordinated beamforming in the multicell downlink with transceiver impairments. In *Proc. IEEE Global Telecommun. Conf.*, pages 4775–4780, 2012.
- [BZB13] R. Brandt, P. Zetterberg, and M. Bengtsson. Interference alignment over a combination of space and frequency. In *Proc. IEEE Int. Conf. Commun. Workshop: Beyond LTE-A*, pages 149–153, 2013.
- [BZBO12] E. Björnson, P. Zetterberg, M. Bengtsson, and B. Ottersten. Capacity limits and multiplexing gains of MIMO channels with transceiver impairments. *IEEE Commun. Lett.*, 17(1):91–94, 2012.
- [CACCO8] S. Christensen, R. Agarwal, E. Carvalho, and J. Cioffi. Weighted sum-rate maximization using weighted MMSE for MIMO-BC beamforming design. *IEEE Trans. Wireless Commun.*, 7(12):4792–4799, 2008.
- [Car78] A. Carleial. Interference channels. *IEEE Trans. Inf. Theory*, 24(1):60–70, 1978.
- [Car88] B. D. Carlson. Covariance matrix estimation errors and diagonal loading in adaptive arrays. *IEEE Trans. Aerosp. Electron. Syst.*, 24(4):397–401, 1988.
- [CC14] S. Chen and R. S. Cheng. Clustering for interference alignment in multiuser interference network. *IEEE Trans. Veh. Technol.*, 63(6):2613–2624, 2014.
- [Cis15] Cisco. Cisco visual networking index: Global mobile data traffic forecast update, 2014–2019. White paper, Cisco, 2015.
- [CJ08] V. R. Cadambe and S. A. Jafar. Interference alignment and degrees of freedom of the K-user interference channel. *IEEE Trans. Inf. Theory*, 54(8):3425–3441, 2008.
- [CLW⁺03] D. Chizhik, J. Ling, P. W. Wolniansky, R. A. Valenzuela, N. Costa, and K. Huber. Multiple-input-multiple-output measurements and modeling in Manhattan. *IEEE J. Sel. Areas Commun.*, 21(3):321–331, 2003.
- [Cox73] H. Cox. Resolving power and sensitivity to mismatch of optimum array processors. *J. Acoustical Soc. America*, 54(3):771–785, 1973.
- [CP15] Y. Cheng and M. Pesavento. Joint discrete rate adaptation and downlink beamforming using mixed integer conic programming. *IEEE Trans. Signal Process.*, 63(7):1750–1764, 2015.
- [CT06] T. M. Cover and J. A. Thomas. *Elements of Information Theory*. Wiley, 2nd edition, 2006.

- [CZO87] H. Cox, R. M. Zeskind, and M. M. Owen. Robust adaptive beamforming. *IEEE Trans. Acoust., Speech, Signal Process.*, 35(10):1365–1376, 1987.
- [DADSC04] S. N. Diggavi, N. Al-Dhahir, A. Stamoulis, and A. R. Calderbank. Great expectations: The value of spatial diversity in wireless networks. *Proc. IEEE*, 92(2):219–270, 2004.
- [DG80] J. H. Drèze and J. Greenberg. Hedonic coalitions: Optimality and stability. *Econometrica*, 48(4):987–1003, 1980.
- [DPS11] E. Dahlman, S. Parkvall, and J. Sköld. *4G LTE/LTE-Advanced for Mobile Broadband*. Academic Press, 2011.
- [DRSP13] H. Du, T. Ratnarajah, M. Sellathurai, and C. B. Papadias. Reweighted nuclear norm approach for interference alignment. *IEEE Trans. Commun.*, 61(9):3754–3765, 2013.
- [EAH12] O. El Ayach and R. Heath. Interference alignment with analog channel state feedback. *IEEE Trans. Wireless Commun.*, 11(2):626–636, 2012.
- [EALH12] O. El Ayach, A. Lozano, and R. Heath. On the overhead of interference alignment: Training, feedback, and cooperation. *IEEE Trans. Wireless Commun.*, 11(11):4192–4203, 2012.
- [ECS+98] R. Ertel, P. Cardieri, K. Sowerby, T. Rappaport, and J. Reed. Overview of spatial channel models for antenna array communication systems. *IEEE Personal Commun. Mag.*, 5(1):10–22, 1998.
- [EPH10] O. El Ayach, S. W. Peters, and R. W. Heath. The feasibility of interference alignment over measured MIMO-OFDM channels. *IEEE Trans. Veh. Technol.*, 59(9):4309–4321, 2010.
- [Eri15] Ericsson. Ericsson mobility report. Technical report, Ericsson, 2015.
- [GBS14] Ó. González, C. Beltrán, and I. Santamaría. A feasibility test for linear interference alignment in MIMO channels with constant coefficients. *IEEE Trans. Inf. Theory*, 60(3):1840–1856, 2014.
- [GBS15] Ó. González, C. Beltrán, and I. Santamaría. On the number of interference alignment solutions for the K -user MIMO channel with constant coefficients. *IEEE Trans. Inf. Theory*, 61(11):6028–6048, 2015.
- [GCJ11] K. Gomadam, V. R. Cadambe, and S. Jafar. A distributed numerical approach to interference alignment and applications to wireless interference networks. *IEEE Trans. Inf. Theory*, 57(6):3309–3322, 2011.

- [GGLF08] B. Göransson, S. Grant, E. Larsson, and Z. Feng. Effect of transmitter and receiver impairments on the performance of MIMO in HSDPA. In *Proc. IEEE Workshop Signal Process. Advances Wireless Commun.*, pages 496–500, 2008.
- [GHH⁺10] D. Gesbert, S. Hanly, H. Huang, S. Shamai Shitz, O. Simeone, and W. Yu. Multi-cell MIMO cooperative networks: A new look at interference. *IEEE J. Sel. Areas Commun.*, 28(9):1380–1408, 2010.
- [GLS14] Ó. González, C. Lameiro, and I. Santamaría. A quadratically convergent method for interference alignment in MIMO interference channels. *IEEE Signal Process. Lett.*, 21(11):1423–1427, 2014.
- [GLV⁺12] Ó. González, C. Lameiro, J. Vía, I. Santamaría, and R. W. Heath. Interference leakage minimization for convolutive MIMO interference channels. In *Proc. IEEE Int. Conf. Acoustics, Speech, Signal Process.*, pages 2829–2832, 2012.
- [GMBS15] H. Ghauch, R. Mochaourab, M. Bengtsson, and M. Skoglund. Distributed precoding and user selection in dense MIMO interfering networks. In *Proc. IEEE Int. Workshop Comput. Advances Multi-Sensor Adaptive Process.*, pages 461–464, 2015.
- [GNCG⁺11] J. A. García-Naya, L. Castedo, Ó. González, D. Ramírez, and I. Santamaría. Experimental evaluation of interference alignment under imperfect channel state information. In *Proc. European Signal Process. Conf.*, pages 1085–1089, 2011.
- [GPK09] S. Gollakota, S. D. Perli, and D. Katabi. Interference alignment and cancellation. In *Proc. ACM SIGCOMM*, 2009.
- [GRS⁺11] Ó. González, R. Ramírez, I. Santamaría, J. A. García-Naya, and L. Castedo. Experimental validation of interference alignment techniques using a multiuser MIMO testbed. In *Int. ITG Workshop Smart Antennas*, pages 1–8, 2011.
- [GS00] L. Grippo and M. Sciandrone. On the convergence of the block non-linear Gauss-Seidel method under convex constraints. *Operations Research Letters*, 26(3):1–10, 2000.
- [GS11] Ó. González and I. Santamaría. Interference alignment in single-beam MIMO networks via homotopy continuation. In *Proc. IEEE Int. Conf. Acoustics, Speech, Signal Process.*, pages 3344–3347, 2011.
- [GSK05] M. Guillaud, D. T. M. Slock, and R. Knopp. A practical method for wireless channel reciprocity exploitation through relative calibration. In *Proc. Int. Symp. Signal Process. Applicat.*, pages 403–406, 2005.

- [Gur14] Gurobi. Gurobi optimizer reference manual. 2014.
- [Haa00] J. Haartsen. The bluetooth radio system. *IEEE Personal Commun. Mag.*, 7(1):28–36, 2000.
- [HG07] A. Hjørungnes and D. Gesbert. Complex-valued matrix differentiation: Techniques and key results. *IEEE Trans. Signal Process.*, 55(6):2740–2746, 2007.
- [HJ85] R. A. Horn and C. R. Johnson. *Matrix Analysis*. Cambridge University Press, 1985.
- [HKB11] E. Hossain, D. I. Kim, and V. K. Bhargava, editors. *Cooperative Cellular Wireless Networks*. Cambridge University Press, 2011.
- [HRLP16] M. Hong, M. Razaviyayn, Z.-Q. Luo, and J.-S. Pang. A unified algorithmic framework for block-structured optimization involving big data: With applications in machine learning and signal processing. *IEEE Signal Process. Mag.*, 33(1):57–77, 2016.
- [HSBL13] M. Hong, R. Sun, H. Baligh, and Z.-Q. Luo. Joint base station clustering and beamformer design for partial coordinated transmission in heterogeneous networks. *IEEE J. Sel. Areas Commun.*, 31(2):226–240, 2013.
- [HT11] H. Holma and A. Toskala. *LTE for UMTS: Evolution to LTE-Advanced*. Wiley, 2nd edition, 2011.
- [IR09] ITU-R. Guidelines for evaluation of radio interface technologies for IMT-Advanced. Technical Report M.2135-1, ITU-R, 2009.
- [Jaf11] S. A. Jafar. Interference alignment: a new look at signal dimensions in a communication network. *Foundations Trends Commun. Inform. Theory*, 7(1), 2011.
- [JAMV11] J. Jose, A. Ashikhmin, T. L. Marzetta, and S. Vishwanath. Pilot contamination and precoding in multi-cell TDD systems. *IEEE Trans. Wireless Commun.*, 10(8):2640–2651, 2011.
- [Jen05] J. L. W. V. Jensen. Sur les fonctions convexes et les inégalités entre les valeurs moyennes. *Acta Mathematica*, 30(1):175–193, 1905.
- [JL10] N. Jindal and A. Lozano. A unified treatment of optimum pilot overhead in multipath fading channels. *IEEE Trans. Commun.*, 58(10):2939–2948, 2010.
- [JPKR11] J. Jose, N. Prasad, M. Khojastepour, and S. Rangarajan. On robust weighted-sum rate maximization in MIMO interference networks. In *Proc. IEEE Int. Conf. Commun.*, pages 1–6, 2011.

- [Kay93] S. M. Kay. *Fundamentals of Statistical Signal Processing: Estimation Theory*. Prentice Hall, 1993.
- [KMT98] F. P. Kelly, A. K. Maulloo, and D. K. H. Tan. Rate control for communication networks: Shadow prices, proportional fairness and stability. *J. Operational Research Soc.*, 49(3):237–252, 1998.
- [Knu11] D. E. Knuth. *The Art of Computer Programming: Combinatorial Algorithms, Part 1*, volume 4A. Addison-Wesley, 2011.
- [KTJ13] P. Komulainen, A. Tölli, and M. Juntti. Effective CSI signaling and decentralized beam coordination in TDD multi-cell MIMO systems. *IEEE Trans. Signal Process.*, 61(9):2204–2218, 2013.
- [KV13] R. Krishnamachari and M. Varanasi. Interference alignment under limited feedback for MIMO interference channels. *IEEE Trans. Signal Process.*, 61(15):3908–3917, 2013.
- [Lö4] J. Löfberg. Yalmip : A toolbox for modeling and optimization in MATLAB. In *Proc. CACSD Conf.*, Taipei, Taiwan, 2004.
- [Lap96] A. Lapidoth. Nearest neighbor decoding for additive non-Gaussian noise channels. *IEEE Trans. Inf. Theory*, 42(5):1520–1529, 1996.
- [Lat05] B. P. Lathi. *Linear systems and signals*. Oxford University Press, 2005.
- [LD60] A. H. Land and A. G. Doig. An automatic method of solving discrete programming problems. *Econometrica*, 28(3):497–520, 1960.
- [LDL11] Y.-F. Liu, Y.-H. Dai, and Z.-Q. Luo. Coordinated beamforming for MISO interference channel: Complexity analysis and efficient algorithms. *IEEE Trans. Signal Process.*, 59(3):1142–1157, 2011.
- [LGGN⁺15] C. Lameiro, Ó. González, J. A. García-Naya, I. Santamaría, and L. Castedo. Experimental evaluation of interference alignment for broadband WLAN systems. *EURASIP J. Wireless Commun. Netw.*, 2015(1):1–21, 2015.
- [LGV⁺12] C. Lameiro, Ó. González, J. Vía, I. Santamaría, and R. W. Heath. Pre- and post-FFT interference leakage minimization for MIMO OFDM networks. In *Proc. Int. Symp. Wireless Commun. Systems*, pages 556–560, 2012.
- [LH05] D. Love and R. Heath. Limited feedback unitary precoding for spatial multiplexing systems. *IEEE Trans. Inf. Theory*, 51(8):2967–2976, 2005.

- [LHA13] A. Lozano, R. Heath, and J. Andrews. Fundamental limits of cooperation. *IEEE Trans. Inf. Theory*, 59(9):5213–5226, 2013.
- [LHLL14] W.-C. Liao, M. Hong, Y.-F. Liu, and Z.-Q. Luo. Base station activation and linear transceiver design for optimal resource management in heterogeneous networks. *IEEE Trans. Signal Process.*, 62(15):3939–3952, 2014.
- [LHNL⁺08] D. Love, R. Heath, V. N. Lau, D. Gesbert, B. Rao, and M. Andrews. An overview of limited feedback in wireless communication systems. *IEEE J. Sel. Areas Commun.*, 26(8):1341–1365, 2008.
- [LKY13] H.-H. Lee, Y.-C. Ko, and H.-C. Yang. On robust weighted sum rate maximization for MIMO interfering broadcast channels with imperfect channel knowledge. *IEEE Commun. Lett.*, 17(6):1156–1159, 2013.
- [LSW03] J. Li, P. Stoica, and Z. Wang. On robust Capon beamforming and diagonal loading. *IEEE Trans. Signal Process.*, 51(7):1702–1715, 2003.
- [LY13] T. Liu and C. Yang. On the feasibility of linear interference alignment for MIMO interference broadcast channels with constant coefficients. *IEEE Trans. Signal Process.*, 61(9):2178–2191, 2013.
- [LZ08] Z.-Q. Luo and S. Zhang. Dynamic spectrum management: Complexity and duality. *IEEE J. Sel. Topics Signal Process.*, 2(1):57–73, 2008.
- [Mad08] U. Madhow. *Fundamentals of Digital Communication*. Cambridge University Press, 2008.
- [MAMK08] M. Maddah-Ali, A. Motahari, and A. Khandani. Communication over MIMO X channels: Interference alignment, decomposition, and performance analysis. *IEEE Trans. Inf. Theory*, 54(8):3457–3470, 2008.
- [MAT15] MATLAB. *version 8.5.0 (R2015a)*. The MathWorks Inc., Natick, Massachusetts, 2015.
- [MBB15] R. Mochaourab, E. Björnson, and M. Bengtsson. Adaptive pilot clustering in heterogeneous massive MIMO networks. *Submitted to IEEE Trans. Wireless Commun.*, 2015. arXiv:1507.04869 [cs.IT].
- [MBGB15] R. Mochaourab, R. Brandt, H. Ghauch, and M. Bengtsson. Overhead-aware distributed CSI selection in the MIMO interference channel. In *Proc. European Signal Process. Conf.*, pages 1043–1047, 2015.
- [McC05] S. T. McCormick. Submodular function minimization. In G. N. K. Aardal and R. Weismantel, editors, *Discrete Optimization*, volume 12 of *Handbooks in Operations Research and Management Science*, pages 321–391. Elsevier, 2005.

- [MFZ15] N. N. Moghadam, H. Farhadi, and P. Zetterberg. Optimal power allocation for pilot-assisted interference alignment in MIMO interference networks: Test-bed results. In *Proc. IEEE Int. Conf. Digital Signal Process*, pages 585–589, 2015.
- [MFZS14] N. N. Moghadam, H. Farhadi, P. Zetterberg, and M. Skoglund. Test-bed implementation of iterative interference alignment and power control for wireless MIMO interference networks. In *Proc. IEEE Workshop Signal Process. Advances Wireless Commun.*, pages 239–243, 2014.
- [MSLT08] E. Matakani, N. Sidiropoulos, Z.-Q. Luo, and L. Tassiulas. Convex approximation techniques for joint multiuser downlink beamforming and admission control. *IEEE Trans. Wireless Commun.*, 7(7):2682–2693, 2008.
- [MZHH12] N. N. Moghadam, P. Zetterberg, P. Händel, and H. Hjalmarsson. Correlation of distortion noise between the branches of MIMO transmit antennas. In *Proc. IEEE Int. Symp. Personal, Indoor, Mobile Radio Commun.*, pages 2079–2084, 2012.
- [NGS12] F. Negro, I. Ghauri, and D. T. M. Slock. Sum rate maximization in the noisy MIMO interfering broadcast channel with partial CSIT via the expected weighted MSE. In *Proc. Int. Symp. Wireless Commun. Systems*, pages 576–580, 2012.
- [Nok14] Nokia. What is going on in mobile broadband networks? Smartphone traffic analysis and solutions. Technical report, Nokia, 2014.
- [NSGS10] F. Negro, S. P. Shenoy, I. Ghauri, and D. T. M. Slock. Weighted sum rate maximization in the MIMO interference channel. *Proc. IEEE Int. Symp. Personal, Indoor, Mobile Radio Commun.*, pages 684–689, 2010.
- [OR96] B. Ottersten and R. Roy. Spatial division multiple access wireless communication systems. *US Patent 5,515,378*, 1996.
- [OSW94] L. Ozarow, S. Shamai, and A. Wyner. Information theoretic considerations for cellular mobile radio. *IEEE Trans. Veh. Technol.*, 43(2):359–378, 1994.
- [PBS⁺13] F. Pantisano, M. Bennis, W. Saad, M. Debbah, and M. Latva-aho. Interference alignment for cooperative femtocell networks: A game-theoretic approach. *IEEE Trans. Mobile Comput.*, 12(11):2233–2246, 2013.

- [PC06] D. P. Palomar and M. Chiang. A tutorial on decomposition methods for network utility maximization. *IEEE J. Sel. Areas Commun.*, 24(8):1439–1451, 2006.
- [PCL03] D. P. Palomar, J. M. Cioffi, and M. A. Lagunas. Joint Tx-Rx beamforming design for multicarrier MIMO channels: a unified framework for convex optimization. *IEEE Trans. Signal Process.*, 51(9):2381–2401, 2003.
- [PD12] D. S. Papailiopoulos and A. G. Dimakis. Interference alignment as a rank constrained rank minimization. *IEEE Trans. Signal Process.*, 60(8):4278–4288, 2012.
- [PH09] S. Peters and R. Heath. Interference alignment via alternating minimization. In *Proc. IEEE Int. Conf. Acoustics, Speech, Signal Process.*, pages 2445–2448, 2009.
- [PH11] S. W. Peters and R. W. Heath. Cooperative algorithms for MIMO interference channels. *IEEE Trans. Veh. Technol.*, 60(1):206–218, 2011.
- [PH12] S. Peters and R. Heath. User partitioning for less overhead in MIMO interference channels. *IEEE Trans. Wireless Commun.*, 11(2):592–603, 2012.
- [PL12] S.-H. Park and I. Lee. Degrees of freedom for mutually interfering broadcast channels. *IEEE Trans. Inf. Theory*, 58(1):393–402, 2012.
- [PLH16] J. Park, N. Lee, and R. Heath. Cooperative base station coloring for pair-wise multi-cell coordination. *IEEE Trans. Commun.*, 64(1):402–415, 2016.
- [RBCL13] M. Razaviyayn, M. Baligh, A. Callard, and Z.-Q. Luo. Robust transceiver design. *Patent WO 2013/044824 A1*, 2013.
- [RBCL14] M. Razaviyayn, H. Baligh, A. Callard, and Z. Q. Luo. Joint user grouping and transceiver design in a MIMO interfering broadcast channel. *IEEE Trans. Signal Process.*, 62(1):85–94, 2014.
- [RBP⁺14] R. Rogalin, O. Bursalioglu, H. Papadopoulos, G. Caire, A. Molisch, A. Michaloliakos, V. Balan, and K. Psounis. Scalable synchronization and reciprocity calibration for distributed multiuser MIMO. *IEEE Trans. Wireless Commun.*, 13(4):1815–1831, 2014.
- [RHL13a] M. Razaviyayn, M. Hong, and Z. Luo. A unified convergence analysis of block successive minimization methods for nonsmooth optimization. *SIAM J. Optimization*, 23(2):1126–1153, 2013.

- [RHL13b] M. Razaviyayn, M. Hong, and Z.-Q. Luo. Linear transceiver design for a MIMO interfering broadcast channel achieving max–min fairness. *Signal Processing*, 93(12):3327–3340, 2013.
- [RLL12] M. Razaviyayn, G. Lyubeznik, and Z.-Q. Luo. On the degrees of freedom achievable through interference alignment in a MIMO interference channel. *IEEE Trans. Signal Process.*, 60(2):812–821, 2012.
- [RSL12] M. Razaviyayn, M. Sanjabi, and Z.-Q. Luo. Linear transceiver design for interference alignment: Complexity and computation. *IEEE Trans. Inf. Theory*, 58(5):2896–2910, 2012.
- [Rud76] W. Rudin. *Principles of Mathematical Analysis*. McGraw-Hill, 3rd edition, 1976.
- [SBH14] C. Shi, R. Berry, and M. Honig. Bi-directional training for adaptive beamforming and power control in interference networks. *IEEE Trans. Signal Process.*, 62(3):607–618, 2014.
- [SCB⁺09] D. A. Schmidt, S. Changxin, R. A. Berry, M. L. Honig, and W. Utschick. Minimum mean squared error interference alignment. In *Conf. Rec. 43rd Asilomar Conf. Signals, Systems and Computers*, pages 1106–1110, 2009.
- [Sch08] T. Schenk. *RF Imperfections in High-rate Wireless Systems: Impact and Digital Compensation*. Springer, 2008.
- [SGHP10] I. Santamaría, Ó. González, R. W. Heath, and S. W. Peters. Maximum sum-rate interference alignment algorithms for MIMO channels. In *Proc. IEEE Global Telecommun. Conf.*, pages 1–6, 2010.
- [SGLW03] S. Shahbazpanahi, A. Gershman, Z.-Q. Luo, and K. M. Wong. Robust adaptive beamforming for general-rank signal models. *IEEE Trans. Signal Process.*, 51(9):2257–2269, 2003.
- [Sha48] C. E. Shannon. A mathematical theory of communication. *Bell Syst. Tech. J.*, 27:379–423, 1948.
- [Sha15] S. Shalmashi. *Device-to-Device Communications for Future Cellular Networks: Challenges, Trade-Offs, and Coexistence*. PhD thesis, KTH Royal Institute of Technology, 2015.
- [SHD⁺09] W. Saad, Z. Han, M. Debbah, A. Hjørungnes, and T. Basar. Coalitional game theory for communication networks: A tutorial. *IEEE Signal Process. Mag.*, 26(5):77–97, 2009.

- [SHZ⁺12] W. Saad, Z. Han, R. Zheng, A. Hjørungnes, T. Basar, and V. Poor. Coalitional games in partition form for joint spectrum sensing and access in cognitive radio networks. *IEEE J. Sel. Topics Signal Process.*, 6(2):195–209, 2012.
- [SM12] J. Shin and J. Moon. Weighted-sum-rate-maximizing linear transceiver filters for the K -user MIMO interference channel. *IEEE Trans. Commun.*, 60(10):2776–2783, 2012.
- [Smi04] G. S. Smith. A direct derivation of a single-antenna reciprocity relation for the time domain. *IEEE Trans. Antennas Propag.*, 52(6):1568–1577, 2004.
- [SRL14] M. Sanjabi, M. Razaviyayn, and Z.-Q. Luo. Optimal joint base station assignment and beamforming for heterogeneous networks. *IEEE Trans. Signal Process.*, 62(8):1950–1961, 2014.
- [SRLH11] Q. Shi, M. Razaviyayn, Z.-Q. Luo, and C. He. An iteratively weighted MMSE approach to distributed sum-utility maximization for a MIMO interfering broadcast channel. *IEEE Trans. Signal Process.*, 59(9):4331–4340, 2011.
- [SSB⁺13] D. Schmidt, C. Shi, R. Berry, M. Honig, and W. Utschick. Comparison of distributed beamforming algorithms for MIMO interference networks. *IEEE Trans. Signal Process.*, 61(13):3476–3489, 2013.
- [SSH04] Q. H. Spencer, A. L. Swindlehurst, and M. Haardt. Zero-forcing methods for downlink spatial multiplexing in multiuser MIMO channels. *IEEE Trans. Signal Process.*, 52(2):461–471, 2004.
- [STB09] S. Sesia, I. Toufik, and M. Baker. *LTE: the UMTS long term evolution*. Wiley, 2009.
- [SWB10] C. Studer, M. Wenk, and A. Burg. MIMO transmission with residual transmit-RF impairments. In *Int. ITG Workshop Smart Antennas*, pages 189–196, 2010.
- [SY15a] G. Sridharan and W. Yu. Can interference alignment impact network utility maximization? In *Conf. Rec. 49th Asilomar Conf. Signals, Systems and Computers*, 2015.
- [SY15b] G. Sridharan and W. Yu. Linear beamformer design for interference alignment via rank minimization. *IEEE Trans. Signal Process.*, 63(22):5910–5923, 2015.
- [TB97] L. N. Trefethen and D. Blau III. *Numerical Linear Algebra*. SIAM, 1997.

- [Tel99] E. Telatar. Capacity of multi-antenna Gaussian channels. *European Trans. Telecommun.*, 10(6):585–595, 1999.
- [TG09] R. Trench and M. Guillaud. Clustered interference alignment in large cellular networks. In *Proc. IEEE Int. Symp. Personal, Indoor, Mobile Radio Commun.*, pages 1024–1028, 2009.
- [TV04] A. M. Tulino and S. Verdú. Random matrix theory and wireless communications. *Foundations Trends Commun. Inform. Theory*, 1(1):1–182, 2004.
- [TV08] D. Tse and P. Viswanath. *Fundamentals of Wireless Communication*. Cambridge University Press, 2008.
- [VGL03] S. Vorobyov, A. Gershman, and Z.-Q. Luo. Robust adaptive beamforming using worst-case performance optimization: a solution to the signal mismatch problem. *IEEE Trans. Signal Process.*, 51(2):313–324, 2003.
- [VKV09] P. Vandewalle, J. Kovacevic, and M. Vetterli. Reproducible research in signal processing. *IEEE Signal Process. Mag.*, 26(3):37–47, 2009.
- [War63] J. Ward. Hierarchical grouping to optimize an objective function. *J. Amer. Statist. Assoc.*, 58(301):236–244, 1963.
- [WBM96] R. Wu, Z. Bao, and Y. Ma. Control of peak sidelobe level in adaptive arrays. *IEEE Trans. Antennas Propag.*, 44(10):1341–1347, 1996.
- [WJN13] M. Wolkerstorfer, J. Jaldén, and T. Nordström. Low-complexity optimal discrete-rate spectrum balancing in digital subscriber lines. *Signal Processing*, 93(1):23–34, 2013.
- [WLM13] H.-T. Wai, Q. Li, and W.-K. Ma. A convex approximation method for multiuser MISO sum rate maximization under discrete rate constraints. In *Proc. IEEE Int. Conf. Acoustics, Speech, Signal Process.*, pages 4759–4763, 2013.
- [WV13] C. Wilson and V. Veeravalli. A convergent version of the MaxSINR algorithm for the MIMO interference channel. *IEEE Trans. Wireless Commun.*, 12(6):2952–2961, 2013.
- [WY11] L.-C. Wang and C.-J. Yeh. 3-cell network MIMO architectures with sectorization and fractional frequency reuse. *IEEE J. Sel. Areas Commun.*, 29(6):1185–1199, 2011.
- [YGJK10] C. Yetis, T. Gou, S. A. Jafar, and A. Kayran. On feasibility of interference alignment in MIMO interference networks. *IEEE Trans. Signal Process.*, 58(9):4771–4782, 2010.

- [YMB⁺16] V. Yajnanarayana, K. E. G. Magnusson, R. Brandt, S. Dwivedi, and P. Händel. Optimal scheduling for interference mitigation by range information. *IEEE Trans. Mobile Comput.*, 2016. Submitted in Feb. 2016.
- [ZBH11] B. Zhuang, R. A. Berry, and M. L. Honig. Interference alignment in MIMO cellular networks. In *Proc. IEEE Int. Conf. Acoustics, Speech, Signal Process.*, pages 3356–3359, 2011.
- [Zet14a] P. Zetterberg. Interference alignment (IA) and coordinated multi-point (CoMP) overheads and RF impairments: Testbed results. In *Proc. IEEE Veh. Tech. Conf.*, pages 1–7, 2014.
- [Zet14b] P. Zetterberg. Interference alignment (IA) and coordinated multi-point (CoMP) with IEEE802. 11ac feedback compression: Testbed results. In *Proc. IEEE Int. Conf. Acoustics, Speech, Signal Process.*, pages 6176–6180, 2014.
- [ZM12] P. Zetterberg and N. M. Moghadam. An experimental investigation of SIMO, MIMO, interference-alignment (IA) and coordinated multi-point (CoMP). In *Proc. Int. Workshop Systems, Signals and Image Process.*, pages 211–216, 2012.
- [ZSGL05] K. Zarifi, S. Shahbazpanahi, A. Gershman, and Z.-Q. Luo. Robust blind multiuser detection based on the worst-case performance optimization of the MMSE receiver. *IEEE Trans. Signal Process.*, 53(1):295–305, 2005.
- [ZT03] L. Zheng and D. Tse. Diversity and multiplexing: a fundamental tradeoff in multiple-antenna channels. *IEEE Trans. Inf. Theory*, 49(5):1073–1096, 2003.